MONASH UNIVERSITY
THESIS ACCEPTED IN SATISFACTION OF THE
REQUIREMENTS FOR THE DEGREE OF
DOCTOR OF PHILOSOPHY
ON..... 8 June 2004.....
.....[redacted].....
Sec. Research Graduate School Committee

Regulated L-Arginine Transport in Heart Failure

A thesis submitted as requirement

for the degree of

Doctor of Philosophy

to the

Faculty of Medicine, Monash University, Melbourne, Australia

Belinda A. Ahlers BBiomedSc (Hons)

Baker Heart Research Institute

Prahran, Melbourne

Australia

October, 2003

Dedication

Dedicated to my family

Mum, Dad, John, Michael, Virginia and Corey.

And my beloved

Yves

Declaration

This thesis contains no material which has been previously been accepted for the award of any other degree or diploma of any university, and to the best of my knowledge contains no material published by another person, except where due reference is made in the text.

[redacted]

Belinda A. Ahlers BBiomedSc (Hons)

Faculty of Medicine

Monash University

Melbourne, Australia

April, 2003

Publications Arising From Work in This Thesis

BA Ahlers, DM Kaye, MM Parnell and JPF Chin-Dusting. Angiotensin II stimulated L-arginine uptake in human endothelial cells mediated by the AT4 receptor. *Hypertension.* Invited for re-submission, currently in review.

BA Ahlers, MM Parnell, DM Kaye and JPF Chin-Dusting. An age related decline in endothelial function is not associated with alterations in L-arginine transport in humans. *J.Hypertension.* Submitted.

DM Kaye, MM Parnell and BA Ahlers (2002) Impaired human myocardial L-arginine transport in congestive heart failure. *Circ Res.* Dec 13;91(12):1198-203.

DM Kaye, BA Ahlers, D Autelitano and JPF Chin-Dusting (2000) In vivo and in vitro evidence for impaired arginine transport in human heart failure. *Circulation.* Nov 28;102(22):2707-12.

JPF Chin-Dusting. BA Ahlers, AM Jefferis and JA Whitworth. The role of L-arginine transport in cortisol-induced hypertension. Accepted. *Hypertension.*

B Rasaratum, BA Ahlers, JPF Chin-Dusting. Arterial vasodilatation in human liver cirrhosis: Upregulation of the L-arginine transporter. *Circulation.* Manuscript invited for re-submission.

Markus P. Schlaich, Melinda M. Parnell, Belinda A. Ahlers, David M. Kaye. Impaired L-arginine transport and endothelial function in hypertensive and genetically predisposed normotensive subjects. *Journal of Clinical Investigation.* Manuscript submitted.

Markus P. Schlaich, Belinda A. Ahlers, Melinda M. Parnell, David M. Kaye. Effect of L-arginine on ß–adrenoceptor mediated vasodilation in early human hypertension. *Journal of Hypertension.* Manuscript submitted.

Acknowledgments

The work contained within this thesis could not have been realised without the help and support of my colleagues and peers at the Baker Heart Research Institute.

Thanks to Dr. Jaye Chin-Dusting for encouraging and supporting for me throughout the PhD programme at the Baker Heart Research Institute. Your willingness of students to take the research data out to both a national and international platform has helped me to develop confidence in communicating with the larger scientific community.

A special thanks to Dr. David Kaye for the mentoring role taken on in my PhD. Also, for the ongoing and continued support throughout my thesis. Your insight and ability in translating data from clinical to experimental models and vice versa is most impressive and inspiring. Sincere gratitude for the opportunity to join your dynamic research team.

A particular acknowledgment of the collective wisdom of Drs. Rob Andrews, Liz Gardiner, Ross Hannan, Yves Brandenburger, Wally Thomas, Dominic Autelitano and Ian Smith at the Baker Institute. Their helpful discussions about specific aspects of the work contained in this thesis, both methodological and theoretical, has been an invaluable source of information. I hope to impart the same sort of passion for the research process to others in the future as well as they have done for me.

Thanks to Samara, Ann-Maree, Margaret, Teneale, Belinda, Elodie and Anna who were always ready and willing to offer laboratory support and work as a team on many projects.

Best wishes to the fellow Baker students in their studies.

Abbreviations

AA	ascorbic acid
Ang II	angiotensin II
Ang IV	angiotensin IV
Ang 1-7	angiotensin 1-7
ANP	atrial natriuretic peptide
AT1	angiotensin receptor type 1
AT2	angiotensin receptor type 2
AT4	angiotensin receptor type 4
BAEC	bovine aortic endothelial cell
BSA	bovine serum albumin
BH4	tetrahydrobiopterin
°C	degrees celcius
Ca^{2+}	calcium ion
CAT	cationic amino acid transporter
CHF	congestive heart failure
DMEM	Dulbecco's Modified Eagle's Medium
D-PBS	Dulbecco's phosphate buffered saline
EA.hy926	human endothelial cell line
eNOS	endothelial nitric oxide synthase
ET-1	endothelin-1
FBS	fetal bovine serum
HCl	hydrochloric acid
hr	hours(s)
IBMX	3-isobutyl-1-methylxanthine
IFN-γ	interferon gamma
IL-1ß	interleukin-1ß
iNOS	inducible nitric oxide synthase
IP_3	inositol 1,4,5-triphosphate
K^+	potassium ion
Km	Michaelis-Menton affinity constant

L	litre
L-Arg	L-arginine
L-[^{3}H]Arg	radiolabelled L-arginine
LPS	lipopolysaccharide
L-NMMA	N^G-mono-methyl-L-arginine
NA	noradrenaline
Na^+	sodium ion
Na OH	sodium hydroxide
NO	nitric oxide
NOS	nitric oxide synthase
M	molar
MAP kinase	mitogen-activated protein kinase
min	minute(s)
Milli Q	double distilled water
mL	millilitre
mM	millimolar
nM	nanomolar
PBM	peripheral blood mononuclear cell(s)
pM	picomolar
PP2A	protein phosphatase 2A
PKC	protein kinase C
PMSF	phenylmethylsulfonyl fluoride
RT	room temperature
RT-PCR	reverse transcriptase-polymerase chain reaction
sec	second(s)
SDS-PAGE	sodium dodecyl sulphate-polyacrylamide gel electophoresis
TNF-α	tumor necrosis factor-α
Tris	Tris
µL	micro litre
µM	micromolar
Vmax	maximum velocity kinetic constant

Synopsis

Clinical studies have shown that the endothelial dysfunction associated with congestive heart failure (CHF) is related to a deficiency in the bioavailability of nitric oxide (NO) in the endothelium. In particular, this abnormality has been identified in the peripheral, pulmonary and coronary circulation of CHF patients through the demonstration of an impaired endothelium-dependent vasodilator response to infused agonists such as acetylcholine *in vivo*. Since endothelial dysfunction in CHF can be significantly improved by exogenous administration of L-arginine, the precursory substrate required for constitutive NO synthase (endothelial NOS) conversion to NO, an impairment of L-arginine transport into the endothelium may be one of the factors contributing to the NO deficiency in this prevalent disease.

As a complementary approach to the clinical *in vivo* studies performed within this laboratory, L-arginine transporter expression and activity were evaluated in the peripheral vasculature of CHF patients. A novel *in vitro* approach was developed in order to assess L-[^{3}H]arginine transport in freshly isolated peripheral blood mononuclear cells from CHF. In accordance with the *in vivo* findings, a major and significant finding of this thesis (Chapter 3) reports on a down-regulation of L-arginine transport in patients with CHF which correlated with a significant decrease in mRNA expression of the major L-arginine transporter, CAT-1, in these cells.

A further *in vivo* approach taken to assess the status of L-arginine transport in the coronary and systemic circulation of CHF performed by Dr. David Kaye has revealed a similar impairment of L-arginine transport in CHF patients. As an *in vitro* complementary approach, a second major finding of this thesis has indicated that a systemic down-regulation of CAT-1 may exist since expression (mRNA) of this transporter was also significantly decreased in the human myocardium of CHF patients (Chapter 3). This down-regulation did not coincide with a down-regulation of the alternate

CAT isoforms present in the myocardium (CAT-2A or CAT-2B) or, an altered NOS (endothelial NOS or inducible NOS) expression profile, indicating that down-regulated L-arginine transport mediated CAT-1 may influence the constitutive production of NO. Collectively, our studies have identified the existence of a systemic down-regulation of L-arginine transport in CHF patients.

Further studies were carried out in order to investigate whether impaired L-Arg transport was related to the effect of important circulating factors in CHF. An initial assessment was made on the ability of CHF serum or major neurohormonal factors (ANP, NE, ET-1Ang II) and cytokines (TNF-α) relevant in the setting of CHF to affect L-arginine transport in a cultured human endothelial cell system. Using a venous endothelial cell type, CHF serum and most of these agents did not have a significant effect on endothelial L-arginine transport, either acutely (<0.5 hr) or long term (>24 hr). Paradoxically, a third major finding of this thesis was that Ang II treatment resulted in a significant up-regulation of L-arginine transport in this cell type that was both time and concentration dependent (Chapter 4). Ang II-enhanced L-arginine transport was shown to be mediated by novel metabolic pathway involving the degradation of Ang II in the culture medium. Activation of Ang IV receptor (AT_4) signalling pathway was involved in this effect since this effect was blocked by AT_4 antagonism and not by other classical receptor types, AT_1 and AT_2. In addition, this mechanism was linked to the production of the metabolically active Ang II degradation product in culture, Ang IV, since Ang IV treatment also led to a significant upregulation of L-arginine transport in this cell type. Ang II enhancing effects on L-arginine transport seemed to be attributable only in part to an increase in CAT-1 mRNA, observed by the induction of CAT-1 mRNA at an early time point only (4 hr), but may involve post-translational regulation of the L-arginine transporter activity at the later time-points (up to 24 hr). An Ang II-mediated increase in CAT-1 activity was shown to involve the PKC signalling pathway(s).

In addition to findings of the previous Ang II study, other groups have indicated that CAT-1 gene expression of CAT-1 does not relate temporally with CAT-1 activity and thus can be a poor predictor of L-arginine transport regulation. Thus, the potential involvement of PKC in (patho-

)physiological CAT-1 regulation were assessed further in cultured endothelial cells. A significant finding of Chapter 5 was that PKC activation, using the well-known PKC activator phorbol-12-myristate ester (PMA), led to a significant and acute (up to 6 hr post treatment) down-regulation of L-arginine transport activity which was not accompanied by changes in CAT-1 gene expression. Long-term treatment (> 6 hr) associated with a depletion of PKC within the cell led to a significant induction of L-arginine transport. Using a CAT-1 antibody produced within the course of this thesis, CAT-1 protein levels were found to remain unaltered throughout the 24 hr time course of PMA treatment, indicating a post-translational mode of regulation. The effects of PKC on L-arginine transport were prevented using the specific PKC inhibitor, bisindoylmalemide I, Bim I. These findings are clearly suggestive of a role for PKC activation in response to various potential stimuli (eg. shear stress, growth hormones, insulin, high glucose) in the regulation of L-arginine transport. The specific PKC isotypes involved in L-arginine transport regulation were not identified. Regulation of L-arginine transport by PKC did not involve changes in the localisation of the transporter at the plasma membrane, phosphorylation status of CAT-1, its co-localisation status with a known interacting structural protein caveolin, or downstream changes in PMA induced-NO and oxidative reactive species (Chapter 6). Preliminary findings in the latter part of this thesis suggest the involvement of a cytoskeletal-associated protein, the Ca+ acitvated-protease calpain, in the regulation of endothelial L-arginine transport by PKC.

Evidence from clinical studies have clearly suggested that there is a correlation between decreased endothelial function and increasing severity of congestive heart failure. Identification of a systemic down-regulation of precursory substrate provision for NO synthesis, through the work contained within this thesis and by others in our laboratory should lead to further efforts in developing alternative therapeutic strategies for the treatment of CHF progression. Since Ang II, altered PKC signalling and cytoskeletal remodelling have also been implicated in the pathophysiology of CHF, findings contained within this thesis have potential impact towards an understanding of the mechanistic events that may be involved in the dysregulation of L-arginine transport in this disease.

Contents

Title		**i**
Dedication		**ii**
Declaration		**iii**
Publications Arising From Work in This Thesis		**iv**
Acknowledgments		**v**
Abbreviations		**vi**
Synopsis		**viii**
Contents		**xi**
Chapter 1	Introduction	1
Chapter 2	Common methodology	76
Chapter 3	L-arginine transport in congestive heart failure	96
Chapter 4	Regulatory factors influencing L-arginine transport in the human endothelium	142
Chapter 5	Modulation of endothelial L-arginine transport by protein kinase C	178
Chapter 6	Mechanisms of protein kinase C modulated L-Arg transport	202
Chapter 7	Conclusions	246
References		254

Chapter One

General Introduction

"THE L-ARGININE-NITRIC OXIDE PATHWAY IN CONGESTIVE HEART FAILURE"

TABLE OF CONTENTS

1.1 Relevance Of The Literature To This Thesis *4*

1.2 Nitric Oxide In The Cardiovascular System *8*

1.3 L-Arginine – Nitric Oxide Pathway *12*

1.3.1 Nitric Oxide Synthases **12**

1.3.2 Endothelial NO Synthase; eNOS **13**

1.3.2.1 eNOS Catalysis 13

1.3.2.2 Regulation of eNOS activity 14

1.3.2.3 Regulation of eNOS Gene Expression 18

1.4 Endothelium Dysfunction *21*

1.4.1 Definition **22**

1.4.2 Identification **23**

1.4.3 Endothelium Dysfunction in Congestive Heart Failure (CHF) **24**

1.4.4 Mechanisms of Endothelium Dysfunction in CHF **27**

1.4.4.1 Free Radical Production and Oxidative stress 27

1.4.4.2 NOS expression and activity 30

1.4.4.3 Lipoproteins 33

1.4.4.4 Substrate and Co-factor Availability for NOS 34

1.4.4.5 Endothelial receptor-signal transduction pathways 35

1.4.4.6 Pro-inflammatory Cytokines and Inflammatory Mediators 36

1.4.4.7 Vasoconstrictor release 37

1.4.5 Treatment of Endothelial Dysfunction **37**

1.4.5.1 Lipid-lowering drugs 38

1.4.5.2 Antioxidants 39

1.4.5.3 ACE inhibitors 39

1.4.5.4 Organic nitrates 40

1.4.5.5 Receptor antagonists and other drugs 40

1.4.5.6 Exercise 41

1.4.5.7 L-Arg supplementation 42

1.5 L-Arg Metabolism *48*

1.5.1 Overview **48**

1.5.2 Regulation of L-Arginine Metabolising Enzymes **50**

1.5.3 L-Arginine Availability and the L-Arginine Paradox **51**

1.5.4 Substrate Provision for the Endothelial L-Arg-NO Pathway **52**

1.5.4.1 Dependence of NO production on Extracellular L-Arg 52

1.5.4.2 Separate Intracellular Pools of L-Arg? 53

1.5.4.3 Preferential Co-localisation of the L-Arg-NO pathway 53

1.5.4.4 Intracellular L-Arg Provision for the NO pathway 55

1.5.5 Nitric Oxide-Independent Vascular Effects of L-Arginine **55**

1.6 L-Arginine Transporters ***58***

1.6.1 L-Arg Transport Systems in Mammalian Cells **58**

1.6.2 Classification of Cationic Amino Acid Transport Systems **58**

1.6.2.1 System y+ cationic amino acid transporters 59

1.6.2.2 Heterodimeric cationic amino acid transporters 61

1.6.2.3 Sodium-dependent cationic amino acid transporters 63

1.6.2.4 Other cationic amino acid transporter types 64

1.7 System Y+/Cationic Amino Acid Transporters (Cat's) ***65***

1.7.1 Discovery **65**

1.7.2 Function **66**

1.7.2.1 CAT1; constitutive expression. 67

1.7.2.2 CAT2A; liver specific isoform 69

1.7.2.3 CAT2B; inducible expression. 70

1.7.2.4 CAT3; neuronal-specific expression. 70

1.7.2.5 CAT4; no known transport function. 71

1.7.3 Regulation **71**

1.7.4 Role of CAT in Endothelial Dysfunction **72**

1.8 Major Aims Of This Thesis ***74***

TABLE OF FIGURES

Figure 1.1	Endothelium-dependent relaxation mediated through the stimulated production of NO.	9
Figure 1.2	Important and beneficial actions of NO in the cardiovascular system.	10
Figure 1.3	Domain arrangement in bovine eNOS.	16
Figure 1.4	Proposed model for eNOS post-translational activation.	20
Figure 1.5	Effects of heart failure on endothelial dysfunction.	25
Figure 1.6	Reactions of superoxide with NO and superoxide dismutase (SOD).	29
Figure 1.7	Metabolic pathways and enzymes related to L-Arginine metabolism.	49
Figure 1.8	Plasma L-Arg availability controls NO synthesis due to compartmentalisation of L-Arg pathways.	54
Figure 1.9	Model for mCAT-1 in the plasma membrane.	68

TABLES

Table 1.1	Factors released from endothelial cells.	11
Table 1.2	Modulation of the L-Arginine-NO pathway in patients with heart failure.	31
Table 1.3	Clinical effects of oral L-Arginine supplementation on endothelial dysfunction.	44
Table 1.4	NO-dependent and independent vascular actions of L-Arginine.	57
Table 1.5	Transport systems described for cationic amino acids.	60

1.1 Relevance Of The Literature To This Thesis

Decreased nitric oxide (NO) bioavailability is thought to be central to endothelial dysfunction. For this reason, the NO pathway and its crucial role in maintaining endothelial function is currently a major topic of investigation. Impaired endothelial function has been identified in congestive heart failure (CHF) amongst other cardiovascular disease states, and is thought to play an important role in excessive peripheral vasoconstriction, a characteristic feature associated with this major cardiovascular disease. Accordingly, evidence suggests that endothelial dysfunction in CHF may affect vascular tone and organ perfusion, particularly during stress situations such as exercise. Since the exact mechanisms underlying endothelial dysfunction in CHF are unclear, an effort has been made within this introduction to review the mechanisms that contribute to the development and progression of endothelial dysfunction. Interventions that potentially improve endothelial function, and their potential impact on the symptoms of heart failure have also been emphasised.

Depletion of the precursory substrate L-Arginine (L-Arg), required by the enzyme endothelial nitric oxide synthase (eNOS) for the synthesis of NO has been proposed as a contributory mechanism in the development of endothelial dysfunction in CHF. L-Arg, is classified as a 'conditionally' essential amino acid and is utilised intracellularly for a variety of different metabolic pathways. An important metabolic fate of L-Arg is through the NO pathway. Importantly, extracellular L-Arg has been proven to be rate limiting for NO production in certain states. However, it is largely unknown what significance this proposed mechanism has in the development of endothelial dysfunction. Additionally, it is not clear whether such a proposed substrate deficiency in the L-Arg-NO pathway may exist in CHF due to decreased substrate concentration in the plasma, decreased transport of substrate across the membrane, or alternatively, intracellular mechanisms which may limit the availability of substrate for NOS.

The major hypothesis of this thesis is that the transport of precursor L-Arg across the cell membrane is impaired and this leads to a decrease in the relative intracellular availability of substrate available for utilisation by eNOS. Development of this working hypothesis is supported

by numerous studies demonstrating the ability of exogenous L-Arg *in vivo* to restore and improve endothelial function (Preli *et al.*, 2002). Beneficial effects of infused and oral L-Arg supplementation have been demonstrated in clinical and experimental models of various cardiovascular disorders associated with endothelial dysfunction (Preli et al., 2002). The major rationale underlying this hypothesis is argued within this chapter.

A number of studies have focused on the role of L-Arg transporters in regulating NO production in response to various (patho-)physiological factors. However, there is a lack of conclusive evidence about the specific role of L-Arg transporters in endothelial dysfunction. Therefore, a portion of this review has been dedicated to describing and identifying transporter systems that have the capability for translocation of L-Arg across the cell membrane in mammals and also their association with substrate provision for the NO pathway. By virtue of its structure, eNOS can function in the absence of L-Arg by utilising molecular oxygen to generate reactive oxygen species (ROS) (Vasquez-Vivar *et al.*, 1998). ROS are important mediators of oxidative stress pathways. As a causal factor implicated in endothelial dysfunction, oxidative stress may be an additional outcome of decreased L-Arg transport across the cell membrane. The pathophysiological effects of oxidative stress pathways on endothelial function are also discussed within this context.

A family of L-Arg transporters termed cationic amino acid transporters (CAT)s predominantly mediates L-Arg transport in humans. Importantly, a specific role of these transporters has emerged in provision of substrate for the NO pathway. As will be discussed, CAT expression and activity can be modulated by factors implicated in the development of endothelial dysfunction and cardiovascular disease. Such evidence makes this family of L-Arg transporters prime candidates for further investigation of their role in endothelial dysfunction.

1.2 Nitric Oxide In The Cardiovascular System

In 1980, Furchgott and Zawadzki (Furchgott and Zawadzki, 1980) discovered that the muscarinic receptor agonist acetylcholine could evoke the release of a non-prostanoid factor from endothelial cells, called endothelial-derived relaxing factor (EDRF), which caused relaxation of smooth muscle and isolated arteries. Further evidence led to the identification of EDRF as the free radical gas, nitric oxide (NO) (Palmer *et al.*, 1987, Ignarro *et al.*, 1987). Furchgott and Zawadzki had also shown that the ability of acetylcholine, mediated by NO, to cause relaxation of rabbit aorta is dependent on the presence of an intact endothelium (Furchgott and Zawadzki, 1980). In addition to acetylcholine, release of NO from endothelial cells was subsequently demonstrated in response to a variety of agonists such as bradykinin, substance P and Ca^{2+} ionophore, resulting in the endothelium-dependent relaxation of blood vessels (Figure 1.1). Following the identification of EDRF as NO, a substantial amount of basic and clinical research on the physiologic and pathophysiologic roles of NO in cardiovascular function has been conducted.

NO is now known to play a vital role in the cardiovascular system and exerts vasoprotective influences in the vascular wall by maintaining important physiological functions such as vascular tone, anticoagulation, leukocyte adhesion, smooth muscle proliferation and, has an antioxidative capability. In addition, NO has also been shown to function in the cardiovascular system in the regulation of cardiac contractility and is produced in large quantities during host defence and immunological reactions. Because NO has cytotoxic properties and is generated by activated macrophages, it is thought to have a role in non-specific immunity (Moncada and Higgs, 1993). Figure 1.2 presents a summary of the important functions that are attributed to the actions of NO in the cardiovascular system.

In the vasculature NO is released by endothelial cells to maintain vascular homeostasis. The synthesis of NO by endothelial cells is primarily responsible for vasodilator tone, and is essential in the regulation of blood pressure. Likewise, regulation of vascular tone is the primary function of

Figure 1.1 Endothelium-dependent relaxation mediated through the stimulated production of NO. eNOS can be activated via various signalling pathways beginning at the cell surface. Phosphorylation of eNOS to its active form begins with the activation of the various receptors (sensing shear stress, bradykinin, acetylcholine, substance P, vascular endothelial growth factor, and β–agonists), followed by signal transduction via their respective signalling pathways. Activation of any of several agonist receptors as well as shear stress glycoproteins converge on the same intracellular pathway that involves G protein activation, IP_3 generation, calcium influx and intracellular calcium release, calmodulin activation, and finally the activation of a protein kinase named Akt (protein kinaseB). Shear stress activates at least two other cascades; one involves endothelial cell membrane hyperpolarization, which leads to an increased calcium influx. β–agonists also activate eNOS although a separate pathway that involves generation of cAMP and activation of A-kinase. Stimulation with calcium ionophore, A23187 leads to receptor-independent activation of eNOS. Activated eNOS hydrolyses the nitrogen atom of the guanidino group of L-arginine to produce NO. Once synthesised NO diffuses to underlying smooth muscle cells. The major physiological target enzyme for NO is soluble guanylyl cyclase (sGC). sGC is activated once NO binds to its haem moiety and converts guanosine triphosphate (GTP) to cyclic guanosine monophosphate (cGMP). This subsequently induces calcium efflux from the smooth muscle cell causing vasodilatation. NO, nitric oxide; PI3K, phosphoinositol 3 phosphate kinase; IP_3, inositol triphosphate; A-kinase, adenylate kinase; p-eNOS, phosphorylated endothelial nitric oxide synthase; B2, bradykinin 2 receptor; BK, bradykinin; NK, neurokinin receptor; SP, substance P; M, muscarinic receptor; Ach, acetylcholine; β2, β2 receptor; Epi, epinephrine; Gs, G-stimulatory protein. SSS GP, shear stress sensing glycoprotein; CAT-1, cationic amino acid transporter-1. Adapted from Maxwell *et al.* 2002 (Maxwell, 2002) with modifications.

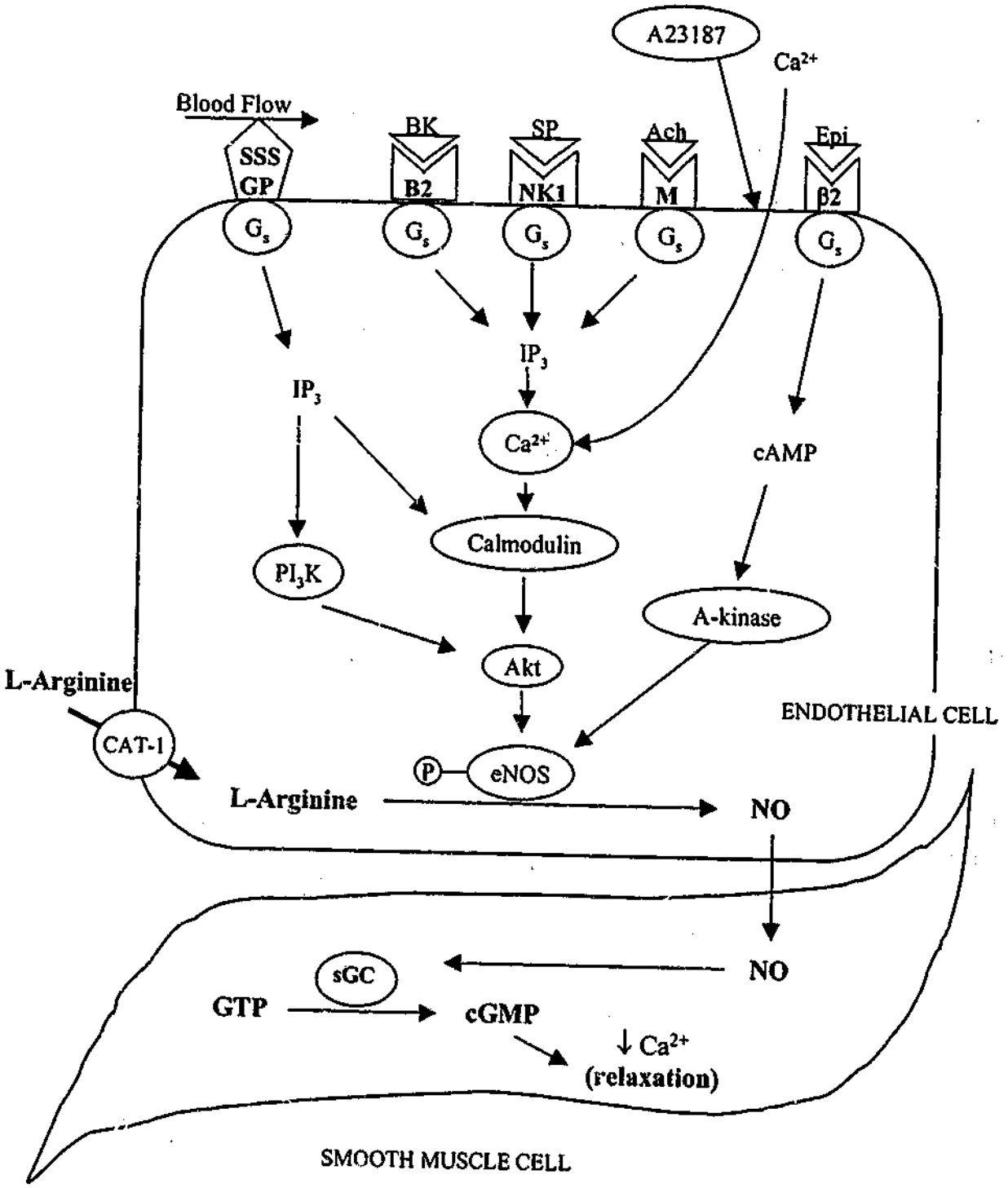

Figure 1.1 **Endothelium-dependent relaxation mediated through the stimulated production of NO.**

the endothelium. Vascular tone is maintained through the endogenous synthesis and release of vasodilator (resulting in dilation of blood vessels), and vasoconstrictor (resulting in constriction of blood vessels) agents by endothelial cells in response to chemical and humoral mediators (Table 1.1). It has also become evident that the role of NO in maintaining endothelium function is of major relevance to cardiovascular disease. Thus, an ongoing and considerable research effort is currently focused on acquiring a better knowledge of the regulatory mechanisms involved in its production, release and bioavailability.

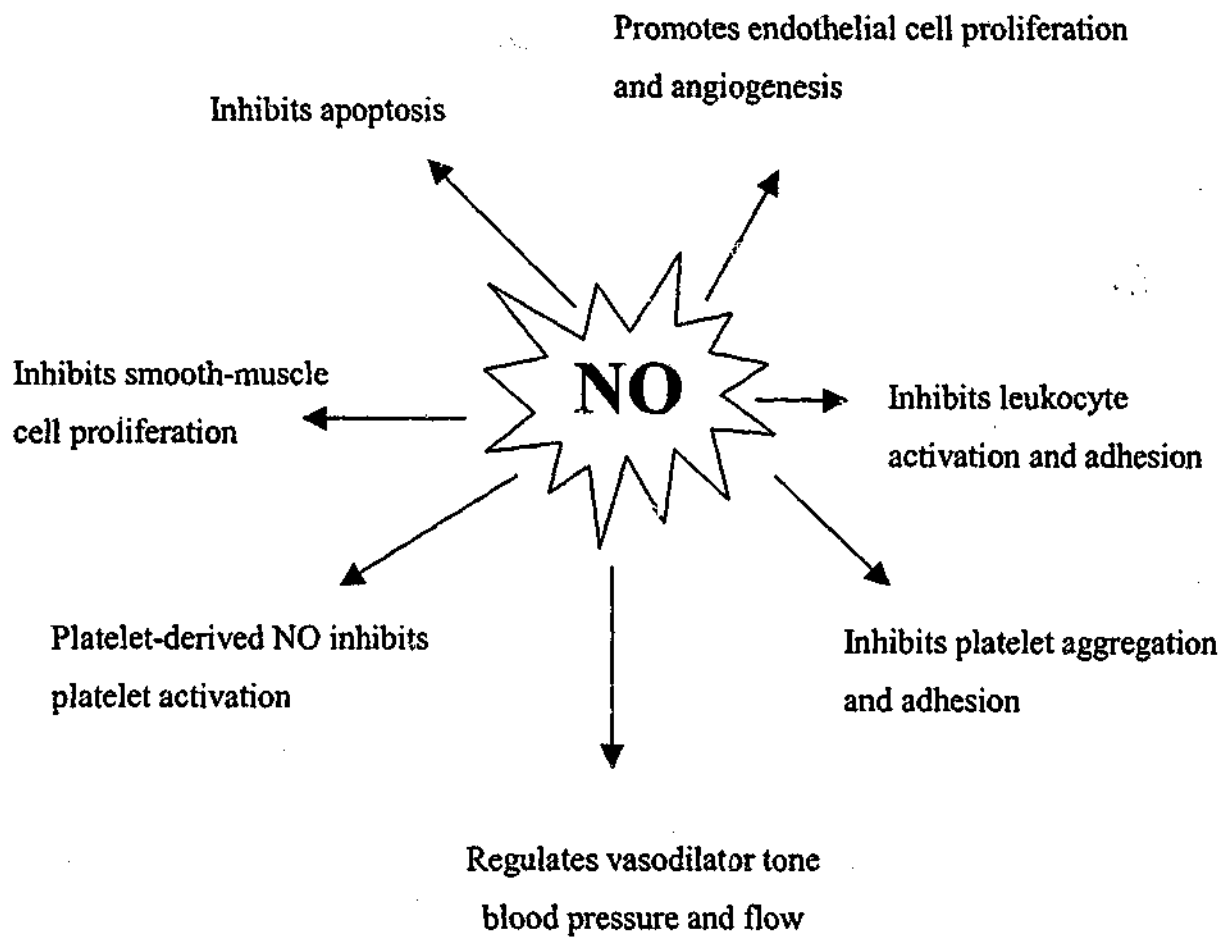

Figure 1.2. Important and beneficial actions of NO in the cardiovascular system. Created from Moncada *et al.* (Moncada and Higgs, 1993).

Table 1.1 Factors released from endothelial cells.*

Vasoactive factors	
Vasodilator	*Vasoconstrictors*
Nitric oxide	Endothelin-1
Endothelium-derived hyperpolarizing factor	Angiotensin II
Prostacyclins, PGI_2	Thromboxane A_2
Natriuretic peptide	Prostaglandin H_2
	Superoxide radicals
	Peroxynitrite, $ONOO^-$
	Hydroxyls, OH^-
Hemostasis and thrombolysis	
Procoagulant, prothrombotic factors	*Anticoagulant, thrombolytic factors*
von Willebrand factor	Tissue factor plasminogen activator
Plasminogen activator inhibitor	Tissue factor pathway inhibitor
Platelet activator	Nitric oxide
	Prostacyclin, PGI_2
	Protein S
Endothelial cell growth modulators	
Promoters	*Inhibitors*
Tumor necrosis factor-α	Nitric oxide
Superoxide radicals	Prostacyclin, PGI_2
	Natriuretic peptide
Inflammatory agents	
Promoters	*Inhibitors*
Tumor necrosis factor-α	Nitric oxide
Superoxide radicals	
Peroxynitrite, $ONOO^-$	

* Adapted from Nilius *et al.* 2001 (Nilius and Droogmans, 2001).

1.3 L-Arginine – Nitric Oxide Pathway

Discovery of NO as the endothelium-derived relaxing factor led to subsequent identification of the enzyme, nitric oxide synthase (NOS), which is capable of generating NO and L-citrulline from its amino acid substrate precursor L-Arginine (L-Arg)(Palmer *et al.*, 1988). The enzyme, NOS, was first isolated and purified in 1990 by Bredt and Snyder (Bredt and Snyder, 1990). The metabolic route by which NO can be synthesised from L-Arg is commonly referred to as the 'L-Arginine-nitric oxide pathway'.

1.3.1 Nitric Oxide Synthases

The synthesis of NO from L-Arg is catalysed by a family of isoenzymes, the nitric oxide synthases. Each NOS isoform type possesses the same structural and binding domains as depicted in Figure 1.3. Although they share structural homology (Sessa, 1994), NOS isoforms are encoded by different genes located on different chromosomes and all have different regulation patterns. Type I NOS (NOS1 or nNOS) is a soluble Ca^{2+}/calmodulin-dependent enzyme (Schmidt and Murad, 1991), located on human chromosome 12, which has been found to be constitutively expressed in neurons (Forstermann *et al.*, 1990). Type II NOS (NOS2 or iNOS) is an inducible isoform, located on human chromosome 17 and found in various cell types, including macrophages (Stuehr *et al.*, 1991) and smooth muscle cells (Koide *et al.*, 1994). Type III NOS (NOS3 or eNOS) is also a constitutively expressed enzyme (Forstermann *et al.*, 1994), located on human chromosome 7 and first identified in endothelial cells (Forstermann *et al.*, 1991, Pollock *et al.*, 1991). The nomenclature nNOS, iNOS and eNOS identify the isoforms based on the cell type they were originally identified in (neuronal, immunocyte and endothelial). It has become clear however, that these isoforms have a wider tissue distribution then what was originally ascribed. For example nNOS is also expressed in skeletal muscle, iNOS expression has been detected in many tissues and, eNOS has been discovered in an array of cell types including cardiomyocytes, blood cells,

trophoblasts, neurons, fibroblasts (Li *et al.*, 2002). This same nomenclature based on the original cellular identification of NOS isoforms will be utilised in this review.

1.3.2 Endothelial NO Synthase; eNOS

Production of NO in the vasculature is largely mediated by eNOS and, and is regulated by changes in eNOS enzymatic activity and/or eNOS gene expression. Active regulation of eNOS and thus NO availability in response to both physiological and pathophysiologic stimuli is a fundamental property of the normal vasculature. The major role of eNOS as an important systemic vasodilator and for cardiovascular function has now been firmly established through the use of eNOS knockout mice developed by several groups (Huang *et al.*, 1995, Gregg *et al.*, 1998, Godecke *et al.*, 2001). Homozygous eNOS knockout mice are hypertensive, lack NO/endothelium-dependent vasodilator capacity, are susceptible to stroke in ischemia models and exhibit increased neointimal proliferation. Heterozygous eNOS knockout mice, which only carry one allele for the gene, have been shown to exhibit exercise intolerance, a characteristic feature of heart failure (Section 1.4.3).

1.3.2.1 eNOS Catalysis

As depicted in Figure 1.3, eNOS protein consists of multiple domains including an N-terminal oxygenase domain and a C-terminal reductase domain, connected by a calmodulin (CaM) binding amino acid recognition sequence (Hemmens and Mayer, 1998). The core region of the oxygenase domain binds L-Arg, tetrahydrobiopterin (BH_4) and heme and, is the active site where NO synthesis takes place (Sessa *et al.*, 1992). The reductase domain binds flavin adenine dinucleotide (FAD), flavin mononucleotide (FMN), nicotinamide adenine dinucleotide phosphate (NADPH) (Pollock et al., 1991).

Calmodulin plays a critical role in activating NOS because its binding is the primary catalyst for the reaction to occur. Initially, a rise of intracellular Ca^{2+} causes its binding to and subsequent activation of calmodulin. The activated Ca^{2+}-calmodulin complex then binds to the calmodulin-

binding domain on eNOS and catalyses the conversion of L-Arginine to NO. During NO synthesis, calmodulin binding prompts reductase flavins, FAD and FMN, to acquire electrons from NADPH and transfer them to the heme iron. This transfer allows the heme iron to bind to the oxygenase domain, activate molecular oxygen (O_2) and catalyse NO synthesis. During the NOS reaction, the substrate L-Arginine undergoes a stepwise five-electron oxidation forming L-citrulline and NO according to the schematic reaction presented below and also depicted in Figure 1.3.

$$\text{L-Arginine} + O_2 + \text{NADPH} \xrightarrow{\text{NOS}} \text{NO} + \text{L-citrulline} + \text{NADP}^+$$

The product of the NOS reaction, NO, is a small reactive molecule constituted by two atoms of nitrogen and oxygen, and comprises a total of 15 electrons. This odd number implies the presence of an unpaired electron, located in the outer orbital of the electron shell. For this reason, NO is a relatively unstable free radical with a reported half-life of 30 seconds and, can easily diffuse through membranes (Lancaster, 1994). In the absence of L-Arg, eNOS can utilise O_2 to produce superoxide anions (Vasquez-Vivar et al., 1998). Superoxide anions produced by eNOS in the absence of substrate and essential co-factors have been implicated as a potential contributor to the adverse vascular effects of oxidative stress in certain pathophysiological states (Section 4.4.1).

1.3.2.2 Regulation of eNOS activity

Under physiological conditions, the vasodilatory action of NO generated by constitutively active eNOS contributes to the control of basal and stimulated regional blood flow in humans (Vallance *et al.*, 1989, Quyyumi *et al.*, 1995). Physiologically, the most important determinant for the continuous generation of NO by eNOS and thus the regulation of local blood flow are mechanical, fluid shear stress and pulsatile stretch (Busse and Fleming, 1998). NO-mediated vasodilation in response to such physical stimuli is the underlying mechanism responsible for flow-mediated vasodilatation (Drexler, 1999a). Ion channels identified on the surface of endothelial cells that are responsive to increased stretch and flow are thought to be involved in shear stress-stimulated NO

production as well as shear stress sensing glycoproteins (Figure 1.1). Shear stress has been shown to modulate eNOS activity both posttranslationally through phosphorylation-dependent mechanisms (Boo *et al.*, 2002) and also by changes in gene expression (Silacci *et al.*, 2000).

A number of endogenously released biochemical and hormonal vasodilator agents including acetylcholine, substance P, adenosine diphosphate, serotonin, thromboxane, and bradykinin are able to stimulate eNOS activity through their respective receptors on the endothelial cell membrane. The activity of eNOS is acutely modulated by these agents through the changes of intracellular Ca^{2+}/calmodulin levels and second messenger intermediates such as cyclic adenosine monophosphate (cAMP) and inositol-1,4,5-trisphophate (IP_3) (Figure 1.1). Receptor-mediated activation of endothelial cells by vasodilator agents generally causes an increase in intracellular Ca^{2+} concentration, which follows depolarisation and activation of voltage-gated Ca^{2+} channels.

The majority of eNOS is reported to be membrane-associated and is predominantly located in caveolae (Busconi and Michel, 1993). Caveolar structures are visualised by electron microscopy as flask-shaped invaginations of the plasma membrane and, serve as specialised compartments for integrating and modulating an array of signalling events at the cell surface. Compartmentalisation in the caveolae facilitates active protein-protein interactions and, Ca^{2+}- and phosphorylation-dependent signal transduction events that modifies eNOS activity (Figure 1.4). Palmitoylation is an essential modification necessary for eNOS targetting to the caveolae (Garcia-Cardena *et al.*, 1996b). The caveolin type 1 isoform, caveolin-1, is the major structural protein of the caveolae and has been shown to co-immunoprecipitate with, and thus, directly interact with eNOS (Garcia-Cardena *et al.*, 1996a). Interaction of caveolin with eNOS occurs via a specific caveolin scaffolding domain located on the former protein (Garcia-Cardena *et al.*, 1997). Association of caveolin negatively regulates eNOS by inhibiting its activity (Ju *et al.*, 1997). In support of this, recent studies have confirmed an enhanced endothelium-dependent vasodilator response in caveolin-1 knockout mice (Drab *et al.*, 2001, Razani *et al.*, 2001).

A

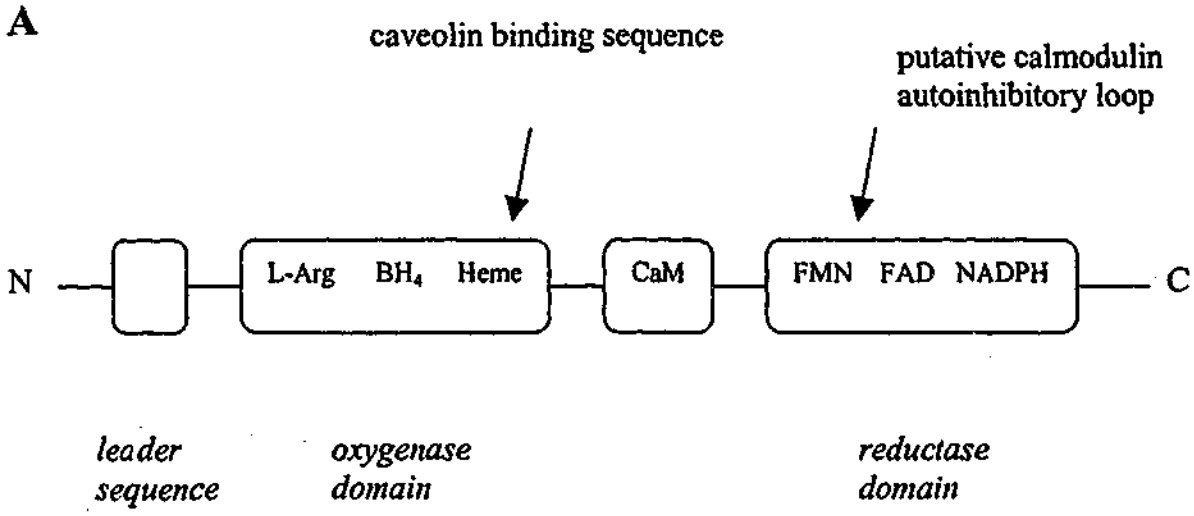

B

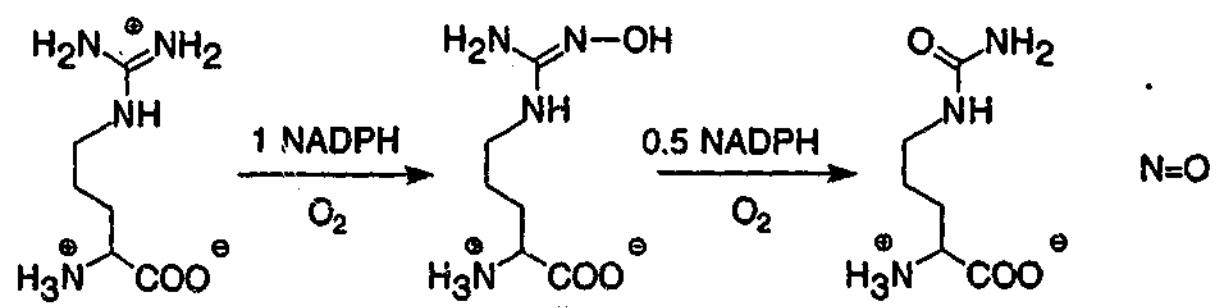

Figure 1.3 A. Domain arrangement in bovine eNOS. A) The structural organisation of nNOS and iNOS are similar to eNOS except that nNOS contains an extensive leader sequence and that the iNOS reductase domain is missing the calmodulin autoinhibitory loop. **B)** Enzyme-catalysed NO synthesis from L-Arg. Hydroxylation of L-Arg generates N-hydroxyarginine (NOHA) as an intermediate. The second step converts NOHA to the products NO and L-citrulline. Figures both adapted and modified from Stuehr *et al.* (Stuehr, 1999)

Receptor mediated increases in intracellular Ca^{2+} by vasodilator agents promotes binding of calmodulin to eNOS and dissociation of eNOS from caveolin-1 (Feron *et al.*, 1998). Thus, the inhibitory conformation of eNOS with caveolin can be reversed by an activated Ca^{2+}/calmodulin complex.

Myristylation at the N-terminal glycine (Pollock *et al.*, 1992, Sessa et al., 1992) and palmitoylation (Robinson *et al.*, 1995) are unique characterisitics of the eNOS isoform. These properties play a key role in the anchorage of eNOS to the plasma membrane. Myristylation of eNOS occurs during translation and is irreversible, whereas palmitoylation occurs post-translationally and is readily reversible. Association of Ca^{2+} with calmodulin after agonist-induced activation initiates the depalmitoylation of eNOS (Prabhakar *et al.*, 1998) and enables the enzyme to translocate away from the plasma membrane to an intracellular compartment.

Although eNOS was traditionally classified as a Ca^{2+}-dependent enzyme, more recent evidence has shown that Ca^{2+} is not always required for eNOS activity. eNOS activity can also be stimulated through a Ca^{2+}-independent pathway (Fulton *et al.*, 2001). Ca^{2+}-independent pathways involving the phosphorylation of eNOS such as that induced by protein kinase B (Akt), can also disrupt the inhibitory association of caveolin and promote eNOS activation (Goligorsky *et al.*, 2002). Phosphorylation of eNOS (bovine) by Akt at serine 1179 enhances eNOS activity by increasing reductase domain activity and also by reducing calmodulin dissociation from activated eNOS in the absence of a raised intracellular Ca^{2+} level (McCabe *et al.*, 2000). An attenuated endothelium-dependent vasodilation in response to acetylcholine in rabbit femoral arteries transduced with, and expressing a dominant negative form of Akt provides further evidence for a role of phosphorylation in eNOS activation (Luo *et al.*, 2000). Phosphorylation in response to various stimuli has also been demonstrated at other sites on eNOS (Fulton et al., 2001).

Additionally, there is evidence for a role of other interacting proteins such as the molecular chaperonin hsp90, and cytoskeletal-associated dynamin, as mediators of eNOS-signalling pathways

(Latchman, 2001). Hsp90 has been shown to bind to eNOS and enhance its activity (Garcia-Cardena *et al.*, 1998). This chaperonin has been shown to facilitate the actions of calmodulin in dissociating caveolin from eNOS (Gratton *et al.*, 2000). Geldanamycin, a specific inhibitor of Hsp90 signalling, has been shown to attenuate acetylcholine-dependent vasodilation in the vasculature of healthy animals but does not prevent vasodilation in response to an endothelium-independent vasodilator, sodium nitroprusside. Recent studies performed in pulmonary artery endothelial cells also suggest that the polymerisation state of the microtubule cytoskeleton can also regulate NO production and eNOS activity in by altering the binding of hsp90 to eNOS (Su *et al.*, 2002).

1.3.2.3 Regulation of eNOS Gene Expression

eNOS activity can be modulated by changes in its gene expression pattern and is known to be regulated both at the transcriptional and posttranscriptional level (Fleming and Busse, 2003). Induction of eNOS gene expression can occur though multiple stimuli such as increased shear stress exercise, proliferation and cell growth, growth factors (such as TGF-β, FGF, VEGF, or PDGF), hormones (such as estrogens, insulin, angiotensin II, or endothelin-1), cytokines and bacterial lipopolysaccharide. For example, various experimental studies have demonstrated an increase in eNOS mRNA levels in cultured endothelial cells exposed to artificial shear stress (Nishida *et al.*, 1992, Noris *et al.*, 1995, Silacci et al., 2000). Increased eNOS mRNA expression and activity in the arterial wall of rats has also been demonstrated *in vivo* by using an experimental model of blood flow and volume overload to chronically increase blood flow and shear stress (Nadaud *et al.*, 1996).

However, some stimuli are also known to downregulate eNOS gene expression. For example, hypoxia has been shown to decrease eNOS mRNA and protein expression in pulmonary endothelial cells (McQuillan *et al.*, 1994) and, impair endothelium-dependent dilation in pulmonary artery preparations (Murata *et al.*, 2001). Bacterial lipopolysaccharide downregulates eNOS mRNA expression in cultured endothelial cells (Lu *et al.*, 1996) and *in vivo* (Liu *et al.*, 1996). Interestingly,

NO itself has been shown to downregulate eNOS mRNA expression in the systemic circulation (Vaziri and Wang, 1999). Although, by contrast, NO has been shown to upregulate eNOS mRNA in the pulmonary circulation (Chen *et al.*, 2001).

The stability of eNOS mRNA can also be regulated by multiple stimuli, including those which are also shown to regulate eNOS gene expression. A few studies have demonstrated that TNF-α decreases eNOS mRNA half-life and thus reduces eNOS protein expression and activity in cultured endothelial cells (Yoshizumi *et al.*, 1993, Aberle *et al.*, 1997). Preliminary evidence has linked an increase in the binding of cytosolic proteins to the 3'-untranslated region of the eNOS mRNA with a decrease in eNOS stability in TNF-α treated endothelial cells (Sanchez de Miguel *et al.*, 1999) and also hypercholesterolemic rabbits (Jimenez *et al.*, 2001). Other stimuli known to target eNOS mRNA stability include statins, thrombin, Rho GTPases, actin cytoskeleton, VEGF, oxidized LDL (oxLDL), glucocorticoids, hypoxia and the proliferation status of the cell (Li et al., 2002).

Figure 1.4 Proposed model for eNOS post-translational activation. Top panel represents myristoylated and palmitoylated membrane-bound eNOS under basal condition (less active). eNOS is associated with caveolin-1 and the fourth intracellular domain of the bradykinin (BK) receptor. Also, under basal conditions, a population of eNOS is thought to be associated with heat shock protein 90 (hsp90). Mitogen-activated protein kinase and protein kinase C (PKC) have been proposed to phosphorylate eNOS, which renders it less active. Endothelial cell stimulation by various stimuli (bottom panel) activates eNOS through its association with Ca^{2+}-activated calmodulin (CaM). Whether, i) CaM is always bound and small changes in Ca^{2+} determine Ca^{2+}-CaM dependence, ii) more CaM is recruited to eNOS by large fluxes in cytoplasmic Ca^{2+} or, iii) how phosphorylation influences the Ca^{2+}/CaM requirements of the enzyme *in situ* is not known. However, the actions of CaM are thought to be facilitated by the recruitment of hsp90 to eNOS and from the dissociation of eNOS from caveolin. BK receptor activation promotes dissociation of eNOS from the receptor, thus lifting its inhibitory effect. Both Ca^{2+}-dependent and -independent stimuli have been shown to induce phosphorylation of serine 1177/1179 eNOS. Phosphorylation of this residue by Akt, protein kinase A (PKA), or AMP-dependent kinase (AmpK) is associated with increased enzyme activity. Other proteins have been shown to be associated with increased eNOS activity or NO release such as dynamin (Dyn). The role of nitric oxide synthase-interacting protein (NOSIP) is less clear, but over-expression of this protein mislocalises eNOS. Taken from Fulton *et al.* 2001 (Fulton *et al.*, 2001).

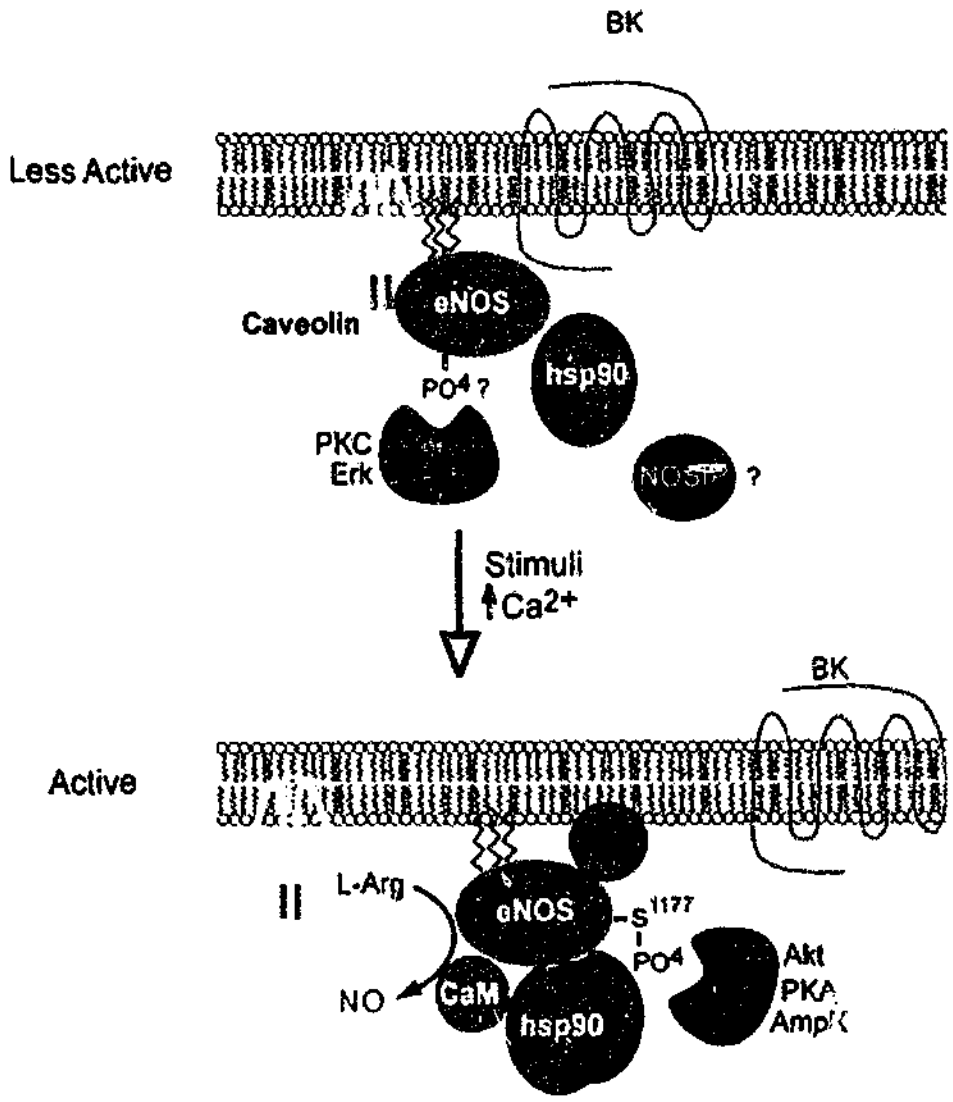
BK
Less Active
eNOS
Caveolin
hsp90
PO4 ?
PKC
Erk
NOSP ?
Stimuli
↑Ca2+
BK
Active
L-Arg
gNOS
S1177
PO4
Akt
PKA
AmpK
NO
CaM
hsp90

1.4 Endothelium Dysfunction

Endothelium function is defined by systemic and local humoral factors, and, by mechanical force generated by the flow of blood. These properties can vary depending upon the local vascular bed stimuli and also its geometry. Endothelial cells line the innermost layer of blood vessels within the arterial and venous circulation of the cardiovascular system and, are located within in all arteries, veins and chambers of the heart. The vascular endothelium, a single cell layer thick, forms a continuous interface between blood and the underlying vessel wall through its tight cell junctions. Due to this locality the endothelium can interact with components of the blood, underlying smooth muscle cells, and extracellular matrix. Although the major role of the endothelium is the maintenance of vascular tone, other roles of the endothelium include the regulation of blood viscosity, coagulation and thrombosis (Vapaatalo and Mervaala, 2001).

The vascular endothelium has been demonstrated to play a pivotal role in the pathogenesis of inflammation, neovascularisation, immunological responses, vascular injury and repair, thrombosis and atherosclerosis. A decline in endothelium function has been implicated as a major contributory factor to the development and/or progression of cardiovascular disorders such as heart failure, hypertension, hypercholesterolemia and diabetes mellitus. The mechanism(s) responsible for an associated decline in endothelium function is not clearly understood. However, an imbalance in the release of various factors by the endothelium (Table 1.1)(Quyyumi, 1998) is thought to contribute to this dysfunction.

In particular, a decline in endothelial NO bioavailability is thought to play a central role in this process (Arnal *et al.*, 1999). During the last two decades it has become apparent that a variety of pathologies are associated with an impairment of endothelium-dependent NO activity. Impaired endothelium-dependent NO activity is observed in blood vessels by an attenuated endothelium-dependent vasodilation in response to NO agonists such as acetylcholine. This is a characteristic feature of endothelial dysfunction. This phenomenon has been found in cardiovascular pathologies

such as atherosclerosis, hypertension, diabetes, hypercholesterolemia, and heart failure. Additional risk factors including obesity, aging, and cigarette smoking can lead to the development of endothelial dysfunction and are also classified as risk factors for the development of cardiovascular disease. The mechanisms underlying altered endothelium-dependent vascular relaxation these various cardiovascular complications are multifactorial. Hence, a current and major challenge in the field of vascular biology is to acquire a better knowledge of the aetiology of endothelium dysfunction. The functional implications of endothelial dysfunction in cardiovascular disease are not well defined, but recent clinical trials have suggested that endothelial dysfunction may affect vascular tone and organ perfusion particularly during stress situations such as exercise. This makes it relevant for diseases such as heart failure, which is characterised by exercise intolerance. Moreover, endothelial dysfunction may represent an early event in the development of cardiovascular diseases such as arteriosclerosis (McVeigh and Cohn, 2003). Therefore, numerous clinical studies have focused on the restoration or improvement of endothelial function using interventions such as L-Arg supplementation, lipid lowering therapy, antioxidants, ACE inhibitors and exercise regimes.

1.4.1 Definition

Cardiovascular diseases and cardiovascular risk factors are associated with impairment in endothelium-dependent vasodilation that seems to be mediated by vasodilators such as nitric oxide and prostacyclin (Drexler and Hornig, 1999). The term 'endothelium dysfunction' is mostly used in the scientific literature to label this type of alteration of vascular endothelial function but, by definition can also include an impairment of other important regulatory processes which the endothelium regulates under normal conditions. Thus, endothelial dysfunction can be generalised to include a dysfunctional regulation of vasodilator tone, dysfunctional control of the balance between anti-coagulant fibrinolysis and thrombosis, dysfunctional control of the inflammatory response, and a dysfunctional regulation of growth of the vascular smooth muscle (Quyyumi, 1998). The use of NO agonists and inhibitors of its production has led to the discovery that NO-

mediated vasodilation is abnormal in many cardiovascular disorders such as heart failure, diabetes, hypertension and hypercholesterolemia (Mombouli and Vanhoutte, 1999). Thus, endothelial dysfunction usually refers to the impairment in endothelium-dependent relaxation that is due to a decrease in NO bioavailability. An enhanced production of endothelium-derived vasoconstrictors may also lead to endothelial dysfunction. An increase in vasoconstrictor action has been reported in various pathophysiological states, particularly in the small resistance vessels and presents an alternative mode of dysfunction separate from that attributed to a reduced capacity of vasodilators (Drexler and Hornig, 1999).

1.4.2 Identification

Endothelium dysfunction is commonly identified in whole animals or individuals by an impaired relaxation of the blood vessel to endothelium-dependent vasodilators such as acetylcholine, serotonin, thrombin and substance P, whilst endothelium-independent relaxation mediated by sodium nitroprusside or glycerol trinitrate is usually preserved (Quyyumi, 1998). Acetylcholine is the most common agent used *in vivo* to assess endothelial function and the release of endothelium-derived NO in humans. N-mono-methyl-L-Arg (L-NMMA), a specific inhibitor of NO synthesis which decreases forearm blood flow by inhibiting the basal release of NO, is also commonly used to assess the contribution of NO to vasodilation in different vascular beds (Quyyumi, 1998).

The NO-mediated vasodilator function of the endothelium is widely studied as a test of endothelial integrity and function in patients with cardiovascular disease. Impaired basal and muscarinic-agonist stimulated components of NO-mediated vascular tone have been found in human coronary, forearm and cutaneous resistance vessels and in coronary and forearm conduit vessels in a many of these diseases (Drexler and Hornig, 1999, Elkayam *et al.*, 2002). The detection of alterations in endothelial function prior to the development of cardiovascular disease has led to the speculation that endothelial dysfunction may significantly contribute to the development of cardiovascular diseases. Impaired vasorelaxation within the coronary artery tree for example has been recognised

before the development of obstructive coronary artery disease (Herrmann and Lerman, 2001). The correlation of endothelial dysfunction with the severity of some cardiovascular diseases also indirectly suggests that it may also play a role in the progression of the disease (Bank *et al.*, 2000, Hayakawa and Raij, 1997, Fang and Marwick, 2002).

1.4.3 Endothelium Dysfunction in Congestive Heart Failure (CHF)

Clinical symptoms and characteristics of congestive heart failure (CHF) include abnormalities of left ventricular (LV) function and neurohormonal regulation, which are accompanied by increased peripheral resistance, exercise intolerance, fluid retention, and decreased longevity (Sullivan and Hawthorne, 1995, Chiariello and Perrone-Filardi, 1999, Opie, 2002). The prevalence of this disease and its implications for the public health are now widely recognised. Prescribed treatments addressing neurohormonal disturbances such as activation of the sympathetic nervous system, stimulation of the renin-angiotensin system, increased activity of the endothelin system, increased production of norepinephrine, and increased circulating levels of cytokines have improved the outcomes of patients, but the prognosis remains dismal (Braunwald and Bristow, 2000, Mak and Newton, 2001). Endothelial dysfunction is also a characteristic feature of CHF and, a number of studies have demonstrated an association between heart failure and endothelial dysfunction (Carville *et al.*, 1998, Bank *et al.*, 1994). Also, a correlation exists between decreased endothelial function and increased severity of CHF (Fang and Marwick, 2002). The clinical implications of endothelial dyfunction in CHF are somewhat unclear. This condition may lead to decrease in organ perfusion, impairment of exercise capacity, and progression of the disease (Elkayam et al., 2002). Therefore, in addition to other conventional treatment regimes, a further exploration of the association between heart failure and endothelial dysfunction may be relevant for a new therapeutic approach in the treatment of heart failure.

Heart failure is thought to be a causal factor in the development of endothelial dysfunction. Although, it is unknown whether endothelial dysfunction results from heart failure or if it results

from a predisposing risk factor for the devlopment of heart failure such as coronary artery disease (Gielen *et al.*, 2002). The pathophysiology of endothelial dysfunction has been associated with increased oxidative stress, abnormal regional flow conditions (eg. decreased peripheral blood flow) and, cytokine and neurohormonal activation (eg. increased angiotensin converting enzyme (ACE) activity) (Katz, 1997). These changes are thought to participate in the development of endothelial dysfunction through the reduction of NO synthesis and release, or, through the increased degradation of NO and increased production of endothelin-1 (Figure 1.5) (Fang and Marwick, 2002).

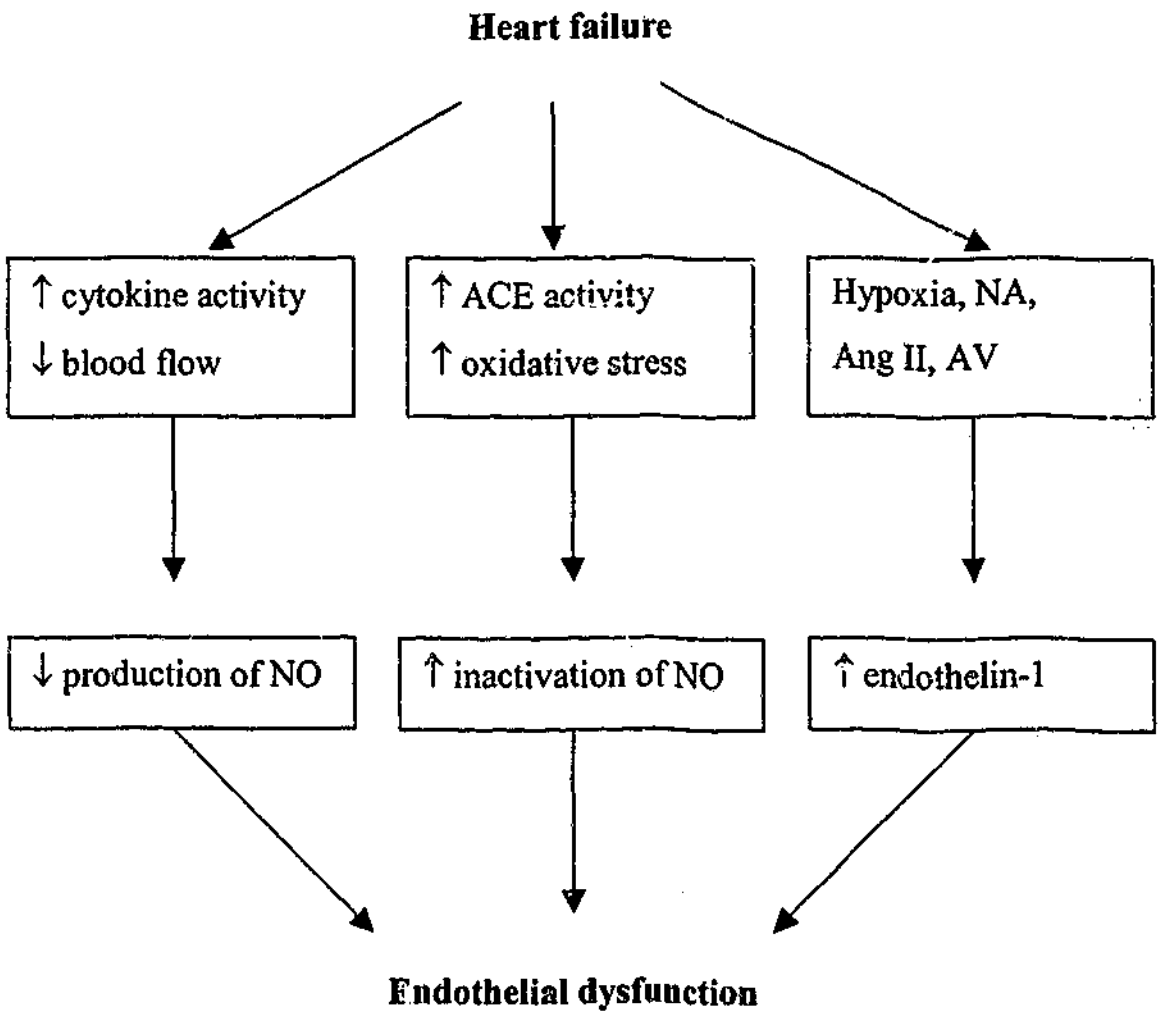

Figure 1.5. Effects of heart failure on endothelial dysfunction. Up arrow, increase; down arrow denotes decrease; NA, noradrenaline; Ang II, angiotensin II; AV, arginine vasopressin. Figure taken from Fang *et al.* (Fang and Marwick, 2002).

Endothelial dysfunction has both peripheral and central actions on the failing heart. These effects may contribute to the progression of heart failure. Under normal conditions the endothelium controls distensibility in large arteries as well as small arteries and arterioles but, this mechanism is impaired in chronic heart failure (Arnold *et al.*, 1991, Nichols and Edwards, 2001). Increased arterial stiffness and reduced compliance resulting from this impairment can lead to increased left ventricular (LV) end-systolic stress, LV dilatation, and failure (Nichols and Edwards, 2001). Increased levels of the vasoconstrictor endothelin-1, due to endothelial dysfunction, can cause increased systemic resistance and increased afterload (Sutsch and Barton, 1999). Additionally, endothelin-1 is also a mitogenic and hypertrophic agent associated with the growth of vascular smooth muscle cells and the stimulation of matrix production. Therefore, the increased actions of endothelin-1 may lead to vascular remodelling and afterload in heart failure (Laurent *et al.*, 1996). Endothelial dysfunction can also affect the heart through its effect on the function of coronary arteries, and may lead to myocardial ischemia (Woodman, 1999).

Although abnormalities in vascular reactivity have been shown to vary considerably within the vasculature in CHF, evidence of endothelial dysfunction demonstrated by an attenuated endothelium-dependent vasodilation has been repeatedly demonstrated in the peripheral, pulmonary, and coronary circulation in response to vasodilatory agents such as acetylcholine or to changes in blood flow (a stimulus for NO release) (Vanhoutte, 1996). In particular, impaired endothelial function is thought to have a major role in increased peripheral vasoconstriction exhibited in CHF (Table 1.2) (Mendes Ribeiro *et al.*, 2001). A growing body of evidence suggests that impaired endothelium-dependent dilation of peripheral resistance vessels in response to endothelial-dependent vasodilators in CHF is due to decreased NO mediation (Table 1.2) (Ferrari *et al.*, 1998). Abnormalities of endothelial function in CHF are thought to contribute to increased peripheral resistance both at rest and during exercise (Katz, 1995). This may be due to an increased release and effect of vasoconstrictor agents or in parallel, an imbalance between the

release of vasodilator (NO and prostacyclin) and vasoconstrictor (endothelium-derived vasoconstrictor) agents (Vanhoutte, 1996).

1.4.4 Mechanisms of Endothelium Dysfunction in CHF

1.4.4.1 Free Radical Production and Oxidative stress

Existing evidence supports a significant role for vascular oxidative stress in the development of endothelial dysfunction in CHF (Mak and Newton, 2001). Major risk factors for the development of heart failure such as coronary artery disease, atherosclerosis and hypertension are also associated with an increase in vascular oxidative stress and are usually accompanied by a decrease in the antioxidative properties of the vascular wall. Increased formation of reactive oxygen species (ROS) consisting of highly reactive, partially reduced intermediates of molecular oxygen (O_2) such as the free-radical superoxide anion (O_2^-) and the hydroxyl radical (OH^-) are associated with oxidative stress and subsequent vascular abnormalities. Excess ROS generation and additionally, an impairment of the antioxidant defence system through decreased expression and/or activity of the enzymatic antioxidant superoxide dismutase (SOD) are thought to be major contributors to vascular oxidative stress exhibited in heart failure (Mak and Newton, 2001). Detrimental effects of superoxide produced intracellularly can be significantly enhanced due to its membrane impermeable nature (because of its negative charge), since its distribution and action is localised to the site of production.

The endothelium is capable of generating substantial amounts of ROS from various sources including nicotinamide adenine dinucleotide/ nicotinamide adenine dinucleotide phosphate (NADH/NADPH) oxidase (Gorlach *et al.*, 2000), xanthine oxidase (Landmesser *et al.*, 2002), cyclooxygenases, NOS (Vasquez-Vivar et al., 1998) and, side products resulting from the mitochondrial respiratory chain under certain conditions (Mak and Newton, 2001). In fact, studies by Landmesser et al. (Landmesser et al., 2002) have indicated that both increased extracellular xanthine-oxidase and reduced extracellular SOD activity, a superoxide scavenger, are closely

associated with increased vascular oxidative stress in patients with chronic heart failure. Pharmacological inhibition of the ROS generating enzyme, NAD(P)H oxidase, has been shown to decrease production of ROS and improve endothelial function in human blood vessels from patients with coronary artery disease (Hamilton *et al.*, 2002).

eNOS can utilise molecular oxygen as a principal substrate to produce superoxide anions when the cellular supply of required co-factors such as BH_4 or substrate, L-Arg, becomes limiting (Vasquez-Vivar et al., 1998). A shift in NOS activity to superoxide formation results in decreased bioavailability of NO by two possible mechanisms. The first is via a direct reduction of NO formation due to a reduced amount of substrate and co factor available for NOS conversion. The second is via indirect reduction in NO levels due to the reaction of NO with superoxide to form peroxynitrite.

If superoxide is formed in the presence of NO then the two react rapidly to form peroxynitrite ($ONOO^-$) (Figure 1.6). Under phyiological conditions, SOD present in the vascular wall is in adequate concentrations to outcompete NO for the formation of peroxynitrite. By constrast, in pathophysiological conditions associated with reduced SOD acitivity (Landmesser et al., 2002) or pathologic levels of NO formed by iNOS can favour the production of peroxynitrite since the rate of superoxide association with NO is faster than with SOD (Figure 1.6) (Gewaltig and Kojda, 2002). Formation of peroxynitrite decreases NO availability and leads to impaired endothelium-dependent vasodilation (Hayashi *et al.*, 1999). Excessive production of peroxynitrite also causes increased platelet aggregation and smooth muscle proliferation (Gewaltig and Kojda, 2002), additional markers of endothelial dysfunction . Additional to its diminishing effect on NO availability, peroxynitrite is a powerful oxidant that can cause further vascular injury through its modulation of various cellular processes. Peroxynitrite nitrates protein tyrosine residues (Ischiropoulos *et al.*, 1992), shears DNA strands (Szabo *et al.*, 1996), affects the intracellular Ca^{2+} homeostasis (Viner *et al.*, 1996), induces lipid peroxidation (Violi *et al.*, 1999), and depletes endothelial glutathione via protein kinase C activation (Phelps *et al.*, 1995).

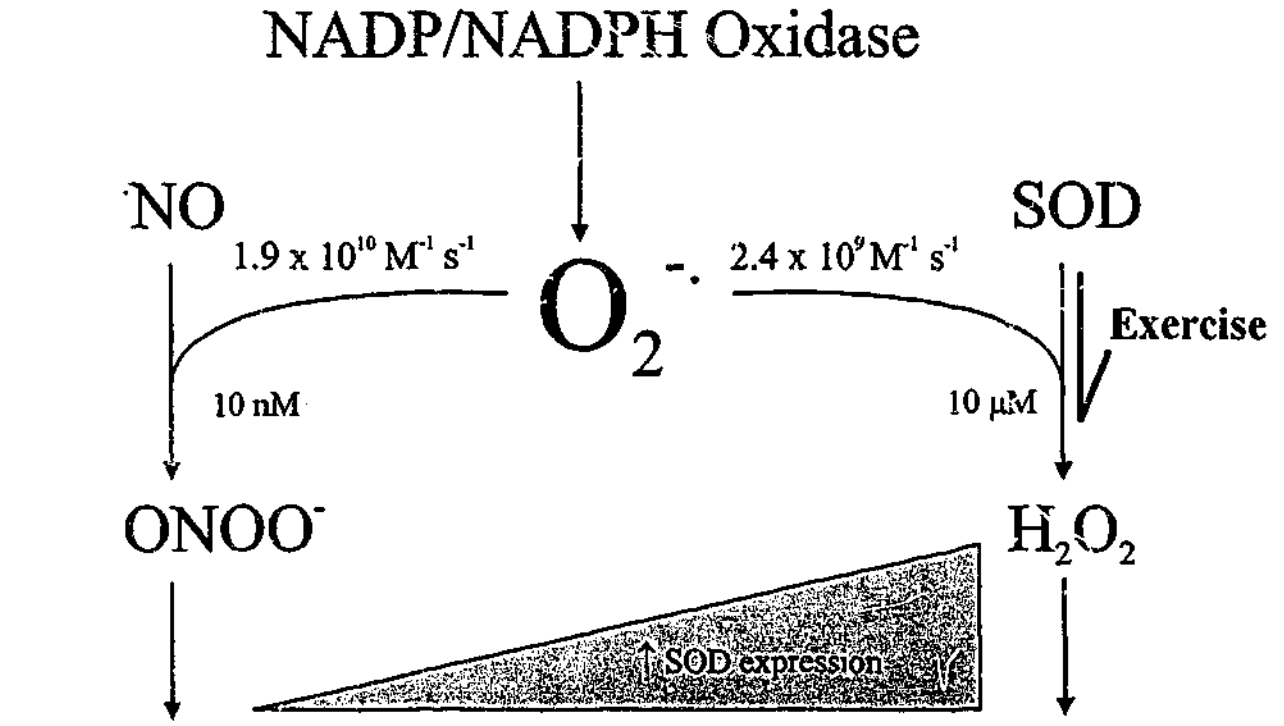

Figure 1.6. Reactions of superoxide with NO and superoxide dismutase (SOD). The reaction constants and the mean concentrations of SOD and NO in the vascular wall suggest the formation of hydrogen peroxide is favoured under physiological conditions. An increase of SOD expression induced by exercise and NO is expected to shift the balance to hydrogen peroxide formation. Both vasoprotective and proatherosclerotic actions of hydrogen peroxide have been reported. Pathophysiological states which lead to high concentrations of NO such as that generated by iNOS or alternatively a decreased SOD activity favour the formation of pexoxynitrite. Figure adapted from Gewaltig *et al.* 2002 (Gewaltig and Kojda, 2002).

1.4.4.2 NOS expression and activity

Reduced NO formation due to reduced eNOS expression and/or activity may contribute to endothelial dysfunction in CHF (Table 1.2). Although eNOS is constitutively expressed within the endothelium, its expression is subject to modulation by various factors which are all relevant in the setting of CHF such as shear stress, atherogenic lipoproteins and cytokines such as TNF-α (Li et al., 2002). A decrease of cardiac output in CHF results in a reduced shear stress on endothelial cells(Vanhoutte, 1996). Since shear stress is an important activator of NOS expression and activity both at rest and during exercise under normal conditions (Fleming and Busse, 2003, Li et al., 2002, Davis *et al.*, 2003), a reduced shear stress in CHF is expected to play a significant role in reduced NO production.

Reduction in eNOS expression due to the effects of increased levels of circulating TNF-α may also contribute to a reduced NO bioavailability in CHF. TNF-α neutralising antibodies have been shown to be beneficial in counteracting the reduction in eNOS expression observed in cultured human cells after treatment with CHF serum (Agnoletti *et al.*, 1999). Yoshizumi *et al.* and others (Yoshizumi et al., 1993, Aberle et al., 1997) have found that TNF-α can decrease eNOS mRNA half-life, eNOS protein expression in cultured human endothelial cells. Treatments which have previously been shown to have beneficial effects on endothelial function such as statin therapy and oestrogen replacement are effective in preventing TNF-α-induced downregulation of eNOS (Sumi *et al.*, 2001, Gonzalez-Fernandez *et al.*, 2001) and preserving NO formation *in vitro*. An unresolved issue is whether or not eNOS expression is actually altered in CHF. A significant decrease in eNOS mRNA and protein as well as basal and stimulated NO production is observed in aortic endothelial cells and the coronary microvasculature of conscious dogs with pacing-induced CHF (Smith *et al.*, 1996, Zhao *et al.*, 1996). In contrast, others have reported unaltered or increased eNOS expression in the ventricular myocardium of failing human hearts and the vasculature (Stein *et al.*, 1998, Bauersachs *et al.*, 1999).

Table 1.2 Modulation of the L-arginine-NO pathway in patients with heart failure.

L-Arg-NO pathway	Reported Change	Summary of findings [a]	Reference[b]
Plasma L-arginine analogues	Increased	↑ L-NMMA plasma concentration in HF	Hanssen *et al.* 1998
	Increased	↑ ADMA plasma concentrations in CHF patients	Usui *et al.* 1998
NO activity,	Increased	↑ Plasma nitrate levels in HF	Winlaw *et al.* 1994
NOS expression,	Increased	↑ Increased vasoconstrictor effect of L-NMMA in HF	Habib *et al.* 1994
Nitrate / nitrite production	Decreased	Administration of L-arg ↓ vascular resistance associated with ↑ of nitrite/nitrate production	Koifman *et al.* 1995
	Decreased	↓ NO release in the coronary circulation in HF	Mohri *et al.* 1997
	Increased	↑ NO_x plasma concentration in HF	Kaye *et al.* 1998
	Increased	↑ NO_x plasma levels in CHF	Usui *et al.* 1998
	Increased/Decreased	↑ Expression of eNOS but not iNOS in the ventricular myocardium of failing hearts	Stein *et al.* 1998
	Increased	↑ Expression of iNOS in skeletal muscle of HF	Reide *et al.* 1998
	Increased	↑ Expression of iNOS in skeletal muscle of HF that was inversely correlated with exercise capacity	Hambrect *et al.* 1998
	Increased	↑ Expression of eNOS and iNOS in the left ventricle endomyocardial of dilated cardiomyopathy	Heymes *et al.* 1999
	Decreased	↓ Urinary nitrates in HF at rest and submaximal exercise	Katz *et al.* 1999
	Increased/Decreased	↑ Expression of iNOS but not eNOS in the ventricular myocardium of failing hearts	Drexler *et al.* 1998
	Increased	↑ Plasma nitrite level in cardiac failure patients	Ramesh *et al.* 1999
	Increased	↑ Plasma nitrite level in HF	Rakhit *et al.* 1999
	Increased	↑Expression of iNOS in myocardium tissue and ↑ serum nitrites/nitrates concentration in patients with idiopathic dilated cardiomyopathy	Orus *et al.* 2000

Table 1.2 Modulation of the L-Arg-NO pathway in patients with heart failure. (Continued)

L-arg-NO pathway	Reported Change	Summary of findings[a]	Reference[b]
Endothelial function	Impaired	↓ Endothelium-dependent relaxation to acetylcholine in the brachial artery of CHF	Drexler *et al.* 1992
	Impaired	↓ Forearm blood flow in HF	Kubo *et al.* 1994
	Impaired	↓ Endothelium-dependent forearm dilation in chronic HF	Takeshita *et al.* 1996
	Impaired	↓ Endothelium-dependent relaxation of internal mammary arteries from HF	Berkenboom *et al.* 1998
	Impaired	Vitamin C ↑ flow-dependent dilation in the radial artery of HF suggesting an ↑ degradation of NO by free radicals in those patients	Hornig *et al.* 1998
	Impaired	↓ Forearm blood flow in HF though not affected by NO inhibition	Maguire *et al.* 1998
	Impaired	↓ Endothelium-dependent vasodilation in response to acetylcholine in internal radial artery was improved by oral L-arginine supplementation and exercise training	Hambrect *et al.* 2000
	Impaired	↓ Forearm blood flow in mild and severe HF	Bank *et al.* 2000

[a] ADMA, asymmetric dimethyl-L-arginine; L-NMMA, N^G-monomethyl L-arginine; NO, nitric oxide; NOS, nitric oxide synthase; iNOS, inducible nitric oxide synthase; eNOS, endothelial nitric oxide synthase; HF, heart failure; CHF, congestive heart failure. Adapted from Table 5, of a recent review by Mendes Ribeiro *et al.* 2001 (Mendes Ribeiro *et al.*, 2001).

[b] Refer to Table 5, Mendes Ribeiro *et al.* 2001 (Mendes Ribeiro *et al.*, 2001) for further details.

A reciprocal role in NO production has been proposed alongside eNOS due to some reports of iNOS induction in CHF (Haywood *et al.*, 1996, Stathopulos *et al.*, 2001). Findings of Ishibashi *et al.* (Ishibashi *et al.*, 2001) indicate that basal NO production in the forearm vasculature of CHF patients is partly mediated by iNOS activation, whereas in normal subjects, it is usually attributed to eNOS activation. Although this may be a compensatory mechanism for reduced eNOS activity, iNOS expression is generally thought to play a pathological role in the progression of CHF (Ikeda and Shimada, 1997). Nitric oxide generated from increased iNOS expression in the failing heart is thought to have negative inotropic actions (Sarkar *et al.*, 2001) and play a role in morphological alterations such as hypertrophy and apoptosis of cardiomyocytes (Drexler, 1999b). Further, iNOS is capable of cytokine-induced pathologic levels of NO production and superoxide generation and is known to cause an attenuation of agonist stimulated endothelium-dependent vasodilation (Mungrue *et al.*, 2002). Therefore, the role of iNOS in endothelial dysfunction is currently unclear.

Pathways regulating eNOS function at the posttranslational level may also play a role in endothelial dysfunction. Protein kinase Akt-dependent phosphorylation of eNOS (bovine) at the serine 1177 and dephosphorylation at threonine 495 residues has been shown to be critical for eNOS activation and subsequent NO release. *In vitro* studies from Chavakis *et al.* (Chavakis *et al.*, 2001) indicate that an oxidised low-density lipoprotein (oxLDL)-induced inactivation of Akt can lead to impaired eNOS activation and subsequent NO release. This may be relevant to the pathophysiology of CHF since plasma levels of oxLDL, an *in vivo* marker of oxidative stress, are correlated with disease severity chronic CHF patients (Tsutsui *et al.*, 2002). Experimental data indicates that an upregulation of caveolin abundance in hypercholestrolemia, a risk factor for the development of heart failure, can contribute to decreased endothelial NO production by promoting an inhibitory caveolin-eNOS interaction (Feron *et al.*, 1999). Other possible contributors to an attenuated NO production include increased levels of endogenous inhibitors of eNOS such as asymmetric dimethyl arginine (ADMA)(Cooke, 2000, Boger *et al.*, 1998), and L-NMMA (Hanssen *et al.*, 1998) which affect eNOS activity at the posttranslational level in CHF (Table 1.2).

1.4.4.3 Lipoproteins

Low-density lipoprotein (LDL) cholesterol and in particular oxidized LDL (oxLDL) appear to play an important role in endothelial dysfunction (Carr and Frei, 2000). In the presence of transition metal ions, superoxide can initiate the oxidation of LDL. In particular, this pathological mechanism has been implicated as the primary cause of endothelial dysfunction in atherosclerosis (Hogg *et al.*, 1993) and is also thought to contribute to the pathophysiology of CHF (Tsutsui et al., 2002). The contribution of oxLDL towards endothelial dysfunction in CHF is not known. The underlying mechanism(s) involved in oxLDL-induced endothelial dysfunction are a contentious issue. oxLDL impairs endothelium-dependent vasodilation both *in vivo* and *in vitro* (Howes *et al.*, 1997) and there is some evidence to suggest that plasma levels of oxidised LDL correlated with the degree of agonist induced endothelium-dependent vasodilation (Matsuoka, 2001). The consensus view is that oxLDL decreases endothelial function by decreasing the release of endothelium-derived NO or, increasing the inactivation of endothelium-derived NO. Direct effects on the NO signalling pathway involving protein kinase C (Kugiyama *et al.*, 1992) and G proteins (Mukherjee *et al.*, 2001, Liao and Clark, 1995) may contribute to the detrimental effects of oxLDL on endothelial function. Studies by Liao *et al.* (Liao *et al.*, 1995) have shown that oxLDL downregulates eNOS expression and activity *in vitro* through the inhibition of eNOS gene transcription and post-transcriptional mRNA destabilisation. By contrast, others have found that oxLDL upregulates eNOS mRNA expression (Drummond *et al.*, 2000). Post-translational effects of oxLDL also may contribute towards the development of endothelial dysfunction. oxLDL has been shown to deplete caveolae of cholesterol and prevent agonist stimulation of eNOS by disrupting a beneficial eNOS localisation complex (Section 3.2.2) that is required for eNOS evoked NO production (Everson and Smart, 2001). oxLDL can in this way disturb the balance of NO and superoxide generation by eNOS and has been shown to direct the reaction towards superoxide generation (Stepp *et al.*, 2002) Lysophophatidylcholine (LPC), a specific component of oxLDL, mimics the effects of oxLDL on endothelial function and may actually be the important mediator of oxLDL. LPC has been shown to significantly increase PKC activity (Murohara *et al.*, 1999) and increase intracellular Ca^{2+} in cultured endothelial cells (Yokoyama *et al.*, 2002).

1.4.4.4 Substrate and Co-factor Availability for NOS

Experimental limitation of substrate availability for eNOS leads to a decrease in NO production (Wu *et al.*, 1999, Escobales *et al.*, 2000) and may be an important determinant of endothelial function *in vivo*. A growing body of evidence demonstrates a restorative effect on endothelial function by oral or infused supplemental L-Arg in CHF and disorders of endothelial dysfunction (Section 4.5.7). This clinical based evidence is strongly suggestive that a deficiency of L-Arg exists for the production of NO by eNOS. The origin and underlying mechanism for this deficiency is unknown. It has been proposed that in human CHF that a substrate deficiency for NOS may exist either due reductions in absolute plasma L-Arg concentrations (Hanssen et al., 1998) or through reduced L-Arg transport. Increased plasma levels of competitive inhibitors of L-Arg transport have previously been demonstrated in CHF (Table 1.2) (Usui *et al.*, 1998, Hanssen et al., 1998). oxLDL, known for its detrimental effects on NO bioavailability (Section 4.4.3), is known to significantly impair L-Arg transport activity and NO production in cultured endothelial cells and platelets (Kikuta *et al.*, 1998, Jay *et al.*, 1997, Chen *et al.*, 1996). Factors that affect CAT-1 activity and the rate of transport of L-Arg in endothelial cells include membrane potential, endotoxin, potassium ion concentrations, L-Arg itself (Section 7.2.1), other cationic amino acids, glucose and insulin (Zharikov and Block, 1998). Hypoxia, a state relevant to CHF (Figure 1.5), is associated with a reduction in L-arginine transport in porcine pulmonary endothelial cells (Zharikov *et al.*, 1997).

Studies that investigate the role of L-Arg transport in endothelial dysfunction are currently lacking. A recent study has provided direct evidence of a link between reduced L-Arg transport and endothelial dysfunction. Patients with lysinuric protein intolerance (LPI), an autosomal recessive disease caused by a mutation in the gene for the L-Arg transporter, y^+LAT1, exhibit impaired L-Arg transport leading to an intracellular L-Arg deficiency and endothelial dysfunction due to a decrease in NO production (Kayanoki *et al.*, 1999). Moreover, supplementation of L-Arg normalised both NO levels and endothelial function in this disease (Kamada *et al.*, 2001). Alternative mechanisms of endothelial dysfunction which might be relevant to a decreased substrate availability for eNOS include increased L-Arg intracellular metabolism by other L-Arg

metabolic pathways (Section 1.5.2) or an inaccessibility of L-Arg intracellularly to the site of eNOS enzymatic activity (Section 1.5.4).

A deficiency of the NOS co-factor, tetrahydrobiopterin (BH_4), has also been implicated in the pathophysiology of endothelial dysfunction in CHF. It is thought that a deficiency of may favour the NOS-evoked formation of superoxide anions and hydrogen peroxide. Beneficial effects of acute and chronic BH_4 supplementation on endothelial function have been reported (Katusic, 2001).

1.4.4.5 Endothelial receptor-signal transduction pathways

Decreased efficacy of cGMP-dependent protein kinase (cGK I) due to decreased NO bioavailability may contribute to endothelial dysfunction. cGK I is the intracellular effector of cGMP in the cardiovascular system and is expressed in human platelets, vascular smooth muscle cells, and cardiac myocytes (Butt *et al.*, 1993). Through its vascular actions it has been shown to lower intracellular Ca^{2+}, endothelial cell permeability, inhibit vascular smooth muscle contraction, platelet activation, thereby acting to preserve endothelial function (Gambaryan *et al.*, 1996). Activity and/or expression of cGK I is vital for modulating NO-induced vasodilation through the cGMP/NO signalling pathway and is also involved in ANP vasodilator actions. ANP and cGMP levels increase with the severity of CHF. However, their efficacies are reported to be lower with increasing severity of CHF (Jakob *et al.*, 1995, Elsner *et al.*, 1995) and is suggestive of a defective NO/cGMP signalling pathway. As a result of this, increased vascular resistance can occur. Studies with cGK-I-deficient mice (cGKI-/-) demonstrated a complete disruption of the NO/cGMP signaling pathway in vascular smooth muscle and also an alteration in markers of endothelial function, characterised by increased vascular adhesion and aggregation of platelets following ischemia (Massberg *et al.*, 1999). Thus, a decrease in the efficacy of cGK I may possibly be relevant for the development of endothelial dysfunction in CHF.

Decreased soluble guanylyl cyclase (sGC) activity may contribute to a decrease in endothelial function independently or in addition to changes in NO bioavailability. sGC has been shown to mediate peripheral and coronary ANP vasodilator actions and, sGC inhibitors such as L-NMMA, that have been detected in CHF (Hanssen et al., 1998), can impair dilatory and hypotensive effects of ANP (Brunner and Wolkart, 2001). NADPH oxidase-induced superoxide production following Ang II stimulation is accompanied by a decrease in sGC expression leading to impaired NO/cGMP signalling and endothelial dysfunction in the vasculature of experimental models (Mollnau *et al.*, 2002b). A downregulation of ANP receptor coupled to GC in peripheral vascular beds of patients with chronic end-stage heart failure has also been suggested (Smits *et al.*, 1993).

Impaired peripheral vasodilation in response to muscarinic agonists such as acetylcholine, commonly used to identify endothelial dysfunction, previously led to the proposal that a defective muscarinic signal transduction pathway in the endothelium may be an underlying cause. However, demonstration that a vasopressin receptor agonist (desmopressin) could stimulate NO production independent of the muscarinic receptor in human heart failure (Rector *et al.*, 1996), have shown that impaired endothelium-dependent vasodilation is not limited to the muscarinic pathway.

1.4.4.6 Pro-inflammatory Cytokines and Inflammatory Mediators

A currently held concept is that the progression of CHF is mediated in part by the effects of proinflammatory cytokines on the heart and the peripheral circulation. Existing evidence suggests that pro-inflammatory cytokines and inflammatory mediators may also contribute to the development of endothelial dysfunction at the concentrations measured in CHF (Birks and Yacoub, 1997). High levels of TNF-α present in the serum of CHF patients have been shown to induce apoptosis and downregulate eNOS expression in cultured endothelial cells (Agnoletti et al., 1999). Anker *et al.* (Anker *et al.*, 1998) has previously shown that circulating TNF-α levels and soluble TNF receptors correlate with the severity of CHF.

1.4.4.7 Vasoconstrictor release

ET-1 has been shown to increase systemic and renal vascular resistance at pathophysiologic concentrations. Plasma endothelin is elevated in humans and animal models with CHF (Lerman *et al.*, 1992).. Effects of elevated endothelin are thought to contribute to excessive peripheral vasoconstriction and endothelial dysfunction in heart failure (Lerman et al., 1992). Elevated angiotensin II is also thought to contribute to a vasoconstrictive state in CHF. Endothelial dysfunction in response to long-term angiotensin II treatment has been attributed to increased superoxide production within the endothelium in experimental models. Subsequent studies have identified an increased expression and activity of NAD(P)H oxidase as the predominant superoxide source in response to Ang II treatment (Mollnau *et al.*, 2002a).

1.4.5 Treatment of Endothelial Dysfunction

There are major ongoing efforts by investigators in assessing the ability of naturally occurring and chemically synthesised factors to improve endothelial function, primarily by increasing NO bioavailability. The association between cardiovascular risk factors and cardiovascular disease with endothelial dysfunction makes it a reasonable to suppose that intervention through risk factor reduction should improve endothelial function and attenuate symptoms associated with the development or progression of cardiovascular disease. Interventions currently favoured include statin therapy, angiotensin-converting enzyme (ACE) inhibitors, and exercise. Of the many vasodilators tested to date in large-scale clinical trials for the treatment of advanced heart failure, overall positive data relating to patient outcomes have emerged from trials of high-dose nitrates with hydralazine and, ACE inhibitors (Elkayam et al., 2002). Both classes of drugs are believed to improve the symptoms, increase exercise tolerance and improve the prognosis associated with advanced heart failure. However, it has not yet been proven whether their effects on patient outcomes are due to beneficial actions on endothelial function.

Cardiovascular disease risk factor reduction by improvement and/or restoration of endothelial function with these recommended interventions, would also be expected to also be beneficial for prevention and relief of symptoms associated with the progression of CHF. Interventions that have demonstrated beneficial clinical and experimental outcomes for the improvement of endothelial function and thus, cardiovascular disease progression and risk factor reduction are discussed with particular emphasis on the potential for dietary modification with supplemental L-Arg.

1.4.5.1 Lipid-lowering drugs

3-Hydroxy-3-methylglutaryl coenzyme A reductase inhibitors or statins are potent inhibitors of cholesterol biosynthesis. Statin-mediated lowering of serum cholesterol has been associated with a significant reduction in cardiovascular morbidity and mortality and may involve the improvement or restoration of endothelial function. Recent studies suggest that additional non-lipid lowering and blood pressure lowering effects of statins are as important in moduiating their effectiveness on endothelial function (Takemoto and Liao, 2001). In cultured endothelial cells, statins have been shown to prevent the inhibitory action exerted by oxLDL on eNOS expression (Hernandez-Perera *et al.*, 1998). Statins attenuate O_2^- formation and simultaneously increase the expression of eNOS, resulting in a beneficial shift in the balance between NO and O_2^- formation that may improve endothelial function (Wagner *et al.*, 2000, Hernandez-Perera et al., 1998). Interestingly, statins have been shown to exert cellular antioxidant effects in vascular smooth muscle cells by decreasing the expression of essential NAD(P)H oxidase subunits and by upregulating catalase expression (Wassmann *et al.*, 2002) and, have also been shown to attenuate angiotensin II-induced ROS production through downregulation of angiotensin type 1 receptor expression (Wassmann *et al.*, 2001). Therefore, an antioxidant capacity may help explain the ability of statins to diminish the pathophysiological effects of Ang II on NO bioavailability. In an experimental model of heart failure, administration of cerivastatin increased left ventricular eNOS expression and reduced peroxynitrite formation (Bauersachs *et al.*, 2001).

1.4.5.2 Antioxidants

Because of the reactivity of ROS and a highlighted role in the pathology of endothelial dysfunction several enzymatic and nonenzymatic antioxidants such as superoxide dismutase, catalase (Muzykantov *et al.*, 1996), glutathione peroxidase (GPX), vitamin E and vitamin C have been tested for treating endothelial dysfunction. Vitamin C (ascorbic acid) and E (α-tocopherol), are found in the human plasma and are associated with an increased NO bioavailability following dietary supplementation (Herrera and Barbas, 2001, Burton *et al.*, 1983). Antioxidant actions of Vitamin C and E are attributed to their ability to scavenge superoxide radicals, inhibit oxidation of LDL, and preserve intracellular levels of pro-vasodilatory factors such as glutathione, thiols and tetrahydrobiopterin. Clinical and experimental studies have demonstrated possible beneficial effects of vitamin C and E on endothelium-dependent vasodilation in cardiovascular disorders associated with endothelial dysfunction (Carr and Frei, 1999). Results of larger scale clinical trials are conflicting (Carr and Frei, 2000) (Esterbauer *et al.*, 1992, Dieber-Rotheneder *et al.*, 1991). Experimental studies have found that co-factor availability for the eNOS reaction may determine the enzyme's capacity for the generation of ROS. The heme moiety is identified as the exclusive source of superoxide production by eNOS. The balance between NO/superoxide reaction pathways may be shifted by addition of exogenous heme-specific agents such as BH_4 and may be of use therapeutically for the treatment of endothelial dysfunction. Certainly, addition of exogenous BH_4 has been found to reduce superoxide production by eNOS in BH_4 deficient mice (Cosentino *et al.*, 2001).

1.4.5.3 ACE inhibitors

Major evidence from clinical studies and experimental models of heart failure suggests that angiotensin-converting enzyme (ACE) inhibition can improve endothelial function (Drexler and Hornig, 1999, Mombouli and Vanhoutte, 1999). ACE inhibitors reduce the risk of major ischaemic events in heart failure patients and therefore it has been proposed that their beneficial effect on the endothelial function may be of major significance to this particular outcome. Inhibition of Ang II production by ACE inhibition reduces superoxide generation from blood vessels and may increase

NO bioavailability (Quyyumi, 1998). Additionally, ACE inhibitors improve endothelial function through decreased degradation of bradykinin, an endogenous agonist for NO release from the endothelium (Mombouli, 1997).

1.4.5.4 Organic nitrates

At therapeutic concentrations, organic nitrates are preferential dilators of venous vessels and conduit arteries and, at higher doses also evoke a beneficial decrease in peripheral resistance (Gewaltig and Kojda, 2002). Organic nitrates such as nitroglycerin and nitroprusside are in widespread use for the treatment of both acute and chronic myocardial ischaemia, as well as CHF. Nitrates cause direct vasodilation following initial enzymatic conversion to NO within endothelial and vascular smooth muscle cells. A body of evidence exists, which documents a variety of mechanisms whereby nitrates increase coronary blood flow, including epicardial coronary artery dilation, prevent or reverse coronary artery vasoconstriction and improve endothelial dysfunction (Abrams, 1996). Inhibition of platelet aggregation by nitrates is another therapeutic effect of nitrates that is linked to an improved endothelial function. Data from a small randomised trial has suggested that high-dose nitrate therapy can significantly improve exercise tolerance and other hemodynamic parameters in patients with chronic, mild to moderate CHF already treated with ACE inhibitors. Short-term use of nitrates is proposed as a beneficial combination with ACE inhibitor therapy for treating heart failure (Elkayam *et al.*, 1999). Long-term treatment with nitrates can lead to endothelial dysfunction (Schulz *et al.*, 2002). Also, hemodynamic resistance to nitrate therapy has been previously documented in CHF and is a major limiting factor for its clinical use (Abrams, 1991).

1.4.5.5 Receptor antagonists and other drugs

Clinical data has provided evidence that TNF-α antagonism with etanercept, a recombinant TNF receptor that binds to and functionally inactivates TNF-α, significantly improves systemic endothelial vasodilator capacity in patients with advanced heart failure (Fichtlscherer *et al.*, 2001). However, since disappointing results were obtained in large clinical trials (RENAISSANCE,

RECOVER and RENEWAL) with respect to patient outcomes after entanercept treatment in heart failure, the prescription of this drug to CHF patients has been largely abandoned. Additionally, an improved endothelial function in response to angiotensin type-1 (AT_1) receptor blockade has been demonstrated in a number of experimental heart failure models (Schiffrin, 2002).. For example, in dilated cardiomyopathic hamsters with advanced congestive heart failure, the selective AT_1 receptor antagonist, candesartan, was shown to improve systemic and femoral hemodynamics by decreasing systemic vascular resistance and increasing blood flow (Goineau *et al.*, 2002). Risk factor-associated disorders for the development of heart failure also display improved endothelial function after AT receptor blockade treatment. Short-term and long-term treatment with AT_1 receptor blockers such as losartan, irbesartan and candesartan have also been shown to improve both flow-mediated and agonist induced endothelium-dependent vasodilation in hypertensive patients (Schiffrin, 2002).

Antagonists and receptor antagonists of the renin-angiotensin-aldosterone system, such as spironolactone and eplerenone, may possibly be of benefit in treating endothelial dysfunction in CHF. Experimental studies have indicated a role for aldosterone in the pathogenesis of endothelial dysfunction in certain cardiovascular disorders (Struthers, 2002). A recent study in healthy humans performed by Farquharson *et al.* (Farquharson and Struthers, 2002), has indicated that acute short-term systemic administration of aldosterone can result in a specific impairment of endothelial function. Other potential candidate drugs for improving NO bioavailability and thus endothelial function include activators of soluble guanylate cyclase, phosphodiesterase inhibitors and β-blockers.

1.4.5.6 Exercise

Outcome of experimental studies and clinical trials relating to treatment regimes for CHF and other cardiovascular disorders such as coronary artery disease, hypertension and diabetes have provided strong evidence for an exercise training benefit in improving endothelial vasodilator function (Gielen et al., 2002). The beneficial effects on hemodynamic parameters make exercise training a

major part of cardiac rehabilitation programs. The precise underlying mechanism(s) involved in the beneficial effects of exercise on endothelial function is unknown. Since exercise increases blood flow to active muscles it might be postulated that exercise-induced shear stress on vessel walls is a stimulus for endothelium-derived NO production, leading to smooth muscle relaxation and vasodilation (McAllister *et al.*, 1995). Shear stress can improve NO availablity by increasing endothelial L-Arg transport, NOS activity and expression, and can also upregulate the production of antioxidant enzymes (extracellular superoxide dismutase andglutathione peroxidase)(Ennezat *et al.*, 2001). Chronic exercise consistently increases eNOS expression in experimental animal models (Laughlin *et al.*, 2001, Sessa *et al.*, 1994). Increased eNOS gene expression demonstrated in both coronary conductance and resistance vessels in response to exercise training in human CHF, might bestow a greater vasodilation capacity to vessels perfusing exercising muscle and enhance enhance exercise capacity (Hambrecht *et al.*, 2000). Another currently favoured view associated with longer-term exercise training regimes in CHF is that increased vessel compliance and reduced arterial stiffening may lead to beneficial structural adaptations in the vessel wall and, improved endothelial function (Bonapace *et al.*, 2003). Due to its attribute as a lifestyle alternative to medication, studies relating to the intensity, duration and frequency of exercise training required for a beneficial effect on endothelial function and, the underlying mechanisms involved are currently an important area of cardiovascular research.

1.4.5.7 L-Arg supplementation

Supplemental L-Arg therapy provides one of the most promising dietary interventions in the treatment of endothelial dysfunction in CHF to date. An early report by (Aisaka *et al.*, 1989) and colleagues was the first study to provide direct evidence of a role for L-Arg in the modulation of endothelium-dependent vasodilatory actions *in vivo*. In experimental models, dietary L-Arg deprivation leading to decreased serum L-Arg levels has been found to impair NO synthesis suggesting that an L-Arg deficiency may contribute to cardiovascular dysfunction due to its effect on decreased NO synthesis (Wu et al., 1999). In the last decade a growing body evidence has documented both in experimental animal studies and clinical studies the ability of supplemental L-

Arg to reverse endothelial dysfunction associated with major cardiovascular risk factors such as hypercholestrolemia, smoking, hypertension, diabetes, obesity and age (Wu and Meininger, 2000), and, also to restore and inhibit the progression of cardiovascular disorders associated with impaired NO synthesis and endothelial dysfunction (Table 1.3). With the beneficial effects established and the lack of any major side effects noted to date, L-Arg is currently being evaluated for its effectiveness in improving or augmenting endothelial function. The long-term effects of L-Arg supplementation in the doses currently accepted in such formulations and as prescribed clinically in trials and are not yet known. Surprisingly little is known about the mechanism(s) involved behind the well-documented beneficial effects of dietary L-Arg supplementation. The mechanism by which L-Arg can increase the production of NO is still debated.

Table 1.3 Clinical effects of oral L-Arginine supplementation on endothelial dysfunction.

First Author	Subjects	Results	Effect of L-arginine supplementation
	Healthy		
Adams	12 healthy men	+	Inhibited platelet aggregation via the NO pathway within platelets
Chin-Dusting	26 healthy males	-	No effect on endothelial function as assessed by forearm blood flow
Lerman	26 healthy subjects	+	Long-term supplementation improved coronary endothelial function, reduced plasma endothelin levels
	CAD		
Blum	29 men with CAD	-	No improvement in NO bioavailability
Adams	10 men with CAD	+	Improved brachial artery endothelial-dependent dilation and reduced monocyte-endothelial cell adhesion
Cenemuzynski	22 CAD patients	+	Improved myocardial perfusion during maximal exercise in patients with stable angina pectoris
	CHF		
Rector	15 CHF patients	+	Improved endothelial function as assessed by forearm blood flow
Chin-Dusting	20 CHF patients	-	No effect on endothelial function as assessed by forearm blood flow
Hambrecht	40 CHF patients	+	Supplementation and exercise improved agonist mediated endothelial-dependent dilation in the brachial artery. Additive effect of interventions.
	Cardiovascular Risk Factors		
Lekakis	35 Essential hypertenensives	+	Improved endothelial-dependent dilation in the brachial artery
Chan	24 hypercholestrolemics	+	Plasma L-arginine/ADMA ratio inversely correlated with mononuclear cell adhesivenss
Theilmeier	20 hypercholestrolemics	+	Reduced mononuclear cell adhesiveness
Wolf	23 hypercholestrolemics	+	Attenuation of increased platelet reactivity
Clarkson	27 hypercholestrolemics	+	Improved endothelial-dependent dilation in the brachial artery
Blum	10 postmenopausal women (not on estrogen)	-	No augmentation of endothelial NO synthesis and release
Adam	8 smokers	+	Reduced monocyte adhesion to endothelium

ADMA, asymmetric dimethyl arginine; CAD, coronary artery disease; CHF, congestive heart failure; NO, nitric oxide. +/- denote positive and negative outcome on beneficial L-arginine effects. Adapted from Preli *et al.* 2002. Please not that studies are listed by their first author. Further details are found within the article.

A common model in the literature proposes that enhanced vasodilation due to supplemental L-Arg administration is due to increased availability of intracellular substrate for eNOS. According to this model, a relative deficiency in intracellular L-Arg stores exists in disorders of endothelial dysfunction (Table 1.3) and therefore the beneficial effect of L-Arg supplementation on vascular function is due solely to restoration of substrate supply and/or augmentation of existing intracellular L-Arg levels available for eNOS conversion to NO. Results of *in vivo* studies that have reported a restoration of endothelial function following supplementation with L-Arg would seem to indicate this possibility. However, an "L-Arg paradox" (further details section 1.5.3) exists where the K_m (Michaelis-Menton affinity constant) of eNOS (3 μM) is far below ambient intracellular L-Arg levels in normal physiologic states. In cultured cells, for example, intracellular L-Arg has been measured at levels 30-800 fold higher than the K_m for NO synthase (Forstermann et al., 1994). Therefore, it is important to note in the context of the present study and many others that this model whereby L-Arg is proposed to serve merely as a substrate for NO synthase has not been validated.

Some evidence suggests that the beneficial effects of L-Arg supplementation on endothelial function may be occurring independent of its role as a substrate for NOS. Exogenous L-Arg may enhance NO production by abolishing the inhibitory effect of the amino acid L-glutamine on NOS. For example, (Arnal *et al.*, 1995) demonstrated that L-Arg dose-dependently reversed L-glutamine inhibition of acetylcholine-stimulated NO release. Interestingly, in that study the inhibitory effect of L-glutamine was not due to change in intracellular L-Arg levels or NO synthase activity but rather due to an interference of the muscarinic receptor-stimulated signal transduction pathway.

Another proposal for the beneficial effects of supplemental L-Arg is that enhanced vasodilation may be non-specific in its actions. D-arg, the enantiomeric form of L-Arg, which does not serve as substrate for endothelial NO synthase (Moncada and Higgs, 1993), has no additive effects on endothelium-dependent vasodilation in response to intraarterial infusion of acetylcholine (40 μmol/min) in young healthy subjects. (Imaizumi *et al.*, 1992) (MacAllister *et al.*, 1995) Additionally, infusion of equimolar amounts of D-arg do not correspond with the enhancing effects

of L-Arg on agonist elicited endothelium-dependent vasodilation of the forearm vasculature in hypercholesterolemic patients (Creager *et al.*, 1992) and the coronary vasculature of patients with coronary atherosclerosis (Quyyumi *et al.*, 1997), or increased blood flow and reduction of blood pressure in acute hyperglycaemic patients (Giugliano *et al.*, 1997a). By contrast, high doses (160 μmol/min) of infused D-arg have been shown to enhance the vasodilatory effects of infused acetylcholine in the forearm vasculature after administration intraarterially (Panza *et al.*, 1993) and increase renal endothelium-dependent vasodilation in patients with essential hypertension (Schlaich *et al.*, 2000). The potential for non-specific effects of L-Arg in its action on endothelium-dependent vasodilation and systemic hemodynamics are currently an important topic for further investigation.

A further possibility highlighted in the current literature is the potential for the release of endogenous factors due to exogenous L-Arg administration, which may contribute to or mediate its beneficial changes to endothelial function. Previous reports have demonstrated that the hormone insulin exhibits vasodilatory properties in the human vasculature of healthy subjects (Steinberg *et al.*, 1994, Cardillo *et al.*, 1999). Increased vasodilation elicited through systemic infusion of L-Arg in healthy human subjects has been partially associated with an increased endogenous insulin secretion (Giugliano *et al.*, 1997b). Indeed, L-Arg is known to stimulate the release of insulin from pancreatic beta-cells (Smith *et al.*, 1997). Human data indicate that insulin-induced vasodilation is mediated by NO (Steinberg et al., 1994). Both insulin and NO have been shown to increase L-Arg uptake in cultured endothelial cells (Simmons *et al.*, 1996, Ogonowski *et al.*, 2000b). Based on these properties, a synergistic effect has been postulated whereby L-Arg increases insulin and NO release, and subsequently, insulin and NO facilitates the uptake of L-Arg by cells thus raising its intracellular availability. Another proposal is that the beneficial effects of L-Arg supplementation with respect to augmentation of exercise-induced vasodilation during exercise (Chauhan *et al.*, 1996, Gryglewski *et al.*, 1996) may involve an inhibitory effect of L-Arg on somatostatin, a neuropeptide inhibitor of growth hormone production (Wideman *et al.*, 2000). It should also be noted however, that the contribution of endothelium-derived NO to exercise-induced vasodilation is not yet clear and somewhat controversial.

An additional and additive benefit on patient immunity and outcome has also been identified with L-Arg supplementation. In fact, some of the earliest reports on the beneficial effects of dietary supplementation with L-Arg, were made with regards to its effect on immune function. A large body of evidence now indicates that dietary L-Arg supplementation enhances immune function in humans and in animal models (Barbul, 1995). In laboratory rats, dietary L-Arg supplementation has been shown to significantly enhance thymic weight, spleen cell mitogenesis, and interferon-activated natural killer cell activity (Reynolds *et al.*, 1990), B-cell maturation in mice (De Jonge *et al.*, 2002) and in humans there is evidence of increased immunostimulation following supplementation such as lymphocyte mitogenesis and increased T cell-mediated immune function. (Barbul *et al.*, 1990, Sigal *et al.*, 1992, Reynolds *et al.*, 1988, Barbul *et al.*, 1984) Studies undertaken with surgical patients in prospective, randomised, double-blinded clinical trials have indicated that administration of nutritional formulas supplemented with L-Arg leads to a decreased post-operative duration of stay in hospital and reduced infection rates (Braga *et al.*, 1999).

In summary, both the NO-dependent and independent effects of L-Arg *in vivo* may contribute to its beneficial effects on endothelium-dependent vasodilation when administered as a dietary supplement in humans (Table 1.4). Overall data from clinical trials using oral and infused doses of L-Arg have shown very encouraging outcomes with fewer side effects displayed than by other endothelial function treatments. The exact mechanism by which L-Arg improves endothelial function is an ongoing topic of investigation. Interestingly, short synthesised polymers of L-Arg are also displaying beneficial properties by stimulating NO production in cultured cells (Uemura *et al.*, 2002) and inhibiting myointimal formation after vein grafting in experimental animal models (Uemura *et al.*, 2000). These polymers can translocate directly across the membrane independently of L-Arg transporters.

1.5 L-Arg Metabolism

1.5.1 Overview

In mammalian cells, the semi-essential amino acid L-Arg is known for its involvement in protein synthesis. L-Arg is classified as a essential amino acid for young mammals, and, in adults including humans during times of metabolic stress or disease when endogenous synthesis is no longer adequate to sustain metabolism (Visek, 1986). For this reason L-Arg has been termed as a 'conditionally' essential amino acid. It is also a substrate for enzymes such as NO synthase, arginase, arginine decarboxylase, or glycine transaminidinase (Ignarro and Murad, 1995) (Figure 1.7). Amongst these pathways, the synthesis of NO and the urea cycle have been proposed to play the most important roles in the metabolism of L-Arg.

The metabolic products of L-Arg utilisation by NO synthase are NO and L-citrulline. L-Arg is metabolised by an enzyme called arginase to form urea. The enzymatic activity of arginase is important for L-Arg metabolism in the urea cycle, an essential metabolic pathway for removal of highly toxic ammonium ions as a result of protein degredation. Arginase also catalyses the conversion of L-Arg to L-ornithine, a precursor of polyamines (spermine, spermidine and putrescine). Polyamines are growth factors that are produced by all cells and are crucial to cell proliferation and differentiation (Vanne etal 1991). Proline, a result of the sequential metabolism of L-Arg and L-ornithine by the enzymes arginase, ornithine decarboxylase and ornithine aminotransferase is essential for the synthesis of many structural proteins, including collagen (Wu and Morris, 1998). In addition, L-Arg is the precursor of creatine, which functions as a high energy-phosphate carrier during muscle contraction and is also involved in energy metabolism in nerves.

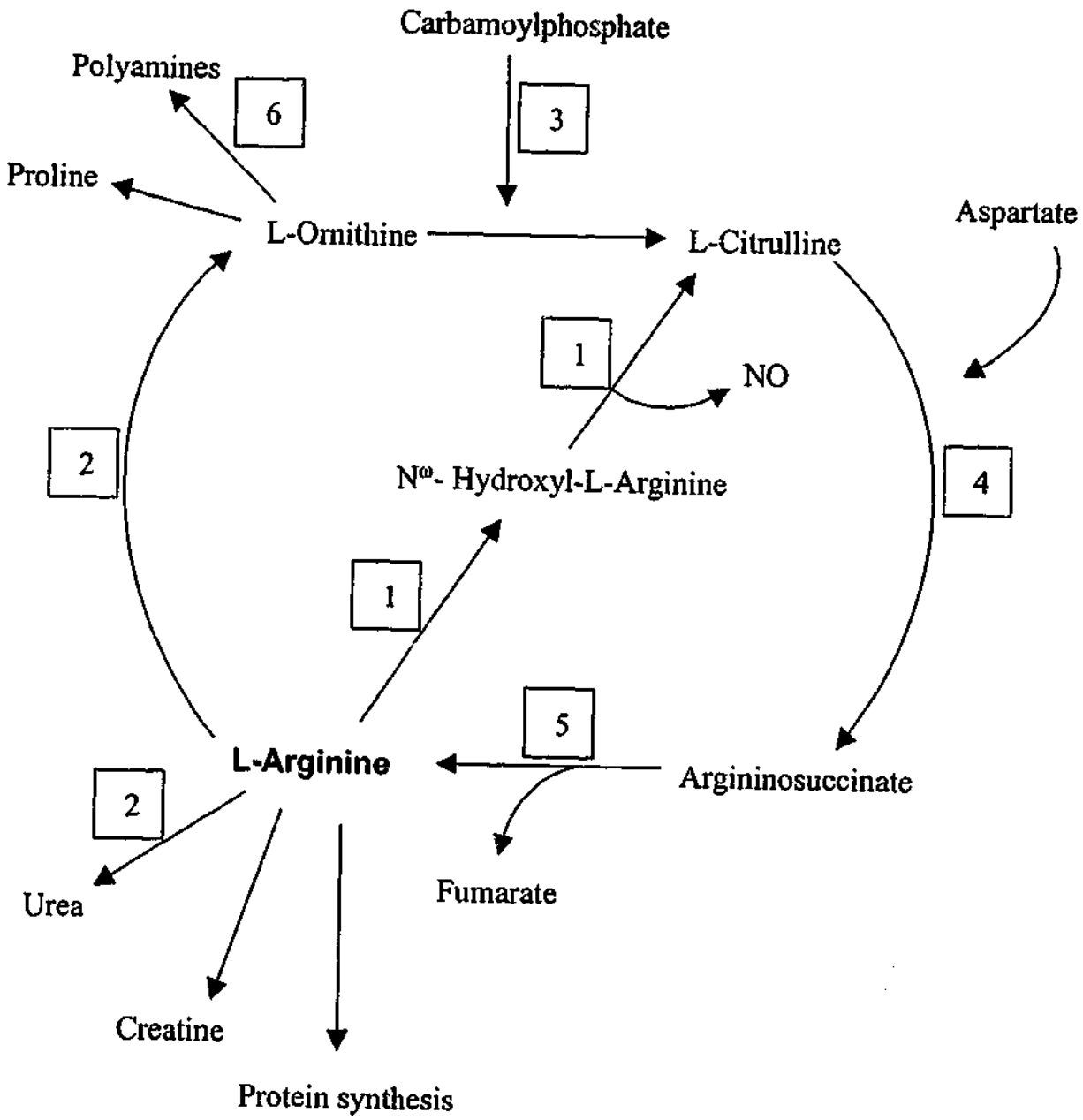

Figure 1.7 Metabolic pathways and enzymes related to L-Arginine metabolism. Some of the enzymes involved are numbered as follows: 1 = nitric oxide synthase; 2 = arginase; 3 = ornithine carbamoyltransferase; 4= argininosuccinate synthase; 5=argininosuccinate lyase; 6= ornithine decarboxylase. Taken from Boucher *et al.* 1999 (Boucher *et al.*, 1999a).

L-Arg homeostasis in humans results from trafficking between organs and involves specific transport proteins (Christensen 1982, 1990). L-Arg is released by a number of cell types such as kidney cells which supply other organs or the endothelial cells of the blood-brain barrier which release L-Arg into the brain. Although L-Arg is not under normal conditions classified as an essential amino acid, only the liver and kidney cells produce useful levels in the body. The kidney is the major source of L-Arg via synthesis from L-citrulline (Barbul 1990). The presence of high arginase activity in liver prevents its export. Therefore, all other cells must import the majority of L-Arg from plasma for their metabolic requirements.

1.5.2 Regulation of L-Arginine Metabolising Enzymes

The resulting product of L-Arg metabolism in a given cell type depends on the activity and regulation of specific L-Arg metabolising enzymes. Furthermore, L-Arg transport across the membrane, the relative expression levels of enzymes involved in L-Arg re-cycling (intracellular synthesis of L-Arg from L-citrulline) and degredation may be important in determining the level of NO production. The function of arginase expression outside the liver is unclear, but has been implicated in the regulation of NO synthesis and cell growth in inflammatory conditions. In activated macrophages various studies have indicated that arginase activity may limit the utilisation of L-Arg by iNOS and suppress the cytotoxic response by these cells (Wang et al., 1995; Modolell et al.,1995; Hey et al., 1997), while polyamine and proline synthesis from L-ornithine (a product of L-Arg metabolism by arginase) may cause cell proliferation and repair of inflammatory lesions. For example, argininosuccinate synthetase and argininosuccinate lyase, L-Arg synthesising enzymes, have been previously shown to be co-induced with iNOS in various cell types including activated macrophages, vascular smooth muscle cells, glial cells, neuronal PC12 cells, and pancreatic beta-cells (Mori and Gotoh, 2000). Arginase can downregulate NO production by metabolic reduction of intracellular L-Arg concentration. iNOS and arginase activities are known to be inversely regulated in macrophages by cytokines and may be a mechanism for sustained and efficient production of NO. By contrast, a study has shown that iNOS and arginase isoforms (type I and II)

are co-induced in LPS-activated macrophages. Durante et al. 1997(Durante *et al.*, 1997) has previously shown that LPC stimulates polyamine synthesis in vascular smooth muscle cells by inducing the expression of specific L-Arg transporters CAT-1 and CAT-2B, ornithine decarboxylase and arginase activity. Minimal information is available about the regulation of L-Arg metabolising enzymes in eNOS expressing cells. Coronary arteriolar endothelial cells (Zhang *et al.*, 2001) and rat aortic endothelial cells (Buga *et al.*, 1996) have been found to express arginase. Furthermore, pharmacological inhibition of arginase potentiated NO-mediated endothelium-dependent coronary artery vasodilation (Zhang et al., 2001). This was presumably due a decreased metabolism of L-Arg by arginase and therefore, an increased L-Arg availability for eNOS. An endogenously produced stable intermediate in the biosynthesis of NO, N^G-hydroxy-L-Arginine (NOHA, see Figure 1.3 and 1.7), has been shown to potently and competitively inhibit arginase activity (Boucher *et al.*, 1994, Boucher *et al.*, 1999b). For this reason, conversion of L-Arg to NOHA as stable intermediate substrate of an active L-Arg-NO pathway may be a preferential mechanism, since it is seems to be somewhat unaffected by the activity of arginase.

1.5.3 L-Arginine Availability and the L-Arginine Paradox

The formation of NO is dependent on an adequate and continuous supply of L-Arg. Studies from several groups have reported that the K_m of eNOS for L-Arg is approximately 3 μM (Pollock et al., 1991) while intracellular L-Arg concentrations range from 0.1 to 0.8 mM in cultured endothelial cells (Mitchell *et al.*, 1990, Block *et al.*, 1995). Therefore, under normal conditions eNOS should be saturated at these concentrations. Similarly, increasing the extracellular L-Arg concentration should not increase NO production any further. Paradoxically, a number of studies have indicated that NO production by vascular endothelial cells could be increased by exogenous L-Arg under physiological conditions, even though intracellular levels of L-Arg are available in excess (Aisaka et al., 1989). This observation has been termed the "L-Arginine paradox" can not be explained by the majority of available data.

1.5.4 Substrate Provision for the Endothelial L-Arg-NO Pathway

1.5.4.1 Dependence of NO production on Extracellular L-Arg

The benefit of supplemental L-Arg on endothelium-dependent vasodilator responses in cardiovascular disorders associated with endothelial dysfunction seems to be suggestive of two possible underlying defects. The first, a dependence for endothelial NO production on extracellular L-Arg and secondly a reduced amount of endogenous L-Arg available for endothelial NO production in the dysfunctional endothelium.

In vitro models of L-Arg depleted endothelial cells have indicated a dependence on extracellular L-Arg for the induction of NO by eNOS in response to various agonists (Escobales et al., 2000). Additionally, in young healthy animal models dietary L-Arg deficiency has been shown to decrease serum L-Arg concentrations and *in vivo* measures of NO production (Wu et al., 1999). Conflicting and inconclusive *in vivo* evidence from human studies exist. For example, even though feeding an L-Arg free diet to healthy humans was shown to reduce plasma L-Arg levels, indirect *in vivo* measures of NO production were unaffected (Castillo *et al.*, 1993, Castillo *et al.*, 1994). Likewise, little data exists on reported endogenous plasma L-Arg concentrations in disorders associated with endothelial dysfunction. Of interest, Hanssen *et al.* (Hanssen et al., 1998) reported significantly reduced plasma concentrations of L-Arg in chronic heart failure patients. However, to date, no correlation has been made between plasma L-Arg levels and endothelial function.

Some of the adaptations which have been reported in the literature for ensuring NO production despite a reduced L-Arg availability include the *de novo* synthesis from citrulline, increased transport across the cell membrane by L-Arg transporters and, reduced breakdown by arginase. Since endothelial dysfunction is associated with a reduced NO bioavailability it is reasonable to suppose that these adaptive mechanisms may either be impaired within the endothelium or alternatively are not sufficient alone to compensate for the loss of NO bioavailability. L-Arg transport across the membrane may actually contribute towards pathophysiological conditions due

to altered L-Arg transporter activity (Section 4.4.4). This mechanism may contribute towards endothelial dysfunction by limiting substrate provision for eNOS intracellularly. Certainly, more recent evidence gained from L-Arginine transporter (CAT-2B, Section 7.2.3) gene knockout mouse models has convincingly demonstrated the dependence of the inducible form of NOS (iNOS) on the transport of L-Arg across the membrane for sustained NO production in response to inflammatory mediators (Nicholson *et al.*, 2001).

1.5.4.2 Separate Intracellular Pools of L-Arg?

The existence of a separate pool of intracellular L-Arg available exclusively for eNOS utilisation was initially proposed by Closs *et al.* (Closs *et al.*, 2000) based on experimental data. In their study, depleting endothelial cells of extracellular L-Arg revealed two separate intracellular pools of L-Arg, one of which was preferential for NOS provision. The authors also speculated that an impaired access to this pool might underlie the L-Arginine paradox. Findings of Flam *et al.* (Flam *et al.*, 2001) also support this proposal. Distinct L-Arg pools are thought to possibly result from a physical compartmentalisation of L-Arg within membrane bound structures that could be selectively accessible by eNOS (Figure 1.8). Alternatively, it has also been suggested that a distinct L-Arg pool for eNOS may not be a physical structure but might be arginine-binding and/or recycling proteins capable of directing L-Arg preferentially towards eNOS conversion. Conversion of L-Arg into its stable metabolite NOHA may also constitute a separate pool of L-Arg preferentially used by eNOS.

1.5.4.3 Preferential Co-localisation of the L-Arg-NO pathway

It has been postulated that endothelial cells can effectively differentiate between the bulk of intracellular L-Arg from the L-Arg required for NO production through the functional co-localisation of L-Arg transporters with eNOS and/or L-Arg regenerating enzymes in the plasmalemmal caveolae. So that, existing intracellular L-Arg may be poorly accessible to eNOS but readily available to other L-Arg metabolising enzymes.

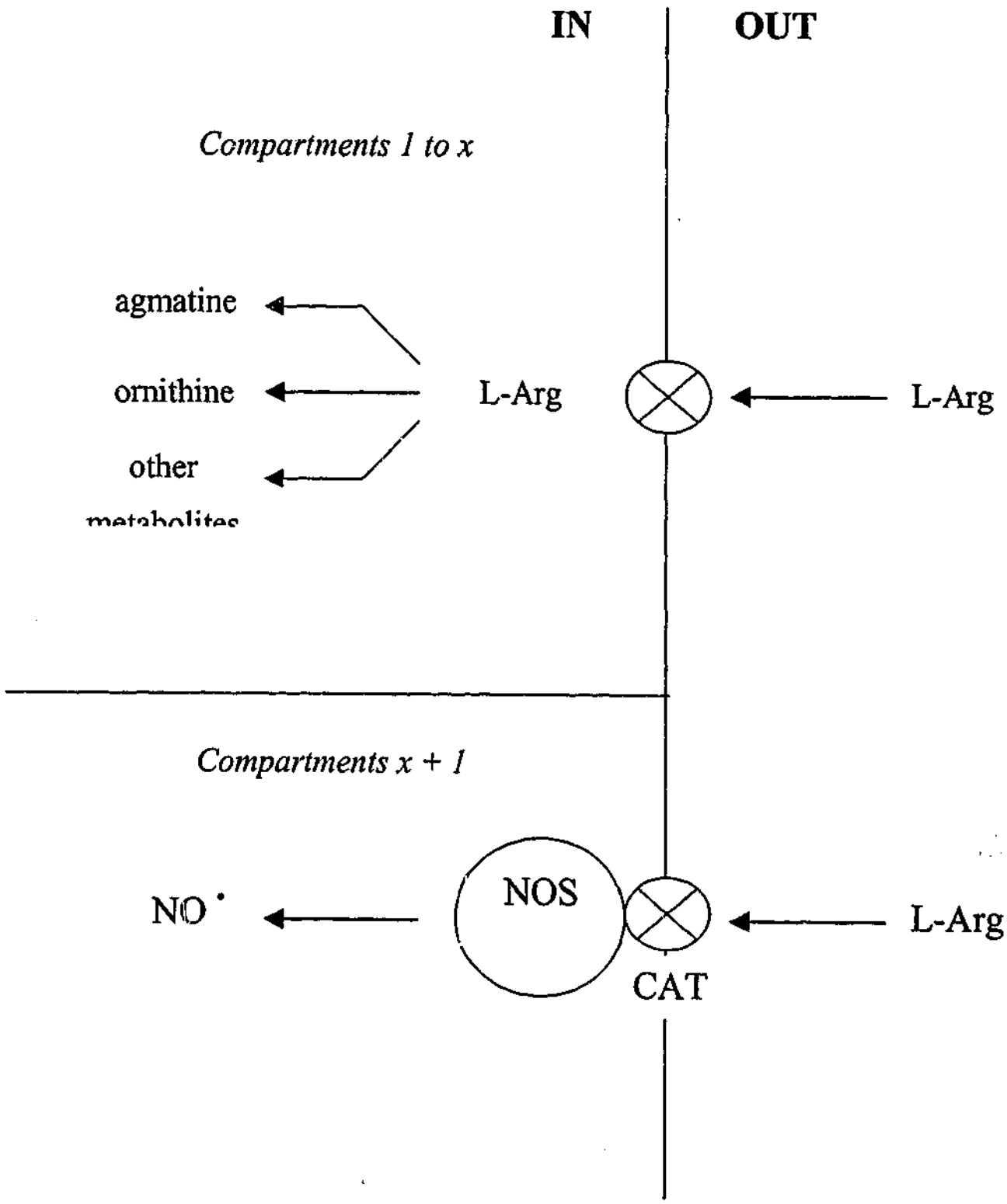

Figure 1.8. Plasma L-Arg availability controls NO synthesis due to compartmentalisation of L-Arg pathways. L-Arg, L-Arginine; NO, nitric oxide; NOS, nitric oxide synthase; CAT, cationic amino acid transporter. Adapted from Cynober *et al.* 2002 (Cynober, 2002).

Colocalisation of the CAT-1 L-Arg transporter with eNOS within caveolae suggests a mechanism for direct delivery of extracellular L-arginine to eNOS, thereby reducing the importance of intracellular L-arginine concentrations and making extracellular L-arginine concentrations and the activity of CAT-1 a potential determinant of the rate of NO synthesis (McDonald *et al.*, 1997).

1.5.4.4 Intracellular L-Arg Provision for the NO pathway

Endothelial L-Arg is mainly derived from the plasma, but can be provided via intracellular synthesis from L-citrulline and the net degredation of intracelullar proteins (Wu and Morris, 1998). Many cell types including endothelial cells have been found to have the capacity to regenerate L-Arg from citrulline, a by-product of the NO synthase reaction, by utilising two of the urea cycle enzymes, argininosuccinate synthase and argininosuccinate lyase (Hecker *et al.*, 1990, Shuttleworth *et al.*, 1995). L-Arg produced via this pathway can be used for NO production and is termed as the citrulline-arginine cycle. Growing evidence suggests that the citrulline-arginine cycle has a preferential role in L-Arg provision for iNOS particularly in non-endothelial cells types such as macrophage and vascular smooth muscle cells (Nussler *et al.*, 1994, Xie and Gross, 1997). This may be due to the requirement for high-output of NO after iNOS activation that would necessitate a high and sustained demand for L-Arg. Studies by Flam *et al.* 2001 have indicated the possibility of a functional association between eNOS and L-Arg regeneration enzymes due to their localisation in the caveolae.

1.5.5 Nitric Oxide-Independent Vascular Effects of L-Arginine

The majority of vascular effects of L-Arg are mediated by NO production. However, L-Arg has also been demonstrated to possess NO-independent hemodynamic modulatory properties (Table 1.4). *In vitro* data provide evidence of an increased NO bioavailability due to the direct superoxide anion scavenging properties of L-Arg (Wascher *et al.*, 1997). This antioxidant property was shown by the ability of L-Arg to reduce copper-induced lipid peroxidation, scavenge O_2^- and inhibit the

release of O_2^- from the endothelium *in vitro*. L-Arg has been found to reduce plasma Ang II levels in humans through an inhibition of angiotensin-converting enzyme (ACE) activity, thus potentiating its hypotensive effect (Higashi *et al.*, 1995). Studies conducted by Komers *et al.* (Komers *et al.*, 2000) found that ACE inhibition and AT_1 receptor blockade resulted in enhanced L-Arg-induced vasodilation both in the systemic and renal vascular beds of humans. Other possible effects of L-Arg independent of NO actions found in the literature, include the *in vitro* stimulation of fibrinogenolysis (Udvardy *et al.*, 1997), inhibition of leukocyte adhesion (Brandes *et al.*, 2000), and, reduced blood viscosity through the regulation of macromolecule binding to red blood cells (Walter *et al.*, 2000).

NO-dependent vascular actions	NO-independent vascular actions
↑ Smooth muscle relaxation	↑ Polarisation of EC membranes
↑ EC proliferation and angiogenesis	↑ Extracellular and intracellular pH
↓ Endothelin-1 release	↑ Release of insulin, GH, glucagon and prolactin
↓ Leukocyte adhesion	↑ Synthesis of urea, creatine, PRO and PA
↓ Platelet aggregation	↑ Plasmin generation and fibrinogenolysis
↓ Superoxide production	↓ Leukocyte adhesion to non-EC matrix
↓ Expression of cell adhesion molecules	↓ Blood viscosity
↓ Expression of monocyte chemotactic peptides	↓ Angiotensin-converting enzyme activity
↓ Proliferation of smooth muscle cells	↓ O_2^- release and lipid peroxidation
↓ EC apoptosis	↓ Formation of TXB_2 , fibrin and platelet-fibrin

Table 1.4 Nitric oxide (NO)-dependent and independent vascular actions of L-Arginine. Abbreviations; EC, endothelial cells; GH, growth hormone; PA, polyamines; PRO, proline; TXB_2, thromboxane B_2. The symbols ↑ and ↓ denote increase and decrease respectively. Taken from Wu *et al.* 2000 (Wu and Meininger, 2000).

1.6 L-Arginine Transporters

1.6.1 L-Arg Transport Systems in Mammalian Cells

Most mammalian cells need to import L-Arg from plasma for their metabolic requirements. In order to sustain these requirements L-Arg can be transported by several different transport systems. An amino acid "transport system" is designated as a functionally distinct transport process. A transport system can result from the expression of a single gene or can be comprised of multiple gene products. Each cell type can express a variety of distinct transport systems, which are capable of transporting several different amino acid substrates, including L-Arg. In addition, broad substrate specificities and overlapping tissue and cell distribution patterns of amino acid transporter types confound the contribution of each individual transport system towards L-Arg uptake *in vivo*. Early pioneering work by Christensen's group and others has resulted in the identification and characterisation of numerous amino acid transport systems, some of which have the capacity to transport L-Arg(Christensen, 1990). This has mostly been achieved through *in vitro* kinetic characterisation studies and the functional identification of cDNA's encoding mammalian amino acid transporters.

1.6.2 Classification of Cationic Amino Acid Transport Systems

At least four different transport pathways have been shown to be responsible for cellular uptake of cationic amino acids into mammalian cells and have been categorised according to transporter properties. These are system y+, heterodimeric, sodium-dependent and other. Kinetically, these transporters have been categorised into two broad classes based on their sodium dependency for the transport of cationic amino acids: Na+-dependent transport ($B^{0,+}$) and Na+-independent transport ($b^{0,+}$, y^+, y^+L). System $B^{0,+}$, a sodium-dependent transporter, is coupled with the plasma membrane Na^+ electrochemical gradient generated by Na^+-K^+ ATPase. The other three transport systems are Na^+-independent and uptake of cationic amino acids occurs via carrier-mediated passive facilitated

diffusion. The driving force of these transporters is derived from the electrochemical potential of the amino acids across the membrane (Palacin *et al.*, 1998). Endothelial cells express both Na+-dependent and Na+-independent transporters. However, transport of L-Arg is predominantly mediated by the Na+-independent y+ system (Palacin et al., 1998). The selectivity and affinity of the various transport systems for cationic amino acids are presented in Table 1.5. Properties listed in this table are commonly utilised in the literature to discriminate between different transport system present in a given cell type. Likewise, work of thesis has identified L-Arg transport systems present in endothelial cells based on these properties.

1.6.2.1 System y+ cationic amino acid transporters

The system y+ cationic amino acid transport system accounts for the majority of L-Arg transport in mammalian cells and importantly, is thought to play a key role in regulating L-Arg supply for NOS isoforms. Accordingly, numerous studies have demonstrated that system y+ is also the main system responsible for L-Arg transport in endothelial cells (Closs and Graf, 1999, Ogonowski *et al.*, 2000a) and, has also been found to be the major cationic amino acid transporter system in other NO producing cells. L-Arg transport occurs mainly via system y^+ at extracelullar L-Arg concentrations of 25 – 200 μM. At higher concentrations (over 1 mM), the influx of L-Arg may be mediated by a second low-affinity system, with K_m values in the millimolar range, or by a process of diffusion (Christensen and Handlogten, 1977). The reported plasma L-Arg level measured in the human ranges from 80-120 μM (Mendes Ribeiro et al., 2001). Uptake of L-Arg under physiological conditions in humans is mediated principally by the high affinity system y+ since the reported K_m of system y+ (0.04-0.25 mM) lies within the physiological concentration range of reported plasma L-L-Arg values (Closs, 1996).

System [a]	y^+	y^+L	b^{0+}	$B^{+,0}$	$b1^+/b2^+$
Transport of cationic amino acids					
+ Na^+	+	+	Lys uptake inhibited	+	+
– Na^+	+	+	+	–	+
Transport of small neutral amino acids					
+ Na^+	+(low affinity)	+/–	+	+	–
– Na^+	–	–	+	–	–
Transport of large neutral amino acids					
+ Na^+	–	+(high affinity)	+	+	
– Na^+	–	–	+	–	
Inhibition by N-ethylmaleimide (NEM)					
	+	–			
Inhibition by 2-aminobicyclo-(2.2.1)-heptane-2-carboxylic acid (BCH)					
	–	–	–	+	–

Table 1.5 Transport systems described for cationic amino acids. Taken from Closs *et al.* 1996 (Closs, 1996).

The transport activity of system y+ is characterised by i) a high affinity for cationic amino acids, ii) sodium independence iii) pH independence, and iv) stimulation of transport by substrate on the opposite (trans-) side of the membrane. System y+ is membrane potential dependent and interacts with neutral amino acids with a very low affinity. Its activity is attributed to the cationic amino acid transporter (CAT) family of monomeric transporters, encoded by SLC7A genes (Section 1.7) . The ubiquitously expressed CAT1, encoded by the gene SLC7A1, and the two transporters CAT2A and CAT2B, derived from the alternative splicing of the SLC7A2 gene, are the most well-characterised members of the family (Deves and Boyd, 1998).

1.6.2.2 Heterodimeric cationic amino acid transporters

Based on sequence homology, the heterodimeric amino acid transporter family is a subfamily of the SLC7 transporter family (the family of CAT transporters encoding cationic amino acid transporters of the system y+ family). Importantly, a major difference of this subfamily with the SLC7 transporter family is the y+L transport system via which heterodimeric transporters are able to facilitate the flux of cationic amino acids (Table 1.5)(Kanai and Endou, 2001). Heterodimeric transporters displaying properties of y+L mediate i) sodium-independent cationic amino acid transport, ii) sodium-dependent transport of neutral amino acids iii) are not regulated by membrane potential and iv) display a much higher affinity for cationic and neutral amino acids than the other systems, displaying apparent K_m values in the range of 5-10 μM (Deves and Boyd, 1998).

Members of the heterodimeric amino acid transporter family are comprised of two subunits, a light chain multiple membrane spanning protein linked via a disulfide bond to heavy chain single membrane spanning membrane glycoproteins such as 4F2hc (a constituent of system y^+L transport) and rbAT (a constituent of system $b^{0,+}$ transport). Light chain subunits are thought to catalyse the translocation of substrate, whereas the heavy chain subunit association is required for intracellular light chain trafficking and insertion in the plasma membrane. The heavy chain rbAT associates with the light chain $b^{0,+}$AT to form the amino acid transport system $b^{0,+}$, whereas the homologous heavy chain 4F2 can interact with several light chains to form system L (with LAT1 and LAT2),

system y^+L (with y^+LAT1 and y^+LAT2), system x^-_c (with xAT), or system asc (with asc1). System y^+L and $b^{0,+}$ are the only two functionally distinct heterodimeric cationic amino acid transport systems characterised which are capable of facilitating the flux of L-Arg at the plasma membrane. System y^+L heterodimeric transporters, 4F2hc/y+LAT1 and 4F2hc/y+LAT2, primarily mediate the efflux of L-Arg, and may be important in the kidney, where L-Arg is produced from citrulline and released into the blood to supply the rest of the body (Broer *et al.*, 2000, Pfeiffer *et al.*, 1999).

System y^+L activity was initially described by Deves *et al.* (Deves *et al.*, 1992) and has since been detected in placenta, intestine, lymphocytes and platelets (Mann *et al.*, 2003). System y^+L activity has generally not been detected in endothelial cells. Although, Sala *et al.*(Sala *et al.*, 2002) and others have reported the presence of endothelial y^+L activity in cultured human umbilical vein endothelial cells, in addition to system y+ activity. System y+L may contribute to the regulation of L-Arg supply for the NO pathway. However, this has not yet been convincingly demonstrated and studies that provide evidence of this are currently lacking.

Transport of cationic amino acids by the rbAT heavy chain/ $b^{0,+}$AT light chain heterodimer display almost identical properties to the amino acid transport system $b^{0,+}$ originally defined by Van Winkle et al. (Van Winkle *et al.*, 1988) in mouse blastocysts. System $b^{0,+}$ activity is principally found in the apical membrane of small intestinal epithelial cells and, the renal tubule epithelial cells of the kidney. System $b^{0,+}$AT light chain mRNA is expressed in kidney and small intestine, and, is also detectable in the heart, liver, placenta, and lung (Wagner *et al.*, 2001). Cationic and neutral amino acids are both transported by this system independently of sodium (Bertran *et al.*, 1992, Van Winkle et al., 1988). The affinity of cationic amino acids is several fold higher than neutral amino acids and so the negative membrane potential produced allows cationic amino acid influx in exchange for neutral amino acid efflux. Expression of system $b^{0,+}$ activity in endothelial cells has thus far only been described in pulmonary artery endothelial cells (Greene *et al.*, 1993). As for system y^+L, the contribution of system $b^{0,+}$ activity for the L-Arg-NO pathway in this endothelial cell type is relatively unknown.

Since heterodimers of system y^+L i) primarily stimulate the efflux of L-Arg, ii) the expression of system $b^{0,+}$ and y^+L heterodimers in endothelial cells is limited and iii) system y+ is the major system of L-Arg transport a major role in regulating L-Arg supply for eNOS in endothelial cells seems unlikely. However, genetic diseases associated with the dysfunctional transport of amino acids via system $b^{0,+}$ and y^+L are thought to contribute towards decreased plasma L-Arg levels in certain instances and influence endothelial function (Palacin *et al.*, 2001, Kayanoki et al., 1999). Under normal conditions polarised expression of system y^+L (4F2/y+LAT1) at the basolateral side of proximal tubule epithelial cells, allows for the efflux of cationic amino acids directly into the blood stream in exchange for large neutral amino acids and sodium ions. A transport dysfunction in the basolateral excretion of L-Arg and lysine from both the kidney tubule cells and intestinal mucosa results from a heritable defect in this transport system. Since the kidney is a major source of L-Arg produced within the body (Section 5.1) decreased levels in the plasma due to a defective y+L contribute to the development of endothelial dysfunction and impaired NO release (Section 4.4.4).

1.6.2.3 Sodium-dependent cationic amino acid transporters

System $B^{0,+}$ represents the only sodium-dependent system for cationic amino acids and neutral amino acids. The substrate affinities of $B^{0,+}$ are similar to system $b^{0,+}$, but also accepts small neutral amino acids. A human cDNA encoding a sodium- and chloride-dependent amino acid transporter with similar properties as system $B^{0,+}$ has recently been isolated and has been named $ATB^{0,+}$ (Sloan and Mager, 1999). Its tissue distribution includes the lung, salivary gland, mammary gland, stomach and pituitary gland. Since cationic amino acid transport in the endothelium is predominantly Na+-independent, system $B^{0,+}$ is thought to have a negligible role in mediating transport of L-Arg and supply for NOS.

1.6.2.4 Other cationic amino acid transporter types

A separate cationic amino acid transport system, b^+ has been previously identified which displays high affinity for L-Arg. There has been no molecular identification of this system to date and it is thought that its expression is confined to the early embryonic stage (Closs, 2002). Additional to the existing transport systems for L-Arg which have been characterised, recent findings indicate that cationic amino acids can serve as substrates for a member of the glutamine transporter family, hNAT3, expressed in the liver (Closs, 2002). There is no evidence to support a role for either of these systems in regulating NO production.

1.7 *System y+/Cationic Amino Acid Transporters (CAT's)*

1.7.1 Discovery

The first member of the cationic amino acid transporter (CAT) family of proteins was originally ascribed a function as integral membrane receptors due to its suseptibility to infection by murine ecotropic leukemia viruses (MuLV). Subsequent studies led to the isolation of cDNA encoding this protein (Albritton *et al.*, 1989). Structural similarities with L-arginine permeases in yeast suggested that this receptor for MuLV might also have transporter properties (Kim *et al.*, 1991). Expression studies in *Xenopus* oocytes led to its identification as a cationic amino acid transporter, re-named CAT-1 (Kim et al., 1991, Wang *et al.*, 1991). CAT-1 cDNA encodes a protein of 622 amino acids (62 kDa). According to the currently favoured model of Albritton *et al.* (Albritton et al., 1989) CAT-1 is an integral membrane protein that is extremely hydrophobic, spans the membrane 14 times, has its N- and C-terminus intracellularly and contains three N-linked glycosylation sites (Figure 1.9). The second member of the family, CAT-2B, was initially identified in a T-lymphoma cell line. (MacLeod *et al.*, 1990). The liver specific-isoform CAT-2A was identified due to to its high sequence homology with CAT-2B (Reizer *et al.*, 1993). In fact, CAT-2A only differs within a sequence stretch of 120 nuclotides encoding a 42 amino acid located within the fourth putative intracellular loop. A 97% sequence similarity between CAT-2A and CAT-2B is due to differential splicing variants of the same gene, SLC7A2 (Closs, 1996). Whilst these two proteins share the same substrate specificities they differ markedly in their affinites for cationic amino acids. The fourth member of the family, CAT-3, was identified exclusively in the rat brain (Hosokawa *et al.*, 1997). A lesser well-characterised member, CAT-4 (Sperandeo *et al.*, 1998) has recently been identified. All CAT proteins are classified as members of the APC family, a family of transporters specific for amino acids, polyamines, and choline, which catalyse solute transport in yeast, fungi and eubacteria (Reizer et al., 1993).

1.7.2 Properties

Cationic amino acid transport by CAT isoforms is dependent on both substrate concentration and cellular voltage gradients. The negative resting membrane potential favours the influx of cationic amino acids (Deves and Boyd, 1998). Since CAT-1 is expressed in most cell types it can be difficult to distinguish the individual contribution of each CAT isoform present. Kinetic analysis does reveal some important differences. Based on their substrate affinities, CAT isoforms are classified as high-affinity transporters (CAT-1, CAT-2B, CAT-3) and low-affinity transporters (CAT-3). Reported affinity constants for L-Arg range from 0.04-0.25 mM for CAT-1, 2-5 mM for CAT-2A, 0.04-0.38 mM for CAT-2B, and 0.04-0.12 mM for CAT-3(Closs and Graf, 1999). Affinity constants for the other cationic amino acid substrates, L-ornithine and L-lysine are similar to that reported for L-Arg for all CAT isoforms. CAT-1 and CAT-2B display a very low affinity for neutral amino acids such as leucine in the presence of sodium ions whereas CAT-3 displays higher affinites for neutral amino acids and a specificity for L-Arg and D-Arg (Closs, 1996).

Facilitated transport by most CAT isoforms is bi-directional (influx and efflux). The direction of transport is dependent on at least two factors. Recognition of substrate on both sides of the membrane by CAT proteins can influence the direction of transport. This property is referred to as *trans*-stimulation and is displayed by an increase in transport when the *trans*-side substrate is increased (Deves and Boyd, 1998). CAT isoforms display different sensitivities to *trans*-stimulation. CAT-1 and CAT-2B are sensitive to trans-stimulation whilst CAT-2A is not suseptible (Closs, 2002).

Tissue and cellular expression profiles of individual CAT isoform(s) might be expected to give an indication of their basic function in meeting the metabolic needs for L-Arg in a particular organ or tissue type. However, multiple CAT isoform types are often found in a single tissue type where the expression of a single CAT isoform should only be required. Aside from their relative affinities for L-Arg and other defined kinetic properties in various culture systems *in vitro*, the major difference

amongst CAT isoforms seems to be their responsiveness to various types of signals. Mitogenic stimuli have been shown to increase both CAT-1 and CAT-2B gene expression in vascular smooth muscle cells, which is thought an important mechanism for increased substrate provision in protein and polyamine biosynthesis (Durante, 2001). Angiotensin II stimulates both CAT-1 and CAT-2B mRNA expression in vascular smooth muscle cells (Low and Grigor, 1995) whereas interleukin-1β and tumor necrosis factor-α stimulate CAT-2B but not CAT-1 expression (Gill *et al.*, 1996). Platelet-derived growth factor treatment of smooth muscle cells strongly induces CAT-2B mRNA expression but only moderately induced CAT-1 mRNA expression (Durante *et al.*, 1996). In cardiac myocytes, interleukin-1β and interferon-γ co-induced CAT-1, CAT-2B, and CAT-2A, whereas insulin increased only CAT-1 levels (Simmons et al., 1996). In resting myocytes, only CAT-1 is expressed (Simmons et al., 1996). In the resting state CAT-2A is exclusively expressed in the liver, however in regenerating liver cells after partial hepatectomy CAT-1 expression is induced (Wu *et al.*, 1994). In cells which are capable of NO production, L-Arg transport activity displaying properties of system y+/CAT transporters is known to be modulated by various factors such as LPS, interleukin-1β, tumor necrosis factor-α, insulin, angiotensin II, and bradykinin (Closs and Graf, 1999).

1.7.2.1 CAT1 (ubiquotously expressed isoform).

The cationic amino acids lL-Arg, L-ornithine and L-lysine are primarily transported into mammalian cells via a distinct amino acid transporter first described in Ehrlich ascites tumor cells by Christensen and colleagues and originally designated as system Ly+ (Christensen and Liang, 1965) .The molecular identity of the cationic amino acid transporter in that early study has since been cloned and is now referred to as cationic amino acid transporter-1 (CAT-1). Its constitutive expression in most cell types signifies a major role for CAT1 in sustaining the basal nutritional requirements of a cell for cationic amino acids. A high degree of sequence conservation between species suggests that the functional properties of CAT-1 are conserved. The deduced amino acid

sequence of mouse CAT-1 is 95.8% and 86.5% identical to rat CAT-1 and human CAT-1 respectively in alignment.

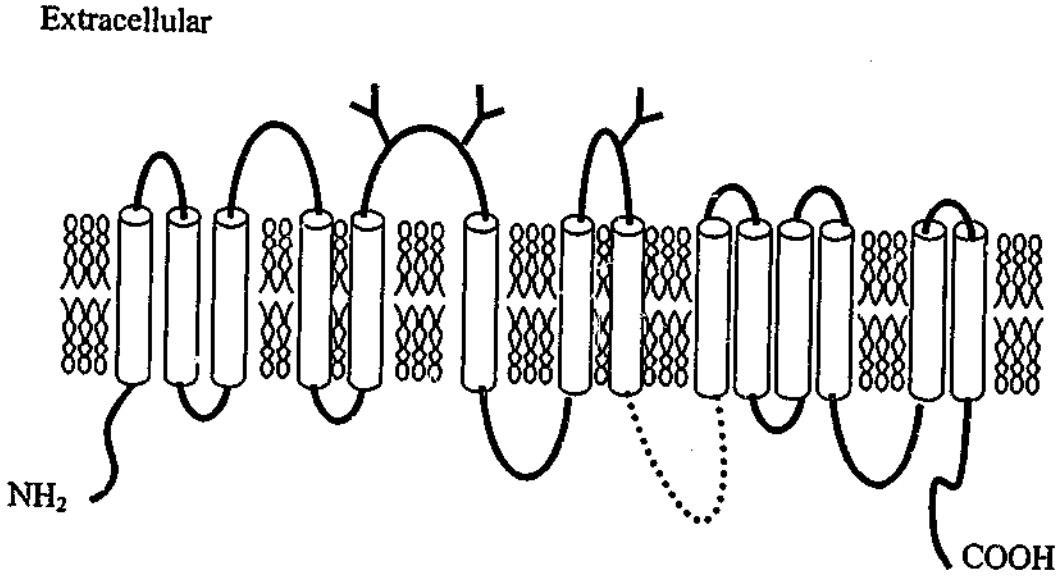

Figure 1.9 Model for mCAT-1 in the plasma membrane. Dashed fork lines displayed are predicted N-linked glycosylation sites in the third and fourth extracellular loop. A single dashed line in the fourth intracellular loop represents the domain that determines transport properties of the various CAT family members. Adapted from Closs *et al.* 1996 (Closs, 1996).

CAT-1 is constitutively and widely expressed and has been found in all tissues investigated with the exception of the liver. The predominant CAT isoform expressed in endothelial cells is CAT-1. Although, in cardiac microvascular and human umbilical vein endothelial cells, cytokine treatment has been reported to induce CAT-2B expression (Irie *et al.*, 1997). A caveolar co-localisation complex with caveolin and eNOS is suggestive of a major role for CAT-1 in NO production (McDonald et al., 1997, Lu and Silver, 2000). Additionally, NO agonists such as histamine, A23187, bradykinin have all been shown to rapidly modulate system y+/CAT-1 activity in

endothelial cells. Bradykinin is thought to modulate system y+/CAT-1 activity through a mechanism involving increased potassium ion permeability and membrane hyperpolarisation (Deves and Boyd, 1998). Whereas membrane hyperpolarisation is known to increase system y+/CAT-1 transport activity membrane depolarisation can result in a reduction in transport activity. Pharmacologic studies in bovine endothelial cells using the NO donor, S-nitroso-N-penacillamine (SNAP), have indicated that the activity of CAT-1 may be modulated by the production of NO itself (Ogonowski et al., 2000b). In addition homocysteine, insulin and glucose have also been shown to modulate system y+ (CAT-1) activity (Jin *et al.*, 2001, Flores *et al.*, 2003).

CAT-1 is expressed at high levels in proliferating cells, emphasising the importance of the CAT-1 protein for growth and development. Various signals that cause transition of cells from the resting state to the proliferating state appear to activate CAT-1 expression (Aulak *et al.*, 1999). Aulak *et al.* (Aulak *et al.*, 1996) identified CAT-1 as a delayed early response gene in the regenerating liver. Hormone treatment with insulin and dexamethasone can also upregulate CAT-1 gene expression in the liver. Increased CAT-1 gene expression is also evident in proliferating T and B lymphocytes (Yoshimoto *et al.*, 1992). A role is cell proliferation has been highlighted by the development of a CAT-1 knockout mouse model. Homozygous knockout mice (CAT-1 -/-) are severly anemic and die within 12 hr of birth. Erythroid maturation was found to be defective in the knockout mice suggestive of an abnormality in cell proliferation and differentiation (Nicholson *et al.*, 1998).

1.7.2.2 CAT2A (liver-derived isoform)

CAT-2A is highly expressed in the liver but can also be expressed in other cell types such as skin, ovary, stomach and skeletal muscle following surgical trauma or fasting. A lack of high-affinity CAT-1 and CAT-2B isoforms in the liver is thought to protect extracellular L-Arg from hydrolysis by hepatic arginase (Palacin et al., 1998). Due to its lower affinity for L-Arg (2-5 mM) CAT-2A allows hepatocytes to rapidly take up cationic amino acids at high plasma concentrations (such as

after a high protein meal), while leaveing a sufficient amount in the circulation for other cell types that express the high–affinity CAT isoforms.

1.7.2.3 CAT2B (T-cell/macrophage-derived isoform)

Inflammatory stimuli have been shown to preferentially upregulate the CAT-2B isoform. Activation of macrophages and brain astrocytes by lipopolysaccharide and interferon-γ results in the parallel induction of CAT-2B/system y+ activity and iNOS. The activity of iNOS is dependent on extracellular substrate for high-output pathologic NO. Thus induction of the CAT-2B transporter is a crucial step for NO production (Nicholson et al., 2001, Kakuda *et al.*, 1999). This has recently been confirmed in CAT-2B knockout mice (Nicholson et al., 2001). Treatment with apolipoprotein E has also been shown to modulate CAT-2B expression in macrophages and increase NO production (Colton *et al.*, 2001). There is evidence to suggest that atrial natriuretic peptides can attenuate inflammatory NO production by macrophages though the suppression of CAT-2B activation and/or induction (Kiemer and Vollmar, 2001). BH_4 has been shown increase the basal expression of CAT-2B in cardiac myocytes (Schwartz *et al.*, 2001).

1.7.2.4 CAT3 (neuronal-specific isoform)

The expression of CAT-3 seems to be regulated in a highly tissue-specific manner since CAT-3 expression is found to be confined to the brain at either the adult or primitive streak stage in mice and rats (Ito and Groudine, 1997, Hosokawa et al., 1997). However, a wider distribution profile has been reported in the 13.5 day post-coitum mouse embryo (Ito and Groudine, 1997). The neuron-specific distribution pattern detected for the CAT-3 transcript in the mouse brain suggests a potentially different role for this transporter. A specific role of CAT-3 in providing substrate for neuronal NOS (nNOS) has been proposed based on the neuron-specific expression of CAT-3 in the rat brain (Hosokawa *et al.*, 1999). By contrast, expression studies performed by Vekony *et al.*(Vekony *et al.*, 2001) have clearly shown that expression of CAT-3 is not confined to the human

brain. In addition to the brain, human CAT-3 is also strongly expressed in the thymus and, at a lower level of expression in other peripheral tissues. The same group found no overlap between CAT-3 and nNOS expression either in the central nervous system, thymus or other peripheral tissues. Therefore, the specific function of CAT-3 remains unknown. Of interest, mouse CAT-3 has been shown to compensate for the loss of functional CAT-1 in fibroblast cells derived from CAT-1 knockout mice (Nicholson et al., 1998).

1.7.2.5 CAT4; no known transport function.

A fourth member, CAT-4, has recently been cloned which exhibits significant sequence homology with the family of human CATs (hCATs) (Sperandeo et al., 1998). Abundant mRNA expression of hCAT-4 has been demonstrated in the brain, testis and placenta. After expressing human CAT-4 in *Xenopus* oocytes, Closs and colleagues (Wolf *et al.*, 2002) were unable to detect any transport activity of cationic, neutral or anionic amino acids. In contrast, earlier work by Sperandeo *et al.* (Sperandeo et al., 1998) reported a significant stimulation of cationic amino acid transport after expression of the same CAT-4 clone in the same cell type. Therefore, it has not been concluded whether CAT-4 has a transport function.

1.7.3 Regulation

Cationic amino acid transport is a regulated process. A growing body of evidence now suggests that regulation of CAT genes may occur at either at the transcriptional, post-transcriptional (see review (Aulak et al., 1996), translational, or post-translational level (Macleod and Kakuda, 1996, Closs, 2002). Targets for CAT-1 and CAT-2 regulation include the long 3' –untranslated mRNA region (Closs, 2002) and 5'-untranslated mRNA region (Fernandez *et al.*, 2001) and N-linked glycosylation sites which have been implicated in the regulation of mRNA stability (Ross, 1996) and membrane trafficking (Helenius and Aebi, 2001, Nguyen and Amara, 1996). A complex

regulation of CAT expression is emerging which is suggestive of specific roles for each individual CAT isoform.

In an earlier *in vitro* study, Baydoun *et al.* (Baydoun *et al.*, 1990) found that after 24 hr of L-Arg deprivation the intracellular concentration of cationic amino acids did not change in cultured endothelial cells. However, the rate of cationic amino acid transport via system y+ was significantly increased. The mechanism for this was not known at that time. Hyatt *et al.* (Hyatt *et al.*, 1997) also demonstrated a similar effect in rat hepatoma cells which was accompanied by a signficant induction of CAT-1 expression. A recent series of publications by Hatzoglou and collegeaus (Fernandez *et al.*, 2002a, Fernandez et al., 2001, Fernandez *et al.*, 2002b) have convincingly demonstrated that increased CAT-1 expression in response to amino acid deprivation is due to a mechanism involving post-transcriptional regulation. An internal ribosome entry sequence was identified within the 5'-untranslated region that causes an increase in translation of CAT-1 mRNA in response to amino acid deprivation. This indicates that CAT-1 gene expression is regulated by nutrient supply. Mechanisms of CAT-2B regulation have not been widely studied to date. CAT-2B and iNOS induction in response to lipopolysaccharide and interferon-γ has been linked to the activities of NK-κB and p38 MAP kinase in macrophages and rat aortic smooth muscle cells (Hammermann *et al.*, 2000, Baydoun *et al.*, 1999).

1.7.4 A Potential Role of CAT-1 in Endothelial Dysfunction

As a potential mechanism for endothelial dysfunction, a great deal of interest surrounds the question of whether the supply of L-Arg might actually be rate-limiting for the synthesis of NO in endothelial cells (Section 5.4.1 and 4.4.4). Interestingly, multiple factors with may affect endothelial function (Section 1.3.4) in CHF have also been shown to modulate L-Arg transporter activity in various cell types (Closs and Graf, 1999). Since CAT-1 predominantly mediates system y+ in endothelial cells and provision of extracellular L-Arg is proposed as a rate limiting factor in NO production *in vitro* (Section 5.4.1) and *in vivo* (Section 4.4.4 and 4.5.7) it is reasonable to

suppose that impairment of L-Arg transport may be a factor in decreased NO production. CAT-1 has recently been shown to co-localise with eNOS in the caveolae and is suggestive that compartmentalisation may be a way for system y+/CAT-1 directed delivery for the NO pathway, rather than be directed towards other L-Arg metabolic pathways (McDonald et al., 1997).

1.8 Major Aims Of This Thesis

Outcomes of numerous basic and clinical studies which seek to identify and characterise mechanisms that may lead to endothelial dysfunction in various cardiovascular disorders, including CHF, point to the involvement of a reduced substrate availability for NOS. Most studies do not demonstrate whether a reduced substrate availability exists. Additionally, such studies do not determine whether reduced substrate availability occurs at the level of intracellular substrate utilisation by NOS, or if it is due to reduced uptake of L-Arg across the cell membrane. Positive outcomes on endothelial function due to L-Arg supplementation studies in CHF are suggestive that a deficiency due to extracellularly derived L-Arg contributes to reduced NO bioavailability in humans. Based on evidence presented within this Chapter, a deficiency might potentially be due to reduced plasma L-Arg concentration, increased levels of endogenous competing agents for system y+ transport or alternatively a reduction in the rate of L-Arg transport. The major hypothesis of this thesis is that a reduced rate of L-Arg transport contributes to endothelial dysfunction in CHF.

The aims of this thesis are:

(1) to design an *in vitro* model for the evaluation of L-Arg transporter activity in human CHF, as a potential mechanism for depressed endothelial function in CHF

(2) to characterise the expression and activity of system y+/CAT L-Arg transporters in the peripheral and coronary CHF circulation

(3) to evaluate the effect of cytokines and neurohormones relevant in the setting of CHF on L-Arg transporter activity on cultured human venous endothelial cells

Based on the results of Chapter 4, Section 2.

(4) to investigate a potential role for the protein kinase C pathway in modulation of endothelial L-Arg transporter activity.

Chapter Two

Common Methodology

TABLE OF CONTENTS

2.0 General Introduction *79*

2.1 Cell Culture *79*

2.1.1 General Maintenance **79**

2.1.1.1 Storage of cells 79

2.1.1.2 Counting of cells 79

2.1.1.3 Subculturing cells 80

2.1.1.4 Serum inactivation 80

2.1.2 Primary Cell Culture of Bovine Aortic Endothelial Cell, BAEC **80**

2.1.3 Cell Culture of Human Endothelial Cell Line, EA.hy926. ..... **81**

2.2 Gene Expression *82*

2.2.1 Extraction of Total RNA **82**

2.2.1.1 Human myocardium 82

2.2.1.2 PBM 82

2.2.1.3 Cultured endothelial cells 83

2.2.2 Analysis of Extracted RNA **83**

2.2.3 Detection of Gene Expression by RT-PCR **84**

2.2.4 Semi-quantitative RT-PCR **86**

2.2.4.1 Limitations 86

2.2.4.2 Protocol 86

2.2.5 Ribonuclease Protection Analysis **88**

2.3 DNA Methodology *90*

2.3.1 Plasmid constructs **90**

2.3.2 Amplification of cDNA constructs **90**

2.3.3 Measurement of DNA concentration 91

2.4 Measurement of endothelial NO Synthase (eNOS) Activity *91*

2.5 Immunoreactivity Studies *92*

2.5.1 Raising CAT-1 rabbit polyclonal antibody 92

2.5.2 SDS-PAGE 94

2.5.3 Western blot 95

2.5.4 Stripping membrane for re-probing 95

2.0 General Introduction

This chapter describes routine procedures and basic protocols performed for the work of this thesis. Modifications, omissions and inclusions to these protocols are detailed in the relevant chapters. Unless noted all general reagents were purchased from Sigma and ICN. Cell culture reagents were from Gibco.

2.1 Cell Culture

2.1.1 General Maintenance

All cells were cultured in a humidified incubator with 5% CO_2 at 37°C and fed with growth medium as required, usually every 2 or 3 days.

2.1.1.1 Storage of cells

Freezing medium (Sigma) containing 1 x 10^7 cells/mL were stored in liquid nitrogen in 1.5 mL freezing vials. Before storage, the cells were cooled to -70°C at a rate equal to approximately 1°C / minute. Cells were recovered from liquid nitrogen by quickly thawing at 37°C in a water bath and adding wash medium dropwise to a final volume of 10 mL. After centrifugation at 500 x g for 5 min, the supernatant was discarded and the cells resuspended gently in 10 mL of growth medium.

2.1.1.2 Counting of cells

Cell count and viability of peripheral blood mononuclear cells were assessed simultaneously using a haemocytometer (Weber Improved Naebauer, BDH). 10 µL of the cell suspension was mixed with an equal volume of 0.1 % w/v trypan blue and flooded into a prepared haemocytometer. Cells excluding the dye were dead cells and excluded. An alternative automated method of cell counting using a Coulter Counter (Beckman Instruments) was a routine option for subculturing endothelial cells.

2.1.1.3 Subculturing cells

Upon reaching confluency, old growth medium was aspirated and the cell monolayer was rinsed once with Dulbecco's phosphate buffered saline (D-PBS; Gibco), calcium and magnesium free. D-PBS was replaced with a cell dissociation solution containing 0.1% w/v Trypsin/ 0.2% w/v Versene solution (CSL Biosciences) applied at 0.05 mL/cm^2. Cell plate was placed in a 37°C incubator until cell dissociation was achieved (~5 min). Cell suspension was transferred to a 14 mL sterile Falcon tube containing an equal volume of growth medium containing 10% fetal bovine serum (FBS; CSL Biosciences) to inactivate trypsin. After centrifugation at 500g for 5 min, cells were resuspended in the appropriate growth medium and divided after initial cell counting according to the experimental protocol.

2.1.1.4 Serum inactivation

Serum supplement used in all protocols was heat-inactivated for 30 min at 56°C to inactive complement. In order to minimise lot-to-lot variation in FBS, one lot was supplied and tested for its ability to promote cell growth equivalent to a laboratory standard.

2.1.2 Primary Cell Culture of Bovine Aortic Endothelial Cell, BAEC.

Primary bovine aortic endothelial cell were cultured according to methods previously described with slight modifications. (Cocks *et al.*, 1985, Cocks and Angus, 1985) Fresh bovine aorta sections were excised and collected from the slaughterhouse, which slaughters healthy cows for human consumption. Excess fat and sinew were removed on site. Approximately four thoracic aortas were rinsed in D-PBS containing magnesium, without calcium and layed out on autoclaved aluminium foil, wrapped and placed on ice for transportation back to the laboratory. Aortas were held with forceps over a sheet of foil and beaker and thoroughly rinsed through with D-PBS before proceeding with primary culture. Aortas were cut longitudinally to expose the lumen. After rinsing the lumen surface with D-PBS, a sterile flat scalpel blade was used to scrape a few times gently along the lumen surface rinsing the blade in a freshly prepared sterile filtered 600 U/mL

collagenase type IV (Sigma), in PBS without FBS after each scrape. Care was taken not to apply excess pressure in order to avoid the risk of smooth muscle cell contamination in the resulting preparation. The collagenase suspension containing cells and debris was then placed in a 5% CO_2/37°C incubator for approximately 15 min, gently pipetting the suspension every 5 min to assist in dispersion of cells. After centrifugation at 100g for 10 min, cells were resuspended in 5 mL 20% FBS + Dulbecco's modified Eagle's medium (DMEM) growth medium containing 5 mM supplemental glutamine (Sigma), 100 U/mL penicillin G, 100 µg/mL streptomycin sulphate, 2.5 µg/mL fungizone solution (Penicillin-streptomycin-fungizone solution, CSL Biosciences) and gentamycin 80,000 IU. Repeat this centrifugation step once more. The resulting cell suspension was transferred to a 60 mm cell culture dish. After 24 hr growth medium was replaced with fresh medium. Upon confluency cells were subcultured according to the methods described in this section and labeled S_1. For experimental purposes, S_1-S_6 were used. Endothelium can be characterised by the presence of factor VIII-related antigen (Booyse *et al.*, 1975). Primary endothelial cells were verified as pure based on morphology and immunohistochemistry staining for factor VIII-related antigen. These cells were also 100% negative for α-actin smooth muscle expression.

2.1.3 Cell Culture of Human Endothelial Cell Line, EA.hy926.

A permanently established and differentiated human endothelial cell line, EA.hy926 (a generous gift from Cora-Jean Edgell, University of North Carolina), was maintained in DMEM supplemented with 10% FBS, 5 mmol/L hypoxanthine, 0.8 mmol/L thymidine, 20 µmol/L aminopterin (HAT supplement, Gibco), 100 U/mL penicillin G, 100 µg/mL streptomycin sulphate and 2.5 µg/mL fungizone. This line was established through the fusion of human umbilical vein endothelial cells with the permanent human cell line A549, a human carcinoma cell line.

2.2 *Gene Expression*

Reagents for bacterial propagation were obtained from Difco. Restriction enzymes were obtained from Promega and all other reagents used were of molecular biology grade. All solutions unless otherwise stated were prepared in distilled/deionised (MilliQ) water and autoclaved. The ribonuclease inhibitor, (DEPC, Sigma), was used to treat MilliQ at a concentration of 0.2% w/v in certain instances.

2.2.1 Extraction of Total RNA

Total RNA was extracted according to the method of guanididium isothiocyanate/phenol/chloroform extraction (Chomczynski and Sacchi, 1987). Alternative steps for initial cell or tissue preparations are as follows:

2.2.1.1 Human myocardium

Frozen tissue (~100 mg) previously stored at -70°C was finely ground under liquid nitrogen and then transferred to a sterile 15 mL Falcon tube containing 1mL of denaturing solution (4 M guanidinium thiocyanate, 25 mM sodium citrate pH 7.0, 0.5% sarkosyl, 0.1 M 2-mercaptoethanol) and given three bursts at high speed with a Polytron homogeniser.

2.2.1.2 PBM

Frozen cell pellets containing 1 x 10^7 cells were thawed on ice and resuspended in 500 µL denaturing solution. Cell suspension was sheared repeatedly using a pre-cooled 1 mL syringe fitted with a 25 G needle. Samples were incubated on ice for 15 min prior to proceeding. All stated volumes were scaled down by half for RNA isolation from PBM in the following steps.

2.2.1.3 Cultured endothelial cells

Cell monolayers in 100 mm petri dishes were rinsed twice with cold D-PBS. Following the final rinse 1 mL denaturing solution was added directly onto petri dish. Cell monolayers were scraped and harvested using a rubber cell scraper. The resulting cellular homogenate was transferred to a sterile 15 mL Falcon tube. Homogenate was then passed through a sterile 1 mL pipette tip several times. Samples were incubated on ice for 15 min before proceeding.

Homogenates of either PBM, myocardium or cultured endothelial cells were sequentially mixed with 1 mL of water saturated phenol, 200 µL chloroform-isoamyl alcohol (49:1) and sodium acetate and then incubated on ice for 15 min. The final mixture was vortexed vigourously and then centrifuged at 10 000 g for 20 min at 4°C. The upper aqueous phase was transferred to a fresh tube and then mixed with an equal volume of 100% isopropanol. Total RNA was cooled at -20°C for 1 hr and then pelleted by centrifugation at 10 000 g for 15 min at 4°C. Supernatant was removed and the pellet was resuspended in 300 µL of denaturing solution. The pellet was vortexed and then precipitated with an equal volume of 100% isopropanol at -20°C for 1 hr. Following centrifugation at 10 000 g for 10 min at 4°C, supernatant was removed and 800 µL 70% v/v ethanol was added to the RNA pellet. After vigourous vortexing to wash the pellet, RNA was left at RT for 10 min to dissolve all contaminating salts and then sedimented by centrifugation at 10 000 g for 10 min at 4°C. This wash step was repeated once more. After removing supernatant from the final wash, the RNA pellet was dried under vacuum for 5 min using a Speedy-Vac. The RNA pellet was dissolved in 100 µL of DEPC-treated water by passing the solution through a pipette tip several times followed by an incubation step for 15 min at 55 °C. Total RNA was stored at -70°C until further use.

2.2.2 Analysis of Extracted RNA

RNA integrity was determined visually by ethidium bromide fluorescence after separation on a 1% formaldehyde agarose gel. Total RNA was quantified by spectrophotometric analysis at 260 nm against reagent blanks. An optical density (OD) reading of 1 was considered to correspond with 40 µg RNA (Sambrook *et al.*, 1989).

2.2.3 Detection of Gene Expression by RT-PCR

RNA (400 ng) from PBM was reverse transcribed using 1X PCR buffer, MuLV RT, dNTP's and oligo(dT) in a 50 µL reaction mixture to produce PCR template cDNAs according to the manufacturers instructions (PerkinElmer). Primer oligonucleotide sequences were synthesised by Genset Pacific Pty Ltd as indicated in Table 2.1. Primer sequences were selected according to the following criteria i) intron spanning to prevent contaminating genomic DNA amplification ii) <50% G/C rich iii) 3' GC end clamping iv) minimai primer/dimer, hairpin secondary structure prediction and v) no significant sequence homology to other known genes contained in a database using the BLAST search engine: (http://www4.ncbi.nlm.nih.gov/BLAST/). For the detection of CAT-1 products, PCR amplification was performed for 40 cycles of 30 sec at 95°C denaturation, 30 sec annealing at 63°C and 1 minute extension at 72°C using *Taq* polymerase and 1.5 mM $MgCl_2$. Sequence verification of the cloned PCR products were determined using the same primers and dideoxy chain-termination methodology (ABI Prism 377 DNA sequencer). PCR cycle parameters were independently optimised for the detection of NOS isofoms listed in Table 2.1.

Table 2.1 Primers employed for RT-PCR

Gene name	Genebank number	Primers (5'- 3')	Size (bp)
CAT1	x59155	**F** CCCCCGGCGTGCTGGCTGAAAA	448
		R CGACACCCCAAAGTAGGCGATGAA	
CAT2A	U76368	**F** CTTTACCCCGAATTCTGTTTG	115
		R AAATGACCCCTGCAGTCAACG	
CAT2B	U76369	**F** CCCAATGCCTCGTGTAATCTA	121
		R TGCCACTGCACCCGATGATAA	
4F2hc	NM_008577	**F** CACAAGAACCAGAAGGATGA	941
		R ACTACCAGAAAACGCTCATT	
β-Actin	NM_001101	**F** GGCTACAGCTTCACCACCAC	490
		R GCTTGCTGATCCACATGTGC	
nNOS	U17327	**F** GTCGAATTCCGAATACCAGCCTGATCCATGGAA	618
		R CGCGGATCCCATGCGGTGGACTCCCTCCTGGA	
eNOS		**F** GTCGAATTCCTGGCGGCGGAAGAGAAAGGAGTC	756
		R CGCGGATCCGGGGCTGGGTGGGGAGGTGATGTC	
iNOS	M89952	**F** AGGGTGGAAGCGGTAACAAAGG	322
		R ATCTGGTAGCCAGCATAGCGGA	

2.2.4 Semi-quantitative RT-PCR

2.2.4.1 Limitations

Briefly the semi-quantitative RT-PCR approach involves reverse transcription of RNA to cDNA and subsequent amplification followed by semi-quantitation of target mRNA expression levels in each sample normalised with respect to an endogenous control, β-Actin, whose expression levels were measured under identical conditions, exclusive of cycle length. This approach was employed in early PhD work to evaluate system y+/CAT mRNA expression in peripheral blood mononuclear cells isolated from healthy controls and heart failure patients. Optimisation of various parameters was performed before semi-quantitation of the various target genes according to standard methods. For example, variation of PCR cycle length for primers enabled the selection of a suitable cycle length based on the linear relationship of PCR product with cycle length (CAT-1 and CAT-2B experiments depicted in Figure 1.1). Whereas significant alterations were detected in the mRNA expression levels of CAT1 in CHF by a quantitative RNAse protection analysis (Chapter 3.2) no alterations of CAT-1 were detected by semi-quantitative RT-PCR when normalised with the expression of β-Actin. A recent study that reports on a two-fold decrease in β-actin gene expression in human CHF (Yang *et al.*, 2000) may contribute to the inconsistent result obtained by semi-quantitative RT-PCR analysis. Thus, the semi-quantitative mRNA approach in pathophysiologic states holds the caveat that expression of normalisation genes may also be altered. For this reason, all semi-quantitative RT-PCR analysis of mRNA expression in this laboratory was replaced by a more quantitative method of mRNA expression, RNAse protection analysis (Chapter 2.2.5).

2.2.4.2 Protocol

Total RNA was extracted from PBM according to the protocol described (Chapter 2.2.1). Integrity and quantification of total RNA was analysed as described (Chapter 2.2.2). An option for removal of contaminating DNA, DNAse I treatment step was included in some instances. The GeneAmp® RNA PCR Core Kit (Perkin-Elmer) was used for the detection and analysis of gene expression. A

reverse transcription reaction mixture was prepared in 0.2 mL tubes for each sample using the manufacturers PCR buffer II containing 1.5 mM $MgCl_2$, 1 mM dGTP, 1 mM dATP, 1 mM dTTP, 1 mM dCTP, 2.5 μM Oligo d(T) primer, 1 U Rnase inhibitor, 1 U MuLV Reverse transcriptase and 400 ng RNA in a total volume of 25 μL. Oligo d(T), the primer used for cDNA synthesis was chosen based on its increased specificity for only reverse transcribing eukaryotic mRNA. All samples were incubated at RT for 10 min and then placed in a Perkin-Elmer GeneAmp® PCR thermocycler 9600 for reverse transcription according to the following conditions: 1 cycle of reverse transcription at 42 °C for 15 min, denaturation at 95 °C for 5 min and a final cooling period at 4 °C for 10 min.

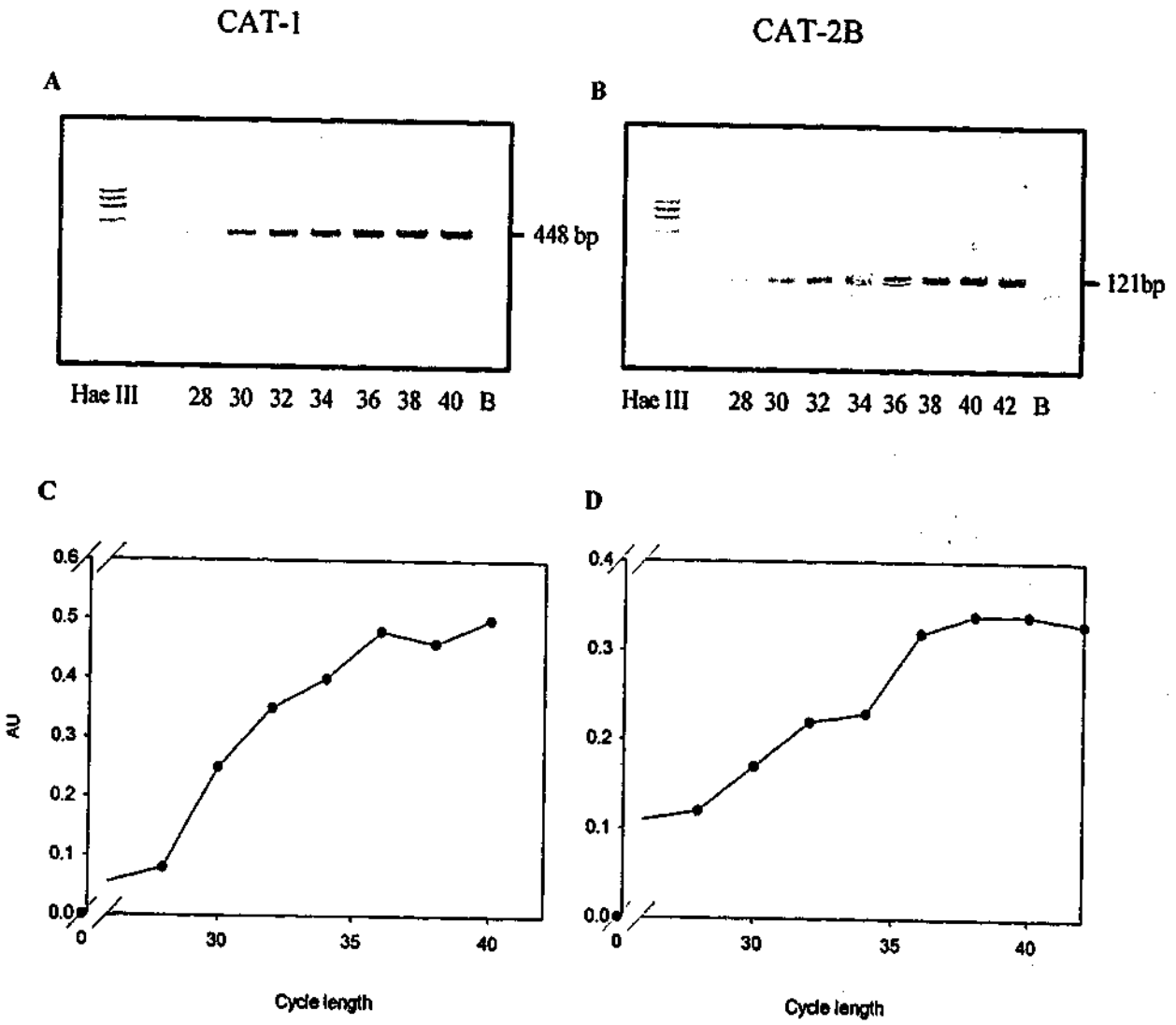

Figure 2.1. Effect of RT-PCR cycle length on CAT-1 and CAT-2B gene expression. 400 ng of total RNA extracted from peripheral blood mononuclear cells were reverse transcribed and then subjected to PCR for different cycle lengths using isoforms specific primers. Amplified fragments and relative densitometric values (AU) corresponding to either CAT-1 (panel A and C) or CAT-2B (panel B and D) are depicted.

Sample (5 μL) from the reverse transcription mixture containing newly synthesised cDNA was combined with 20 μL preparations of PCR mixture using the manufacturers PCR buffer II containing 1.5 mM $MgCl_2$, 2.5U of *Taq* polymerase, and 150 pM of relevant sense and anti-sense primer pairs. PCR was performed according to the following conditions: Initial denaturation cycle at 94°C for 30 sec, followed by 35 cycles of denaturation at 94°C for 30 sec, annealing at 63°C for 30 sec and extension at 72 °C for 1 minute, and a final cycle of extension at 72 °C for 10 min. Cycle length was modified to 18 cycles for amplification of β-Actin cDNA. The PCR cycle numbers were optimised for each primer to ensure that the comparison of the level of expression of each gene was within the linear phase of amplification in order to obtain a proportional relationship between input RNA and densitometric readout (Figure 1.1). Aliquots (10 μL) of all PCR products were combined with 1X DNA loading buffer (Sambrook et al., 1989) and subjected to electrophoresis alongside DNA markers on a 1.8 % agarose gel containing ethidium bromide in Tris borate EDTA buffer. A HaeIII digest of ϕ-X174 DNA (Promega Inc.) was used as the standard marker. Polaroids were taken using Black and White negative film (Kodak). The abundance of the PCR product was semi-quantified by further analysis of the negative image on a scanning densitometer. Output values were expressed as relative densitometric units (RDU).

2.2.5 Ribonuclease Protection Analysis

Human probes for CAT-1, CAT-2B and eNOS were constructed from cloned cDNA fragments. To synthesise CAT-1 and CAT-2B cDNA fragments, 400 ng of total RNA from PBM was reverse transcribed using 1X PCR buffer, MuLV RT, dNTP's and oligo(dT) in a 50 μL reaction mixture to produce PCR template cDNAs. For the synthesis of eNOS cDNA fragments, 400 ng of total RNA from EA.hy926 was reverse transcribed using an identical protocol.

Reverse transcription–polymerase chain reaction (RT-PCR) amplification of total RNA from mononuclear cells was used to construct cDNA fragments of CAT-1 and CAT-2B, with species-

and isoform-specific sequences as follows: CAT-1 sense 5'-CCCCCGGCGTGCTGGCTGAAAA-3' and antisense 5'-TTCATCGCCTACTTTGGGGTGTCG-3' (GenBank accession number x59155); CAT-2B sense 5'-GATCCATTTTCCCAATGCCTCG-3' and antisense 5'-GGTGCAGTGGCAGCTTTGAT-3' (GenBank accession number u76369). Primer oligonucleotide sequences were synthesised by Genset Pacific Pty Ltd as indicated in Table 2.1. Primers for CAT-2A and CAT-2B have been formulated on the basis of the different sequences resulting from the alternative splicing of the SLC7A2 transcript. In order to synthesise CAT-1 and CAT-2B cDNA fragments, 400 ng of total RNA from PBM was reverse transcribed according to the manufacturers instructions (PerkinElmer) using 1X PCR buffer, MuLV RT, dNTP's and oligo(dT) in a 50 μL reaction mixture. PCR amplification was performed for 40 cycles of 30 sec at 95°C denaturation, 30 sec annealing at 63°C and 1 minute extension at 72°C using *Taq* polymerase and 1.5 mM $MgCl_2$. The amplified cDNA was cloned into pGEM-T vector (Promega, Madison, WI). DNA orientation and sequence verification of the cloned PCR products were determined from these plasmid templates using the dideoxy chain-termination method (ABI Prism 377 DNA sequencer). The cloned CAT-1 and CAT-2B fragments were then used as templates to generate ^{32}P-labeled riboprobes for use in ribonuclease protection assays, as previously described (Autelitano, 1998). Generated radiolabelled antisense RNA probes were purified by incubation with DNase I for 15 min at 37°C and then precipitated with ammonium acetate and ethanol according to standard protocols (Ausubel *et al.*, 1990). When linearised with Nco I riboprobe CAT-1 gave a protected fragment size of 354 bp. The riboprobe CAT-2B gave a protected fragment size of 289 bp and unprotected size of 307 bp when linearised with EcoRI. A plasmid containing a cDNA fragment of human CAT-2A (pBluescript II SK +/-, rCAT-2A, protected fragment size 185 bp) was generously provided by Dr. Ellen Closs (Department of Pharmacology, Johannes Gutenberg University, Mainz, Germany).

A ribonuclease protection assay kit was utilised (RPA III™, Ambion) for detection and quantitation of mRNA. Briefly, this assay involves hybridisation of the radiolabelled antisense RNA probe with

complementary sequence on the extracted RNA samples to protect the complementary sequence from subsequent ribonuclease digestion. The protected fragments are then analysed. Labelled antisense RNA probes were hybridised at 42°C overnight to complementary RNA isolated from peripheral blood mononuclear cells, EA.hy926 or human myocardium or a negative control, sheared torulla yeast RNA. To control for equal loading of RNA, the samples were simultaneously hybridised with a human GAPDH probe The following day total RNA samples were digested 30 min at 37°C with a combination of ribonuclease A and ribonuclease T1. The protected fragments were then separated and analysed on a 5% denaturing polyacrylamide/urea gel according to standard protocols (Ausubel et al., 1990). Radioactive signals were quantitated using a phosphorimager (Fuji BAS-1000). Data were expressed as a ratio of CAT to GAPDH signal.

2.3 DNA Methodology

2.3.1 Plasmid constructs

Human caveolin-1 full length cDNA was a gift from Dr. Chris Fielding, Cardiovascular Research Institute, University of California, San Francisco, USA. Full length bovine eNOS cDNA was provided by Dr. Thomas Michel, Cardiovascular Division, Brigham and Women's Hospital, Department of Biological Chemistry and Molecular Pharmacology, Harvard Medical School, Boston, Massachusetts, USA. Green fluorescent protein (gfp) tagged full length murine CAT-1 and CAT-2A cDNA clones were provided by Dr. Mari Masuda, Department of Microbiology, Graduate School of Medicine, University of Tokyo, Tokyo. Murine full length CAT-1 and CAT-2B cDNA clones were a generous gift from Dr. Daniel Markovich with permission of Dr. Donald Kakuda of the University of Queensland, Brisbane, Australia).

2.3.2 Amplification of cDNA constructs

Full length cDNA clones generated by PCR using *pfu* polymerase were initially purified from plasmid DNA by electrophoresis through 1% agarose gels and then isolated from gel slices by silica bead adhesion using a commercially available kit (Quantum). Full length cDNA clones kindly provided in sequencing vectors were excised through restriction digests using the appropriate restriction endonucleases indicated and separated from plasmid DNA by electrophoresis and purified using the gel extraction kit (Quantum). Full-length clones were subcloned into mammalian expression vectors using T4 DNA ligase (Promega) and transformed in bacterial cells using either the chemically competent strains xL Blue, JM109, DH5α, DH10β or electro-competent strains DH5α and DH10β E.coli cells by standard techniques. Resulting clonal colonies were then propagated in nutrient LB broth containing appropriate antibiotics as previously described (Sambrook et al., 1989). Plasmid DNA was subsequently isolated by the alkaline lysis method using a plasmid isolation kit (Quantum). Positive selection was performed on the basis of restriction endonuclease analysis and subsequent sequence analysis of suitable clones using an ABI Prism 377 DNA sequencer. After DNA isolation, all plasmids were purified by an additional phenol:chloroform extraction step according to standard protocols (Sambrook et al., 1989). cDNA constructs prepared in this manner were used directly in cDNA transfection of mammalian cells.

2.3.3 Measurement of DNA concentration

DNA was quantified by spectrophotometric analysis at 260 nm against reagent blanks. An optical density (OD) reading of 1 was considered equivalent with 50 μg DNA (Sambrook et al., 1989).

2.4 Measurement of endothelial NO Synthase (eNOS) Activity

Confluent endothelial monolayers were rinsed twice with 2 mL physiological saline solution (BSS) composed of (mM) NaCl 130, CaCl2 1.5, KCl 5, MgCl2 1, glucose 10, and HEPES 20 (pH 7.4) and were incubated with 2 mL BSS at 37°C with or without treatment. After treatment, endothelial cells were immediately harvested in homogenisation buffer (50 mM Tris-HCl, pH 7.5, 1 mM

EDTA, 1 mM EGTA), sonicated, and centrifuged at 1000 x g for 5 min, and the supernatant was used to measure NOS catalytic activity by the conversion of L-[^{3}H]Arg to L-[^{3}H]citrulline (Bredt and Snyder, 1990). Briefly, conversion of [^{3}H] L-Arg to [^{3}H] L-citrulline in either 100 µg of cellular homogenates was measured in the presence of unlabelled L-Arg totalling 100 µmol/L combined in a reaction mix containing 50 mmol/L Tris-HCl (pH 7.4), 1 mmol/L $CaCl_2$, 1 mmol/L EDTA, 1 mmol/L NADPH, 4 µmol/L FAD, 4 µmol/L FMN, 10 µM BH_4, 10 µg/mL calmodulin and 1 mmol/L dithiothreitol and incubated for 10 min at 37°C. The reaction was stopped by adding 3 mL of 20 mM HEPES, pH 5.5, 2 mM EDTA and 2 mM EGTA. The resulting samples were applied to 1 mL columns of Dowex AG50WX-8 (Na+ form), and the radioactivity in the flow through was determined by liquid scintillation counting (Model LS3801, Beckman Instruments). Specific eNOS activity was calculated as citrulline production from the above reaction mixture with 10 µM $CaCl_2$ minus citrulline production from the above reaction mixture with 5 mM EDTA. Data were expressed as pmol L-[3H]citrulline/µg protein/min.

2.5 Immunoreactivity Studies

2.5.1 Raising CAT-1 rabbit polyclonal antibody

A 21-mer synthetic peptide, ECY4, corresponding to a region of the fourth extracellular loop of CAT-1 according to the topology described by Kim *et al.*(Kim *et al.*, 1991)was used to raise polyclonal antibodies based on the known amino acid sequence (PubMed Accession #NP_031539, CLDIDSPLPGAFKHQGWEEAK). Synthesised ECY4, purified by HPLC and characterised by mass spectrometry, was purchased from Auspep, Melbourne, Australia. Peptide (2 mg) containing a Cys residue at the N-terminus to facilitate coupling was solubilised immediately before use in 0.05 M sodium phosphate, pH 7.0. Coupling of ECY4 peptide to a large carrier protein, keyhole limpet hemocyanin (KLH; Sigma, St Louis, IL, U.S.A.), was carried out according to a method previously described by Lerner *et al.* 1981 (Lerner *et al.*, 1981). The resulting conjugated peptide-KLH was then divided into six 0.5-mL aliquots, and stored at -70^{o}C. The peptide-KLH conjugate,

was used for a total of 6 injections into two rabbits. For each round of injection, a single aliquot was thawed and was adequate for two rabbits. A one-sixth aliquot diluted to a total of 2 mL distilled water was divided in half, and a 1 mL aliquot was used for each rabbit. One millilitre of the peptide-KLH conjugate antigen mixture was added to an equal volume of Freund's adjuvant (Sigma, St Louis, IL, U.S.A.), and the sample was thoroughly mixed using a 5 mL syringe and a 21 gauge needle until no separation of phases was evident after 20 min rest at RT. The mixture was taken up in the syringe, and a clean needle was substituted for subcutaneous injection at two sites. To stimulate the immune response, Freund's complete adjuvant (85 % w/v mineral oil, 15% w/v mannide monooleate, and containing 1 mg heat-killed *Mycobacterium tuberculosis* cells) was used for the first injection. Freund's incomplete adjuvant (lacking the bacterial cells) was used for the 5 remaining injections. The standard protocol for raising antisera involved three injections at 3 week intervals, with bleeds carried out as follows:

Day 1.	1st Injection	(Complete adjuvant)
Week 3	2nd Injection	(Incomplete adjuvant)
Week 6	3rd Injection	(Incomplete adjuvant)
Week 7	1st Bleed	
Week 8-9	2nd Bleed	(10-12 days later)
Week 10	4th Injection	(Incomplete adjuvant)
Week 11-12	3rd Bleed	(10-12 days later)
Week 13-14	4th Bleed	(10-12 days later)

Approximately 30 mL of blood per rabbit was collected from an ear vein into a tube without anti-coagulant, and allowed to clot at room temperature for 2-3 hrs. Serum was obtained from the clotted blood following after an additional overnight incubation at 4°C, and stored at –20°C. Affinity-purification of anti-peptide IgG from rabbit serum was performed using ECY-coupled affinity resin. Peptide-Affigel affinity resin was prepared as previously described (Andrews *et al.*, 1998), by coupling a 2 mL mixture of ECY4 peptide alone (0.25 mg/mL) and a 4 mL mixture of peptide-BSA conjugate (0.125 mg/mL) in coupling buffer (0.05 M sodium phosphate, pH 7.0). A 5

mL mixture (1:1) of Affigel-10/15 (Bio-Rad, Richmond, IL, U.S.A.) was washed sequentially in a sintered glass funnel with one bed volume of ice-cold isopropanol and two bed volumes of distilled water. Slurry of washed resin in ice-cold coupling buffer was added to the ECY or ECY-BSA mixture and rocked overnight at 4°C. Unreactive sites were blocked by incorporating 10 mM ethanolamine, pH 8.0 into the mixture for the final hr of incubation. ECY4-Affigel (10/15) and ECY4-BSA-Affigel (10/15) resins were pooled to obtain a 10 mL bed volume, then washed three times in column buffer (0.01M Tris-HCl, 0.15 sodium chloride, pH 7.4) by performing an 800 g centrifugation for 10 min at RT. Dialysed serum (10 mL) pooled from multiple rabbit bleeds, was loaded onto a column of ECY4-BSA-Affigel at a rate of 20 mL/h and washed thoroughly with column buffer. Bound antibody was eluted with 0.1 M glycine, pH 2.8. Four millilitre fractions were collected and neutralised with 1 M Tris-HCl, pH 8.5 to a final concentration of 0.2 M Tris-HCl. Peak fractions were then dialysed overnight at 4°C in 0.01 M Tris-HCl and 0.15 M sodium chloride, pH 7.4. The resulting CAT-1 polyclonal antibody concentration was determined and small aliquots stored at -20°C.

2.5.2 SDS-PAGE

The following protocol was routinely used in most instances with alterations according to the specific nature of the antibody and target protein. Alterations and details of specific protocols are included in the following chapters. After exposure to experimental conditions cell monolayers were washed twice in D-PBS then lysed using the appropriate lysis buffer. Protein content was determined by the Lowry assay using a commerically available kit modified for detergent containing samples.(BioRad). Prepared protein lysates prepared as detailed in the following chapters were analysed by reducing SDS-PAGE gel in SDS-PAGE running buffer using the Bio-Rad mini Protean II assembly for 3 hrs at 100 V according to the manufacturers instructions.

2.5.3 Western blot

Proteins were transferred onto Immobilon-P membranes (Amersham) at 4°C using a Bio-Rad mini Protean II Western blot assembly for 1.5 hrs at 100 V in transfer buffer according to the manufacturers instructions. After transfer, the membrane was blocked for 2 hr at RT in TBS-T (0.1% Tween-20, 20 mM Tris-buffered saline, pH 7.6) containing 5% skim milk powder. The membrane was then incubated with a primary antibody in TBS-T containing 5% skim milk overnight at 4°C and then washed four times in TBS-T for 5 min each. A species-specific secondary antibody conjugated to horseradish peroxidase was added to membrane and incubated in TBS-T containing 1% skim milk powder for 1 hr at RT. Following extensive washing in TBS-T, the protein of interest was detected by enhanced chemiluminescence (ECL) and the signal developed by exposure of the membrane to film for various lengths of time using X-OMAT film (Kodak).

2.5.4 Stripping membrane for re-probing

After three initial 5 minute washes in TBS-T the membrane to be stripped of antibodies was placed into a sealed plastic bag containing 2% w/v SDS, 62.5 mM Tris pH 6.8 and 100 mM β-Mercaptoethanol and incubated for 30 min at 70°C. After this time, the membrane was extensively through six washes for 5 min each in TBS-T. Immunodetection was initiated though the addition of blocking agents (5% w/v skim milk in TBS-T).

Chapter Three

L-Arg Transport in Congestive Heart Failure

TABLE OF CONTENTS

3.0 General Introduction *99*

3.1 Development Of An In Vitro Model To Assess L-Arg Transport In Humans. *101*

3.1.1 Introduction **101**

3.1.2 Methods **103**

3.1.2.1 Experimental design 103

3.1.2.2 Separation of peripheral blood mononuclear cells (PBM) from whole blood 103

3.1.2.3 Concentration-dependent L-[^{3}H]Arg transport in PBM 104

3.1.2.4 Time course of L-[^{3}H]Arg transport in PBM 105

3.1.2.5 Competitive inhibition of L-[^{3}H]Arg transport 106

3.1.2.6 FACS analysis of PBM 106

3.1.2.7 Identification of L-arginine transport systems: RT-PCR analysis 107

3.1.3 Results **107**

3.1.3.1 Characterisation of L-arginine transport in PBM 107

3.1.3.2 Detection L-Arg transporter and NOS expression in PBM by RT-PCR 109

3.1.3.3 FACS analysis 111

3.1.4 Discussion **115**

3.2 L-Arg Transport In Congestive Heart Failure *118*

3.2.1 Introduction **118**

3.2.2 Methods **120**

3.2.2.1 Patient recruitment 120

3.2.2.2 L-[^{3}H]Arg transport in PBM isolated from CHF patients 120

3.2.2.3 Ribonuclease protection assay 121

3.2.2.4 NOS Western blot 121

3.2.2.5 Statistical analysis 121

3.2.3 Results **122**

3.2.3.1 L-[^{3}H]Arg transport in PBM from CHF patients 122

3.2.3.2 L-arginine transporter mRNA expression in PBM of CHF patients 124

3.2.3.3 L-Arg transporter and NOS expression in human CHF myocardium 124

3.2.4 Discussion **129**

3.2.4.1 Evidence of L-Arg transport abnormalities in the peripheral vasculature 129

3.2.4.2 Evidence of L-Arg transport abnormalities in the coronary vasculature 132

3.3 L-Arg Transport In Age-Related Endothelial Dysfunction ***135***

3.3.1 Introduction **135**

3.3.2 Methods **136**

3.3.2.1 Exclusion criteria for aging individuals 136

3.3.2.2 L-[^{3}H]Arg transport in peripheral blood mononuclear cells 136

3.3.3 Results **136**

3.3.3.1 PBM L-[^{3}H]Arg transport in the aging population 136

3.3.4 Discussion **137**

TABLE OF FIGURES

Figure 3.1 Time course of L-Arg transport in the presence and absence of sodium ions. 108

Figure 3.2 System y^+ transport of L-Arg in PBM. 110

Figure 3.3 RT-PCR Analysis of CAT and NOS isoforms present in PBM 111

Figure 3.4 FACS analysis of cell-surface CD45 antigen expression in peripheral blood mononuclear cells. 113

Figure 3.5 FACS analysis of cell-surface CD14 antigen expression in peripheral blood mononuclear cells. 114

Figure 3.6 L-[^{3}H]Arg transport kinetics in PBM obtained from control subjects and CHF patients. 123

Figure 3.7 Ribonuclease protection assay for GAPDH and CAT-1 mRNA abundance in isolated peripheral blood mononuclear cells from control and CHF subjects. 125

Figure 3.8 RT-PCR detection of CAT isoform expression in human heart samples. 126

Figure 3.9 RNAase protection assay of CAT-1 mRNA expression normalised to GAPDH expression in healthy control versus CHF myocardial samples. 127

Figure 3.10 RNAase protection assay showing CAT-2A and CAT-2B mRNA expression in control versus CHF myocardial samples. 128

Figure 3.11 Western blot of eNOS and iNOS in the human CHF myocardium. 129

Figure 3.12 L-Arg transport in isolated PBM from young , middle-aged and older healthy individuals. 137

3.0 General Introduction

The work in this chapter forms an important basis of all further studies contained within this thesis and reports on the development of a novel *in vitro* model of L-arginine (L-Arg) transport in humans using freshly isolated peripheral blood mononuclear cells. This model has been utilised for assessing the status of L-Arg transport in congestive heart failure (CHF), as a potential contributory mechanism for endothelial dysfunction (Chapter 1, Section 4.4.4). The three major three aims of this chapter were *i)* to develop a non-invasive *in vitro* model for assessing the rate of L-Arg transport in humans utilising freshly isolated peripheral blood mononuclear cells (PBM), *ii)* to evaluate the rate of L-Arg transport in PBM isolated from CHF patients and, *iii)* to investigate in healthy human PBM controls whether there are variations in L-Arg transport rate within the population based on age and gender criteria. Major findings from Section 3.1 and 3.2 of this chapter relating to L-Arg transport in CHF have contributed to two recent publications in conjunction with the clinical findings of Dr. David Kaye and colleagues (Kaye *et al.*, 2002, Kaye *et al.*, 2000). In addition, major elements of the work contained within Section 3.1 and 3.3 have been combined in a recent manuscript submission to the Journal of Hypertension entitled "An age related decline in endothelial function is not associated with alterations in L-arginine transport in humans." This manuscript has been written in conjunction with clinical findings of Dr. Melinda Parnell.

3.1 Development Of An In Vitro Model To Assess L-Arg Transport In Humans.

3.1.1 Introduction

Core elements of the L-Arg-nitric oxide (NO) pathway include the transport of L-Arg from the plasma across the endothelial cell membrane via carrier-mediated transporters, adequate utilisation of intracellular L-Arg by endothelial nitric oxide synthase (NOS), an adequate supply of NOS co-factors (BH_4, FAD, FMN and NADPH), and a catalyst for the reaction to occur either through a rise in intracellular Ca^{2+} levels (Ca^{2+}/camodulin complex) and/or by direct phosphorylation of the enzyme in response to various physiological stimuli (Chapter 1, Section 3.2). The product of the NOS reaction, NO, exerts its biological effects principally through its vasodilatory actions within the vasculature (Chapter 1, Section 2). Decreased functionality of this pathway is thought to be a major contributor to the well-documented endothelial dysfunction in both clinical and experimental models. Importantly, various reports have identified that a deficiency at any of the regulatory points in the L-Arg-NO pathway described above can lead to impaired release of NO and subsequently endothelial dysfunction (Chapter 1, Section 4.4).

Endothelial function in humans can be measured in both in the coronary circulation by coronary angiography and Doppler flow wire and in the peripheral circulation by plethysmography and ultrasound Doppler equipment (Luscher and Noll, 1996). Such techniques commonly involve the assessment of NO-dependent responses in response to infused vasodilatory agents (Chapter 1, Section 4.2). For example, impaired vasodilatory responses measured by changes in forearm blood flow in response to regional administration of acetylcholine (Ach) is used widely as an indicator for endothelial dysfunction in the human circulation, whilst simultaneous infusion of a NOS inhibitor, gives an indication of the NOS-independent part of the Ach response. Other commonly employed markers and assays for endothelial dysfunction in humans involve the measurement of the stable NO metabolites nitrate NO_3. and nitrite NO_2., from plasma and urine and, assays of different circulating markers. Whilst these techniques are useful for identifying whether a decline in endothelial function is associated with an impaired L-Arg-NO pathway the data obtained does not

indicate the point where the deficiency exists within the L-Arg-NO pathway. In order to determine more precisely the origin of a deficiency in the L-Arg-NO pathway which may lead to endothelial dysfunction, NOS expression in humans has been assessed by specific NOS immunoblotting in skeletal muscle (Comini *et al.*, 1996) and myocardial sections (Stein *et al.*, 1998) whilst the level of NOS enzymatic activity is commonly reported on the basis of plasma and urinary nitrite/nitrate levels (Katz *et al.*, 1999, Ramesh *et al.*, 1999). Contrasting evidence exists on the reporting of NOS isoform activity and expression in human CHF (Chapter 3, Section 3.2).

The status of substrate and co-factor provision for this pathway remains poorly addressed to date which is surprising given that a decrease in the availability of either one can cause NOS to utilise molecular oxygen and produce highly reactive and destructive superoxide species. Oxidative stress due to superoxide species formed within the endothelium is a major causal factor linked to the development of endothelial dysfunction. Certainly, a growing body of clinical evidence indicates that a deficiency may in fact exist at the level of substrate and co-factor availability for NOS in endothelial dysfunction. In order to develop more selective strategies for treating endothelial dysfunction in humans a methodological approach in evaluating each input point in the L-Arg-NO pathway needs to be attained. These approaches have become increasingly more attractive given that recent evidence gained from eNOS-overexpressing transgenic mice as a potentially beneficial regime *in vivo* actually leads to eNOS dysfunction. Evidence of eNOS dysfunction was detected in these mice by lower NO production relative to eNOS expression and enhanced levels of deleterious superoxide production in the endothelium (Ozaki *et al.*, 2002) and, in another study, reduced NO-dependent vasodilation of thoracic aortas (Yamashita *et al.*, 2000). Interestingly, Ozaki *et al.* (Ozaki et al., 2002) has convincingly demonstrated that supplementation with the NOS co-factor tetrahydrobiopterin reversed eNOS dysfunction in the eNOS-overexpressing mice, further demonstrating the importance of adequate substrate and co-factor requirements for maintaining physiologic NO production.

The potential for L-Arg to become a rate-limiting factor in NO production has also been indicated (Chapter 1, Section 5.4.1). Absolute plasma L-Arg substrate concentrations have been reported in the literature as an indication of L-Arg provision into the cell. However, in the absence of a such measurements reported L-Arg plasma concentrations can only be used speculate on such a process since L-Arg transporters are known to be actively regulated (Chapter 1, Section 7). In order to compensate for the lack of existing methodology available to assess L-Arg transport in humans, the kinetics of radiolabelled (L-[^{3}H]Arg) L-Arg transport were examined using freshly isolated peripheral blood mononuclear cells (PBM).

3.1.2 Methods

3.1.2.1 Experimental design

Given the intended usage of PBM as a model of L-Arg transport within the human endothelium a thorough assessment and characterisation of the predominant L-Arg transport system kinetic in freshly isolated PBM was undertaken. To establish a sound methodological approach for evaluating the kinetics of PBM L-Arg transport an analysis of concentration-dependent L-Arg transport (kinetic constants V_{max} and K_m were obtained from this data by Lineweaver-Burk kinetic plots and Eadie-Hofstee transformation of the data), time-dependent L-Arg transport and competitive inhibition of L-Arg for the major L-Arg transport system by other amino acids was carried out. Additionally FACS (fluorescent activated cell sorter) analysis was used to analyse isolated PBM cell populations and RT-PCR studies identified the presence of CAT and NOS isoforms.

3.1.2.2 Separation of peripheral blood mononuclear cells (PBM) from whole blood

There are various methods available by which a population of human PBM can be prepared prior to analysis. In this study, a centrifugation method of whole blood separation was employed whereby PBM are isolated according to the principles of differential cell migration on a density gradient by using a commercially available sterile Ficoll-Paque® (Pharmacia Biotech) separation medium.

Advantages of this technique include the isolation of pure lymphocyte populations, removal of platelets, erythrocytes, cellular debris and dead cells prior to further analysis with the additional of assurance of an endotoxin-free product. Approximately 25 mL of freshly isolated peripheral venous blood was collected into sterile EDTA tubes and kept at RT. Anti-coagulant treated whole blood was then diluted with an equal volume of balanced salt solution (BSS) containing 0.01% D-glucose, 5 μM $CaCl_2$, 10 μM $MgCl_2$, 0.5 mM KCl, 14.5 mM Tris-HCl and 140 mM NaCl; pH 7.4. Diluted blood was gently layered over Ficoll-Paque® Plus reagent (density = 1.077) in a 4:3 volume ratio. After centrifugation of layered whole blood at 400 g for 40 min (RT) the upper layer containing plasma was carefully removed using a Pasteur pipette and stored at –80°C. A visible white band containing PBM was harvested by transferral from the separation medium interface using a clean Pasteur pipette into a 14 mL centrifuge tube (Falcon) containing 3 volumes of BSS. Cells were washed by centrifugation at 100 g for 10 min at RT. Following an initial wash, the supernatant was discarded and the resulting cell pellet resuspended in 6 volumes of BSS and centrifuged at 100 g for 10 min (RT). Supernatant was removed after the final wash and the cell pellet containing PBM were gently resuspended in freshly prepared, pre-gassed (5% CO_2/95% O_2 mixture) Krebs-Henseleit solution (131 mM NaCl, 5.5 mM KCl, 1 mM $MgCl_2$, 2.5 mM $CaCl_2$, 25 mM $NaHCO_3$, 1 mM NaH_2PO_4 and 5.5 mM D-glucose at pH 7.4) and incubated for a brief period at 37°C prior to initiation of L-[^{3}H]Arg transport studies. Cell count and viability of isolated PBM were assessed simultaneously using a haemocytometer according to manufacturer instructions (Hausser Scientific™, Sigma). PBM cell counts were independently confirmed using an automated cell counter (Coulter Z2, Coulter Corp.). Aliquots (300 μL) of cells were transferred to eppendorf tubes at a density of 5 x 10^5 cells/mL and incubated at 37°C in preparation for transport studies.

3.1.2.3 Concentration-dependent L-[^{3}H]Arg transport in PBM

Self-inhibition L-Arg transport kinetics were performed using a fixed concentration of 100 nM labelled L-[2,3-^{3}H]Arg (53 Ci/mmol, from a stock solution of 1 mCi/mL New England Nuclear) in the presence of incremental unlabelled Arg concentrations totalling 1 – 300 μM that was added to

cells in separate tubes. This experiment was repeated in the presence of saturating (10 mM) L-lysine (SIGMA), a competitor with similar affinity for system y+ transport, in order to elucidate specific L-Arg transport activity of PBM. Concentration-dependent L-[^{3}H]Arg transport studies were initiated through the addition of 200 µL Krebs-Henseleit solution mixture containing L-[^{3}H]Arg. Transport was determined under initial rate and linear conditions at 37°C over a time interval of 5 min. Where sodium-independent L[^{3}H]Arg transport was assessed, a sodium-free Krebs-Henseleit solution was prepared by substitution of sodium ions with eqimolar choline ion concentrations. After a 5 min of L-[^{3}H]Arg transport measurement, amino acid transport was terminated by transferring eppendorfs immediately to melting ice. Cells were then washed three times in 1 mL of ice-cold Krebs-Henseleit solution by brief centrifugation at 15 000 g for 10 sec, 4°C. Washing three times with ice-cold Krebs-Henseleit buffer either containing 10 mM L-Arg or 10 mM L-Lys to prevent possible diffusion of L-Arg extracellularly did not alter the total amount of radiolabel recovered (data not shown). Additionally, the current data are consistent with the washing procedure removing non-specific bound radiolabeled L-Arg from the cell surface since placing cells on ice, washing and measuring radioactivity immediately after the addition of the L-[^{3}H] mixture at 37°C accounted for <5% of total radioactivity obtained. After the final rinse, supernatant was carefully discarded and pellets left to air dry. Samples were digested with 200 µL 0.1% w/v SDS and the digested samples transferred into 5 mL plastic liquid scintillation counting vials and mixed with 4.3 mL scintillation fluid. In order to calculate specific L-Arg transport activity, the radioactivity associated with the cells in the presence of saturating L-lysine concentrations (10 mM) for each data point was subtracted from the corresponding data point in the absence of L-Lysine. Specific L-Arg transport calculated from these values was expressed as pmol L-Arg /10^5 cells/ 5 min. All experiments were performed in duplicate for the each subject.

3.1.2.4 Time course of L-[^{3}H]Arg transport in PBM

Time-dependent L-Arg transport was determined in freshly isolated PBM by adding a fixed concentration of 100 nM labelled L-[^{3}H]Arg in the presence of unlabelled L-Arg concentration totalling 100 µM for various lengths of time (30 sec – 64 min). Radioactivity associated with

transport was measured as described above. The same experiment was also conducted in the presence of saturating L-lysine concentrations (10 mM) to elucidate the specific L-Arg transport activity of PBM.

3.1.2.5 Competitive inhibition of L-[^{3}H]Arg transport

Cross-inhibition of L-Arg transport by L-leucine, L-Arg and L-lysine in the presence and absence of sodium ions was determined by adding each amino acid at a saturating concentration (10 mM) to a 100 μM mixture of L-[^{3}H]Arg and measuring L-Arg transport for 5 min at 37°C as described above. Additionally, a specific inhibitor of system y+ transport, N-ethyl maleimide (NEM, ICN Biomedicals) was added to cells at various concentrations (1-1000 μM) for 20 min at 37°C prior to transport measurement with a 100 μM mixture of L-[^{3}H]Arg for 5 min at 37°C.

3.1.2.6 FACS analysis of PBM

PBM isolated from 8 healthy subjects were used to determine the constitution of lymphocyte populations (CD45 positive cell surface marker) and lymphocyte positive (CD45+) monocyte populations (CD14 positive, CD14+, cell surface marker). Both cell subsets, were determined using a fluorescence activated cell sorter (FACS) that detected cells labelled with fluorescein-conjugated monoclonal antibodies specific for either CD14/CD45. Briefly, PBM at a concentrations of 3 x 10^5 cells/mL were resuspended in 100 μL phosphate-buffered saline (PBS, pH 7.4; SIGMA) containing 1% BSA. Non-specific binding was blocked using 1% goat serum in PBS (Dako, Glostrup). Cells were then processed for dual staining of surface markers CD14 and CD45 by addition of fluorescein-conjugated monoclonal antibodies (Fluorescein isothiocyanate (FITC)-conjugated CD45 and phycoerythrin (PE)-conjugated CD14 were from Pharminogen) for possible reaction with specific cell markers for 30 min at 4°C. Cells were also stained with corresponding FITC or PE conjugated isotype matched control human IgG (Becton Dickinson) as negative controls. After incubation, cells were washed twice by centrifugation at 100 g for 10 min at 4°C and resuspended in PBS containing 1% BSA for further analysis using FACS. Fluorescence was determined by

FACS using a 488 nm argon laser (Becton Dickinson, Mountainview, CA), and data relating to gated cell populations were collected. Measurement of mean fluorescence intensity (MFI) and analysis of data were done using Cell Quest Software (Becton Dickinson).

3.1.2.7 Identification of L-arginine transport systems: RT-PCR analysis.

Total RNA was extracted from PBM according to the method described in Chapter 2, Section 2.1.2. Isoform-specific primers were used in RT-PCR analysis in order to detect the presence of either system y+ transporters (CAT-1, CAT-2A or CAT-2B) or NOS isoforms (nNOS, iNOS or eNOS) as previously described in Chapter 2, Section 2.3.

3.1.3 Results

3.1.3.1 Characterisation of L-arginine transport in PBM

PBM were chosen as a model of the human endothelial L-Arg-NO pathway, as they are reported contain the same predominant L-Arg transporter system y+ (Boyd and Crawford, 1992), and an intact and functional L-Arg-NO pathway (Amin *et al.*, 1995). To confirm this, the predominance of system (y+) L-Arg transport in isolated PBM from healthy individuals were evaluated. At least four functionally distinct L-Arg transport systems have been identified in mammalian cells and can be defined by their sodium dependence and affinity for different amino acid types (Deves and Boyd, 1998). System y+ can be defined by its high affinity for cationic amino acids (L-Arg, L-lysine, L-ornithine), sodium independence, sensitivity to the sulfhydryl reactive reagent NEM and, has a low affinity for neutral amino acids (L-leucine) in the presence of sodium (Chapter 1, Table 1.5). These properties were used as tools in the present study to dissect out the separate systems which may exist in human PBM using standard methods (Deves *et al.*, 1992). The time course of L-[^{3}H]Arg transport (30 sec – 60 min) in PBM and the contribution of sodium-dependent and independent systems to total transport of L-Arg was initially investigated. In the presence of 100 μM L-Arg, transport of L-[^{3}H]Arg in PBM occurred linearly with time for at least 5 min (Figure 3; depicts the initial 16 min time course). To ensure a linear transport model, an incubation time of 5 min was

chosen for all further transport studies. Substitution of sodium ions did not significantly influence L-[^{3}H]Arg transport kinetics (Figure 3.1), indicating that the major L-Arg transport system present in PBM is sodium-independent and accounts for over >80 % of total L-Arg transport. These findings exclude a significant role for the sodium-dependent system $B^{+,0}$ (Chapter 1, Table 1.5) in PBM.

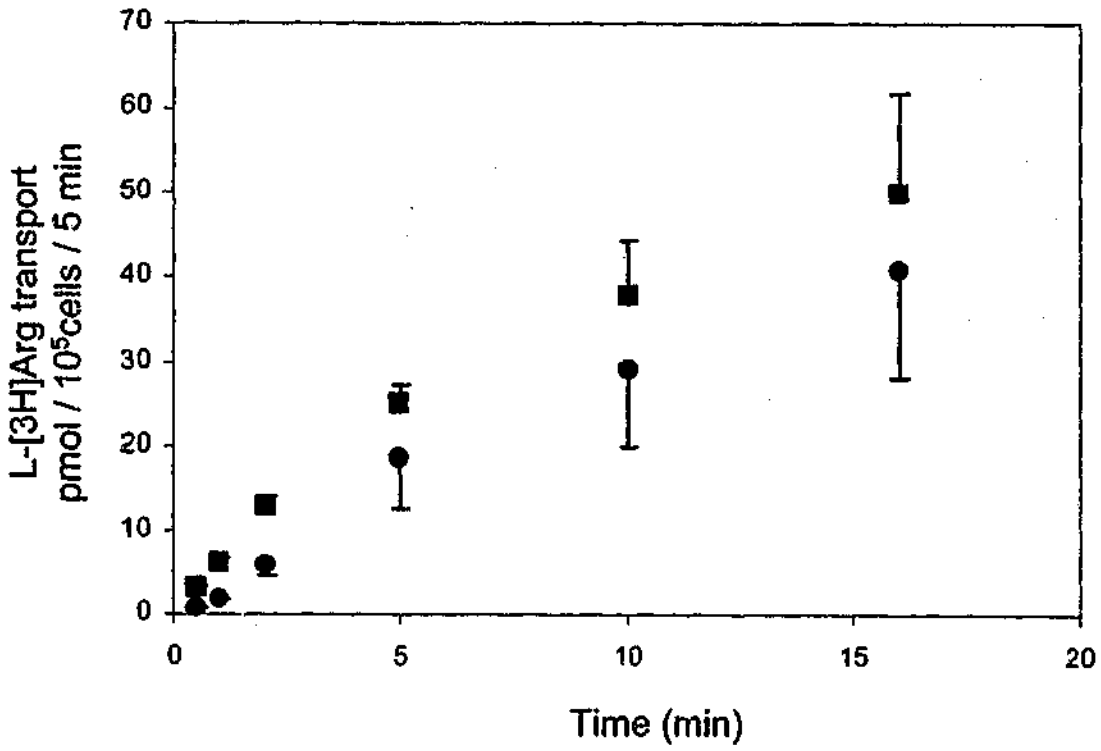

Figure 3.1 Time course of L-Arg transport in the presence (closed squares) and absence (closed circles) of sodium ions. This figure depicts a time course of L-Arg uptake in PBM using a solution containing 100 μmol/L L-Arg (100 nmol/L [^{3}H] L-Arg). Data are expressed as pmoL L-arg / 10^5 cells and represented as mean ± SEM, n=6.

Affinity of the predominant L-Arg transport system for cationic and neutral amino acids was addressed in PBM, by assessing the capacity for L-Arg (100 μM) transport in the presence of 10 mM L-leucine, L-Arg and L-lysine (Figure 3.2A). In accordance with system y+ properties, sodium-dependent (Figure 3.2A) and -independent (results not shown) L-[^{3}H]Arg transport was

significantly and competitively inhibited by the cationic amino acids L-Arg and L-lysine. L-leucine, which has a high-affinity for system y+L in the presence of sodium ions is reported by others to have a weak affinity for system y+ transport in the presence of sodium ions. In the present study L-Leucine was found to be a poor inhibitor of L-Arg transport at a competitor concentration of 10 mM (86% of control). Thus, the presence of $b^{0,+}$ in PBM was excluded on the basis of its transport properties (Chapter 1, Table 1.5) since L-Arg transport was not inhibited by large neutral amino acids (leucine) in the absence of sodium ions (results not shown). Thus, sodium-independent properties, the ability of L-Arg and L-Lys to competitively inhibit L-Arg transport whilst L-leucine was not an effective competitive inhibitor is strongly suggestive of a predominant system y+ in PBM. Additional evidence for the predominance of system (y+) L-Arg transport in PBM was detected in these cells by their demonstrated sensitivity to the selective system y+ inhibitor, NEM (Figure 3.2B). Extension of the pre-incubation time with NEM was not found to further influence the inhibitory effect on L-Arg transport in PBM. L-Arg transport in PBM was found to be concentration-dependent over a physiological range of extracellular L-Arg concentrations (1- 300 μM) Figure 3.6 (healthy controls). Eadie-Hofstee transformation of this kinetic data revealed the presence of two L-Arg transport systems: the first with an apparent K_M 185±37 μM and V_{max} 49.8±7.1 pmol/10^5 cells/ 5 min and the second with an apparent K_M 3.2 ± 0.9 μM and a V_{max} of 8.7 ±2.4 pmol/10^5 cells/ 5 min.

3.1.3.2 Detection L-Arg transporter and NOS expression in PBM by RT-PCR

RT-PCR analysis of isolated PBM mRNA detected the presence of the system y+ transporter isoforms CAT-1 and CAT-2B in all subjects tested whereas the liver-specific CAT-2A isoform was undetectable (Figure 3.3A). Additionally, gene expression of the eNOS isoform was detected in PBM (Figure 3.3B) whereas nNOS and iNOS isoforms were not detectable (not shown).

A

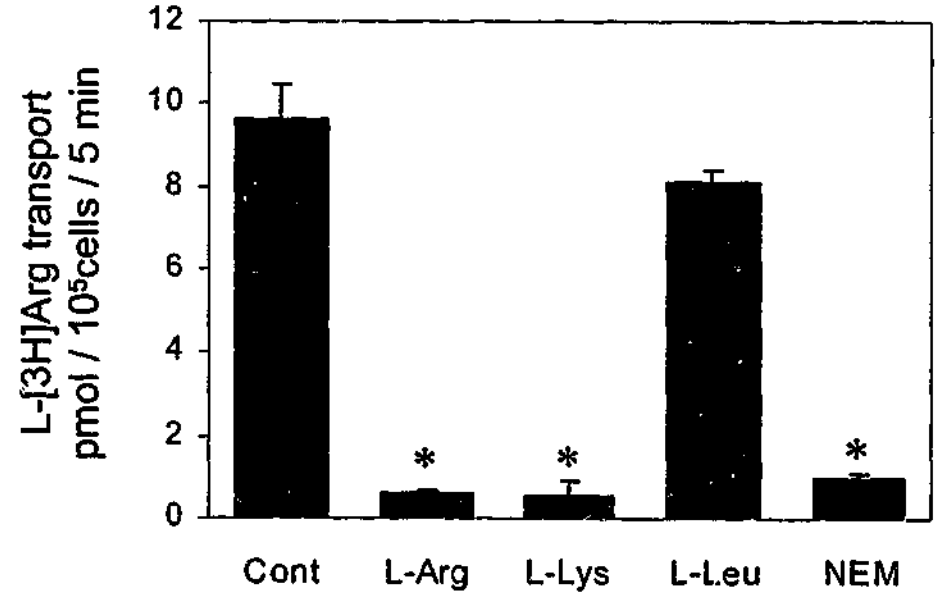

B

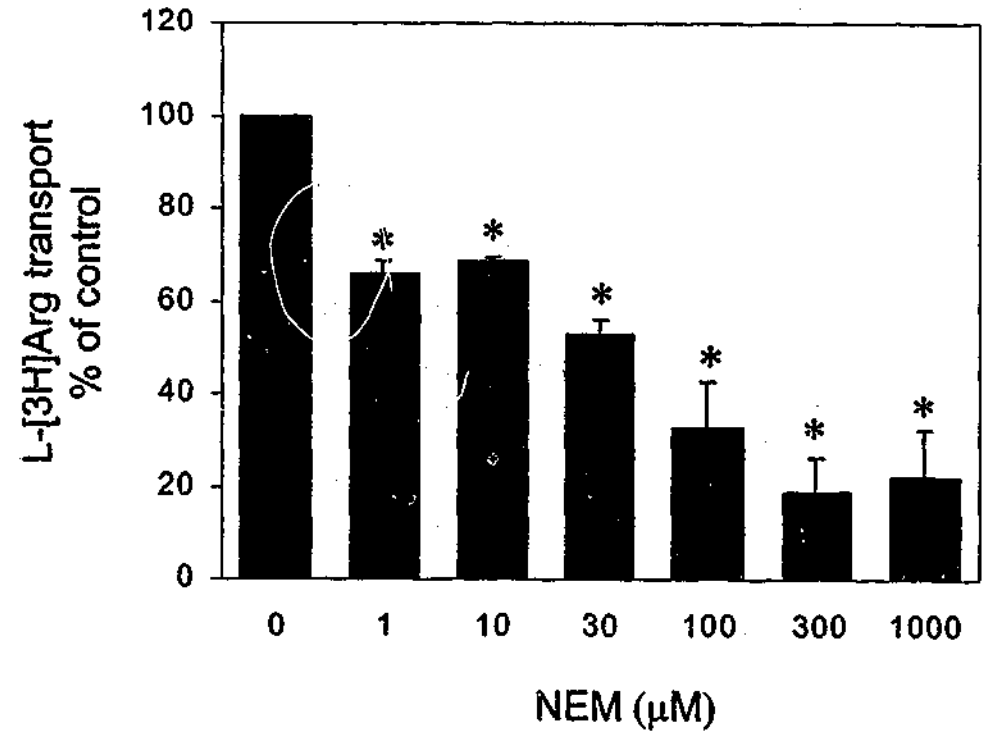

Figure 3.2. System y^+ transport of L-Arg in PBM, A) in the presence of 10 mM L-Arg, L-lysine (L-Lys), L-leucine (L-Leu) and after a 15 min pre-incubation with 200 μM NEM. Data are expressed as pmoL L-arg / 10^5 cells/ 5 min and represented as mean ± SEM, n=6. *p<0.05 versus untreated control. **B)** Concentration dependent inhibition of system y^+ by NEM. A 20 min NEM pre-incubation with the concentration indicated was performed prior to initiation of L-Arg transport studies. Data are expressed as percentage change from untreated controls (100 %) and represented as mean ± SEM, n=6 experiments $^*P< 0.05$ versus untreated control.

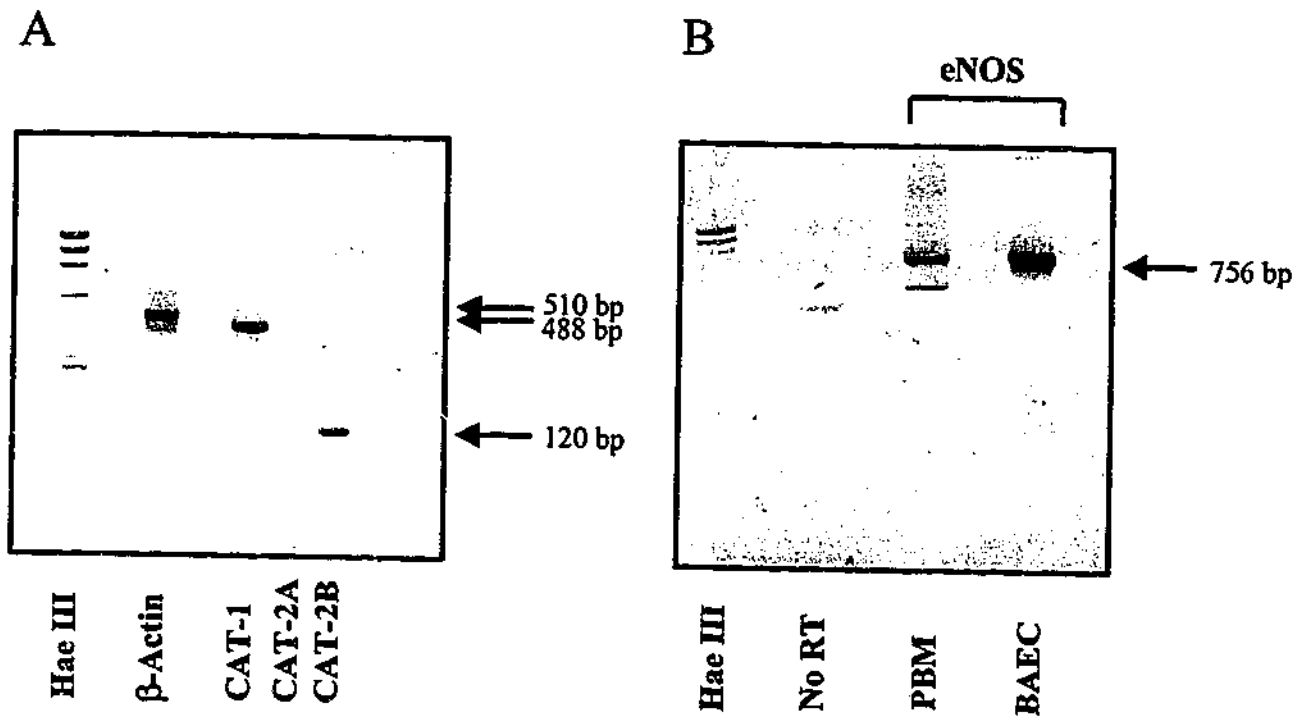

Figure 3.3 RT-PCR Analysis of CAT and NOS isoforms present in PBM. Isoform-specific primers were used to detect the presence of A) L-Arg transporter (CAT) isoforms –1, -2A, -2B and also B) the eNOS isoform in total RNA extracted from PBM as described in Methods. Primers specific for the detection of β-Actin in PBM, panel A, were used as an internal control. Controls for the detection of eNOS in PBM included no reverse transcriptase in a separate PCR experiment tube (no RT) and as a positive control, the detection of eNOS in total RNA extracted from bovine aortic endothelial cells (BAEC). Hae III markers (Hae III, Promega) were resolved alongside PCR products on a 1.8% agarose gel.

3.1.3.3 FACS analysis

The manufacturer of the peripheral blood mononuclear Ficoll-Paque separation medium indicates that the resulting mononuclear cell population isolated contains ~90% lymphocytes, 10% monocytes, granulocytes and other. In the present study an analysis of the proportion of lymphocytes isolated was undertaken in order to verify that the methodology used was reproducible and that a uniform population of cells was being obtained from each subject. Mononuclear cell populations have different capacities for L-Arg transport. In particular, lymphocytes and monocytes are both known to have a large capacity for L-Arg transport once

activated (Boyd and Crawford, 1992, Kakuda *et al.*, 1999). Therefore, a further analysis was undertaken to determine the proportion of monocytes in the PBM population for each subject.

Expression of CD45 is found on all hemopoietic cells, e.g. granulocytes, monocytes, macrophages and lymphocytes, except mature erythroid cells. In peripheral blood cells, a distinction can be made between lymphocytes (CD45+,CD14 -) and monocytes (CD45+, CD14+) on the basis of their cell surface specific antigens. To quantify the percentage of lymphocytes and monocytes, CD45 (FITC-conjugated) and CD14 (PE-conjugated) cell surface antigens specific for lymphocytes and monocytes respectively were determined by FACS. Samples were gated on forward-scatter versus side-scatter to include all cell populations. A second gate was set around the FITC- or PE-positive cells. The lymphocyte-specific marker (CD45) was detected in isolated mononuclear samples from all subjects and represented 92.6 ± 6.5 % of the total cell population (Figure 3.4). As shown, two separate and distinct populations of lymphocytes were detected both within R2 and R3 gating as depicted on the top panel scatter plot. Similarly, the monocyte-specific marker (CD14) was detected in all of the subject samples tested but represented only 1.2 ± 0.3 % of the total PBM cell population (Figure 3.5).

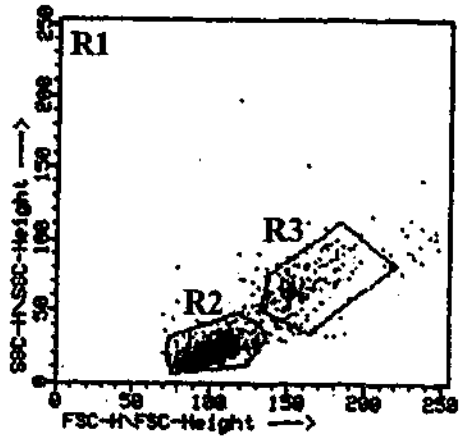

CD-45 positive in each population

Gate	%	Total
R2	97.5	
R3	97.6	91.7%

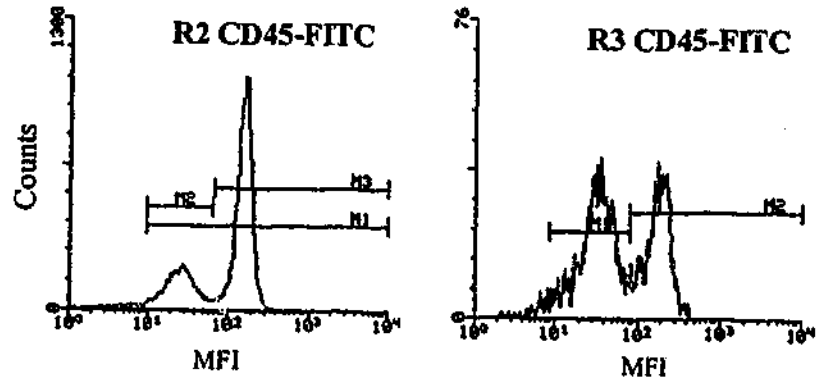

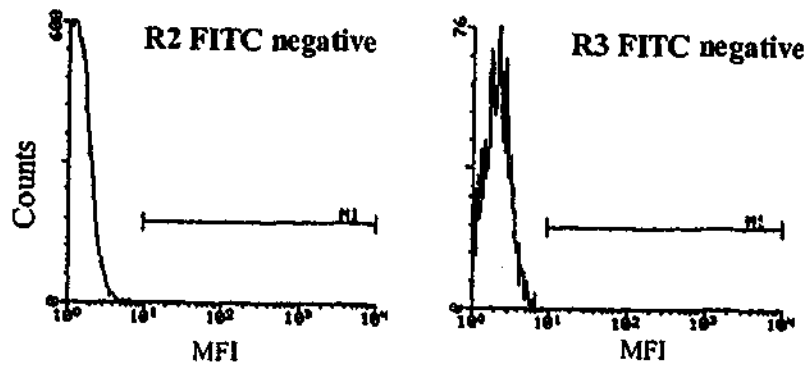

Figure 3.4. FACS analysis of cell-surface CD45 antigen expression in peripheral blood mononuclear cells. The scatter plot at the top represents the two major cell populations identified (R2 and R3 gating) in an isolated PBM population by forward and side-scatter of light analysis. The histograms in the middle panels represent CD45+ positive cells within the R2 and R3 gating of the scatter plot shown in the top panel. Histograms on the bottom panels represent the isotype-matched control IgG antibodies for FITC within the R2 and R3 gating of the scatter plot shown in the top panel. The x-axis is a logarithmic scale of mean fluorescence intensity (MFI) and the y-axis displays the number of cell counts (Counts) in the sample. This figure is representative experimental data obtained from the peripheral blood of one healthy human subject (n=8 in total).

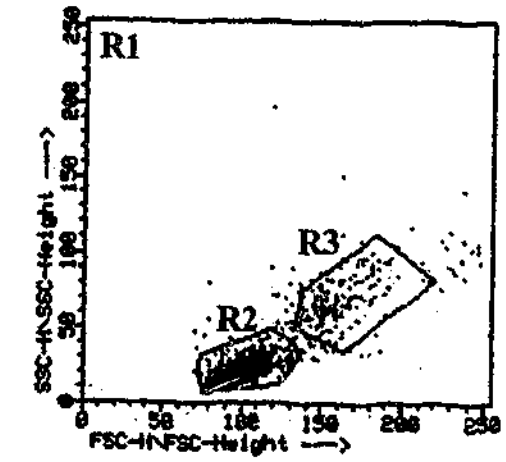

CD-14 positive in each population

Gate	%	Total
R2	0.4	
R3	91.7	1.2%

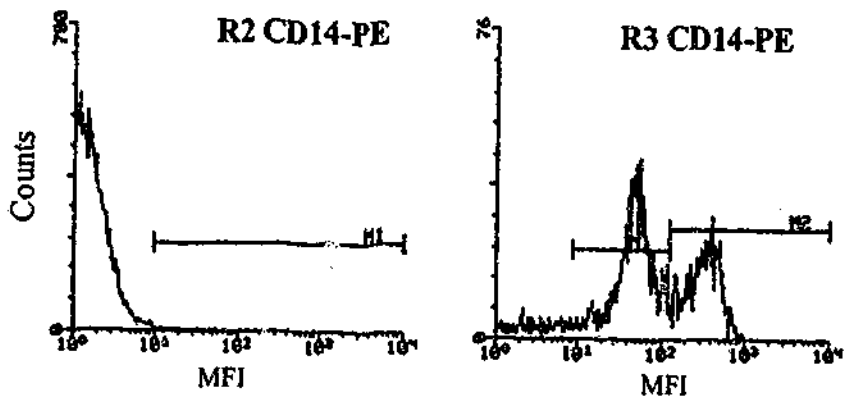

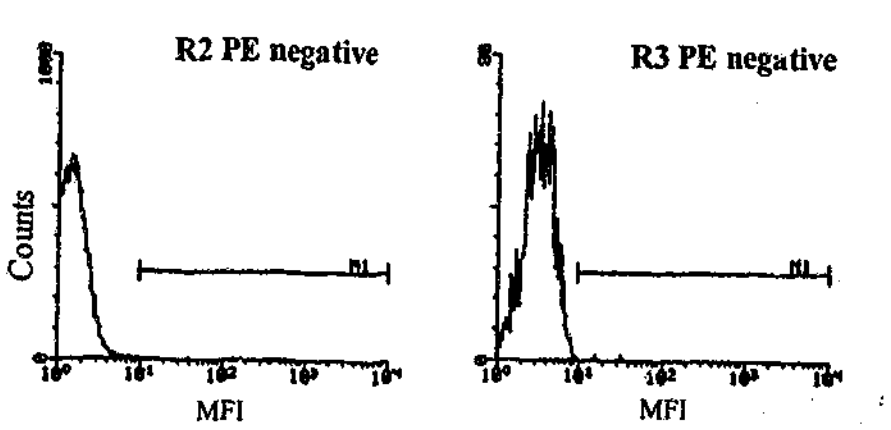

Figure 3.5. FACS analysis of cell-surface CD14 antigen expression in peripheral blood mononuclear cells. The scatter plot at the top represents the two major cell populations identified (R2 and R3 gating) in an isolated PBM population by forward and side-scatter of light analysis. The histograms in the middle panels represent CD14+ positive cells within the R2 and R3 gating of the scatter plot shown in the top panel. Histograms on the bottom panels represent the isotype-matched control IgG antibodies for PE within the R2 and R3 gating of the scatter plot shown in the top panel. The x-axis is a logarithmic scale of mean fluorescence intensity (MFI) and the y-axis displays the number of cell counts (Counts) in the sample. This figure is representative experimental data obtained from the peripheral blood of one healthy human subject (n=8 in total).

3.1.4 Discussion

Current evidence clearly indicates that limitations of L-Arg transport across the cell-membrane may be rate-limiting in NO production, the role of L-Arg transport activity in conditions associated with decreased NO availability such as endothelial dysfunction needs to be clarified (Schapira *et al.*, 1998). In the present study we have attempted to address this by developing and characterising an *in vitro* model for assessing L-arginine transport in freshly isolated human PBM.

The methodological approach taken for characterising L-Arg transport in PBM in the present study is a common approach used by investigators to kinetically define and identify the contribution of the various L-Arg transport systems which may exist in a particular cell type and allows direct comparison of kinetic constants across studies (Chapter 1. Section 6.2). The identity of the major L-Arg transport system in PBM was confirmed as system y+ on the basis of its transport properties (Chapter 1, Table 1.5): sodium-independence, sensitivity to the system y+ inhibitor NEM, a lack of affinity for L-leucine and similarities with the reported kinetic properties of system y+. System y+ was found to account for 85% of total L-Arg transport in PBM at physiologic levels of extracellular L-Arg (Figure 3.6A). Eadie-Hofstee transformation data (Figure 3.6B) revealed the presence of two kinetically distinct L-Arg transport systems in PBM with different affinities for L-Arg, possessing apparent K_m values of 185±37 μM and 3.2±0.9 μM respectively. In accordance, reported K_m values for system y+ transporters CAT-1 (250-380 μM) and CAT-2B (140-250 μM) closely match the lower affinity component. Indeed, further RT-PCR analysis in the present study confirmed the expression of both isoforms, CAT-1 and CAT-2B in human PBM. Interestingly, expression of CAT-1 has been reported by MacLeod *et al.* (MacLeod *et al.*, 1990) in resting lymphocytes whereas CAT-2B isoform was only detectable in mitogen-activated lymphocytes. Since their results were derived from a homogenous population of cultured lymphocytes differential expression of CAT-2B in the present study may result as a consequence of a heterogenous *in vivo* PBM population constituted by lymphocytes in different states of immunologic activation.

Alternatively, CAT-2B expression detected in the present study may be derived from other mononuclear populations present in isolated PBM such as monocytes since activated monocytes/macrophages are known to express the CAT-2B isoform (Kakuda et al., 1999).

Data from the present study has also suggested the presence of system y+L in PBM since a small proportion of the total L-Arg transport (<15%) displayed insensitivity to the system y+ inhibitor (NEM Figure 3.2B) and was sensitive to competitive inhibition by leucine (Figure 3.2A). In addition, the reported K_m of system y+L (10 μM)(Mendes Ribeiro *et al.*, 1999) matches closely to the second L-Arg transport component detected (3.2±0.9 μM) in the present study. In summary and in accordance with the literature system y+ was the predominant form of L-Arg transport detected, y+L was also detectable whereas other classified L-Arg transport systems such as $B^{o,+}$ and $b^{o,+}$ have not been described in PBM (Mendes Ribeiro *et al.*, 2001).

Expression of NOS was also evaluated in PBM since this model was developed for assessing the role of L-Arg transport in the NO pathway. Contrasting evidence exists in the literature on the NOS isoform types expressed in human PBM and other circulating cell types. PBM isolated from all subjects by the methods employed in the current study were shown to uniformly express eNOS whereas nNOS and iNOS isoforms were undetectable. These results are in agreement with a study by Reiling et al.(Reiling *et al.*, 1996), who demonstrated expression of eNOS at the both the mRNA and protein level in a pure population of human lymphocytes. In the present study FACS analysis revealed a PBM population largely constituted by lymphocytes (93%) and monocytes (1%). Contaminating platelets, monocytes and red blood cells also reportedly contain eNOS isoforms (Chen and Mehta, 1998, Sase and Michel, 1995, Mehta *et al.*, 1995). Reported differences in the literature are probably due in part to the variety of isolation methods employed for isolating populations of PBM. Contamination with neutrophils, monocytes or red blood cells for instance can lead to detection of the inducible NOS isoform (iNOS), which is known to be "constitutively" expressed in both cell types (Amin et al., 1995). Contamination with human polymorphonuclear leukocytes may lead to the detection of the neuronal NOS isoform, nNOS (Chen and Mehta, 1996).

A functional L-Arg-NO pathway in human PBM has been demonstrated by the detection of basal NO production using the fluorescent NO indicator, DAF-2 DA (Toomtong and Young, 2001) and also the conversion of L-[^{3}H]Arg into a by-product of the NOS reaction, L-[^{3}H]citrulline (Amin et al., 1995).

Substrate availability for the L-Arg-NO pathway has been largely addressed by employing methods aimed at detecting total plasma and tissue L-Arg concentrations by high-performance liquid chromatography. Resulting levels of tissue and plasma L-Arg can give an indication of L-Arg metabolism *in vivo*. To date, interpretation of such data as indicators of endothelial dysfunction has been limited since reporting of tissue and plasma L-Arg concentrations are highly variable in similar disease states possibly reflecting on the measured vascular bed origin and also the sensitivity limits of the detection method employed. In particular, it is though that measured tissue and cellular L-Arg levels do not necessarily indicate the level of L-Arg available to eNOS since this measure is a combination of both L-Arg bound in proteins and free unbound intracellular L-Arg. In this regard, measurement of a stable intermediate in the NO reaction, N-hydroxy-L-arginine (NOHA; Chapter 1, Section 5), may be a better marker of intracellular substrate availability for eNOS (Garlichs *et al.*, 2000).

Reported millimolar levels of intracellular L-Arg are far in excess of that required for eNOS conversion to NO (K_m 10 μM) within the endothelium. However, in view of an L-Arg paradox within the endothelium (Chapter 1, Section 5.3) whereby extracellular L-Arg can increase NO production. or even become rate-limiting for eNOS there is perhaps a need to more accurately assess the rate of L-Arg delivery in humans. We believe the PBM model employed in the present study for measuring L-Arg transport provides a sound, relatively non-invasive approach for assessing the status of L-Arg substrate provision in humans, with particular relevance to eNOS substrate provision. As such, it is believed that human PBM model may be beneficial in elucidating the role of L-Arg transport in pathophysiological states associated with endothelial dysfunction and is complimentary to other existing measures of the L-Arg-NO pathway.

3.2 *L-Arg Transport In Congestive Heart Failure*

3.2.1 Introduction

Reduced cardiac performance in humans leads to the activation of neurohumoral sympathetic and renin-angiotensin systems which can result in the adverse clinical manifestations of congestive heart failure (CHF) (Chapter 1, Section 4.3). One of the underlying features of heart failure involves the abnormal release of nitric oxide (NO). It is generally thought that this abnormality contributes to a sustained reduction in cardiac performance and an increased peripheral vascular resistance in CHF. Increased peripheral vascular resistance is related to diminished endothelium-dependent NO release in CHF whereas elevated production of NO by the failing heart is thought to cause adverse effects on ventricular contractility in its capacity as a negative inotrope (Sarkar *et al.*, 2001). The demonstration of differential release of this molecule within the same pathophysiology of CHF has caused significant controversy during the past decade.

As a major contributor towards increased peripheral resistance in CHF endothelial dysfunction is well documented but poorly understood. Intravenous or oral supplementation of L-Arg, the substrate precursor of NO, in CHF patients has been shown to result in increased NO production, peripheral and coronary vasodilation and increased cardiac output (Chapter 1, Section 5.4.7, Table 1.3). These outcomes suggest a beneficial hemodynamic and therapeutic effect for L-Arg in restoring normal vasodilator responses and reversing endothelial dysfunction. They may also highlight a relative deficiency of L-Arg in CHF. Based on such observations, a concept proposed is that reduction in the rate of transport of L-Arg may lead to relative intracellular substrate depletion for NO synthase.

Paradoxically, elevated NO production in CHF has been proposed by several groups on the basis of increased expression of the inducible NO synthase (iNOS) in the failing myocardium (Haywood *et al.*, 1996, Vejlstrup *et al.*, 1998). Such evidence is partly substantiated by reports of elevated NO

byproducts in the CHF plasma (Ramesh et al., 1999). Although, direct biochemical evidence of increased NO generation within the failing myocardium has yielded contrasting results (Kaye *et al.*, 1998). Thus, it has not yet been established whether excess myocardial NO generation due to an increase in NOS expression and/or activity might play a role contractile dysfunction and the pathophysiology of CHF. The major hypothesis of this collaborative study is that an observable paradox of increased NOS expression in the face of reduced NO production detected in CHF could be explained by a relative limitation in the intracellular availability of L-Arg attributable to downregulation of the major L-Arg transport system.

Since L-Arg transport activity is now known to be an absolute requirement for sustaining the pathologic levels of NO production mediated by iNOS in other models (Chapter 1, Section 5.4.1) it is reasonable to suppose that increased substrate provision via L-Arg transport into the myocardium may also be required for the reported increases in the L-Arg-NO metabolic pathway in CHF. In order to address this further in the present study, expression levels of the major L-Arg transporters present in CHF myocardium are determined in conjunction with an independent evaluation of iNOS and eNOS isoform expression. Previous studies have detected mRNA expression of the three major isoforms of CAT: -1, -2A and -2B in mouse hearts (MacLeod *et al.*, 1994). Since a downregulation of NO bioavailability is generally associated with the peripheral vasculature in CHF (Chapter 1, Section 4.3), we further sought to determine the expression of CAT in peripheral blood mononuclear cells (PBM). To assess the status of substrate provision, an *in vivo* approach has been developed within this laboratory to assess regional and intrinsic L-Arg transport kinetics in both the peripheral and coronary circulation of CHF patients (Kaye et al., 2000). As a complementary index to this *in vivo* approach, the present study also reports on the kinetic assessment of L-Arg transport in CHF using freshly isolated peripheral blood mononuclear cells (PBM).

3.2.2 Methods

3.2.2.1 Patient recruitment

Groups of 12 heart failure patients (NYHA class II-III; mean age ± SEM, 52 ± 3 years) and 10 age/sex-matched healthy control subjects (mean age ± SEM, 41± 2 years) were studied. The cause of heart failure was non-ischemic in 8 patients and myocardial ischemia in 2 patients. All patients were treated with an ACE inhibitor and diuretics, 10 received digoxin, and 1 received a ß-blocker. Left ventricular ejection fraction was 23± 4% (mean± SEM). Healthy subjects had blood pressure, glucose, cholesterol and triglycerides within the normal range and no history of cardiovascular disease. All patients participated after giving informed consent, and the study was conducted with the approval of the Alfred Hospital Ethics Review Committee.

3.2.2.2 L-[^{3}H]Arg transport in PBM isolated from CHF patients

To obtain an index of L-Arg transport in healthy subjects and patients with heart failure, the kinetics of L-[^{3}H]Arg transport by freshly isolated PBM were investigated. Peripheral blood (30 mL) was collected from 10 CHF patients and 14 healthy control subjects in tubes containing EGTA. PBM were then isolated by Ficoll-Paque (Pharmacia) density gradient centrifugation according to the manufacturer's instructions (Chapter 3, Section 1.2.2). The resultant lymphocyte-rich band typically contained at least 90% lymphocytes (as assessed by fluorescence-activated cell sorter analysis; data not shown), and 90% of the cells were viable (asassessed by trypan blue exclusion). The PBMC band was resuspended in 17 mL of Krebs-Henseleit buffer and divided into 32 aliquots of 500 µL. L-[^{3}H]Arg transport studies were conducted as previously described for concentration-dependent L-[^{3}H]Arg transport measurement (Chapter 3, Section 1.2.3). Briefly, PBM were incubated in Krebs-Henseleit transport buffer containing L-Arg in concentrations ranging from 1 to 300 µM, which included 100 nM L-[^{3}H]Arg, for a period of 5 min at 37°C. Transport studies were performed in duplicate. For each subject, additional parallel transport studies were performed in the presence of 10 mM L-lysine, a specific competitor for transport by the cationic amino acid transport system. At the conclusion of the incubation period, tubes were rapidly cooled on ice, washed twice in ice-cold Krebs-Henseleit buffer and then lysed in 0.1%

Triton X-100 for subsequent liquid scintillation spectroscopy. L-Arg transport by cationic acid transporter(s) was calculated as the difference between uptake in the absence and presence of 10 mM lysine in the transport buffer.

3.2.2.3 Ribonuclease protection assay

Expression of the major system y+/CAT isoforms, CAT-1, -2A and –2B, were assessed in PBM and myocardial tissue specimens from CHF patients. Myocardial tissue samples were obtained from 5 unused donor hearts and from the explanted hearts of 7 patients undergoing cardiac transplantation. Total RNA from human myocardial tissue preparations and isolated PBM were prepared according to previously described methods (Chapter 2 Section 2.1.2). 20 μg of myocardial RNA and 10 μg of PBM RNA respectively were used for hybridisation. RNA loading was assessed with a human GAPDH riboprobe. Of note, RNAse protection analysis did not detect any changes in GAPDH expression between healthy control and CHF patient groups nor has this been reported elsewhere in the literature to the authors knowledge.

3.2.2.4 NOS Western blot

Myocardial homogenates were obtained from 4 unused donor hearts and from the explanted hearts of 5 patients undergoing cardiac transplantation. Expression of endothelial NOS (eNOS) and inducible NOS (iNOS) protein in 40 μg of tissue homogenate was evaluated by Western blot using the appropriate monoclonal antibodies (Transduction Laboratories), as previously described (Kaye *et al.*, 1997). Protein content was determined by a modification of the Lowry method (BioRad).

3.2.2.5 Statistical analysis

Data are presented as mean±SEM. Between-group differences were compared using an unpaired Student's t test. $P<0.05$ was considered statistically significant.

3.2.3 Results

3.2.3.1 L-[^{3}H]Arg transport in PBM from CHF patients

L-Arg transport kinetics were examined in PBM obtained from patients with CHF and healthy age-matched subjects. Transport of L-[^{3}H]Arg was detected over a physiological range of L-Arg concentrations (1- 300 μM) in both groups, healthy volunteers and CHF patients (Figure 3.6). A significant reduction (75%, $P<0.001$) in the rate of L-Arg transport in PBM isolated from patients with CHF was demonstrated compared with healthy subjects, and was particularly evident at an extracellular plasma L-Arg concentration of 100 μM. Eadie-Hofstec transformation of the data depicted in Figure 3.6B for control subjects (left panel), demonstrated the existence of two transport components with different Vmax and K_m values: the higher affinity transport system had a K_m 3.2 ± 0.9 μM and a Vmax of 8.7 ±2.4 pmol/10^5 cells/ 5 min. whereas the lower affinity transport system had a K_m 185±37 μM and V_{max} 49.8±7.1 pmol/10^5 cells/ 5 min. The biphasic nature of this plot was consistent with the previous identification of two kinetic L-Arg transport systems, y+ (the lower affinity component) and y+L (the higher affinity component), in PBM (Chapter 3, Section 1.3.1). Similarly, kinetic analysis of the L-[^{3}H]Arg transport rate in CHF patients revealed the presence of two transport systems (right panel, Figure 3.6B). A significantly depressed L-Arg transport rate observed in CHF corresponded with a reduction in the V_{max} for the lower affinity transport system y+ when compared to healthy individuals (10.1±1.3 versus 49.8±7.1 pmol/10^5 cells/5 min, $P<0.001$). No significant change or in the affinity of system y+ for L-Arg transport (K_m) was apparent (CHF versus control, 107±43 versus 185±37 μM). Likewise, no significant alterations in the kinetic constants for system y+L were apparent. Further work performed within our laboratory has demonstrated that L-Arg transport in isolated PBM significantly correlates with L-Arg transport in the forearm vasculature.

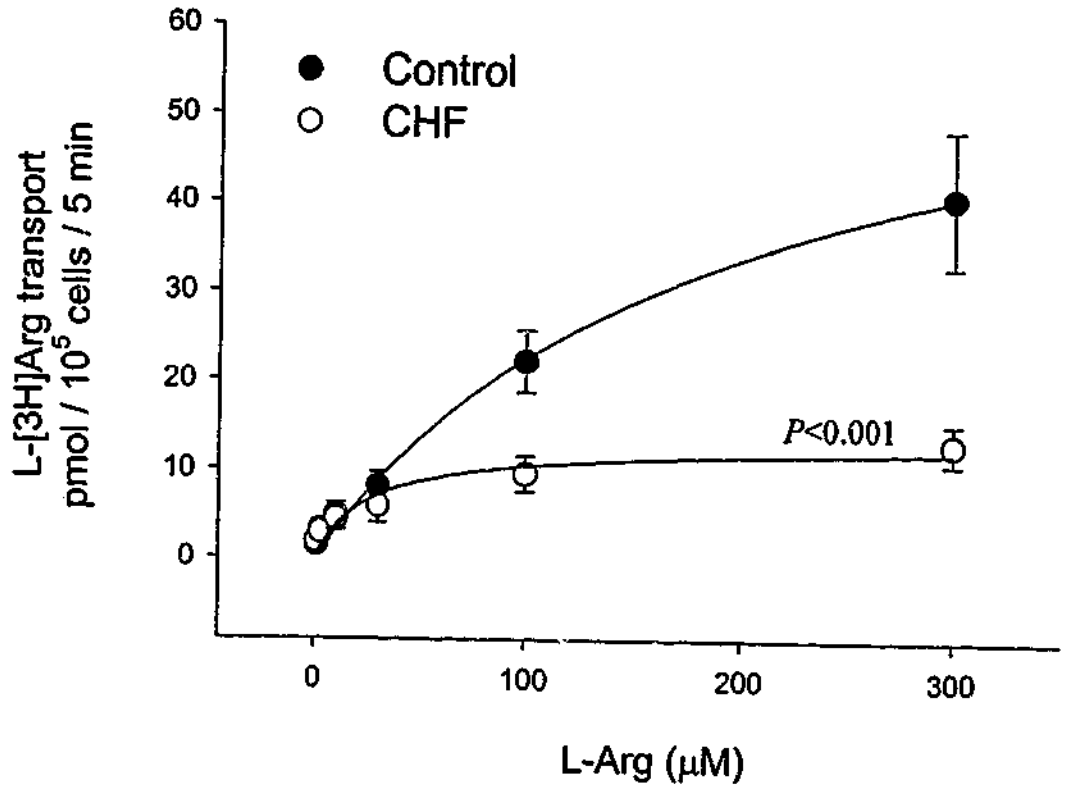

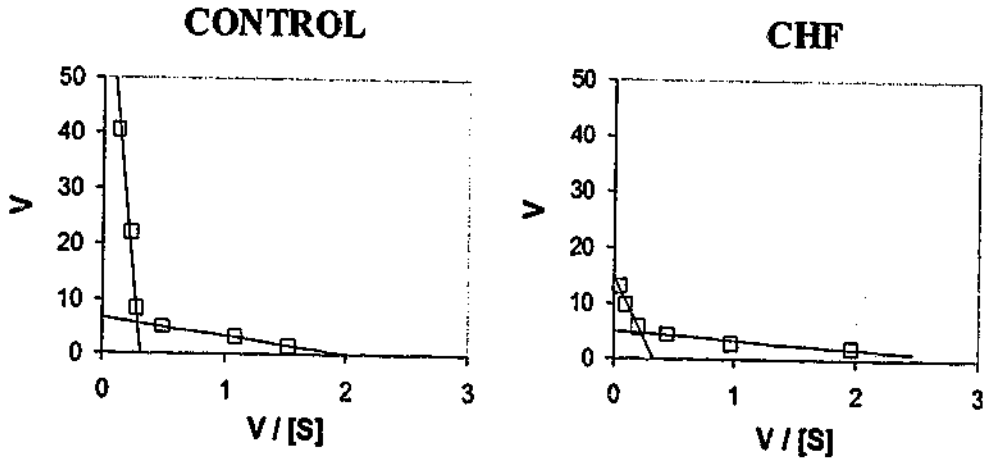

Figure 3.6. L-[^{3}H]Arg transport kinetics in PBM obtained from control subjects (n=14) and CHF patients (n=10). A) The rate of concentration-dependent L-[3H]Arg transport in PBM over a concentration range of 1- 300 μM in the extracellular medium for both healthy and CHF subjects as described in methods. **B)** Eadie-Hofstee transformation data from panel A. This plot is a representative plot of one healthy control (left panel) and CHF patient (right panel) respectively. Two kinetic systems of L-Arg transport in PBM were detected by the presence of two distinct linear regression curves.

3.2.3.2 L-arginine transporter mRNA expression in PBM of CHF patients

To determine whether the reduction in system (y+) L-Arg transport rate in CHF was due to changes in the expression of system y+ transporters (CAT-1, CAT-2A or CAT–2B isoforms) total RNA from either control or CHF PBM were analysed by RNAse protection assay. As shown in Figure 3.7, a significant reduction (76±7%, $P<0.05$; n=3) in mRNA expression for CAT-1 was observed in PBM isolated from CHF patients and was readily detected by ribonuclease protection assay using 10 μg total RNA. Expression of CAT-2B in PBM was negligible and did not differ in between control subjects and CHF patients. Expression of CAT-2A was not measured in this study, because preliminary studies carried out using RT-PCR did not detect CAT-2A mRNA expression in either control or CHF PBM (results not shown). Further, RNAse protection analysis did not detect any changes in GAPDH expression between healthy control and CHF patient groups nor has this been reported elsewhere in the literature to the authors knowledge.

3.2.3.3 L-Arg transporter and NOS expression in human CHF myocardium

By extending a recently developed method for studying the kinetics of regional L-arginine transport *in vivo* (Kaye et al., 2000), Dr. Kaye has demonstrated that the fractional extraction of L-[^{3}H]Arg during passage though the coronary circulation is significantly reduced in patients with CHF. These results clearly suggest that an abnormality of L-Arg transport also exists in the human failing heart. In order to address this further *in vitro*, gene expression of cationic amino acid transporter isoforms,CAT1, CAT-2A and CAT2B, were evaluated in human myocardial tissue from failing hearts (explanted hearts of patients undergoing cardiac transplantation). In accordance with previous findings in mouse heart tissue (Macleod and Kakuda, 1996, Finley *et al.*, 1995), initial RT-PCR analysis of total RNA from human myocardium in the present study detected the presence of all three major CAT isofroms-1, -2A and -2B (Figure 3.8). These results were subsequently verified by DNA sequencing using CAT2A and CAT2B primers.

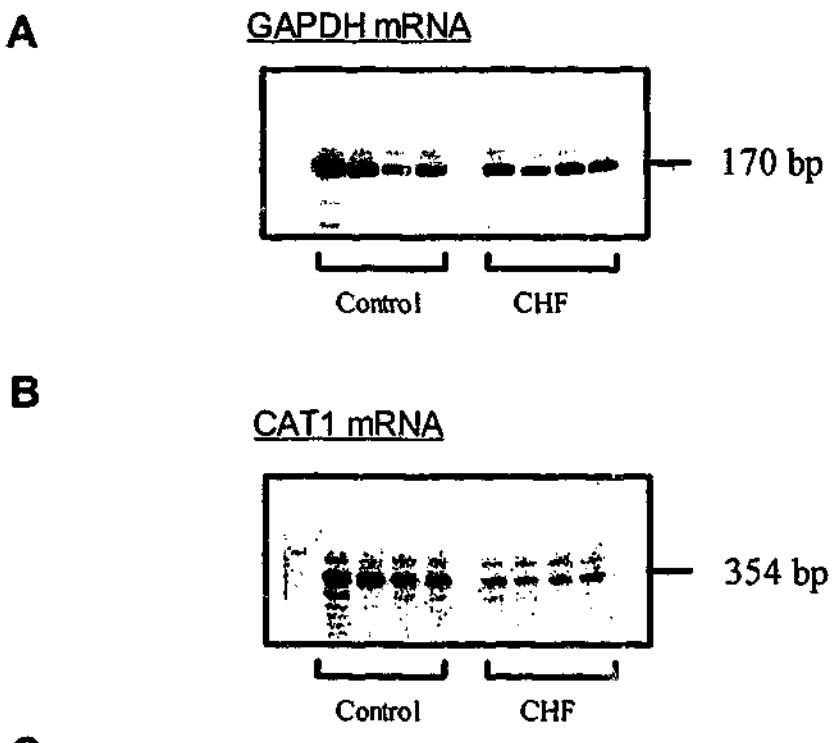

Figure 3.7. Ribonuclease protection assay for A) GAPDH and **B)** CAT-1 mRNA abundance in isolated peripheral blood mononuclear cells from control and CHF subjects. **C)** CAT-1 to GAPDH mRNA ratio from control (n=7) and CHF (n=5) subjects. $^{**}P<0.01$.

In comparison with nonfailing hearts, RNAse protection analysis revealed a significant reduction (38%, $P<0.05$) in the level of CAT1 mRNA in the failing human heart after normalisation with the expression of GAPDH (Figures 3.9A and B). In contrast, no significant differences in the

expression of CAT-2A or CAT2B (Figure 3.10) were detected in failing hearts compared with unused nonfailing donor hearts. In conjunction with this study, the level of NOS protein expression in control and failing myocardium was determined. In these studies, no significant differences were observed in the levels of both iNOS (Figure 3.11, top panel) and eNOS expression (Figure 3.11, lower panel) between the two groups.

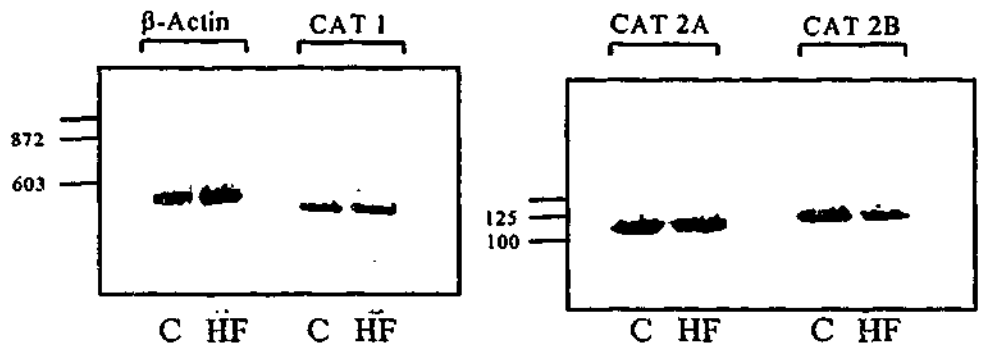

Figure 3.8. RT-PCR detection of CAT isoform expression in human heart samples. 1 μg of total RNA extracted from healthy human hearts were subjected to RT-PCR analysis using isoform specific primers for CAT isoforms and for CAT-1 (448 bp), CAT-2A (115 bp) and CAT-2B (125 bp). β-Actin was used to verify equivalent amounts of starting material.

A

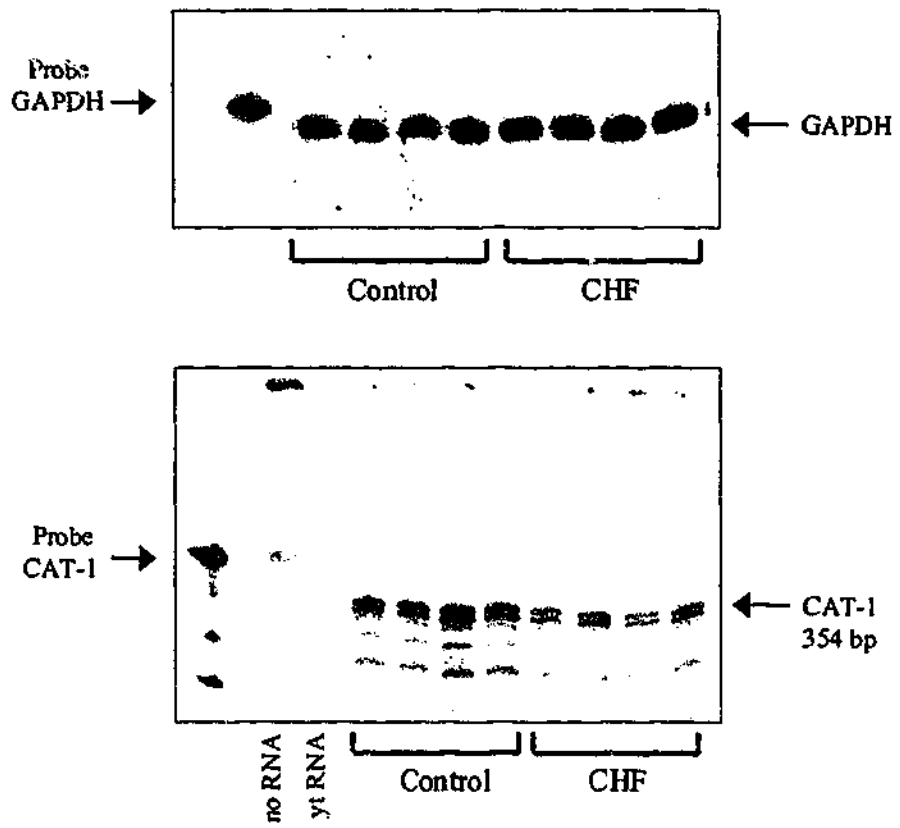

B

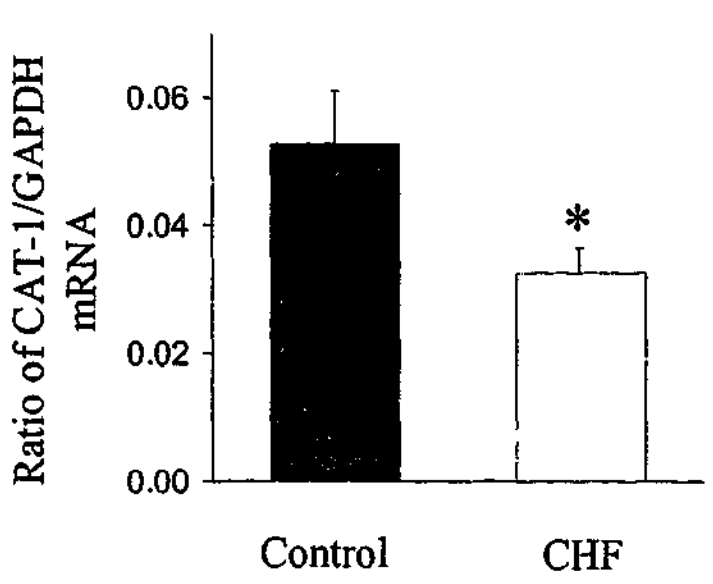

Figure 3.9 A) RNAase protection assay of CAT-1 mRNA expression normalised to GAPDH expression (top panel) in healthy control versus CHF myocardial samples. B) Bar graph showing the expression of CAT-1 mRNA relative to GAPDH mRNA as determined by ribonuclease protection assay in myocardial samples obtained from donor controls and explanted failing hearts. No RNA control indicates complete digestion of the unprotected probe. Sheared yeast tortilla RNA (ytRNA) was used to indicate specificity of the probe for CAT-1 target mRNA. *$P<0.05$.

A

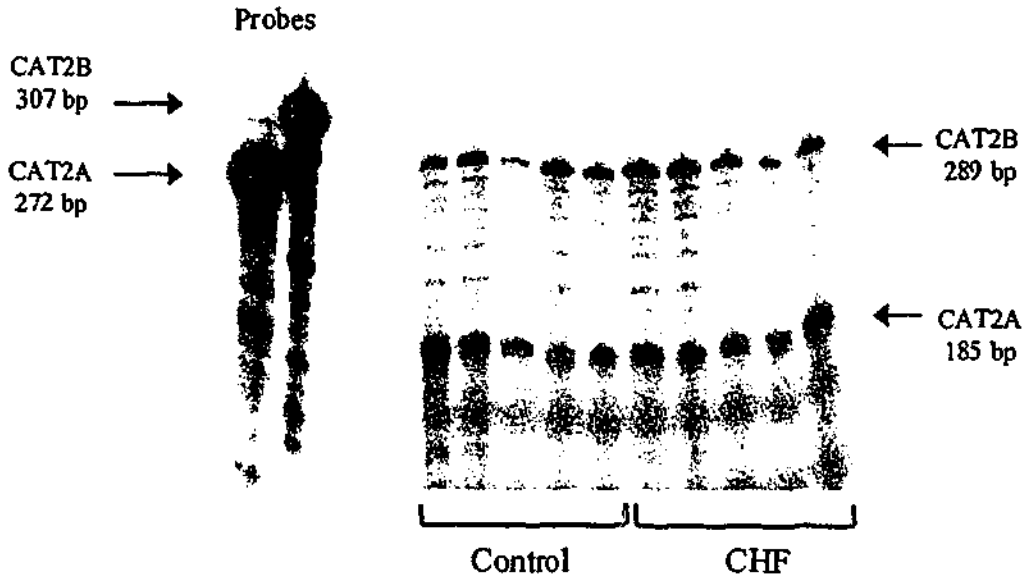

B

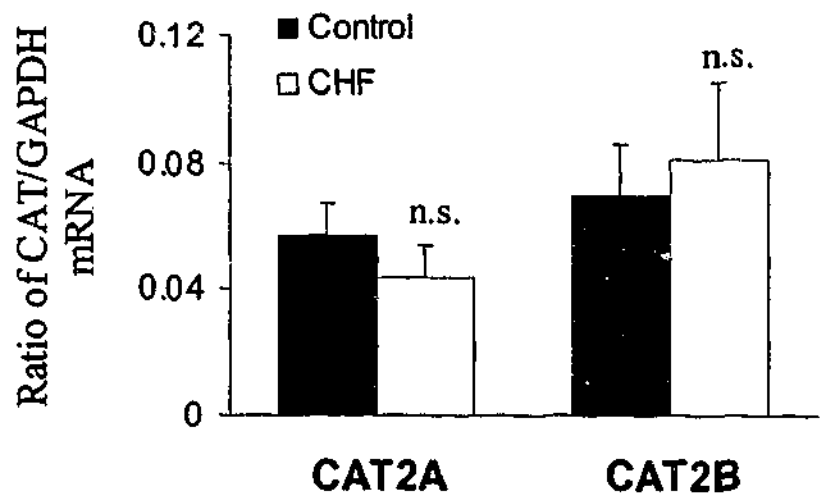

Figure 3.10 A) Representative RNAase protection assay showing CAT-2A and CAT-2B mRNA expression in control versus CHF myocardial samples. B) Bar graph showing the expression of CAT-2A mRNA and CAT-2B mRNA relative to GAPDH mRNA as determined by ribonuclease protection assay in myocardial samples obtained from donor controls and explanted failing hearts. The abbreviation n.s means not significant.

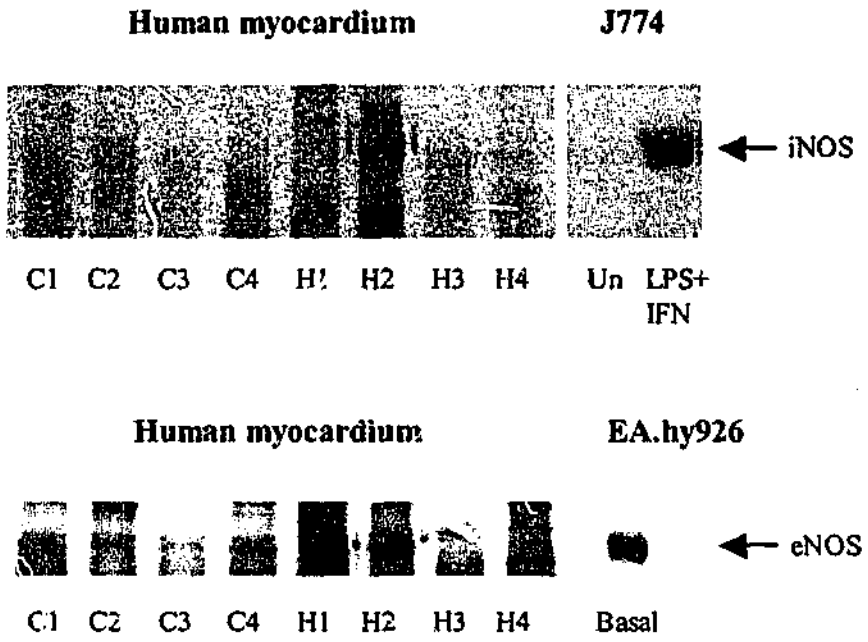

Figure 3.11. Western blot of eNOS (bottom panel) and iNOS (top panel) in the human CHF myocardium. Cellular homogenates were prepared from either unused healthy donor hearts (C1-C4) and from the failing hearts of patients undergoing cardiac transplantation (H1-H4) as described in Methods. Controls for iNOS were derived from J774 mouse macrophage cells (J774), either untreated (Un, negative control) or stimulated with 1 ug/mL lipopolysaccharide + 100 U/mL of γ-interferon (LPS+IFN, positive control) for 24 hr. The positive control for eNOS was the human endothelial cell line, EA.hy926, which exhibits basal expression of this isoform.

3.2.4 Discussion

3.2.4.1 Evidence of L-Arg transport abnormalities in the peripheral vasculature

Although the mechanism leading to the development of endothelial dysfunction in pathophysiological states probably represents a diverse array of predisposing factors, a common feature of endothelial dysfunction in human heart failure is a reduction in the biological actions of NO. The majority of evidence to support this is drawn largely from clinical studies reporting impaired endothelial-dependent vasodilatation mediated by NO mechanisms, such as in response to infused acetylcholine (Chapter 1, Section 4.3). In human heart failure, impaired NO-vasodilator responses have been observed in multiple vascular beds, including the forearm, lower limb, coronary circulation, and isolated resistance arteries (Kaye et al., 2000).

Beneficial effects of L-Arg supplementation on endothelial function is suggestive of a possible L-Arg deficiency in heart failure. However, these observations do not distinguish whether the deficiency is extracellular or intracellular. In a combined effort by members of our laboratory group, we tested the hypothesis that an impairment of cellular L-Arg transport was present in human heart failure. Using a novel *in vivo* approach in the human forearm, Dr. Kaye demonstrated a substantial reduction in the rate of clearance of L-[^{3}H]Arg from the circulation, consistent with an abnormality of endothelial L-Arg transport. The presence of endothelial dysfunction in the heart failure cohort of the present study, was evident by the presence of a significantly attenuated response to intra-arterial infusions of acetylcholine.

To further assess L-Arg transport in CHF, the kinetics of L-[^{3}H]Arg transport by freshly isolated PBM from healthy subjects and CHF patients were examined . In keeping with the findings of the *in vivo* radiotracer study, a substantial reduction (76% versus healthy controls) in the rate of L-[^{3}H]Arg accumulation by PBM over a range of physiologically relevant concentrations was demonstrated. This was shown to be due to a reduction in the maximal transport capacity for L-Arg (V_{max}) rather than due to changes in the affinity of transporters for L-Arg (K_m). We have further shown that a significant reduction in CAT-1 gene expression may account for the reduction in L-Arg transport in the peripheral vasculature of CHF patients.

Although system y+ accounts for the major proportion of L-Arg transport, it is possible that changes in expression of other L-Arg transporting systems, including the $B^{+,o}$, $b^{o,+}$ or y+L system, could explain our findings. However, this would seem unlikely given the fact that heart failure was associated with up to an 80% reduction in L-Arg transport rate, suggesting the involvement of the predominant L-Arg transport system. Of note, kinetic characterisation of cationic amino acid transport in PBM has previously identified a second system with properties of y+L in PBM that accounts for approximately 10% of total L-[^{3}H]Arg transport. Kinetic parameters (V_{max} and K_m) for the second system (Figure 3.6B) of L-Arg transport identified in PBM from CHF patients were not found to vary significantly from healthy subjects .

L-Arg transport in freshly isolated red blood cells (RBC) has also been utilised by others for assessing the status of intracellular L-Arg provision and its role in the L-Arg-NO pathway in heart failure. By contrast, Hanssen *et al.* (Hanssen *et al.*, 1998) have reported an absolute increase in total L-Arg transport rate in RBC from CHF patients. Whilst the aetiology and treatment regimes described for CHF patients in both studies have similarities, a few noted differences may potentially help to explain the apparent discrepancies in data, i) the present study determined specific L-[^{3}H]Arg transport properties on the basis of L-lysine insensitive transport values whereas Hanssen *et al.* determined specific L-[^{3}H]Arg transport properties on the basis of system y+ sensitivity to the sulfhydryl reactive chemical NEM. Whilst this inhibitor is thought to be useful in detecting y+ activity, it is important to mention that the selectivity of NEM for y+ inhibition has not formally been proven since many amino acid and other membrane transport systems also contain reactive sulfhydryl (-SH) groups (van Iwaarden *et al.*, 1992). ii) both studies have utilised non-linear least squares curve fitting of initial rate self-inhibition L-Arg transport values to the Michaelis-Menton equation and Eadie-Hofstee transformation of the resultant data in order to express system y+ and y+L components. However, only the Vmax for the major transport component (system y+) was affected in PBM whereas an increased affinity of y+L for L-Arg and an increased maximal transport rate of y+ was detected in CHF RBC. Increased affinity of y+L for L-Arg may impact upon transport rates in RBC since on the basis of NEM discrimination between system y+ and y+L, 50% of total L-Arg transport is attributable to y+L in red blood cells (Deves *et al.*, 1993) whereas only 10% of L-Arg transport is attributable to system y+L in PBM (Chapter 3.1) iv) whilst eNOS expression has been detected in RBC by sensitive RT-PCR methods, the enzyme is not thought to be catalytically active in RBC (Kang *et al.*, 2000). Further, in the absence of a nucleus RBC lack the capacity for regulated gene expression (Hirono and Miwa, 1996). This is an important difference since system y+/CAT transporters and eNOS are both known to be regulated at the gene expression level.

In summary, it is conceivable that a significant decrease in the rates of substrate provision via system y+ CHF may lead to a relative deficiency of intracellular L-Arg and subsequently affect NO synthesis.

3.2.4.2 Evidence of L-Arg transport abnormalities in the coronary vasculature

The main source of cardiac NO is generated through eNOS expressed by coronary endothelial cells and cardiac myocytes whereas iNOS is generally not present in healthy hearts (Schulz and Triggle, 1994). In addition to a coronary vasodilator role, NO is known to modulate cardiac contractile function (Moncada and Higgs, 1993, Shah and MacCarthy, 2000). In pathological situations such as heart failure an increase in myocardial NO generation is proposed to occur exerting deleterious negative inotropic effects on the heart, through a reduction in ventricular contractility, leading to contractile dysfunction. This proposal has been based on a few reports of increased NO metabolites in CHF, increased iNOS and/or eNOS expression and enzymatic activity in skeletal and myocardial tissue (Haywood et al., 1996, Vejlstrup et al., 1998, de Belder *et al.*, 1993). (Chapter 1, Table 1.2) in the face of an apparent reduction in the endothelial L-Arg NO pathway (Chapter 1, Section 4). However, increased myocardial NO generation in CHF remains controversial as evidenced by conflicting reports. Also, more direct biochemical evidence in the failing human heart has not reported on alterations in NO production (Kaye et al., 1998). Alternatively, a reduction in basal NO production has been reported in an experimental pacing-induced model of heart failure (Recchia *et al.*, 1998). In accordance, data from the present study does not support an upregulation of either eNOS or iNOS expression (the present study) or NOS activity (work of Dr. Parnell) in the CHF myocardium. Thus, the pathophysiological role of NO in this context remains largely equivocal.

Based on the existing lines of evidence, we hypothesised that reports of increased NOS expression in the face of reduced NO production could be explained by a relative limitation in the intracellular availability of L-Arg due to a decreased rate of L-Arg transport. Certainly, strong evidence gained from transgenic L-Arg transporter knockout mice has convincingly demonstrated the absolute

dependence on a co-ordinate induction of the system y+ transporter CAT-2B isoform with iNOS expression for sustained and pathologic levels of NO production in response to inflammatory cytokine mediators (Nicholson *et al.*, 2001). There is no evidence from the present findings of an induction of either CAT-2B mRNA, iNOS protein and NOS activity in the CHF myocardium.

In an attempt to address possible alterations in substrate provision for the NO pathway within the failing heart, Dr. Kaye has assessed fractional extraction of L-[^{3}H]Arg in the coronary circulation (Kaye et al., 2002). A major finding of our study was a significantly reduced fractional extraction of L-[^{3}H]Arg during passage through the coronary circulation consistent with a reduced rate of L-Arg transport in patients with CHF. Furthermore, this decline correlated with a significant reduction (P<0.05) in mRNA for the system y+ transporter, CAT1, in failing heart samples compared with healthy unused donor myocardium. Reduced CAT-1 expression but no detectable changes in the level of eNOS protein or NOS activity are suggestive that a deficiency of L-Arg provision may in exist within the CHF myocardium. Existing evidence based on myocyte-specific eNOS overexpressing mice, eNOS knockout mice and pharmacologic NO donors suggests that an increased NO release derived from eNOS activity in myocytes may have a cardioprotective role in pathophysiological states that are associated with decreased NO bioavailability (Brunner *et al.*, 2001). Thus, a possible reduction in L-Arg provision for the NO pathway may result in an abolition of beneficial eNOS-derived NO effects on the heart.

A limitation of the current study is that myocardial gene expression studies from explanted failing hearts were not performed in the same group of CHF and healthy subjects that underwent assessment of *in vivo* L-Arg kinetics for evident reasons. Accordingly, the degree of disease severity was greater in CHF myocardial tissue than in the CHF patients (NYHA Class II-III). Thus is a possibility that reduced CAT-1 expression is a consequence of end-stage failing heart aetiology rather than due to a generalised defect in CHF. Collective *in vivo* and *in vitro* studies from our laboratory did not precisely identify the cell types accounting for reduced L-Arg transport capacity in the failing heart. Furthermore, a correlation of *in vivo* L-Arg transport rate with NOS enzyme

activity from explanted failing hearts could not be established. Collectively, our data has provided evidence for the cardiac impairment of L-Arg transport which may be explained by a reduction in mRNA expression for the major L-Arg transporter in the myocardium, CAT-1.

3.3 L-Arg Transport In Age-Related Endothelial Dysfunction

3.3.1 Introduction

Aging is associated with various abnormalities in the coronary vasculature such as progressive endothelial dysfunction (Quyyumi, 1998, Mayhan *et al.*, 1990, Dohi *et al.*, 1990). Numerous clinical studies have demonstrated that the aging process is associated with impaired endothelium-dependent vasodilation characterised by the blood flow response to administered acetylcholine (ACh), including the coronary epicardial arteries and microvasculature (Yasue *et al.*, 1990, Egashira *et al.*, 1993, Chauhan *et al.*, 1996), brachial arteries (Taddei *et al.*, 1995, Andrawis *et al.*, 2000), dorsal hand vein (Dachman *et al.*, 1992) and renal vasculature (Higashi *et al.*, 1997). ACh dilates normal vessels by releasing the endothelium-derived relaxing factor, nitric oxide (NO) (Palmer *et al.*, 1987). Additional contributory factors may include decreased prostacyclin and/or EDHF(s) release (Ref).

Reversal of endothelial function by L-Arg supplementation is known to be beneficial in aging individuals, where acute L-Arg administration has been shown to augment skeletal muscle vasodilation (Meneilly *et al.*, 2001) and restore coronary microvascular function (Chauhan et al., 1996). An age-related decline in endothelial function has been linked to a decreased NO bioavailability (Matz *et al.*, 2000). Such findings suggest that decreased substrate availability for eNOS may lead to a decrease in NO production and therefore contribute to endothelial dysfunction.

While it is well established that the function of the endothelium decreases with age, the mechanism(s) behind this dysfunction are not fully documented. The present study sought to investigate whether the age-related decline in endothelial function is due to a mechanism involving reduced L-Arg transport.

3.3.2 Methods

3.3.2.1 Exclusion criteria for aging individuals

Healthy volunteers were recruited from the general population to provide 30 mL of peripheral venous blood. All recruits had blood pressure, glucose, cholesterol and triglycerides within the normal range and no history of cardiovascular disease. Thirty healthy volunteers were divided into one of three groups according to age: young (n=14; mean age 22.8 ± 0.7; range 19-27 years), middle age (n=13; 39.4 ± 1.9; range 30-48 years) and older (n=10; 61.5 ± 2.1; range 50-69 years). These subjects were recruited from the Alfred and Baker Risk Clinic, following the same inclusion criteria as the *in vivo* study.

3.3.2.2 L-[^{3}H]Arg transport in peripheral blood mononuclear cells

As previously described in Chapter 3.2.2.2.

3.3.3 Results

3.3.3.1 PBM L-[^{3}H]Arg transport in the aging population

To investigate the association of aging with a decline in endothelium function, L-Arg transport was measured in freshly isolated PBM from healthy volunteers. Complementary to the *in vivo* study, L-Arg transport was measured in freshly isolated PBM from a healthy aging population. As shown in Figure 3.12, no significant difference in L-Arg transport was detected between the young, middle-aged or older age groups in PBM. Variations in L-Arg transport from within the normal healthy population were detectable in all groups. Outcomes of various experimental and clinical studies have indicated that a beneficial effect the sex steroid oestrogen on endothelial function may exist in premenopausal women due in part to its effects on the L-Arg-NO pathway. The possibility of a confounding gender-related effect on L-Arg transport in the same cohort of healthy individuals was investigated. Further analysis of the L-Arg transport data revealed no significant differences in individuals grouped as healthy males versus healthy pre-menopausal females (25-25 year of age;

results not shown) or post-menopausal women (>50 years of age) versus pre-menopausal women (< 30 yrs of age; results not shown).

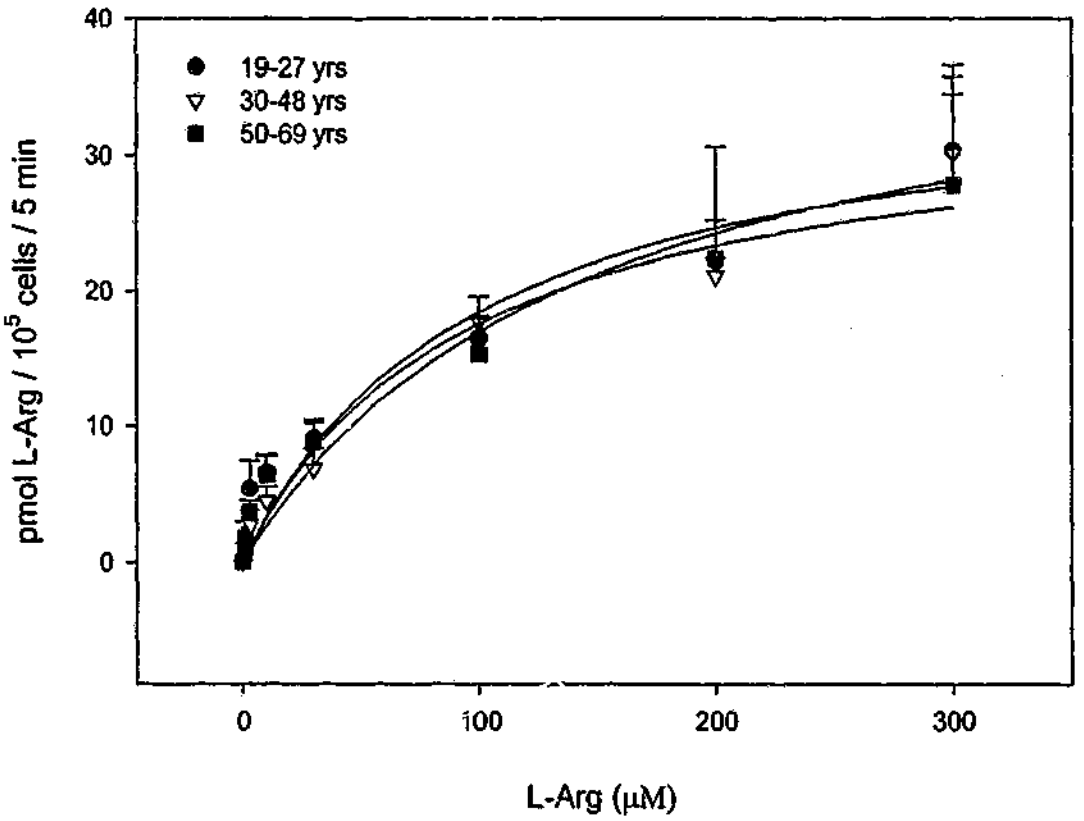

Figure 3.12 L-Arg transport in isolated PBM from young (closed circles), middle-aged (open triangles) and older (closed squares) healthy individuals (p=ns). Self-inhibition kinetics were performed on isolated PBM from each individual for 5 min using a fixed concentration of 100 nmol/L labelled [^{3}H] L-Arg in the presence of incremental unlabelled L-Arg concentrations from 1 – 300 μmol/L. Data are expressed as pmoL L-arg / 10^5 cells/ 5 min and represented as mean ± SEM, n=10 for each group.

3.3.4 Discussion

Work performed within this laboratory by a colleague (Personal communication Dr. Parnell) supports previous findings that ACh-induced vasodilation decreases with age in healthy subjects (Andrawis et al., 2000, Taddei et al., 1995). In accordance with the current literature, endothelial-

independent vasodilation was preserved with aging in the present study (Andrawis et al., 2000). However, data from the present study and our laboratory has revealed that the age-related decline in endothelial function was not associated with a reduction in L-Arg transport activity as assessed by *in vivo* and *in vitro* techniques. Therefore, mechanisms other than reduced L-Arg transport mediate the age-related decline in endothelial function.

Since the present study suggests that there is adequate substrate availability for eNOS in the aging human population it is likely that factors further downstream in the L-Arg-NO pathway may be associated with the age-related decline in endothelial function. Alterations in the localisation of eNOS, NOS expression and/or activity, NOS co-factor availability and an altered NO half-life have all been previously reported to modulate NO production in a broad range of experimental models (Shaul, 2002, Papapetropoulos *et al.*, 1999, Katusic, 2001). In accordance, reduced eNOS activity in aging rats has also been demonstrated by others both *in vivo* (Chou *et al.*, 1998) and *in vitro* (Sato *et al.*, 1993). In the present study venous [^{3}H] L-citrulline concentration, a by-product of [^{3}H] L-Arg conversion in the NOS reaction, was determined in response to intraarterial infusion of acetylcholine as a marker of NOS activity *in vivo* (data not shown). Whilst a trend for reduced NOS activity with age was observed, no significant difference across the age-spectrum was detected in humans. Increased levels of the endogenous NOS inhibitors such as ADMA have also been reported to reduce NO production. Accordingly, a previous study has detected elevated serum levels of ADMA in aged rats with endothelial dysfunction (Xiong *et al.*, 2001). ADMA is a known competitor of L-Arg for transport by system y+ (Cooke, 2000). Since our collective results did not reveal age-related changes in L-Arg transport *in vivo*, the current data suggests that circulating factors such as ADMA do not contribute to the age-related decline in human endothelial function by modulating L-Arg transport activity.

An age-related decrease in growth hormone leads to a reduction in circulating IGF-I and changes in the expression of IGF-binding proteins (Khan *et al.*, 2002). Previous studies have demonstrated that IGF-I stimulates endothelial NO production and has been shown to induce endothelium-dependent

vasodilation in experimental animal models as well as in humans (Boger, 1999). Moreover, growth hormone treatment has been shown to augment endothelial function when administered to congestive heart failure patients (Napoli *et al.*, 2002). Therefore, decreased growth hormone and IGF-1 may also be linked to the age-related decline in endothelial function. Numerous studies have highlighted the susceptibility of the aging endothelium to oxidative stress and free radical damage (Yu and Chung, 2001). Taddei and colleagues demonstrated that vitamin C increased ACh-induced vasodilation and restored the inhibitory effect of L-NMMA in elderly sedentary subjects (Taddei *et al.*, 2000). In addition, the finding that vitamin C has no beneficial role in the blood vessels of endurance trained elderly athletes with preserved endothelial function (Taddei et al., 2000) highlights an importance of oxidative stress in age-related endothelial dysfunction. *In vivo* formation of peroxynitrite and increased lipid peroxidation has also been shown in various vessel types in aging experimental animal models (Drew and Leeuwenburgh, 2002, Csiszar *et al.*, 2002). Thus, oxidative stress is a likely major contributing factor to age-related endothelial dysfunction.

Of the numerous reports investigating the basis of endothelial dysfunction, many have implicated alterations in the equilibrium between endothelium-derived vasodilatory and constricting factors. An increase in circulating levels of vasoconstrictor hormones such as noradrenaline and endothelin-1 have been associated with aging (White *et al.*, 1997). In addition to impaired ACh-induced vasodilation, aging has been reported by some to lead to an impairment of beta-adrenoceptor mediated (van der Zypp *et al.*, 2000) and prostanoid vasodilatory pathways (Singh *et al.*, 2002) as well as a reduction in NO-independent and NO-dependent adenosine responses (Hinschen *et al.*, 2001). Thus, decreased vasodilation due to a decreased production of NO and, in some arteries, endothelium-derived hyperpolarizing factor (Urakami-Harasawa *et al.*, 1997) as well as reports of an increased vasoconstriction mediated by endothelin-1 and cyclooxygenase products such as COX-1 and thromboxane A2 may contribute to age-related impairment of endothelium-dependent vasodilation (Matz et al., 2000, Heymes *et al.*, 2000).

There is clear evidence demonstrating that endothelium-dependent vasodilation is impaired in the aging human population. A decline in endothelial function has been associated with the development and progression of cardiovascular disease. Therefore, strategies to enhance endothelial function may become increasingly attractive. While impaired L-Arg transport has been demonstrated in cardiovascular diseases such as hypertension and heart failure, the present study excludes the hypothesis of impaired substrate availability in the elderly as a major contributor to endothelial dysfunction.

Chapter Four

Regulatory Factors Influencing L-Arginine Transport In The Human Endothelium

TABLE OF CONTENTS

4.0 General Introduction 146

4.1 Effect Of Neurohormones And Cytokines On L-Arginine Transport In The Human Endothelium 148

4.1.1 Introduction 148

4.1.2 Methods 150

4.1.2.1 Experimental screening regime 150

4.1.2.2 Serum preparation 150

4.1.2.3 Cell culture 151

4.1.2.4 L-[^{3}H]Arg transport in EA.Hy926 151

4.1.3 Results 153

4.1.3.1 Time and concentration dependent L-[^{3}H]Arg uptake in EA.Hy926 cells 153

4.1.3.2 Effects of CHF serum treatment on L-[^{3}H]Arg transport 156

4.1.3.3 Effects of CHF cytokines and neurohormones on L-[^{3}H]Arg transport 157

4.1.4 Discussion 159

4.1.4.1 Properties of L-Arg transport in EA.Hy926 159

4.1.4.2 Cytokines and neurohormonal effects on endothelial L-Arg transport 160

4.2 Ang II stimulated L-Arginine transport in human endothelial cells is mediated by the AT4 receptor. 163

4.2.1 Introduction 163

4.2.2 Methods 164

4.2.2.1 L-[^{3}H]Arg transport assay 164

4.2.2.2 Ribonuclease protection assay 164

4.2.2.3 eNOS Western blot 165

4.2.2.4 Materials 165

4.2.2.5 Statistical analysis 166

4.2.3 Results 166

4.2.3.1 Ang II stimulates transport of L-Arg in EA.Hy926 cells 166

4.2.3.2 Increased CAT-1 gene expression by Ang II 167

4.2.3.3 AT_1 and AT_2 receptor blockade effect on Ang II stimulated L-Arg transport 170

4.2.3.4 AT_4 receptor antagonist effect on Ang II stimulated L-Arg transport 170

4.2.3.5 PKC activation is associated with Ang II- stimulated L-Arg transport 171

4.2.3.6 Effects of Ang II on NOS Expression and Activity 173

4.2.4 Discussion 173

TABLE OF FIGURES 4

Figure 4.1 A) Specific L-Arg uptake by EA.hy926 cells as a function of time. B) Concentration-dependent specific L-Arg uptake in EA.hy926 cells. 154

Figure 4.2 *Trans*-stimulation of L-Arg transport in BAEC. 156

Figure 4.3 Assessment of L-Arg transport in EA.hy926 after treatment with CHF serum. 157

Figure 4.4 Time dependent L-Arg transport in response to neurohormones and cytokines. 158

Figure 4.5 Induction of L-Arg transport activity and CAT-1 mRNA expression by Ang II in EA.hy926 cells. 168

Figure 4.6 Ribonuclease protection analysis of CAT-1 mRNA following treatment of EA.hy926 with Ang II for the indicated times. 169

Figure 4.7 Effect of Ang II receptor antagonists on Ang II stimulated L-Arg transport. 170

Figure 4.8 Effect of Ang II degradation fragments on L-Arg transport in endothelial cells. 171

Figure 4.9 Effect of PKC inhibition on Ang II stimulated L-Arg transport. 172

4.0 General Introduction

Alongside a clinical approach taken by Dr. Kaye (Kaye *et al.*, 2000), *in vitro* data from Chapter 3 has demonstrated the existence of a depressed L-Arg-NO pathway both in the peripheral vasculature, myocardium and circulating peripheral blood mononuclear cells (PBM) of patients with CHF. Specifically, a decreased maximal velocity rate for intracardiac and vascular L-Arg transport was evident with no detectable changes in the apparent affinity of the major L-Arg transport system present for its substrate (K_m). A decreased rate of L-Arg transport in CHF corresponds with a significantly decreased gene expression of the major L-Arg transporter, CAT-1, detectable both in PBM and the myocardium of patients with CHF. These findings might lead to the concept that decreased expression of CAT-1 protein at the plasma membrane is an underlying mechanism, amongst others, in endothelial dysfunction by contributing to a reduction in substrate provision and therefore bioavailablity of NO. Since the *in vitro* data collected in Chapter 3 were from PBM that had been freshly isolated from an *in vivo* setting these results are suggestive that circulating factors present in CHF plasma may have an influence on the expression and/or activity of the L-Arg transporter.

The present chapter sought to assess the potential of factors relevant in the setting of CHF to modulate the L-Arg transport pathway in the human endothelium. In Chapter 3, isolated PBM from CHF patients were used as a model of L-Arg transport in the human endothelium since they are exposed to the same range of pathological stimuli *in vivo*, thereby providing a minimally invasive approach for assessing the status of *in vivo* L-Arg transporter activity. In order to isolate and identify regulatory factors relevant in the setting of CHF, which may affect endothelial L-Arg transport, cultured endothelial cells were employed as a suitable model for all subsequent studies presented within this thesis.

Surprisingly, treatment of cultured endothelial cells with either CHF serum or most of the major pathophysiologically relevant factors in CHF did not significantly reduce basal L-Arg transport activity. Thus, a conclusion to the work presented in this chapter is that alternative processes (eg. shear stress) relevant in CHF may underly this L-Arg transport abnormality. A major finding of this study was the ability of Ang II to significantly modulate L-Arg transporter activity and expression (CAT-1) in the endothelium. Paradoxically, L-Arg transport activity was significantly increased in human endothelial cells in response to treatment within a physiological concentration range of Ang II by a novel pathway that seems to involve a metabolically active degradation product of Ang II in the culture media. Given the context of the present chapter these findings are surprising. However, this work may provide an insight into the mechanisms by which Ang II exerts its actions *in vivo* and potentially reveal a beneficial therapeutic strategy in the treatment of endothelial dysfunction. The data and its relevance to endothelial dysfunction is presented within a separate section of Chapter 4 (Section 4.2).

4.1 Effect Of Neurohormones And Cytokines On L-Arginine Transport In The Human Endothelium

4.1.1 Introduction

The course of heart failure can be characterised by progressive left ventricular deterioration in association with activation of compensatory neurohormone pathways. Activation of these systems is accompanied by increases in the circulating levels of noradrenaline, aldosterone, angiotensin II and endothelin (Stanek *et al.*, 2001). .In certain instances, the level of activation of these major systems has been shown to correspond to the severity of heart failure (Dargie, 1999). Additionally, elevated circulating levels of pro- and anti-inflammatory cytokines, interleukin (IL)-10, IL-6, IL-1β, tumor necrosis factor-alpha (TNF-α) and their soluble receptors have been reported in many forms of human heart failure. The predominant cardiovascular action of many of these compounds is peripheral vasoconstriction. Interestingly, many of these factors have been demonstrated to exert their vasoactive properties by modulating or inactivating the L-Arg-NO pathway.

Table 4.1 is a compiled list of the major cytokines and neurohormones that are known to be released or that are elevated in human plasma in the later stages of heart failure (New York Heart Association Class, NYHA, II-IV) along with reported plasma concentrations. All data controls used in the determination of the levels were healthy individuals matched on the basis of age alone and exclusion criteria for any individuals with pre-existing cardiovascular risk factors and conditions. Reporting of these levels is found to vary widely in the literature that seems likely to be due to the method of detection used and categorisation of patient groupings. It is noteworthy to state here that the absolute plasma concentrations of the factors listed are not necessarily representative of their local tissue-based concentration, nor of their specific role in endothelial dysfunction.

Table 4.1 Neurohormonal and cytokine factors elevated in congestive heart failure.

Factors		Healthy	CHF	Fold change
NA; pg/mL		294	1004	↑3
Aldosterone; pg/mL		45	505	↑10
ANP; pg/mL		26	445	↑17
BNP		n.a.	n.a.	n.a.
Ang II ; pM [1]		12	81	↑8
ET-1 ;	pg/mL[2]	7	14	↑2
	pg/mL[3]	7	12	↑1.5 – 2
IL-10[4]		n.a.	n.a.	n.a.
IL-6[5]		n.a.	n.a.	n.a.
IL-1β[6]		n.a.	n.a.	n.a.
TNF- α ;	pg/mL	22	47	↑2.5
	U/mL[7]	9	115	↑10
sTNF-RI;	ng/mL	1	5	↑5
sTNF-RII;	ng/mL	2	10	↑5

Table partially adapted from Agnoletti *et al.* (Agnoletti *et al.*, 1999); [1]Ang II (Pedersen *et al.*, 1986); [2,3] ET-1 (Rodeheffer *et al.*, 1992) and (Lerman *et al.*, 1992); [5] IL-6 (Dibbs *et al.*, 1999); [7]TNF (Levine *et al.*, 1990); n.a. data not available; NA, noradrenaline, ANP, atrial natriuretic peptide; BNP, brain natriuretic peptide; Ang II, angiotensin II; ET-1, endothelin-1; IL, interleukin; TNF-α, tumor necrosis factor-alpha; sTNF-RI and RII, soluble tumor necrosis factor receptor 1 and II; ↑ and ↓ denotes increase and decrease respectively.

Nevertheless, these circulating factors (Table 4.1) provide a working list of potential candidates that may modulate L-Arg transport in the endothelium. Accordingly the work in this chapter has sought to use a human endothelial cell model in order to explore separately the direct effects of elevated circulating factors present in the plasma of CHF patients or CHF serum on L-Arg transport activity.

4.1.2 Methods

4.1.2.1 Experimental screening regime

The cytokines and neurohormones selected for this study are listed in Table 4.2. Appropriate concentrations for use under culture conditions are also listed. Concentration ranges were tailored to be within the accepted standard ranges for treatment for cultured cells in the published literature. In order to assess any potential dose-dependent effects of these agents cells were treated within the dosage range as stated in Table 4.2 and after a 24 hr incubation time in culture. After incubation, L-Arg transport was determined and values compared to controls (treated with the appropriate vehicle). For the assessment of time-dependent effects, L-Arg transport was determined at defined time points as indicated in Results after cells had been treated separately with each agent at the upper dosage limit listed in Table 4.2 (100 nM ANP, 100 nM Ang II, 100 nM ET-1, 10 μM NE or 100 nM TNF-α). Where an agent demonstrated a significant effect on L-Arg transport, a further investigation with this agent was carried out (Section 4.2).

4.1.2.2 Serum preparation

Whole blood was obtained from CHF patients recruited from the Heart Failure Service, Alfred Hospital, Melbourne, Australia, and healthy control volunteers. Left ventricular ejection fraction was 23±4% (mean±SEM), and all patients had New York Heart Association class III symptoms of CHF. All patients participated after giving informed consent, and the study was conducted with the approval of the Alfred Hospital Ethics Review Committee. Approximately 30 mL of whole blood was collected in 10 mL stopper tubes. The blood was allowed to clot at RT for 30 min. After

allowing the clot to form, tubes were centrifuged at 3000 x g for 15 min at 4°C. The serum was carefully removed using a Pasteur pipette. Samples were then frozen at -80°C until further use.

Table 4.2 Cell culture experimental dosage range for neurohormone and cytokine treatment.

Cytokine/Neurohormone	Dosage Range	Additional Factors In Culture *
ANP	100 pM - 100 nM	
Ang II	1 pM - 100 nM	
ET-1	1 pM - 100 nM	
NA	100 pM - 10μM	1 mM Ascorbic acid;
TNF-α	1 pM - 100 nM	

* Note that NA was added to cells alongside ascorbic acid. Ascorbic acid is known to preserve NA and prevents its rapid breakdown of under *in vitro* culture conditions (Dillon *et al.*, 2000). Ang II, angiotensin II; ANP, atrial natriuretic peptide; ET-1, endothelin-1; NA, noradrenaline; TNF-α, tumor necrosis factor-α.

4.1.2.3 Cell culture

A permanently established endothelial cell line EA.hy926 that is derived from the HUVEC cell type (a generous gift from Cora-Jean Edgell, University of North Carolina), was maintained in Dulbecco's modified Eagle's medium (DMEM) supplemented with 10% fetal bovine serum, 5 mM hypoxanthine, 0.8 mM thymidine, 20 μM aminopterin (HAT supplement), 100 U/mL penicillin, 100 μg/mL streptomycin and 2.5 μg/mL fungizone.

4.1.2.4 L-[^{3}H]Arg transport in EA.Hy926

Confluent monolayers of EA.hy926 cells were prepared in 24 well plates. Cells were serum deprived in DMEM containing 0.5 % fatty acid free BSA 24 hr prior then rinsed twice with pre-

warmed Locke's solution (in mM: 154 NaCl, 5.6 KCl, 2 $CaCl_2$, 1 $MgCl_2$, 10 HEPES pH 7.4, 3.6 Na HCO_3 and, 5.6 glucose) prior to all L-Arg transport measurements. Prior to treatment regimes a characterisation of L-Arg transport in EA.hy926 cells was carried out as follows. For an analysis of time-dependent L-Arg transport in these cells, transport buffer (Locke's solution containing 100 nM L-[^{3}H]Arg and unlabelled L-Arg totalling 100 μM) were placed in all wells and incubated for defined lengths of time. Linear conditions of transport were determined at 5 min or less. Concentration-dependent L-Arg transport was determined after a 5 min (linearity) incubation of 100 nM L-[^{3}H]Arg with unlabelled incremental L-Arg concentrations added (0.1 – 1000 μM) into each well. The effect of competing amino acids and compounds on L-Arg transport was evaluated by adding saturating concentrations of either 10 mM L-Arg, 10 mM L-Lysine, 10 mM of the L-Arg analogue L-NMMA or 100 μM L-Leucine in the transport buffer. In trans-stimulation experiments, cells were deprived of amino acids for 2 hr with Locke's solution. After this time cells were pre-loaded with defined concentrations of L-Arg (unloaded control) for an additional 1 hr and L-[^{3}H]Arg transport measured as indicated in Results. Where indicated, treatment regimes were initiated by adding either serum obtained from CHF patients or each factor listed in Table 4.2 separately to the culture media for time and dose indicated. After incubation with the relevant factor, cell monolayers were rinsed twice with pre-warmed Locke's solution prior to transport measurement.

Transport of L-Arg by EA.hy926 cells was initiated by adding 500 μL of transport buffer containing the radiolabelled L-[^{3}H]Arg for the times indicated in Results. Transport of L-Arg was terminated by the addition of ice-cold transport buffer and wells were rinsed three times with 1 mL of ice-cold transport buffer. Cell monolayers were then air-dried followed by solubilisation in 500 μL 0.2% SDS + 0.2 M NaOH. For treatment regimes non-specific L-Arg transport correction was determined for each data point by subtracting the radioactivity associated with 100 μM L-Arg transport in the presence of 10 mM saturating lysine, a competitor for the same transport system, in parallel treatment wells. Specific L-Arg transport was expressed as pmol L-Arg / μg protein/ 5 min.

Non-specific bound L-Arg accounted for <5% of radioactivity counts and was considered negligible. Protein content was determined by the Lowry assay (Lowry *et al.*, 1951). Radioactivity associated with each sample was determined by liquid scintillation spectroscopy.

4.1.3 Results

4.1.3.1 Time and concentration dependent L-[^{3}H]Arg uptake in EA.Hy926 cells

Prior to measuring the effects of various factors, preliminary studies were conducted in order to characterise the major L-Arg transport system present in this cell type. The time course of L-Arg transport was evaluated initially (Figure 4.1A). L-Arg transport was time-dependent with linear transport kinetics determined for at least 5 min. Thus, in order to maintain linearity of the L-Arg transport kinetics an incubation time of 5 minutes was selected for the remaining studies. Concentration-dependent L-[^{3}H]Arg transport was measured for 5 min at 37°C over a range of incremental L-Arg concentrations (0.1- 1000 μM) (Figure 4.1B). A maximal uptake velocity of (V_{max}) of 1.4 ± 0.1 pmol/L L-Arg/μg protein/5 min was evident in this cell type. Eadie-Hofstee linear transformation of this data revealed a single high-affinity transporter with a Michaelis constant (K_M) of 72.6 ± 13.8 μmol/L.

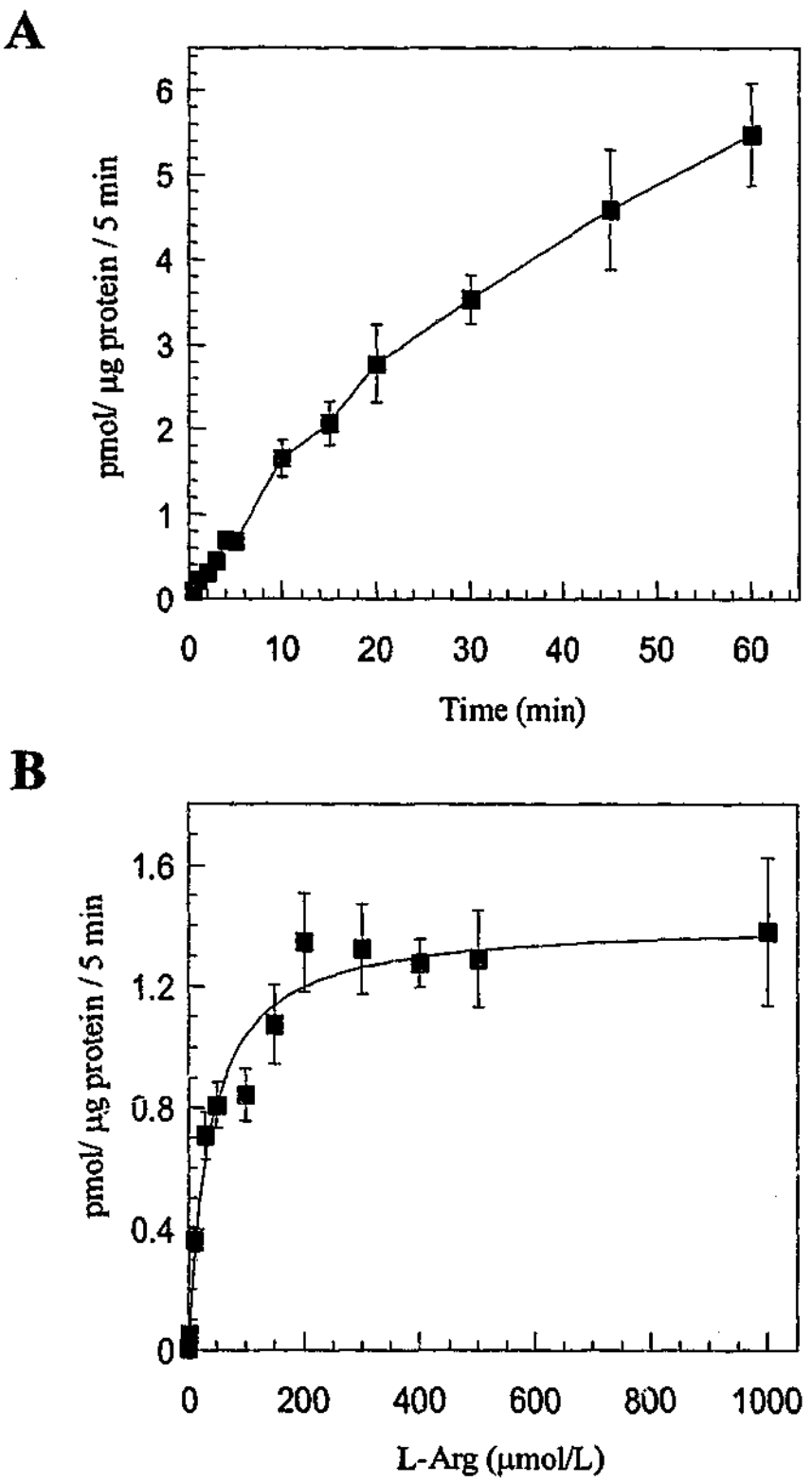

Figure 4.1 A) Specific L-Arg uptake by EA.hy926 cells as a function of time. Uptake of 100 µM L-Arg incorporating 100 nM L-[^{3} H]Arg and unlabelled L-Arg was measured over a time course of 0 - 60 minutes. Data are expressed as pmol/L L-Arg/ µg protein/5 minutes and represent mean ± SEM, n=4 experiments. **B) Concentration-dependent specific L-Arg uptake in EA.hy926 cells.** Uptake of 100 nM was measured for 5 min over a range of unlabelled L-Arg concentrations (0.1 – 1000 µM). Data are expressed as pmol/L L-Arg /µg protein/5 minutes and represent mean ± SEM, n=4 experiments.

The majority of L-[^{3}H]Arg was transported in a Na+-independent manner, because substitution of Na+ ions with choline ions in the external transport buffer resulted in a minor 7% reduction in L-[^{3}H]Arg transport by EA.hy926 cells (results not shown). These findings are consistent with recently published data from Closs *et al.* (Closs *et al.*, 2000) using the same cell line.

Transport of 100 μM L-Arg was measured in the presence (10 mM) and absence of various cationic (L- and D-isomers) and neutral amino acids (results not shown). L-Arg transport was found to be stereo-specific and was inhibited significantly by cationic amino acids (L-Arg, L-Lysine and L-Ornithine) and also by the cationic L-Arg analog N^G-monomethyl-L-Arg (L-NMMA), which is also a potent inhibitor of eNOS. In contrast, the neutral amino acid L-Leucine (93% of control) and the neutral L-Arg analog inhibitor of eNOS, L-NAME (89% of control), were all poor inhibitors in the presence of Na+ ions. To verify, that the Na+-independent transport of L-Arg was being mediated exclusively by system y+ as opposed to system y+L or $b^{0,+}$ which also transport L-Arg in the absence of Na+ ions (Kilberg *et al.*, 1993, Deves *et al.*, 1993), L-Arg transport was measured in the presence of N-ethyl maleimide (NEM), a sulfhydryl reactive agent that has been reported to inhibit transport via system y+ (Deves et al., 1993). Treatment with 200 mM NEM caused a significant reduction in L-Arg transport (16% of untreated control, $P<0.05$).

As described in Chapter 1.6.2.1, one of the distinctive properties cationic amino acid transport mediated by system y+ is the *trans*-stimulation of amino acid transport when the substrate concentration is sufficiently high on the opposite side of the membrane. A detailed mechanism of this phenomenon has not yet been fully defined. To study this particular property of the system y+ transport in cultured human venous endothelial cells, cells were initially deprived of amino acids then pre-loaded with either 100 nM, 100 μM or 1 mM of L-Arg for 1 hr. The transport of L-[^{3}H]Arg (physiological concentration of 100 μM) was compared to L-Arg transport by cells without an initial pre-loading step (control transport). A significant *trans*-stimulatory effect of all

pre-loaded intracellular L-Arg concentrations was apparent for L-Arg transport when compared to unloaded cells (Figure 4.2).

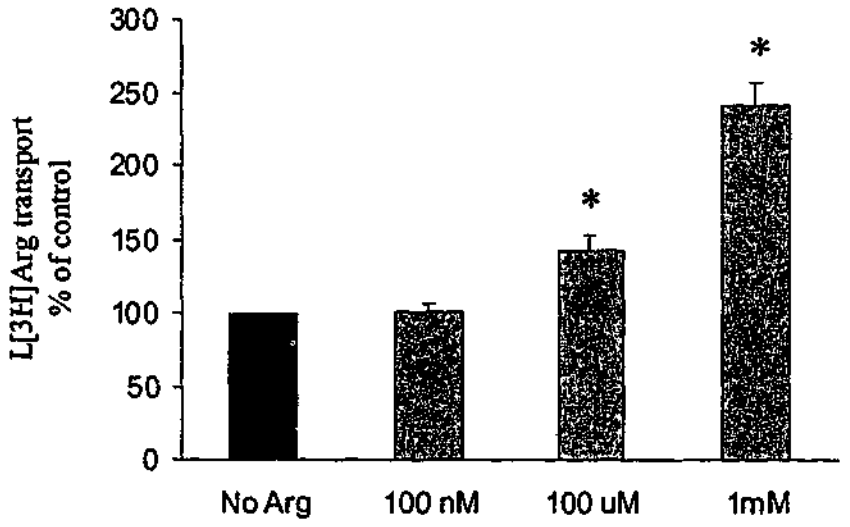

Figure 4.2 ***Trans*-stimulation of L-Arg transport.** L-Arg transport (100 μM, 5 min, 37°C) in amino-acid deprived cells preincubated (1 hr) in Locke's solution in the absence (control) or presence of 100 nM, 100 μM or 1mM L-Arg. Transport assays were performed in cells exposed to 100 μM L-Arg for the last 5 min of the 1-hr incubation period with L-Arg. Values are mean±SEM (n=3). *$P<0.05$ vs all other values.

4.1.3.2 Effects of CHF serum treatment on L-[^{3}H]Arg transport

The effect of CHF serum containing the same range of circulating factors that are present *in vivo* Serum was collected from clotted whole blood of either age-matched healthy controls or CHF patients (NYHA Class II–IV) and stored at –80 °C until required. EA.hy926 that had been serum deprived for 24 hr (0.5%BSA) were incubated for an additional 24 hr in fresh DMEM with 20% or 40% serum (v/v) from either the healthy controls or patients with CHF. After this time L-[^{3}H]Arg transport was assessed. As shown in Figure 4.3, the L-Arg transport activity of cells treated with either 20 or 40% CHF serum for 24 hr was not significantly different from that determined in cells that had been treated with equivalent amounts of healthy control serum.

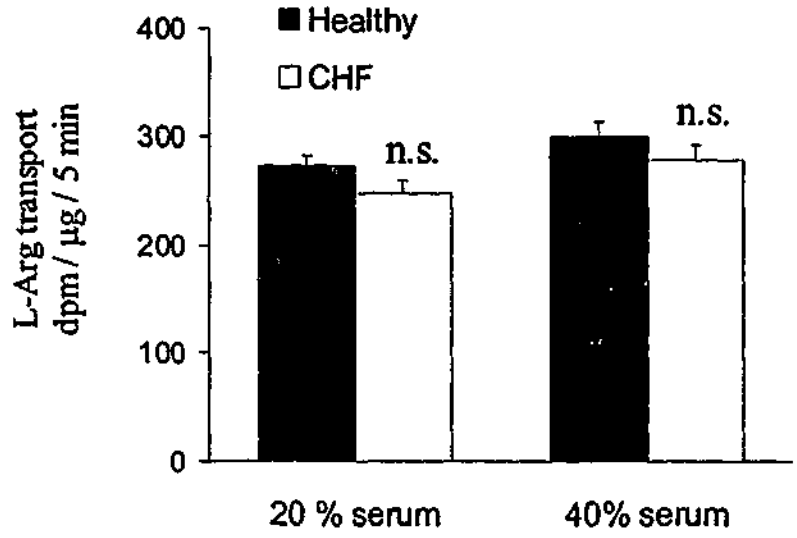

Figure 4.3 Assessment of L-Arg transport in EA.hy926 after treatment with CHF serum. Serum deprived EA.hy926 cells were incubated with either 20% or 40% serum from normal controls (n=6), and patients with CHF (n=7, NYHA Class II-IV). After 24 hr of incubation with serum L-Arg transport was assessed as described in Methods. Results are expressed as the rate of transport dpm/µg protein/5 min. Data are mean ± SEM of three separate experiments with serum from the same population. n.s. indicates not significant.

4.1.3.3 Effects of CHF cytokines and neurohormones on L-[^{3}H]Arg transport

With the exception of Ang II (Chapter 4, Section 4.2), none of factors listed in Table 4.2 were shown to have any individual effect with respect to L-Arg transport in EA.hy926 cells when treated alone in culture. This was evident from both time-course (Figure 4.4) and dose-response (results not shown) experiments. At the dosage commonly used in the previous literature for cell culture studies, 24 hr treatment within a range of 1- 10 µM resulted in a trend for decreased L-Arg transport (n.s. % vs untreated control) in response to NA at the higher dose (10 µM) but this effect was also found to be accompanied by a significant decrease in total cellular protein content (>60%) and cell death as measured by Lowry assay and Trypan blue staining respectively. The presence and absence of ascorbic acid (1 mM) in the culture medium was without effect on cell viablility (results not shown) which indicated a selective toxicity for NA on endothelial cells within the

dosage range of 1-10 μM. As a proper control, all L-Arg transport values obtained from NA treated cells with ascorbic acid were normalised to cells treated in the presence of ascorbic acid alone. EA.hy926 treated with 1mM ascorbic acid alone did not cause any affect on basal L-Arg transport activity as compared with untreated controls (results not shown).

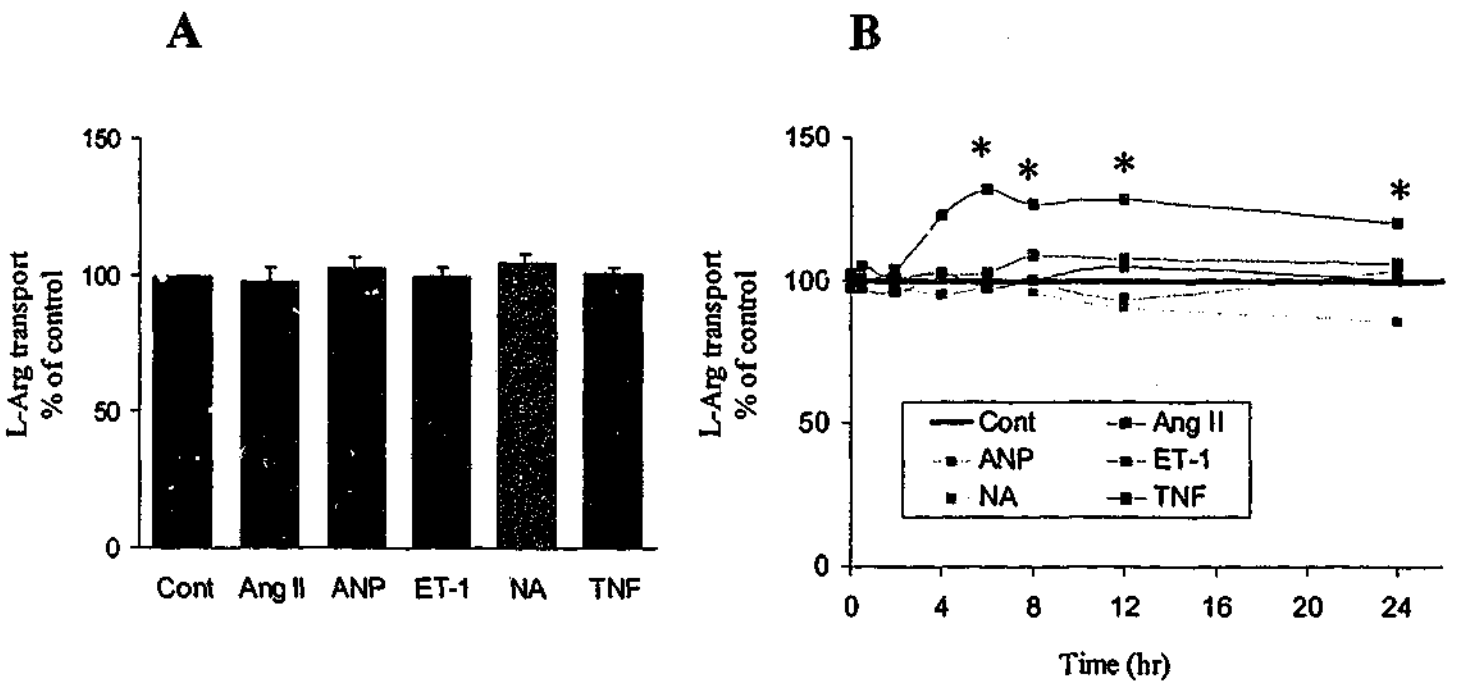

Figure 4.4 Time dependent L-Arg transport in response to neurohormones and cytokines. EA.hy926 were serum deprived for 24 hr (0.5% fatty-acid free BSA) and then treated with the factors listed for either **A,** 5 min or **B,** longer incubation times as indicated on the x-axis. At the end of the incubation period, culture medium was removed and an assessment of L-Arg transport was carried out as described in Methods. Data are expressed as a percentage of untreated time-matched control L-Arg transport values and are the mean ± SEM, n=6. *P<0.05 versus untreated control (with vehicle). Ang II, angiotensin II; ANP, atrial natriuretic peptide; ET-1, endothelin-1; NA, noradrenaline; TNF-α, tumor necrosis factor-α.

4.1.4 Discussion

This is the first study of its kind to assess the effects of cytokines and neurohormones relevant in CHF on L-Arg transport in the human endothelium.

4.1.4.1 Properties of L-Arg transport in EA.Hy926

This study demonstrates that the major system of L-Arg transport in EA.hy926 is system y+. A single high affinity transporter was revealed by Eadie-Hofstee transformation of the Lineweaver-Burk plots with a Michaelis constant of 72.6 ± 13.8 μmol/L and a V_{max} of 1.4 ± 0.1 pmol L-Arg/μg protein/5 min. In the present study, RT-PCR analysis of total mRNA isolated from EA.hy926 cells using isoform specific primers did not detect CAT-2A and –2B isoforms in this cell type (results not shown). In the course of these studies a published study by Closs *et al.* (Closs et al., 2000) has also confirmed through similar methodology that the major L-Arg transport system in EA.hy926 cells is the high affinity L-Arg transporter, CAT-1. In the present study, L-Arg transport in EA.hy926 was shown to be sensitive to the effects of *trans*-stimulation, which is also in agreement with previously reported properties of the CAT-1 isoform. Existing models of *trans*-stimulation predict that the conformation change of the carrier occurs much more rapidly in the presence of substrate and thus, the return of the transporter to the *cis*-conformation is slow when the substrate concentration on the transmembrane side is low (Stein, 1990). Although, the precise mechanisms responsible for this phenomenon are unclear a specific role for potassium ions in the mechanism of *trans*-stimulationhas been suggested (Zharikov and Block, 1998). The ability of similar amino acid structures such as L-Lysine and L-NMMA to *trans*-stimulate L-Arg uptake has been documented previously in endothelial cells (Closs and Graf, 1999). The contribution of *trans*-stimulation by system y+ L-Arg transport in pathophysiological disorders where intracellular L-Arg may become limiting at the local site of eNOS action needs to be addressed further.

4.1.4.2 Cytokines and neurohormonal effects on endothelial L-Arg transport

With the exception of Ang II, the cytokines and neurohormones selected as candidates for depressed L-Arg transport in CHF in this human endothelial culture system (Table 4.2) were without effect on L-Arg transport activity. The effect that these agents have either alone or in combination on different regulation points of L-Arg-NO pathway both in the endothelium and other cell types have been found to vary widely in the literature. For example, IL-1β stimulation of rat vascular smooth muscle cells increased L-Arg transport and NO production in a concentration-dependent manner (Gill *et al.*, 1996). This was attributed to an increase of CAT-2B mRNA expression and iNOS, while CAT1 mRNA levels remained constant. By contrast, Ang II in the presence of IL-1β up-regulated L-Arg transport by selectively inducing CAT1 while having no effect on iNOS or CAT-2B. The findings of Escobales *et al.* (Escobales *et al.*, 2000) contrast to the findings of Gill *et al.* (Gill et al., 1996) where both the induction of L-Arg transport and NOS expression by IL-1β were inhibited by Ang II in the same species and cell type. IL-1β alone or in combination was not explored within the present study. However, a stimulatory effect of Ang II on system y+ L-Arg transport with dose and time was observed in human endothelial cells and is consistent with previous studies conducted using rat vascular smooth muscle cells (discussed further in section 4.2.5). TNF-α treatment of primary bovine aortic and human umbilical endothelial cell cultures at the same concentration used in the present study was previously shown to result in a time-dependent and concentration dependent increase in L-Arg transport (Irie *et al.*, 1997, Durante *et al.*, 1996). In both instances the increase in L-Arg transport was attributed to the selective induction of CAT-2B mRNA accompanied also by a significant increase in NO production. However, the enhancement of L-Arg transport due to the effects TNF-α treament was not observed in the present study. These differences are likely explained by the differences in the origin and metabolism of this cell type (EA.hy926).

Existing literature documenting the effects of various (patho-)physiological on L-Arg transport in mammalian cells is suggestive of a complex network of regulatory pathways which regulate L-Arg

transport in a transport system-specific, cell-specific and species-specific manner. This is not surprising given the metabolic demands for L-Arg within the cell. Since there is a poor correlation between neurohormones and systemic vascular resistance it may be likely that other systems are involved in pathophysiological regulation of the L-Arg- NO pathway (Katz *et al.*, 1994) (Packer, 1995).

Treatment with CHF serum should have exposed the endothelial cells to the same complement of circulating factors as would be expected *in vivo*. These studies failed to reproduce our previous observations on L-Arg transport activity as observed in the peripheral forearm vasculature and in freshly isolated peripheral blood mononuclear cells (Chapter 3, Section 2.3.1, 75% reduction) (Kaye et al., 2000). The effect of extended incubation times were not pursued in the present study. It might be interesting to speculate that longer incubation times may have produced a stronger influence on the L-Arg transport activity. Since the population numbers were fairly small in this study perhaps a larger cohort of both subject groupings would have revealed significant differences. Alternatively, degradation of factors can occur rapidly in the culture medium. Without replenishment form the circulation, cultured endothelial cells may only be transiently exposed to the CHF circulating environment, thus potential L-Arg transport modulators may be degraded in culture over this time period. This aspect needs to be addressed further.

Due to the lack of effects of circulating factors and CHF serum demonstrated in the present study, it seems likely that structural and mechanical alterations to the vasculature in congestive heart failure may account for the previously observed depression of L-Arg transport activity *in vivo*. For example, a decreased cardiac output in CHF results in a reduced shear stress on endothelial cells (Vanhoutte, 1996). Since shear stress is an important activator of NOS expression and activity both at rest and during exercise under normal conditions (Fleming and Busse, 2003), reduced shear stress in CHF is expected to play a significant role in reduced NO production. Reduced shear stress may also potentially affect transport of its substrate precursor across the membrane *in vivo*. Shear

stress has previously been shown to induce uptake of L-arginine in endothelial cells *in vitro* (Posch *et al.*, 1999). In the same study, the formation of NO in response to shear stress was found to critically depend on extracellular L-Arg.

4.2 Ang II stimulated L-Arginine transport in human endothelial cells is mediated by the AT4 receptor.

4.2.1 Introduction

In Section 4.1 we observed a significant effect of the neurohormone Ang II on L-Arg transport activity in endothelial cells. Therefore, this effect was further explored in the present study. Elevated circulating or local production of the vasoconstrictory factor Ang II has been associated with endothelial dysfunction in cardiovascular disorders such as hypertension and heart failure (Loscalzo, 2000, Napoli and Ignarro, 2001, Hughes, 1998). Ang II induced superoxide anion O(2)(-) production through the local actions of NADH/NAD(P)H oxidase is known to contribute to reduced NO bioavailability and a decline in endothelial function (Lang *et al.*, 2000). Paradoxically, there is a body of evidence to suggest that Ang II also has NO-mediated vasodilatory actions which can occur though activation of angiotensin type-1 (AT_1) or angiotensin type-2 (AT_2) receptors on isolated arteries (Boulanger *et al.*, 1995, Thorup *et al.*, 1999), and cultured endothelial cells (Pueyo *et al.*, 1998) (Carey *et al.*, 2000). Interestingly, metabolically active Ang II degradation fragments such as Ang III, Ang 3-8 (Ang IV) or Ang 1-7 have also been shown to elicit NO-mediated vasodilatory responses in several tissue and cell types (Seyedi *et al.*, 1995, Patel *et al.*, 1998, Chen *et al.*, 2000, Brosnihan *et al.*, 1996, Gorelik *et al.*, 1998).

While regulation of CAT's by inflammatory cytokines and growth factors is well documented (Nelin *et al.*, 2001, Nicholson *et al.*, 2001, Durante *et al.*, 2001, Matthews *et al.*, 1999, Irie et al., 1997, Macleod and Kakuda, 1996), the role of endogenous neurohormones such as Ang II in the regulation of L-Arg transport is lesser known. In the context of the role of endothelial dysfunction in the pathophysiology of cardiovascular disease and the frequent association of increased renin-angiotensin system activity, the aim of the present study was to further explore our initial observations (Section 4.1) of Ang II-modulated L-Arg transport in endothelial cells.

4.2.2 Methods

4.2.2.1 L-[^{3}H]Arg transport assay

Transport of radiolabelled L-[^{3}H]Arg by EA.hy926 cells was determined by previously described methods (Chapter 4, Section 1.3)(Kaye et al., 2000). Confluent monolayers of EA.hy926 cells in 24 well plates were serum deprived in DMEM containing 0.5 % fatty acid free BSA 24 hr prior to experimental studies. In order to measure the effects of Ang II treatment time on L-Arg transport activity, cell monolayers were incubated in a fresh DMEM medium containing 0.5% fatty acid free BSA and 100 nM Ang II for various lengths of time. At the appropriate time point cell monolayers were rinsed twice in pre-warmed Locke's buffer (in mM: 154 NaCl, 5.6 KCl, 2 $CaCl_2$, 1 $MgCl_2$, 10 HEPES pH 7.4, 3.6 Na HCO_3 and, 5.6 glucose) prior to transport measurement. All other experiments including Ang II dose-response experiments were performed by incubating cells with the appropriate treatments for 6 hr prior to initiation of L-Arg transport measurement. Where relevant, cells were pre-incubated with antagonists for 30 min prior to the addition of Ang II.

4.2.2.2 Ribonuclease protection assay

Total RNA was isolated after relevant treatments and times from EA.hy926 cells by guanididium isothiocyanate/phenol/chloroform extraction according to previously described methods (Chapter 2, Section 2.1.3) (Chomczynski and Sacchi, 1987). Probes for human CAT-1 and CAT-2B were constructed from cloned cDNA fragments according to previously described methods (Chapter 3, Section 2.2.3) (Kaye et al., 2000). A human CAT-2A probe was a gift provided by Dr. Ellen Closs (Johannes Gutenberg University, Mainz, Germany). Probes were hybridised to 15 µg total RNA from EA.hy926 cells or a negative control, sheared yeast tRNA (ytRNA), followed by digestion with ribonuclease A and ribonuclease T1. To control for equal loading of RNA, the samples were simultaneously hybridised to a GAPDH probe (Kaye et al., 2000), The protected fragments were separated and analysed on a 5% denaturing polyacrylamide/urea gel. Radioactive signals were quantitated using a phosphoimager (Molecular Dynamics, Sunnyvale, CA).

4.2.2.3 eNOS Western blot

After exposure to experimental conditions cell monolayers were washed twice in Dulbecco's phosphate-buffered saline followed by lysis in ice-cold RIPA (mM; 50 Tris pH 7.5, 150 NaCl, 1% Nonidet P-40, 0.25% Na+ deoxycholate, 2 EDTA, 1 phenylmethylsulfonyl fluoride, 10 μg/mL leupeptin, pepstatin and aprotinin). Cell lysates were sonicated and then centrifuged at 1000g for 5 min, 4°C. After discarding the pellet, the protein content of the resultant homogenates was determined by the Lowry assay. Whole cell homogenates (40 μg) were analysed on a 10 % SDS-PAGE gel and the proteins transferred to an Immobilon-P membrane as previously described (Chapter 2, Section 5.2 and 5.3). After transfer, the membrane was blocked for 2 hr at RT in TBS-T (0.1% Tween 20 and 20 mM Tris-buffered saline, pH 7.6) containing 5% skim milk powder. Following a brief rinse in TBS-T the membrane was incubated with a rabbit eNOS primary antibody (1:1000 dilution, BD Transduction Laboratories) in TBS-T containing 5% skim milk overnight at 4°C and then washed four times in TBS-T for 5 min each. The primary antibody was detected with and anti-rabbit IgG secondary antibody conjugated to horseradish peroxidase (1:5000 dilution, Bio-Rad) that was added to membrane and incubated in TBS-T containing 1% skim milk powder for 1 hr at RT. eNOS protein was detected by chemiluminescence (Amersham) using X-OMAT film (Kodak).

4.2.2.4 Materials

DMEM and HAT supplement were purchased from Life Technologies, Grand Island, NY. Fetal bovine serum and antibiotic/antimycotic agents was from CSL Bioscience Ltd. Ang II human acetate salt, L-Arg hydrochloride, L-lysine monohydrochloride were obtained from Sigma Chemical Co. (St.Louis, MO). Ang IV human acetate salt was from ICN Biomedicals Inc. Candesartan and PD123319 were from DuPont Merck Pharmaceuticals and Research Biochemicals International respectively. Bim I and Bim V were obtained from Calbiochem. L-[2,3,4-^{3}H] Arg monohydrochloride (45.2 Ci/mmol) was obtained from New England Nuclear, Boston, MA. Insta-

Gel Plus scintillation fluid and counting vials were obtained from Packard Instrument Company Inc. Lowry protein assay kit II was obtained from BioRad. Ribonuclease protection assay kit was obtained from Ambion. Restriction enzymes, T7 polymerase, Sp6 polymerase, DNAse and RNAsin were obtained from Promega Co. All other reagents were purchased from Sigma.

4.2.2.5 Statistical analysis

Data are expressed as mean ± SEM values for the number of experiments indicated in the figure legends. Statistical significance was evaluated by one-way analysis of variance. Final analysis was made using the least significant difference multiple range test. $P<0.05$ was considered significant in all experiments.

4.2.3 Results

4.2.3.1 Ang II stimulates transport of L-Arg in EA.Hy926 cells

The effect of Ang II on L-Arg transport in endothelial cells was determined by measuring transport of L-[^{3}H]Arg into EA.hy926 cells. Treatment of these cells with Ang II resulted in a significant increase of L-Arg transport in a time (Figure 4.5A) and concentration-dependent (Figure 4.5B) manner. A significant L-Arg transport increase of 23.5 ± 4.9 % ($P<0.05$) over basal values in response to Ang II was detectable by 4 hr post treatment. Maximal stimulation of L-Arg transport was observed 6 hr (29.7 ± 3.6 %, $P<0.05$) after the addition of Ang II and was significantly enhanced over the 24 hr experimental duration. For this reason, 6 hr Ang II treatment time was chosen for subsequent L-Arg transport experiments. A dose-response of Ang II-stimulated L-Arg transport within a dose range of 10 pmol – 1 μM is presented in Figure 4.5B. Ang II dose-dependently stimulated L-Arg transport. As shown, stimulation of L-Arg transport occurred maximally at 100 nM Ang II, with a significant threshold response also observed as low as 1 nM Ang II. While (patho-)physiological concentrations of Ang II has previously been reported to range from 12 – 81 pmol (Pedersen et al., 1986), an Ang II dosage range in cultured cells has been used

in the current study, consistent with that presented by others for pathological studies (eg. 10 nM – 10 μM (Gragasin *et al.*, 2003), 1 nM – 0.1 μM (Zhang *et al.*, 1999)). Since the *in vitro* environment is not subject to Ang II replenishment from the circulation, higher initial levels of Ang II are necessary to ensure a physiological range of Ang II is met through an experimental 24 hr time period. There were no associated changes in the total protein content following Ang II treatment in this cell type during the time examined.

4.2.3.2 Increased CAT-1 gene expression by Ang II

The major L-Arg transport system present in EA.hy926 cells is mediated by the high affinity L-Arg transporter, CAT-1 (Graf *et al.*, 2001). Expression of CAT-1, the mediator of L-Arg transport present in endothelial cells, in response to 100 nM Ang II treatment was measured to determine whether increased L-Arg transport activity was due to changes in mRNA expression. Quantitation of CAT-1 mRNA by ribonuclease protection analysis normalised to GAPDH showed an induction of mRNA at 4 hr, to 131% of untreated control values ($P<0.05$), which returned to baseline levels over the 24 hr experimental duration (Figure 4.6). Induction of CAT-1 mRNA by Ang II at 4 hr post treatment corresponded with significantly enhanced L-Arg transport activity. However, after this time point the CAT-1 mRNA expression profile differed from L-Arg transport activity levels which remained significantly increased in comparison to untreated controls throughout the 24 hr experimental duration in response to Ang II. CAT–2A or –2B isoform mRNA transcripts were undetectable in either untreated control or Ang II treated EA.hy926 cells.

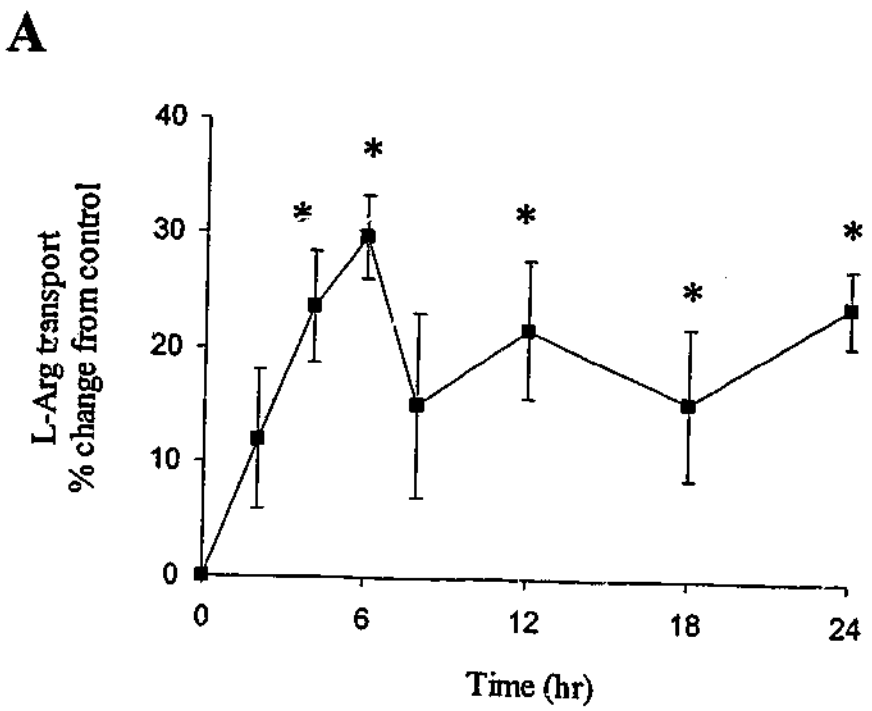

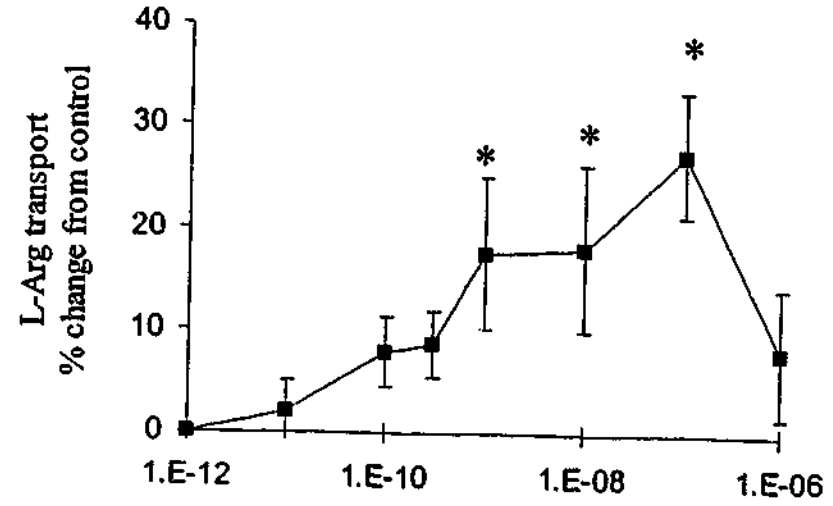

Figure 4.5 Induction of L-Arg transport activity and CAT-1 mRNA expression by Ang II in EA.hy926 cells. **A)** Time course of specific L-Arg transport after 100 nM Ang II treatment. Data are expressed as percentage change from untreated controls and represented as mean ± SEM, n=6 experiments. **B)** Concentration-dependent Ang II stimulated L-Arg transport activity. Cells were incubated with an Ang II concentration range of 10 pM to 1 μM for 6 hr. Results are expressed as the percentage change from untreated control values. Data are mean ± SEM, n=6.

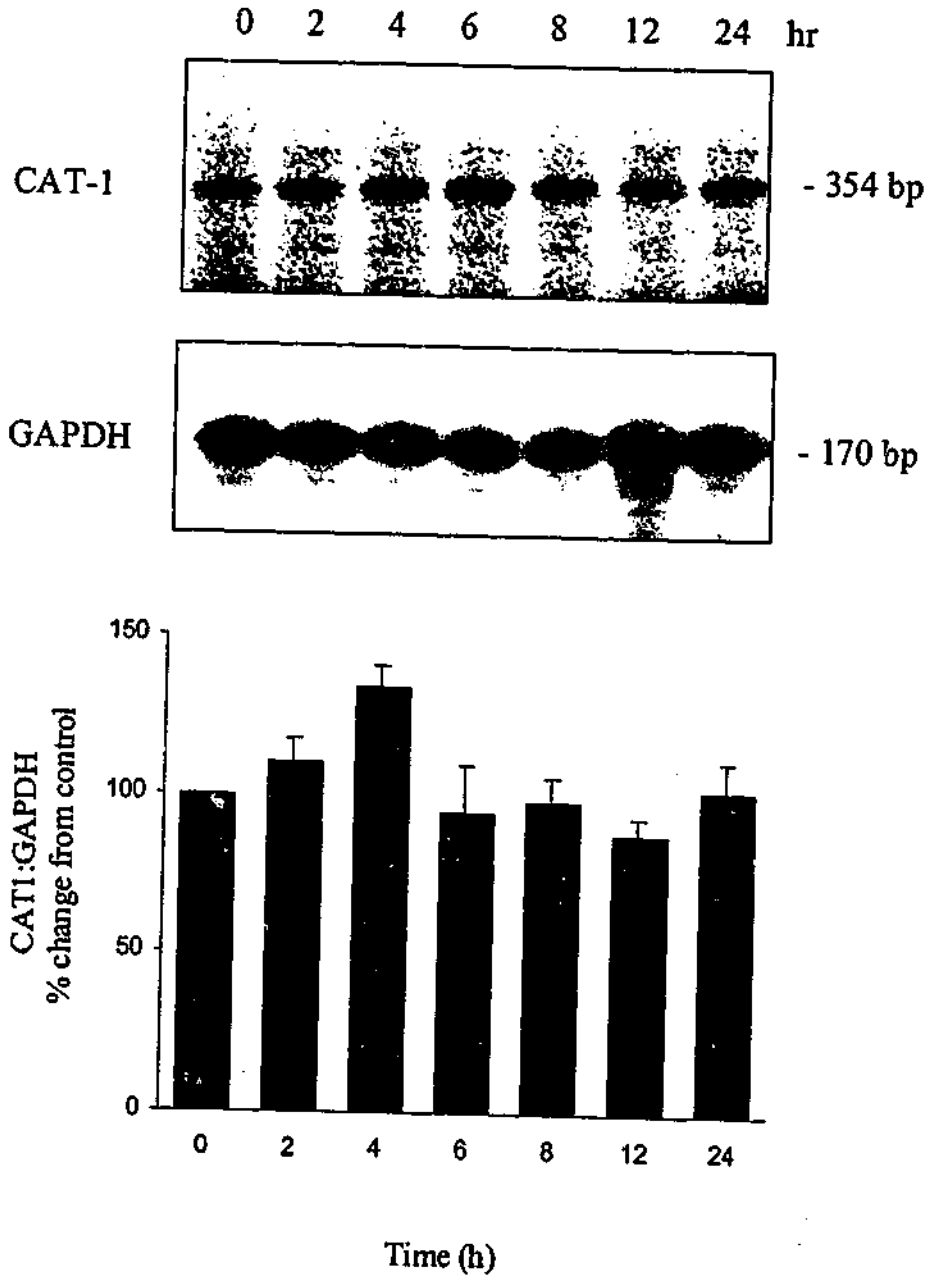

Figure 4.6 Ribonuclease protection analysis of CAT-1 mRNA following treatment of EA.hy926 with Ang II for the indicated times. The top panel shows a representative image of protected fragments of CAT-1 and GAPDH. The bottom panel represents CAT-1 mRNA levels derived from phosphoimager analysis of protected fragments and expressed as a ratio of CAT-1 mRNA versus GAPDH mRNA. Data was expressed as arbitrary units and is represented as percentage change from untreated control values (mean ± SEM, n=3). * $P <$ 0.05, versus untreated control.

4.2.3.3 AT_1 and AT_2 receptor blockade effect on Ang II stimulated L-Arg transport

Ang II stimulated L-Arg transport was not prevented by either AT_1 receptor blockade using 1 μM Candesartan, or by AT_2 receptor blockade with 1 μM PD123319 (Figure 4.7). A combination of the two Ang receptor blockers, similarly did not affect Ang II stimulated L-Arg transport suggesting the involvement of a non-classical AT receptor subtype and/or an Ang II metabolic product.

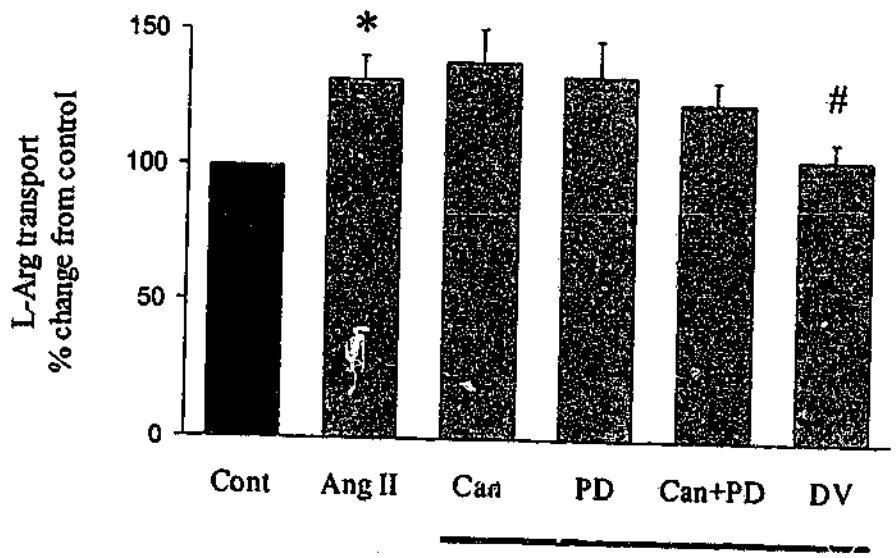

Figure 4.7 Effect of Ang II receptor antagonists on Ang II stimulated L-Arg transport. Cells were incubated for 6 hr with 100 nM Ang II in the presence or absence of 1 μM Candesartan (Can), PD123319 (PD) or Divalinal (DV). Results are expressed as the percentage change from untreated control (Cont) values. Data are mean ± SEM, n=4. *P<0.05 versus untreated control. # P<0.05 versus Ang II stimulated cells.

4.2.3.4 AT_4 receptor antagonist effect on Ang II stimulated L-Arg transport

To further investigate the mechanism for the Ang II mediated effect we evaluated the role of the AT_4 receptor subtype, given that Ang II has the capacity to weakly bind to this receptor subtype (Harding *et al.*, 1994). Using a specific AT_4 receptor antagonist, divalinal (1 μM), a significant reduction in the effect of Ang II on L-Arg stimulated transport was demonstrated (P<0.05 versus Ang II treated cells). Supplementary to this finding, we next investigated whether the Ang II

metabolic fragment Ang IV, a ligand with high affinity for the AT_4 receptor, or Ang 1-7, a ligand with no affinity for the AT_4 receptor subtype, had the potential to elicit a stimulated L-Arg transport response. 1 μM Ang IV treatment of EA.hy926 cells resulted in a significant induction of L-Arg transport (19.4 ± 6.3 %, $P<0.05$) to a similar degree as that elicited by 100 nM Ang II treated cells versus untreated controls (Figure 4.8). Importantly, AT_4 receptor blockade inhibited Ang IV stimulated L-Arg transport. At the same concentration, Ang 1-7 was found to have no effect on L-Arg transport (Figure 4.8).

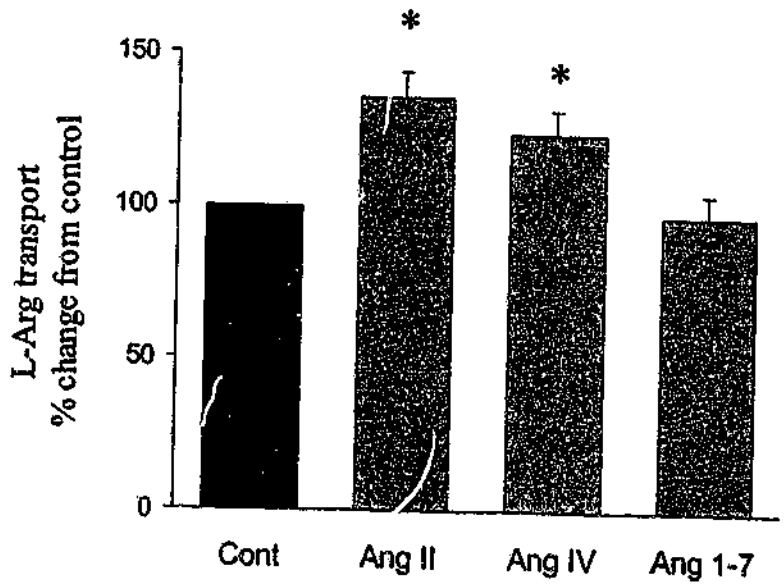

Figure 4.8 Effect of Ang II degradation fragments on L-Arg transport in endothelial cells. Cells were incubated for 6 hr in the presence or absence of 100 nM Ang II, 1 μM Ang IV or 1 μM Ang 1-7. Results are expressed as the percentage change from untreated control (Cont) values. Data are mean ± SEM, n=4. *$P<0.05$ versus untreated control.

4.2.3.5 PKC activation is associated with Ang II- stimulated L-Arg transport

Having demonstrated that Ang II stimulates L-Arg transport in this cell type we determined whether induction of transport was dependent on PKC activation. In order to investigate this, L-Arg transport activity was measured in the presence of the PKC inhibitor, bisindolylmaleimide I (Bim

I). Bim I shows high selectivity for PKC α-, β_{II}–, γ–, δ–, α and ε isozymes (K_i ~10 nM). As shown, pre-treatment of cells with 1 μM Bim I significantly abolished the stimulatory effect of both Ang II and Ang IV on L-Arg transport (Figure 4.9). The effectiveness of Bim I at nanomolar doses in attenuating Ang II- and Ang IV stimulated L-Arg transport was also observed (results not shown). Additionally, the inactive analogue of Bim I, Bisindoylmalemide V (Bim V), was used as a negative control for these series of experiments and displayed no inhibitory effect on L-Arg transport (results not shown).

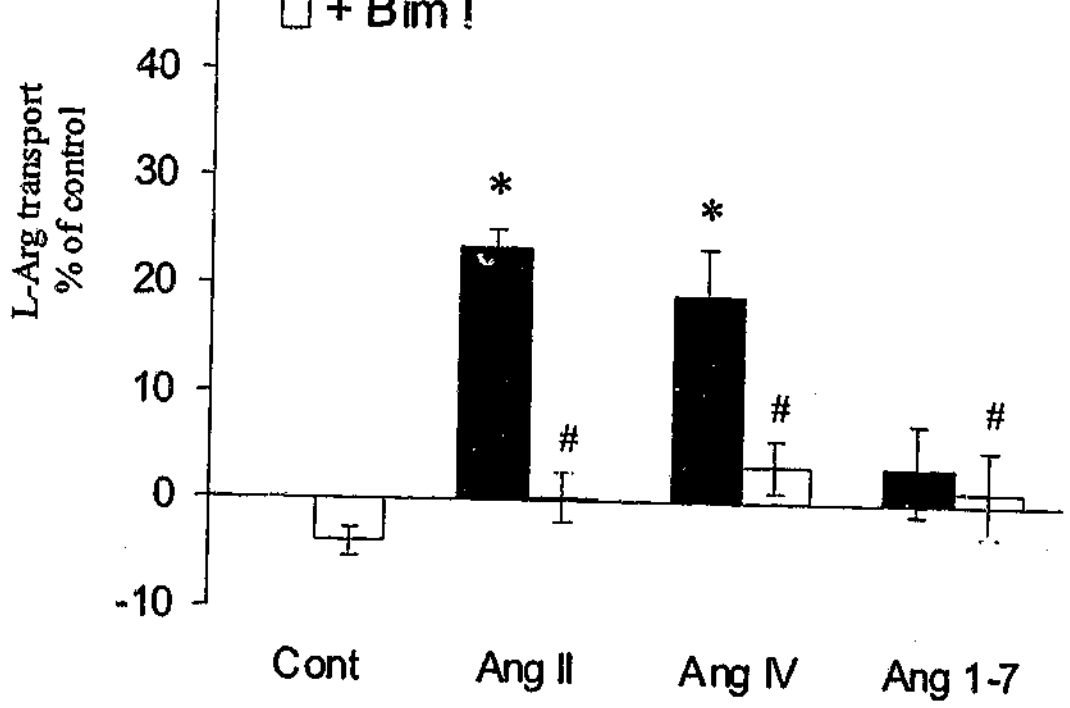

Figure 4.9 **Effect of PKC inhibition on Ang II stimulated L-Arg transport.** Cells were incubated for with either 100 nM Ang II, 1 μM Ang IV or 1 μM Ang 1-7 for 6 hr in the presence or absence of 1 μM Bim I. Results are expressed as the percentage change from untreated control (Cont) values. Data are mean ± SEM, n=4. *P<0.05 versus untreated control. # P<0.05 versus Ang II stimulated cells.

4.2.3.6 Effects of Ang II on NOS Expression and Activity

In order to examine the effect of Ang II on NO production, total eNOS expression and NOS activity were evaluated in this cell type. Total eNOS expression was quantitated at defined time points over a 24 hr incubation period in the presence of 100 nM Ang II. No significant changes to eNOS protein levels over time were detected in Ang II-treated EA.hy926 cells. Interestingly, a trend for increased NOS activity measured in intact cells as previously described (Lantin-Hermoso *et al.*, 1997) after 6 hr of treatment with Ang II (the maximal peak time of Ang II-induced L-Arg transport) was evident compared to unstimulated time-matched controls (42 ± 11% $P<0.1$; n=3).

4.2.4 Discussion

The major finding of this component of Chapter 4 is that Ang II stimulates L-Arg transport in human venous endothelial cells in a dose and time-dependent manner. This effect of Ang II is not mediated via either AT_1 or AT_2 receptor subtypes, but rather appears to be mediated by activation of the AT_4 receptor. Furthermore, this effect of Ang II could be mimicked by its degradation fragment Ang IV (a high affinity ligand for the AT_4 receptor) but not by the Ang II metabolite, Ang 1-7. This leads to the conclusion that Ang II stimulated L-Arg transport by CAT-1 in EA.hy926 is mediated via AT_4 receptors, either through the binding of Ang II or Ang IV produced locally.

Our finding of an early transient up-regulation of CAT-1 mRNA at 4 hr by Ang II which resulted in significantly elevated L-Arg transport over 24 hr parallels that previously reported in vascular smooth muscle cells (Low and Grigor, 1995, Gill et al., 1996). We interpret this finding as indicative of a slow turnover of CAT-1 protein from the plasma membrane. Alternatively, Ang II may alter expression of CAT-1 associated regulatory protein(s) resulting in a post-translational modification of L-Arg transport. Changes in the nutritional status of the cell have previously been

shown to lead to increased CAT-1 mRNA levels and L-Arg transport activity in the cell through a mechanism involving increased CAT-1 mRNA stability (Aulak *et al.*, 1999). Additionally, this might lead to the speculation that early up-regulation of CAT-1 mRNA by Ang II in the current study (Figure 1C) is associated with transient changes in CAT-1 mRNA stability rather than changes in the absolute transcription/mRNA turnover rate.

Previous studies in vascular smooth muscle cells indicated that Ang II stimulated L-Arg transport was temporally associated with an increase in total cellular protein content, an effect associated with cellular proliferation (Low and Grigor, 1995). Data from the present study suggests that up-regulation of L-Arg transport by Ang II in endothelial cells within the same time period is not associated with cellular proliferation since changes in protein content indicative of a proliferative response were not evident within the 24 hr of Ang II treatment. Interestingly, findings of Hall et al (Hall *et al.*, 1995) have suggested a proliferative response of endothelial cells after longer-term exposure to Ang IV by demonstrating a significant increase in DNA synthesis after 3-11 days of treatment. In addition to its contribution for new protein synthesis, L-Arg is also required for various processes including production of NO, polyamine growth factors, and collagen synthesis. Amongst these roles, the synthesis of NO is a crucial pathway for the metabolism of L-Arg. The existence of a CAT-1-eNOS protein-protein interaction demonstrated in pulmonary artery endothelial cell preparations is suggestive of a functional association of these two proteins that is advantageous for directed delivery of substrate for the NO pathway (McDonald *et al.*, 1997). Furthermore, eNOS co-localisation with CAT-1 in structural compartments called caveolae is thought to facilitate receptor-signalling events at the plasma membrane that are involved in modulating NO production (Shaul and Anderson, 1998). Localisation and translocation of eNOS away from this caveolar complex association are major determinants of eNOS activity (Goligorsky *et al.*, 2002). Interestingly, Ang II has been shown to significantly increase NOS activity in endothelial cells (Pueyo et al., 1998, Olson *et al.*, 1997).

Since the effects of Ang II were not inhibited by either AT_1 nor AT_2 blockers we explored the possibility that Ang II was acting via its biologically active metabolic products. Production of the biologically active peptides (Ang) I, II, III, IV and Ang 1-7 is dependent on the activities of exopeptidases, including several aminopeptidases and carboxypeptidases (Wright *et al.*, 1995). Ang II to Ang IV conversion involves aminopeptidase cleavage of two NH2-terminal amino acids from the former peptide (Wright and Harding, 1995, Johnson and Erdos, 1977). Our data demonstrate that Ang IV can mimic the effect of Ang II, and also that increased L-Arg transport activity by both agonists can be inhibited by the selective AT_4 receptor antagonist divalinal. This receptor subtype displays high affinity for Ang IV, with a reported $k_d = 1$ nM as determined by an [^{125}I]Ang IV receptor binding and displacement assay (Harding *et al.*, 1992), and is present in cultured endothelial and smooth muscle cells (Moeller *et al.*, 1999, Hall *et al.*, 1993). In this context, it is of interest that Ang IV has been demonstrated to mediate vasodilation and as such has been shown to increase cerebral (Kramar *et al.*, 1998) and renal blood flow (Coleman *et al.*, 1998). Moreover, AT_4 has been demonstrated to mediate Ang IV induced NO production in cultured pulmonary aortic endothelial cells (Patel *et al.*, 1999). Findings of Chen and colleagues suggest that Ang IV mediated vasodilation is endothelium-dependent and regulated by intracellular calcium release through mechanisms involving receptor coupled G proteins, phospholipase C and PI3 kinase signalling pathways (Chen et al., 2000). Beneficial effects of AT_4 mediated vasodilation through increased activity of the L-Arg-NO pathway may act to counteract the detrimental effects of increased NAD(P)H oxidase activity and oxidative stress in endothelial cells attributed to Ang II (Zhang et al., 1999, Griendling *et al.*, 1994).

In the current study NOS activity was measured in intact cells (results not shown) by measuring the intracellular level of [^{3}H]L-citrulline conversion following initial treatment with [^{3}H] L-Arg (Lantin-Hermoso et al., 1997). A trend for a temporal association of increased NOS activity with increased L-Arg transport after 6 hr of treatment with Ang II was observed compared to

unstimulated time-matched controls (42 ± 11% P <0.1; n=3). Therefore, increased L-Arg transport in response to Ang II in the human endothelium suggests that this may be part of a counter-regulatory process to Ang II-mediated oxidative stress via stimulation of the L-Arg-NO pathway.

AT receptor activation is associated with activation of PKC mediated pathways (Capponi, 1996). In the current study PKC inhibition abrogated Ang II stimulated L-Arg transport in EA.hy926 cells and suggests that PKC activation via AT receptors may regulate CAT-1 at the gene expression level or post-translationally. PKC activation and increased CAT-1 mRNA expression was previously shown to be required for the proliferative response induced by Ang II in smooth muscle cells (Taubman *et al.*, 1989). Interestingly, down-regulation of PKC activity by specific PKC inhibition and phorbol ester depletion has been shown to inhibit Ang II stimulated NO production in bovine endothelial cells associated with AT_1 receptor activation (Saito *et al.*, 1996). In addition, Ang II has been shown to up-regulate cytokine induced NOS expression in cardiac myocytes through a PKC mediated pathway (Ikeda *et al.*, 1995). The specific PKC isoform(s) required in these processes was not identified.

Recent molecular evidence has identified the AT_4 receptor as the enzyme insulin-regulated aminopeptidase (IRAP) in humans (Albiston *et al.*, 2001). Substrates or ligands of AT_4 /IRAP include oxytocin, vasopressin and angiotensin metabolites (Herbst *et al.*, 1997). The role of AT_4/IRAP as a signalling receptor is presently unclear. As such, we believe the present study implicates AT_4/IRAP involvement as an important signalling receptor in the regulation of L-Arg transport activity.

The findings of the present study seem to indicate that increased intracellular L-Arg delivery requires conversion to Ang IV and subsequent AT_4 receptor binding. However, a limitation of the present study is that we cannot absolutely exclude the possibility that a differential pattern of regulation exists in non-immortalised endothelial cell types. If correct, the mechanism by which

Ang IV may modulate the L-Arg-NO pathway could potentially be exploited therapeutically in pathophysiological conditions such as heart failure where the net effect between vasoconstriction and vasodilation is shifted towards net vasoconstriction due to a reduced NO bioavailability within the endothelium. It is conceivable that reduced NO bioavailability might involve a localised L-Arg deficiency at the site of eNOS activity additional to other contributing factors which are already well documented. Certainly in Chapter 3, a defective L-Arg transport pathway was evident in congestive heart failure where endothelium dysfunction, defined by an impaired vasodilator response, had been established (Kaye et al., 2000). Since all the heart failure patients in the study presented in Chapter 3 were on ACE inhibitor medications it is difficult to know whether breakdown products of Ang II may play a significant role in L-Arg transport regulation *in vivo*.

Chapter Five

Modulation Of Endothelial L-Arginine Transport By Protein Kinase C

TABLE OF CONTENTS

5.0 General Introduction *181*

5.1 Alterations in Endothelial L-Arg Transport by Protein Kinase C *183*

5.1.1 Introduction **183**

5.1.2 Methods **185**

5.1.2.1 L-[^{3}H]Arg transport assay 185

5.1.2.2 Protein lysate preparation and Western blot analysis 186

5.1.2.3 Statistics 187

5.1.3 Results **187**

5.1.3.1 Characterisation of L-Arg transport In BAEC 187

5.1.3.2 Stimulation of PKC is associated with decreased L-Arg transport 191

5.1.3.3 Downregulation of PKC is associated with increased L-Arg transport 193

5.1.3.4 PMA-mediated effects on L-Arg transport are blocked with a PKC inhibitor 194

5.1.3.5 PKC does not alter CAT-1 expression levels 195

5.1.4 Discussion **196**

TABLE OF FIGURES

Figure 5.1 Time Course Of L-Arg Transport In BAEC. 189

Figure 5.2 System y+ Properties Of L-Arg Transport In BAEC. 190

Figure 5.3 PKC Activation Selectively Inhibits The Maximum Velocity Of L-Arg Transport In BAEC. 192

Figure 5.4 Effect Of PMA Incubation Time On L-Arg Transport In BAEC. 193

Figure 5.5 PKC Inhibition Prevents The Effects Of PMA On L-Arg Transport In BAEC. 194

Figure 5.6 CAT-1 Protein Expression Levels In Response To PMA Treatment. 196

5.0 General Introduction

An important finding arising from the study of Ang II-modulated L-Arg transport in the previous Chapter 4 (Section 4.2) is that CAT-1 gene expression is not a good predictor of changes in CAT-1 transport activity. This intriguing and perplexing fact has also become evident elsewhere in the literature. Gill and Grigor (Low and Grigor, 1995) were the first to report that CAT-1 gene expression does not necessarily match the temporal profile of altered CAT-1 activity in response to growth hormone stimuli. Closs *et al.* and Hatzoglou *et al.* groups have also discussed the significance of this phenomenon in more recent publications (Graf *et al.*, 2001). The half-life of CAT-1 mRNA in rat hepatoma cells is reportedly between 1.5 – 4 hr (Aulak *et al.*, 1996). It would thus seem unlikely that increased L-Arg transport activity, sustained up to 24 hr after Ang II treatment in the previous chapter (Figure 4.5A), could have been due soley to changes in CAT-1 gene expression (induction at 4 hr post-treatment only, Figure 4.6) unless there is a slow turnover of CAT-1 from the plasma membrane or alternatively a form of post-translational regulation that mediates changes in CAT-1 activity. In the absence of a specific antibody for CAT-1 in human tissues we were unable to explore whether Ang II caused changes in the abundance of CAT-1 protein. Since PKC was implicated as a mediator of increased L-Arg transport by Ang II (Chapter 4, Section 2.3.5), we have started to explore the latter explanation, possibly due to the effects of PKC in a more physiologically relevant primary endothelial phenotype, the bovine aortic endothelial cell (BAEC).

The recent development of reliable methodologies for CAT-1 antibody generation have revealed that large changes in CAT-1 mRNA expression in response to various stimuli more often translate to only small changes in absolute CAT-1 protein levels (Graf et al., 2001). In response to changes in cell amino acid availability, this has been interpreted as a change in the efficiency of mRNA translation for CAT-1 in a series of landmark publications by Hatzoglou and colleagues (Aulak *et al.*, 1999, Fernandez *et al.*, 2001, Hyatt *et al.*, 1997, Fernandez *et al.*, 2002). In the absence of

CAT-1 protein changes modulation of CAT-1 activity by cytoskeletal interacting agents, NO itself, and PKC have also been demonstrated (Zharikov and Block, 2000, Graf et al., 2001, Zharikov *et al.*, 2001). The aim of the present chapter was to determine whether activation of PKC affects CAT-1 mediated L-Arg transport in the endothelium utilising a species compatible CAT-1 antibody.

5.1 Alterations in Endothelial L-Arg Transport by Protein Kinase C

5.1.1 Introduction

A growing body of evidence suggests that more rapid, post-translational modulation of L-Arg transporter expression is required to match the altered metabolic demands for intracellular L-Arg. Earlier L-Arg transport studies have indicated the potential for post-translational regulation of CAT activity by protein kinase C (Racke *et al.*, 1998, Hortelano *et al.*, 1993, Bode *et al.*, 1998) since protein synthesis was not a requirement for PKC-induced changes in L-Arg transport. One postulated mechanism is that PKC may be involved in L-Arg transport regulation either by altering CAT-1 protein turnover at the plasma membrane or by more direct modulation of CAT-1 transport rate at the plasma membrane (Graf et al., 2001). An important observation deriving from these earlier studies is that PKC has a differential role in modulating L-Arg transport activity, which is dependent on the cell type. For example, treatment with the PKC activator, phorbol-12 myristate-13 acetate (PMA) is reported to increase L-Arg transport activity in peritoneal macrophages (Racke et al., 1998, Hortelano et al., 1993), intestinal Caco-2 cells (Pan and Stevens, 1995) and human umbilical endothelial cells (Pan *et al.*, 1995) whereas in human hepatoma cells PMA treatment leads to a downregulation of L-Arg transport activity (Bode et al., 1998). There is also evidence to show a differential modulation of CAT-1 expression by PKC. In mouse B-lymphocytes a significant induction of CAT-1 mRNA is observed after PMA treatment whereas in the human leukemia cell line PMA-induced terminal differentiation of HL-60 cells leads to a downregulation of CAT-1 mRNA (Yoshimoto *et al.*, 1992).

It is highly conceivable that such reported discrepancies in response to PMA treatment may be accounted for by differential expression of PKC isotypes in various cell types, the identity of the CAT isoform involved in mediating the PMA response or alternatively the precise duration of treatment. The phorbol ester (PMA) used in many of the previous studies has a biphasic action on PKC activity that is dependent on the duration of cell exposure. That is, short-term treatment of

cells with PMA results in PKC activation (Ma *et al.*, 2001) whereas long-term activation of the PKC by phorbol ester treatment with PMA is commonly used throughout the literature to degrade and deplete PKC activity (Srivastava *et al.*, 2002).

To date, 12 isotypes of PKC are known to exist. PKC isotypes are divided into three subgroups due to the properties of their respective N-teminal regulatory region (Mellor and Parker, 1998). Calcium, diacylglycerol, and phosphatidylserine are necessary requirements for classical PKC isotype (α,β1,β2,and γ) activation. Novel PKC isotypes (δ,ϵ,θ,η) require diacylglycerol and phosphatidylserine. Atypical PKC isotypes (ι,λ,ζ and μ) require phosphatidylserine only. Such differences in subgroup properties suggest that PKC isotypes may be regulated by different stimuli and target divergent downstream signaling molecules. A growing amount of evidence suggests that PKC isotype groups provide distinct functions, but as yet, these isoforms and their specific roles remain to be elucidated. Diacyglycerol analogues such as the phorbol ester, phorbol-12-myristate-13 acetate (PMA) are useful agents for evaluating the role of PKC function (classical and novel PKC isotypes) in various signalling pathways.

The localised expression pattern of PKC in bovine aortic endothelial cells (BAEC) has previously been determined. Immunoreactivity studies have confirmed the presence of the classical PKC isotype alpha (α), the novel PKC isotype epsilon (ε) and the atypical PKC isotype zeta (ζ) in BAEC whilst beta, gamma, delta, eta and theta isotypes were not detected (Patel *et al.*, 1996). PMA, a diacyglycerol analogue, binds strongly to and activates the classic and novel PKC isotypes (Liu and Heckman, 1998). Patel and colleagues (Patel et al., 1996) have convincingly demonstrated in BAEC that after PKC activation (>1 min) with PMA, the predominantly cytosolic PKC-α isotype translocates to the membrane (Triton X-100 soluble) whereas PKC-ε remains associated with a Triton X-100 insoluble membrane fraction. PKC-ζ was found in both soluble and membrane bound (Triton X-100 soluble) fractions in the unstimulated cells and was found to be unaffected by

short-term treatment with PMA. By contrast, long-term treatment with PMA (>6 hr) in BAEC results in a 90% downregulation of PKC-α, while the expression of -ε and -ζ isoforms is unaltered.

An initial aim of the studies within this chapter was to determine whether PKC has a role in modulating L-Arg transport activity in the primary endothelial cell type, BAEC. Furthermore, the effects of short-term and long-term exposure to PMA on L-Arg transporter expression and activity were also determined. The major transporter responsible for mediating L-Arg transport activity in BAEC was also characterised and identified.

5.1.2 Methods

5.1.2.1 L-[^{3}H]Arg transport assay

BAEC were seeded at a density of 1 x 10^5 per well in 24 well plates (Falcon) and grown to 90% confluence. Cells were then washed twice in pre-warmed Locke's solution (in mM: 154 NaCl, 5.6 KCl, 2 $CaCl_2$, 1 $MgCl_2$, 10 HEPES pH 7.4, 3.6 Na HCO_3 and, 5.6 glucose). Cells in each well were then pre-incubated 37°C in 200 µL Locke's solution containing 100 µM L-Arg and the relevant treatments, at the time and dosage indicated in the Results section. Inhibitors were added to the incubation medium 0.5 hr prior to the addition of treatments. At the end of the treatment period, transport assays were performed using the same 24-well plates and the equipment described by Gazzola *et al* (Gazzola *et al.*, 1981) for rapid-measurement of solute transport. Pre-incubation buffer was replaced by the same solution in the absence of treatments containing 100 nM L-[^{3}H] Arg (1 mCi/mL with a specific activity of 45.2 Ci/mM from New England Nuclear) and unlabelled L-Arg up to a total concentration of 100 µM ("Transport buffer"). Initial-rate transport measurement was allowed to proceed for only 60 sec at 37°C in order to achieve linearity. In selected experiments, treatments were added directly into the Transport buffer. L-Arg transport was terminated by rapidly decanting and shaking the transport buffer into a collection container and immediately washing the cells three times with ice-cold Locke's solution with the plate kept on ice.

Cells were detergent solubilised in 0.2% SDS and 0.2 M NaOH. Radioactivity associated with L-arg transport was quantified by liquid scintillation counting of extracts in a β-counter (Packard Instruments). The total cellular protein in each sample was determined by the Bio-Rad detergent method, which uses a modification of the Lowry assay (Lowry *et al.*, 1951) with BSA as a standard. Regression analysis and rectangular hyperbola transformations were made using GraphPad Prism 2 software (GraphPad Inc.). K_m and V_{max} calculations were made from these analyses.

5.1.2.2 Protein lysate preparation and Western blot analysis

BAEC were grown to 90% confluence in 100 mm plates (Chapter 2 Section 1.2) and treated as indicated in Results. At the end of the treatment period cells were rinsed twice with Dulbecco's phosphate buffered saline (pH 7.4) (D-PBS; SIGMA). Cells were then scraped in 1 mL of D-PBS and transferred to eppendorfs. Cells were then pelleted by centrifugation at 15,000 g for 10 sec and the supernatant discarded. Resultant pellets were resuspended in 200 µL lysis buffer (mM; 50 Tris pH 7.5, 100 NaCl, 1% Nonidet P-40, 1% sodium deoxycholate, 2 EDTA, 1 phenylmethylsulfonyl fluoride, 10 µg/mL leupeptin, pepstatin and aprotinin) and placed on ice for 0.5 hr. Cellular debris were removed by 4°C centrifugation of lysates at 15, 000 g for 15 min. The supernatant was retained and used for protein determination by Lowry assay. In selected experiments 100 µg lysates were treated with 20 U N-glycosidase F and 0.1% SDS (v/v) for 3 hr at 37°C. An equal volume of 1X SDS-Urea loading buffer (Laemmli buffer supplemented with 8M urea) was added and incubated at 65 °C for at least 15 min prior to loading on a gel. SDS-PAGE and Western Blot analysis was carried out as detailed in Chapter 2.5.2 and 2.5.3 with modifications. Briefly, 30 µg of cell lysate in each lane was resolved by 10% SDS-PAGE and transferred to PVDF for 1.5 hours at 100 V. Blots were rinsed briefly in TBS-T solution (Tris-HCl, pH 7.5, buffered saline and 0.1% Tween) containing 5% non-fat powdered milk. After an initial blocking period of 2 hr at RT in the same solution, blots were incubated with a 1:500 dilution of primary affinity-purified CAT-1 antibody (Chapter 2, Section 5.1) overnight at 4°C in fresh 5% milk solution. Blots were then

incubated for 1 hr at RT with a 1:5000 dilution of a peroxidase-conjugated secondary goat anti-rabbit antibody (Bio-Rad). Development of signal was achieved with Western blot detection reagents (enhanced chemiluminescence, Amersham Biosciences, Inc.), X-OMAT film (Kodak) and a Kodak developer.

5.1.2.3 Statistics

The following statistical considerations were applied throughout the present chapter. Results are expressed as mean±SEM. Except where noted, results were normalised to the protein content. Statistical evaluation of the data was performed by two-tailed Student's *t*-test for unpaired observation. When more than two groups were compared, the significance of the difference between group means was analysed by one-way ANOVA with post-hoc analysis by the Tukey test. SigmaStat 2.0 software (Jandel Scientific, San Rafael, CA, USA) was utilised for all statistical analyses. Values were considered to be statistically different at a value of $P<0.05$.

5.1.3 Results

5.1.3.1 Characterisation of L-Arg transport In BAEC

Transport of L-Arg in BAEC was found to be time- (Figure 5.1) and concentration- (Figure 5.3A) dependent. N-ethyl maleimide (NEM), the selective inhibitor of system y+, can be employed to discriminate between the various transport systems (Chapter 1, Section 6.2) that mediate the influx of cationic amino acids (Deves *et al.*, 1993). As shown, a 200 μM pre-treatment with NEM resulted in a significant inhibition of L-Arg transport in BAEC (Figure 5.2A, $P<0.05$). Time-dependent L-Arg transport studies in the presence and absence of sodium ions revealed that L-Arg was almost completely Na+ independent in BAEC, consistent with the transport properties of system y+ (Figure 5.1). Linear uptake of 100 μM was evident for at least 60 sec after the addition of L-Arg mixture and thus, 60 sec was chosen as the appropriate time for all further initial-rate L-Arg transport measurements in BAEC. Other characteristics of system y+ (Chapter 1, Section 6.2) were also exhibited in BAEC: L-Arg transport was significantly inhibited by an excess (10 mM) of

competing cationic amino acids (L-Arg or L-Lysine) in the transport buffer and, in the presence of sodium ions the neutral amino acid L-Leucine (100 μM) was a poor inhibitor of L-Arg transport (Figure 5.2A). In comparison to the NOS inhibitory L-Arg analogue L-NMMA (17% of control, $P<0.05$), the NOS inhibitor L-NAME was a poor inhibitor of L-Arg transport (86% of control)(Figure 5.2A). Although, L-NAME is known to be a more potent inhibitor of NOS activity in endothelial cells.

Another known property of the CAT-1 isoform transporter activity is its sensitivity to substrate concentrations on the opposing side of the membrane called *trans*-stimulation (Chapter 1, Section 1.7.2). In order to assess this in BAEC, cells were amino-acid depleted for 2 hr then preloaded with either 1mM L-Arg, L-NMMA or L-NAME for a further 1 hr and then L-[^{3}H]Arg transport (100 μM) was measured as outlined in Methods.

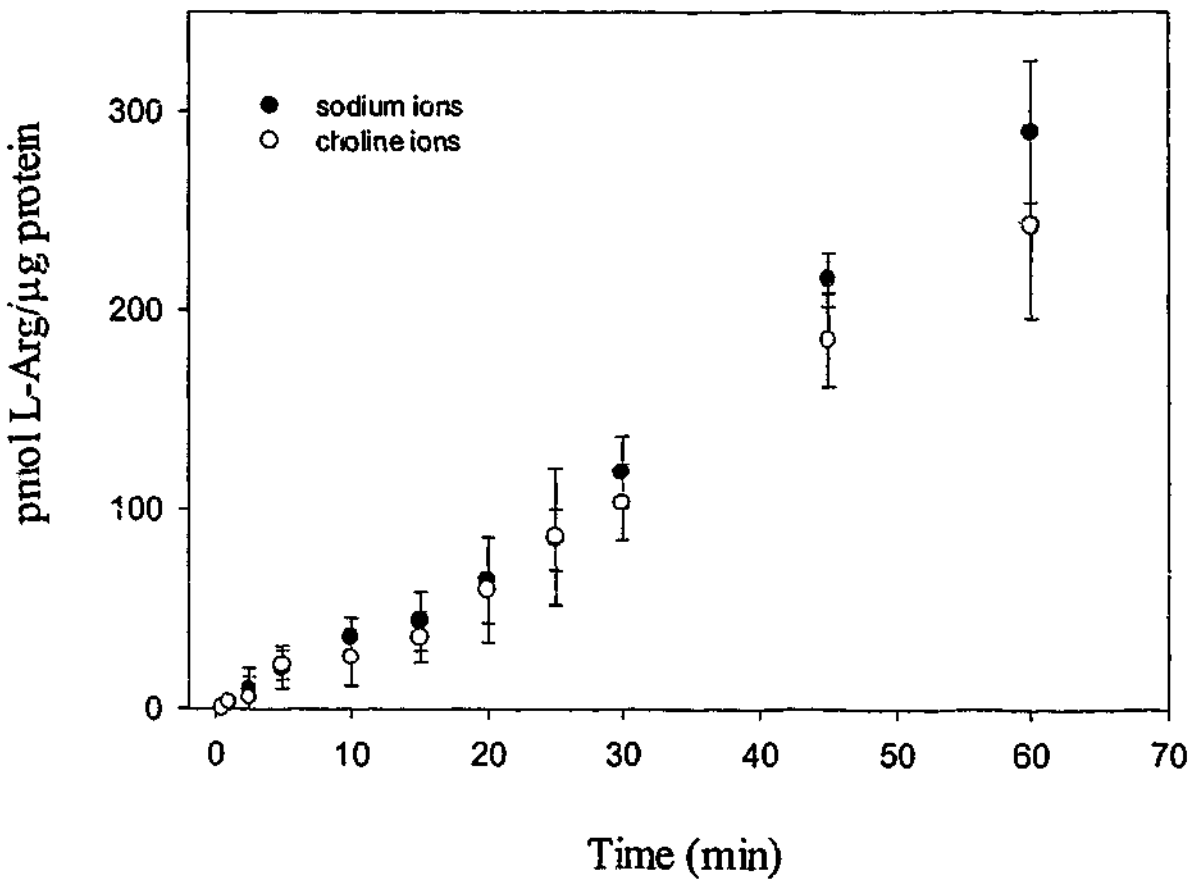

Figure 5.1 **Time course of L-Arg transport in BAEC.** Confluent BAEC were incubated in transport buffer containing a 100μM L-[^{3}H]Arg mixture for various length of times as indicated on the x-axis. L-Arg transport measurements (y-axis) were performed in the presence (•) and absence of sodium ions (○) as described in Methods. This figure depicts the results of four independent experiments (n=4).

As shown in Figure 5.2B pre-loading with a physiological concentration of L-Arg (100 μM) resulted in a significantly higher L-Arg transport rate than in conditions where the intracellular L-Arg concentration would be expected to become limiting (no pre-loading of L-Arg). L-Arg transport was also significantly *trans*-stimulated by the presence of the NOS inhibitory L-Arg analogue L-NMMA at the intracellular face when compared to BAEC that had not been pre-loaded , whereas L-NAME was without effect. These observations are in accordance with the major L-Arg transporter system y+ displayed by other endothelial cell types (Bogle *et al.*, 1996). In summary, these results confirm that in BAEC L-Arg transport is predominantly due to the activity of system

y+. In order to test the suitability of this L-Arg transport assay to measure known changes in L-Arg transport in response to physiological agents, early passage cells (between splits 1-2) were pre-treated with bradykinin (10 μM) in Locke's solution for 10 min before the addition of L-[^{3}H]Arg mixture to the same solution for 60 sec. Treatment of cells with bradykinin caused a significant increase in L-Arg transport in BAEC (Figure 5.2A, 143% of control untreated cells; $P<0.05$). This increase is within a similar magnitude reported by others in endothelial cellsz (Hardy and May, 2002).

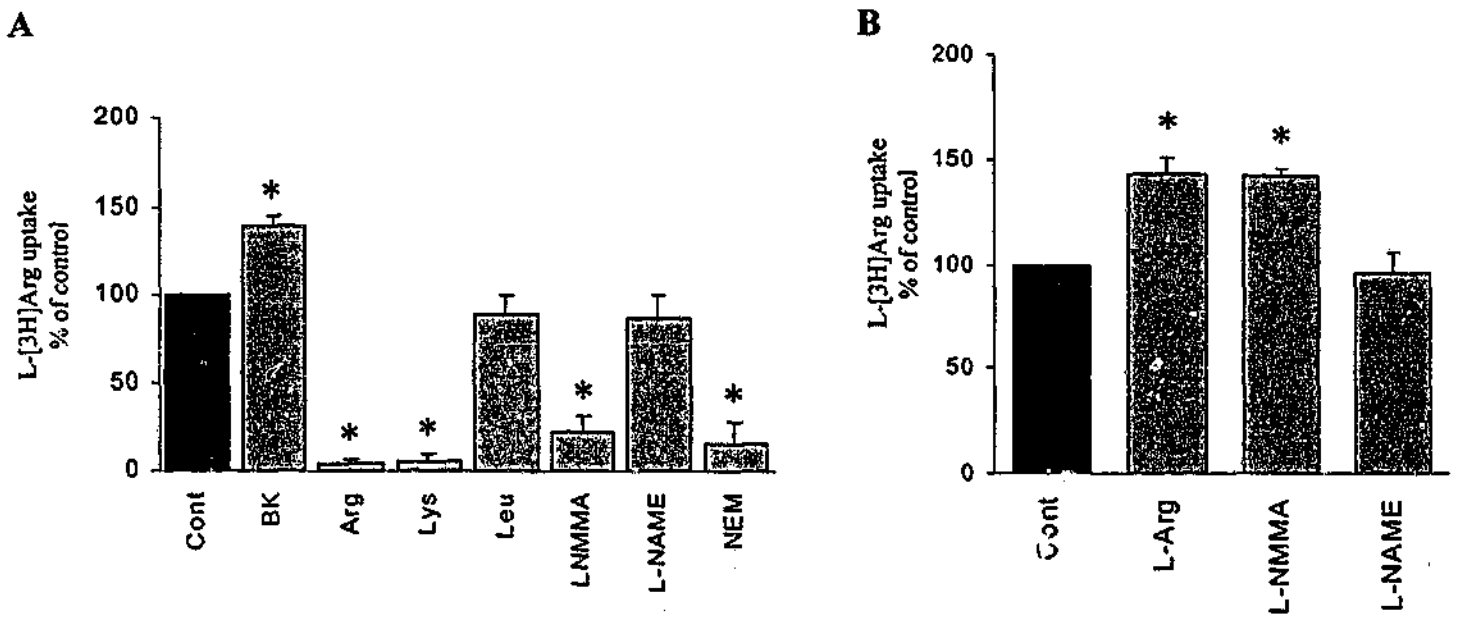

Figure 5.2 **System y+ properties of L-Arg transport in BAEC. A,** L-Arg transport (100 μM L-[^{3}H] Arg mixture) was measured in the presence of either 10 μM bradykinin (BK), 10 mM L-Arg (Arg), 10 mM L-Lysine (Lys), 100 μM L-Leucine (Leu), 1 mM L-NMMA, 1 mM L-NAME or 200 μM NEM as described in Results and Methods. **B,** *Trans*-stimulation of L-Arg transport by either 1 mM of L-Arg, LNMMA or L-NAME at the opposing side of the membrane as described in Methods. Control cells did not contain any pre-loaded amino acids (Cont). This figure depicts the results of four independent experiments (n=4). * $P<0.05$ versus untreated controls (Cont).

5.1.3.2 Stimulation of PKC is associated with decreased L-Arg transport

In order to test whether PKC has a role in endothelial L-arginine transport, BAECs were treated with either vehicle (0.1% DMSO) or the PKC activator PMA (100 nM) for 0.5 hr and then assayed for an evaluation of L-Arg transport activity. Kinetic analysis was undertaken for this purpose to measure the concentration dependence of L-Arg transport. In this assay, transport of L-[^{3}H]Arg was measured in the presence of defined incremental extracellular L-Arg concentrations for both PMA treated and untreated cells. As shown an increase in the concentration of extracellular L-Arg facilitated the transport of L-Arg in a dose-dependent manner for both PMA treated and untreated cells (Figure 6.3A). Treatment with PMA for 0.5 hr prior to transport measurement (100 nM) reduced the maximum transport rate (*V*max; 3.2 ± 0.4 versus 1.5 ± 0.1 pmol/μg protein/min; $P<0.05$) particularly at higher physiological concentrations of extracellular L-Arg (100-300 μM), indicating an impaired rate of L-Arg transport in response to PKC activation. Eadie-Hofstee transformation of this kinetic data (Figure 6.3B) revealed that a single high-affinity L-Arg transport system was mediating L-Arg transport in both PMA treated and untreated cells. The affinity of this L-Arg transport system for L-Arg in BAEC after PKC activation was not significantly different from that in untreated cells (K_m; 116 ± 9 versus 106 ± 16 μM). Dose-response experiments measuring the effects of PMA pre-treatment (0.5 hr) on L-Arg transport indicated a significant threshold inhibition of L-Arg transport at a dosage of 1 nM (data not shown, $P<0.05$).

A

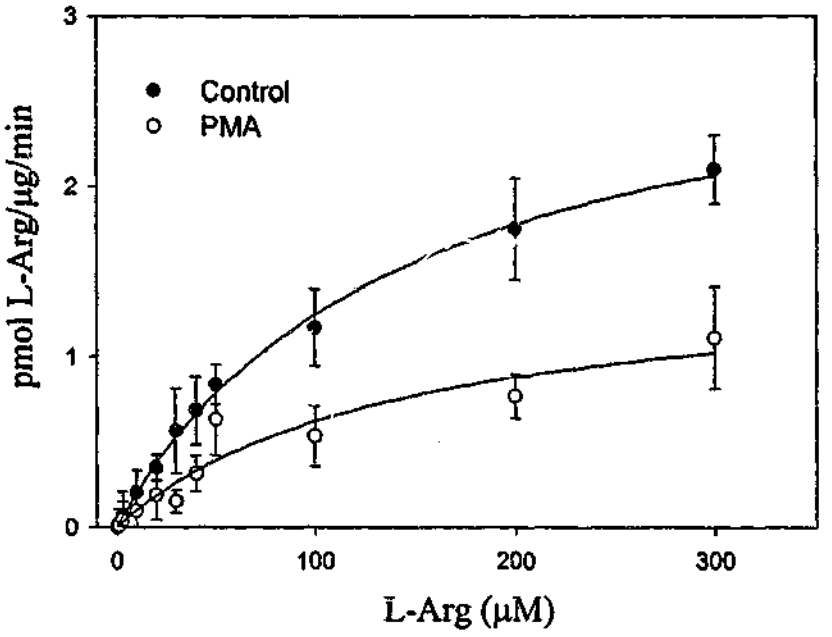

B

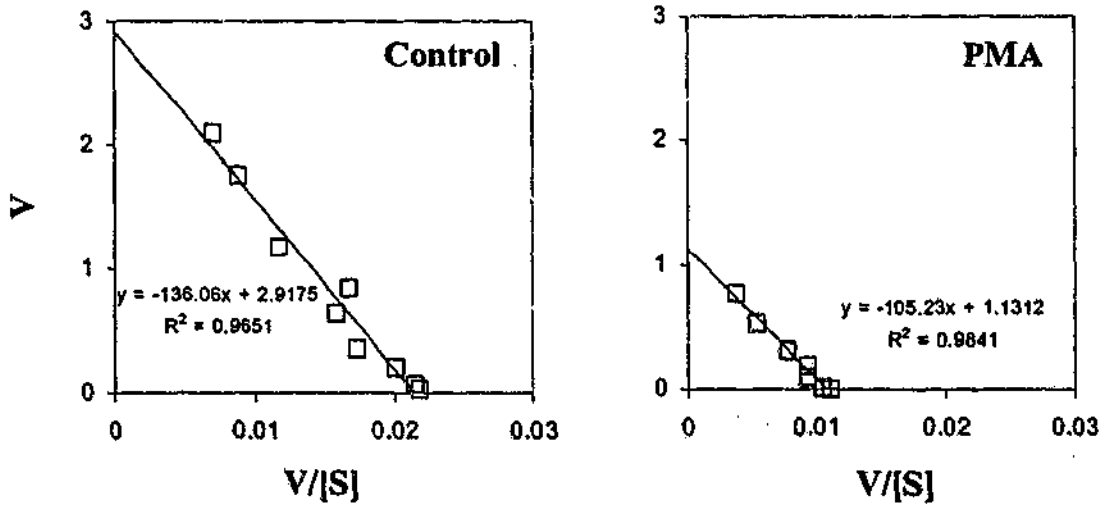

Figure 5.3 PKC activation selectively inhibits the maximum velocity of L-Arg transport in BAEC. A, Effects of concentration of extracellular L-Arg on the uptake by BAEC with (○) or without (●) pretreatment with PMA (100 nM for 0.5 hr). The velocity of L-Arg uptake by BAEC treated with or without PMA was determined in the presence of different amounts of L-Arg in the transport buffer as outlined in Methods. **B,** Eadie-Hofstee plot of L-Arg transport by BAEC. The data from panel A are rearranged in the Eadie-Hofstee plot where V/[S] represents velocity on the x-axis and V represents velocity divided by the extracellular L-Arg concentration on the y-axis. L-Arg transport by BAEC consists of a single high-affinity transport system. Values in panel A are mean±SEM of four independent experiments with triplicate values obtained per experiment (n=4). Values in panel B are from one representative experiment.

5.1.3.3 Downregulation of PKC is associated with increased L-Arg transport

The effects of PMA on L-Arg transport were dependent on the duration of treatment. As mentioned in the Introduction (Chapter 5, Section 5.1.2) short-term treatment with PMA (less than 6 hr) is associated with PKC activation whereas long-term treatment (more than 6 hr) is associated with PKC degradation and downregulation in BAEC (Patel et al., 1996). A 0.5 to 4 hr treatment with PMA significantly inhibited L-Arg transport (0.5 hr, 45 ± 4%; $P<0.05$) whereas long-term treatment (12-24 hr) with PMA significantly induced L-Arg transport (12 hr, 189±29%; $P<0.05$) (Figure 5.4). Long-term treatment with PMA corresponded with a significantly increase in L-Arg transport capacity (Vmax 3.2 ± 0.4 versus 6.0 ± 0.6 pmol/ μg protein/min; $P<0.05$) but no measurable change in transport affinity (K_m 116 ± 9 versus 111 ± 10 μM).

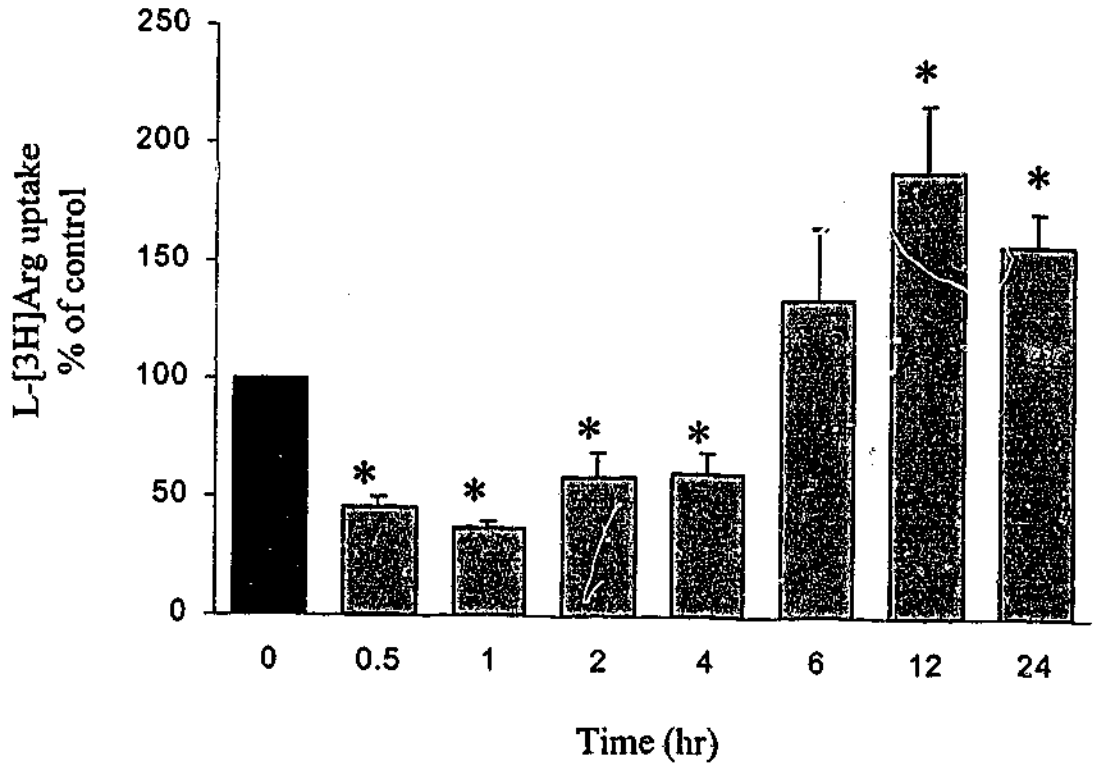

Figure 5.4 Effect of PMA incubation time on L-Arg transport in BAEC. L-Arg transport by BAEC was measured after incubation of cells with 100 nM PMA over the time course indicated and as described in Methods. Values are expressed as a percentage of time-matched controls (100%) and are the mean±SEM of four independent experiments with triplicate values obtained per experiment (n=4). *P<0.05 versus untreated control.

5.1.3.4 PMA-mediated effects on L-Arg transport are blocked with a PKC inhibitor

To investigate whether the effects of PMA treatment time on L-Arg transport was mediated specifically by activation of PKC, PMA effects on L-Arg transport were measured in the presence of the PKC inhibitor bisindolylmaleimide I (Bim I) or its inactive analogue bisindoylmaleimide V (Bim V). Based on the previous literature (Budworth and Gescher, 1995) (Toullec *et al.*, 1991), a Bim I dose of 1 μM was chosen for all studies in order to block PKC activity in cultured endothelial cells. Incubation of the BAEC in 1 μM of the inactive phorbol ester Bim V alone or in the presence of PMA for either 0.5 hr or 12 hr did not affect the basal transport activity for L-Arg (Figure 6.5 A/B).

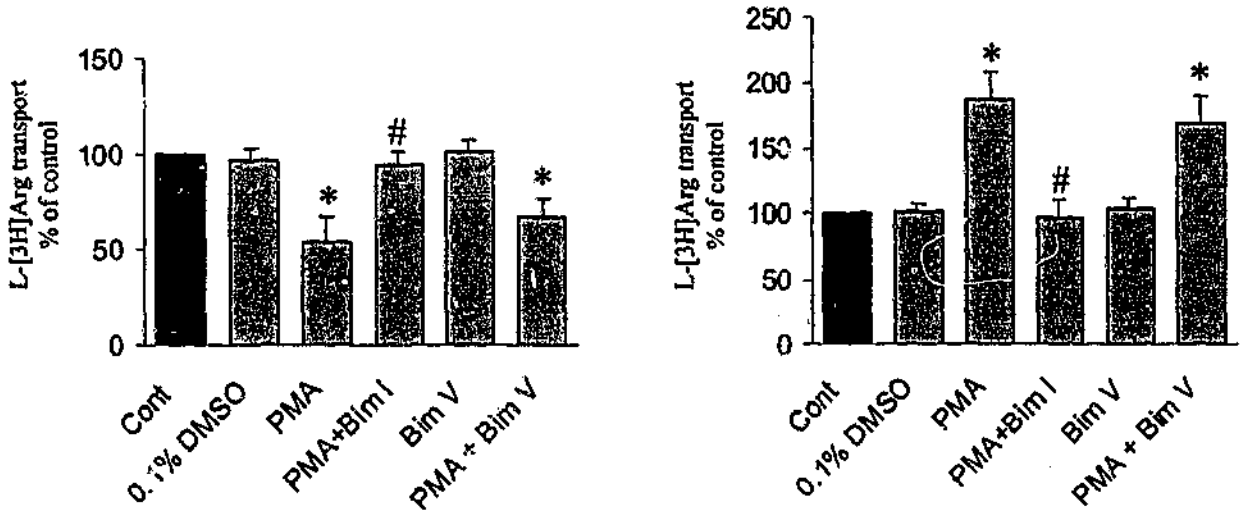

Figure 5.5 PKC inhibition prevents the effects of PMA on L-Arg transport in BAEC. BAEC were treated with 100 nM PMA in the presence or absence of the PKC inhibitor Bim I, or its inactive analogue Bim V. Cells were incubated with Bim I or Bim V for 0.5 hr prior to the addition of PMA. L-Arg transport was measured after **A**, 0.5 hr or **B**, 12 hr of PMA treatment as described in Methods. Values are expressed as a percentage of control cells treated with vehicle (0.1% DMSO) and are mean ± SEM of four independent experiments with triplicate values obtained in each experiment (n=6). *$P<0.05$ versus control. #$P<0.05$ versus PMA alone treated cells.

Both the downregulatory (0.5 hr PMA, Figure 5.5 left panel) and stimulatory (12 hr, Figure 5.5 right panel) effects of PMA on L-Arg transport in BAEC were abolished in the presence of Bim I (Figure 5.5, #$P<0.05$). In order to verify its effectiveness at lower doses, the dose-response of Bim I (1 nM – 10 μM) on L-Arg transport was examined in BAEC under basal conditions and after 0.5 hr of PKC stimulation with PMA (100 nM). A significant threshold blockade effect of Bim I on PKC-stimulated downregulation of L-Arg transport was also evident at lower concentrations (100 nM) (results not shown).

5.1.3.5 PKC does not alter CAT-1 expression levels

Western blot analysis of protein lysates from PMA-treated BAEC demonstrated that changes in the L-Arg transport induced by short-term and long-term PMA treatments were not due to significant changes in CAT-1 protein expression (Figure 6.6A and B). In order to confirm equal loading in each lane and quantitate CAT-1 protein, CAT-1 signals were normalised to the expression of β-tubulin. The expression of β-tubulin was not altered in response to PMA treatment nor is it known to be by others (Harrison *et al.*, 1990). Changes in glycosylation status are known to affect the activity of some glycan-linked membrane proteins (Samih *et al.*, 2003), although CAT-1 L-Arg transport activity is not known to be subject to regulation by its N-linked glycosylation status (Closs, 1996). In accordance, the total glycosylation level of the CAT-1 protein was not significantly altered by incubation with PMA as shown in top panel of Figure 6.6A. Although, some differences in individual glycosylated forms were detectable (glycosylated forms detected as the three signal visualised between 80-100 kDa in Figure 6.6A, top panel). An additional and potentially dimerised form of CAT-1 protein was observed at a higher molecular weight form ~120 kDa in figure 6.6A, top panel. This form has been reported by two other groups (Masuda *et al.*, 1999, Lu and Silver, 2000)is generally observed after boiling cell lysates at a temperature higher than 70°C but may alternatively represent a highly glycosylated form of CAT-1.

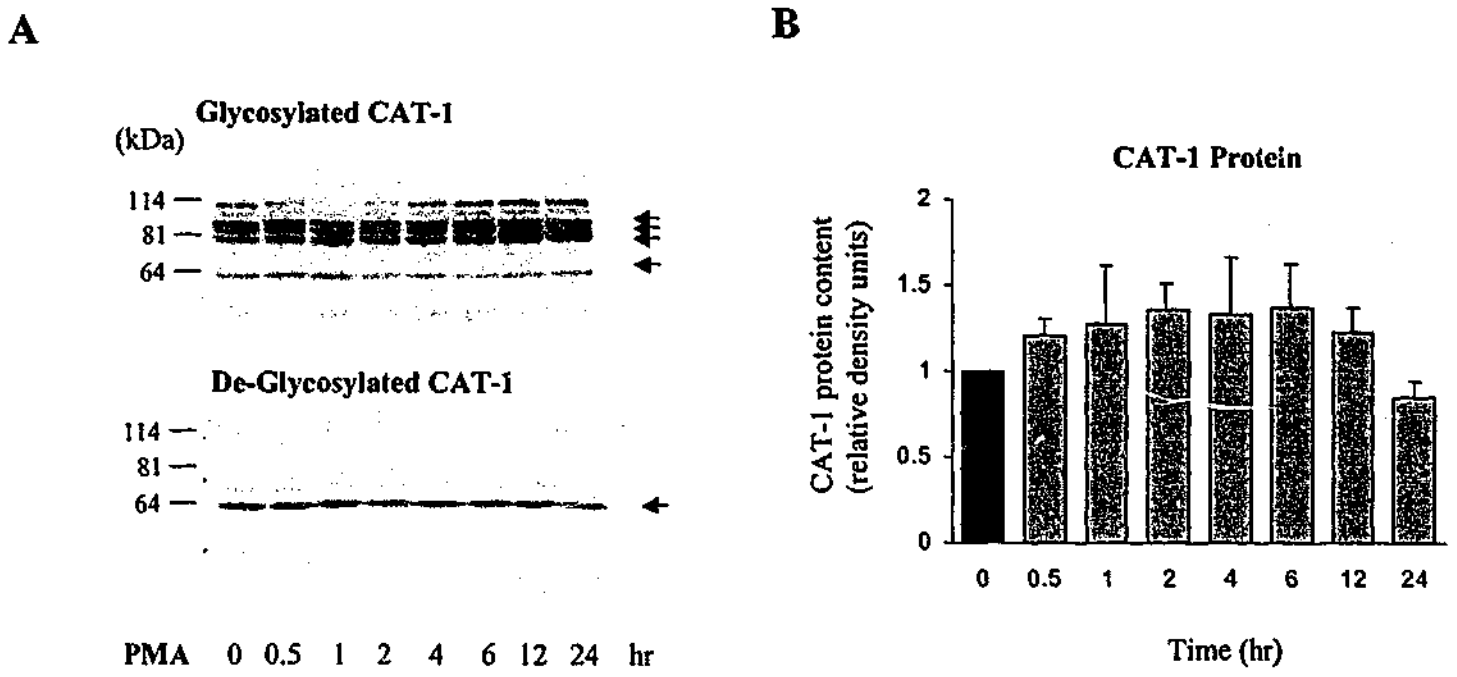

Figure 5.6 **CAT-1 protein expression levels in response to PMA treatment. A,** Western blot analysis of CAT-1 was performed as described in Methods using PMA treated BAEC-lysates at the times indicated. Glycosylated and de-glycosylated forms of CAT-1 are evident in the top panel and are marked with black arrows. In the bottom panel, cell lysates were pretreated with Glycosidase F to remove N-linked glycans prior to SDS-PAGE. The de-glycosylated form of CAT-1 is marked with a single black arrow. **B,** Graphical depiction of CAT-1 protein levels after PMA incubation for various times. Results are expressed as densitometric units relative to time matched controls (mean±SEM) and are from three independent experiments (n=3).

5.1.4 Discussion

System y+ was identified as the major kinetic L-Arg transport system present in primary BAEC isolated from this laboratory. Further RT-PCR studies conducted with this endothelial cell type revealed a singular expression of the system y+/CAT-1 isoform with no detectable presence of alternate CAT-2B or –2A isoforms (data not shown). Furthermore, the apparent affinity for L-Arg (K_m, 116 ± 9 μM) in BAEC measured in the current study is consistent with the range of values

(140-380 μM) reported in various other molecular and physiological models of CAT-1 expression (Closs, 1996). Together, this evidence confirms that the major system of L-Arg transport in BAEC is mediated by CAT-1.

In the present study PKC activation resulted in a significantly decreased L-Arg transport activity in BAEC which was not accompanied by changes in the apparent affinity of the L-Arg transporter for L-Arg but rather due to a significantly decreased L-Arg transport capacity. PKC depletion due to long-term PMA treatment resulted in an induction of L-Arg transport activity that was due to an increased L-Arg transport capacity without changes in the apparent substrate affinity. Receptor-mediated and kinase- mediated changes in L-Arg transport capacity (*V*max) with little or no change in apparent substrate affinity (K_m) have previously been reported in cultured endothelial cells (Pan et al., 1995) which may seem to indicate a decrease of functional transporter units. Interestingly, in some instances changes in L-Arg transport rate were not associated with alterations in either CAT gene or protein expression. For example, Zharikov *et al.*(Zharikov et al., 2001) have shown that disruption of the microtubule cytoskeleton results in a significantly decreased L-Arg transport activity that does not correspond to changes in CAT protein expression. Similarly in the present study, changes in L-Arg transport activity observed after PKC activation (decreased L-Arg transport) or depletion (increased L-Arg transport) with PMA were not associated with alterations in CAT-1 protein expression. Additionally, the level of CAT-1 protein glycosylation was not altered by PMA treatment time indicating that there were no abnormalities to the way in which this protein was post-translationally modified and processed by the endoplasmic reticulum, as a preparation for targeting to the plasma membrane. Thus, the present study and others are strongly indicative that a post-translational mode of L-Arg transport regulation by PKC exists in endothelial cells.

A major property of CAT-1 is the sensitivity of L-Arg transport activity to *trans*-stimulation when substrate concentrations are high enough on the opposite side of the membrane (Closs, 1996). In BAEC, it was evident that at a physiological concentration of L-Arg on the extracellular face of the

membrane (100 μM), the rate of L-[3H]Arg transport was significantly reduced in cells which had been previously deprived of L-Arg compared to those which had been pre-loaded with 100 μM of L-Arg (Figure 5.2B). Such a requirement of CAT-1 for cationic amino acids on the *trans*-side of the plasma membrane for its activity may possibly play a role in the sustained depression of L-Arg transport shown in response to PKC activation by PMA, although this was not tested within the present study. According to this proposed theory, a decreased rate of L-Arg entry or an increased metabolic rate of intracellular L-Arg utilisation due to PKC activation may result initially in a lowered intracellular concentration and, in turn, lead to a further decline in L-Arg transport activity. Thus, a positive feedback loop may exist for CAT-1 regulation involving its own substrate. Although the (patho-)physiological relevance of this phenomenom is still unknown, this may contribute to a deficiency of L-Arg in endothelial cells and will be explored in future studies. Intracellular L-Arg concentrations were not measured within the current study after the L-Arg deprivation period. However, two independent previous reports using bovine aortic endothelial cells have confirmed that after 2 hr of L-Arg deprivation intracellular L-Arg levels are reduced by more than 50% without affecting viability of the cells (Baydoun *et al.*, 1990, Preik-Steinhoff *et al.*, 1995). A decrease in intracellular L-Arg levels caused by extracellular deprivation of L-Arg over this time period has been attributed to its demand by other essential metabolic pathways within the cell (Chapter 1, Section 5), but might also be partially due to the effects of extracellular diffusion and efflux.

Since inhibition of L-Arg transport in response to PKC activation in BAEC is not accompanied by a reduction in the expression of its major transporter, it is possible that PMA-induced internalisation or inactivation of CAT-1 by PKC may account for the altered transport activity of L-Arg across the cell membrane. Inhibition of the human dopamine transporter (Daniels and Amara, 1999), rat serotonin transporter (Jess *et al.*, 2002), and rat glutamate/aspartate transporter activity by activated PKC is known to involve a trafficking process of transporter internalisation from the plasma membrane. Alternatively, PKC-induced inactivation of amino acid transporter activity has been proposed to involve direct phosphorylation of the transporter. According to the 14

transmembrane model proposed by Albritton *et al.* (Albritton *et al.*, 1993) the amino acid sequence of CAT-1 (mouse) contains five putative PKC phosphorylation sites. Three of putative PKC phosphorylation sites are located on the intracellular loops. CAT-1 also contains consensus sequences for casein kinase II phosphorylation sites. Therefore, CAT-1 transport activity may potentially be regulated by phosphorylation events involving activated PKC or alternatively through the actions of casein kinase II. Interestingly both kinases are known to regulate the activity of membrane transporter proteins through phosphorylation events (Kalandadze *et al.*, 2002, Krantz *et al.*, 1997) and also to regulate trafficking events to and from the plasma membrane (Melikian and Buckley, 1999, Shi *et al.*, 2001).

An additional possibility is that activated PKC may elicit indirect actions on CAT-1 activity through an interaction with a potential CAT-1 regulatory protein. Cell-specific expression and activation of a putative regulatory CAT-1 protein in response to activation of PKC may explain the contrasting effects of PKC activation on L-Arg transport activity in other cell types. It is noteworthy that since eNOS and caveolin-1 are both known substrates for PKC (Sukumaran *et al.*, 2002, Michell *et al.*, 2001), have been shown to co-localise with CAT-1 (Lu and Silver, 2000, McDonald *et al.*, 1997) and are also expressed in a cell -specific manner they might be likely candidates as potential CAT-1 regulatory proteins.

The use of PMA as an activator of classical and novel PKC isotypes holds the caveat that each isotype of PKC can be differentially activated and/or depleted. Thus, PMA usually only gives an indication of the class of PKC involved in a response. Since α- and ε- are the only classical and novel isotypes identified in BAEC this allowed the discrimination of two likely candidates for their involvement in modulation of L-Arg transport activity in the current study. In particular, since the translocation and depletion patterns of the PKC-α isotype (Patel et al., 1996) closely matched the temporal profile of altered L-Arg transport activity in response to PMA: translocation of PKC-α from cytosolic to the membrane fraction after PKC stimulation with PMA for less than 6 hr

corresponds with a decreased L-Arg transport activity in the present study wherease depletion of PKC-α expression after 6 hr of treatment with PMA corresponds with a significantly increased L-Arg transport activity. Taken together, this evidence is suggestive of a possible role for the PKC-α isotype in the regulation of CAT-1 activity.

Previous work by others has suggested that endothelial cells can express a different complement of PKC isoforms in different areas of the circulation (Krizbai *et al.*, 1995) and also within immortalised endothelial cell lines (Li *et al.*, 1998). Identification of the PKC expression pattern elsewhere in the vasculature may thus be an important part in identifying mechanisms that may alter CAT activity and expression in response to the local physiological stimulus. More recently, Graf *et al.* (Graf et al., 2001) have indicated that PKC is involved in modulation of L-Arg transport activity in the immortalised endothelial cell type, EA.hy926. In agreement with the present data, PKC activation significantly reduced L-Arg transport activity. However, by contrast to the effect in BAEC (increased L-Arg transport activity), long-term PKC depletion with PMA resulted in a sustained decrease in L-Arg transport activity that corresponded temporally with an increased CAT-1 mRNA expression and a moderate but non-significant increase in CAT-1 protein levels.

It is possible that either the vascular bed origin or aberrations in the endothelial phenotype that occur after immortalisation may explain the difference in this effect in both of these endothelial cell studies. Since the observations in the present study were carried out on primary cultures of endothelial cells it is thought that these findings may have particular relevance to the normal endothelial response *in vivo*.

The functional consequence of altered L-Arg transport activity in response to changes in PKC activation status within endothelial cells is not known. The PKC family is known to participate in endothelial proliferation, angiogenesis and cytoskeletal remodelling (Mellor and Parker, 1998). However, individual members of the PKC family involved in these processes are unknown. It is thought that individual PKC isotypes are likely to provide distinct functions, which give rise to

distinct signalling pathways. For example, two PKC isotypes have been shown to have important but reciprocal roles in the mitogenic response of endothelial cells to growth factors. BAEC stably transduced with and overexpressing PKC-α have been shown to exhibit reduced proliferation *in vitro* whereas cells transduced with PKC-β1 exhibited increased growth (Rosales *et al.*, 1998). Interestingly, PKC-α and β- isotypes have also been shown to play an important role in the mechanism of agonist-induced endothelial barrier dysfunction (Siflinger-Birnboim and Johnson, 2003) and impaired release of NO by the endothelium in response to vasoactive mediators (Beckman *et al.*, 2002). Given the important requirement of L-Arg transport activity in the processes mentioned above, further work in elucidating the mechanisms involved in PKC modulation of L-Arg transport activity is warranted.

Chapter Six

Mechanisms of Protein Kinase C Modulated L-Arg Transport

TABLE OF CONTENTS

6.0 General Introduction *206*

6.1 Effect of PKC on CAT-1 (Co-)localisation Status in BAEC *208*

6.1.1 Introduction **208**

6.1.2 Methods **209**

6.1.2.1 Immunofluorescence 209

6.1.2.2 Separation of membrane and cytosolic fractions from BAEC 209

6.1.2.3 (Co)-Immunoprecipitation studies 210

6.1.2.4 Western blot analysis 211

6.1.2.5 NOS catalytic activity 212

6.1.2.6 Statistical analysis 212

6.1.3 Results **212**

6.1.3.1 PKC does not affect plasma membrane localisation of CAT-1 212

6.1.3.2 Effect of PKC on caveolin expression in BAEC. 214

6.1.3.3 Effect of PKC on NOS expression in BAEC 215

6.1.3.4 Effects of PKC on NOS activity in BAEC 216

6.1.3.5 Antioxidants do not affect PKC regulation of L-Arg transport. 217

6.1.3.6 Caveolin associates with CAT-1 under basal conditions in BAEC. 219

6.1.3.7 PKC does not affect CAT-1 association with caveolin. 221

6.1.4 Discussion **221**

6.1.4.1 Membrane localisation of CAT-1 is not affected by PMA in BAEC 221

6.1.4.2 PMA modulation of caveolin and NOS expression in BAEC 223

6.2 Effect of PKC on CAT-1 Phosphorylation Status in BAEC 224

6.2.1 Introduction 224

6.2.2 Methods 225

6.2.2.1 Plasmids 225

6.2.2.2 Generation of CAT-1 mutants 226

6.2.2.3 Transfection of BAEC 227

6.2.2.4 Metabolic labelling of BAEC 228

6.2.2.5 Immunoprecipitation of CAT-1 and Western blot analysis 228

6.2.2.6 L-[^{3}H]Arg transport assay 230

6.2.3 Results 230

6.2.4.1 Activation of L-Arg transport due to overexpression of CAT-1 230

6.2.4.2 CAT-1 is a phosphoprotein 233

6.2.4.3 Effect of PKC activation on CAT-1 phosphorylation status 234

6.2.4.4 A role for putative PKC sites in basal expression of CAT-1 236

6.2.4 Discussion 237

6.3 PKC –Modulated L-Arg Transport is Mediated by a Cytoskeletal-Associated Protease. 239

6.3.1 Introduction 239

6.3.2 Methods 239

6.3.2.1 L-[^{3}H]Arg transport assay 239

6.3.2.2 Western blot analysis of isolated membrane fractions 240

6.3.3 Results 240

6.3.3.1 Calpain inhibition prevents effects of activated PKC on L-Arg transport 241

6.3.3.2 Calpain inhibition prevents the long-term effects of PMA 241

6.3.4 Discussion 243

TABLE OF FIGURES

Figure 6.1	Activation of PKC does not affect CAT-1 plasma membrane localisation.	213
Figure 6.2	Subcellular fractionation of PMA-treated and untreated BAEC into membrane and cytosolic fractions.	214
Figure 6.3	Effect of PMA treatment time on the expression of caveolin protein.	215
Figure 6.4	Effect of PMA treatment time on the expression of eNOS protein.	216
Figure 6.5	NOS activity in BAEC homogenates after PMA treatment.	217
Figure 6.6	Effect of antioxidant treatment on PMA-modulated L-Arg transport.	218
Figure 6.7	Interaction of caveolin with CAT-1 in BAEC under basal conditions.	220
Figure 6.8	Association of CAT-1 with caveolin in response to PMA treatment in BAEC.	220
Figure 6.9	Serine to alanine substitutions at intracellular PKC phosphorylation sites on CAT-1.	226
Figure 6.10	L-Arg transport activity and expression of CAT1-FLAG in BAEC.	232
Figure 6.11	Effect of PKC activation on the activity of overexpressed CAT1-FLAG in BAEC.	233
Figure 6.12	Basal phosphorylation of CAT-1.	234
Figure 6.13	Phosphorylation status of CAT-1 after PKC activation.	235
Figure 6.14	Ablation of putative PKC sites on CAT-1 reduces basal L-Arg transport.	236
Figure 6.15	Effect of calpain inhibition on PKC mediated inhibition of L-Arg transport.	241
Figure 6.16	Calpain inhibition prevents the induction of L-Arg transport caused by long-term PMA treatment.	242
Figure 6.17	Calpain inhibition prevents the effects of long-term PMA treatment on caveolin and NOS expression.	243

6.0 General Introduction

Protein kinase C (PKC) isotypes participate in the regulation of processes such as cellular differentiation, proliferation, gene expression, membrane transport and, the organisation of cytoskeletal and extracellular matrix proteins (Mellor *et al.*, 1998). Within the endothelium, PKC isotypes participate in biological responses that control angiogenesis, cell proliferation, cytoskeletal reorganisation and the nitric oxide (NO) pathway (Siflinger-Birnboim *et al.*, 2003). Known physiological activators of PKC in the endothelium include high glucose (diabetes mellitus and hyperglycaemia), thrombin, angiotensin, oxidised LDL, fluid and shear stress and, growth factors such as vascular endothelial growth factor.

There is now increasing evidence to suggest that PKC is an important mediator of endothelial dysfunction (De Vriese *et al.*, 2000). PKC-induced endothelial dysfunction in disorders of high glucose is associated with impaired endothelium-dependent vasodilation *in vivo* (Beckman *et al.*, 2002) and, downregulation of eNOS activity (Chakravarthy *et al.*, 1998), increased oxidative stress (Cosentino *et al.*, 2003), induction of vasoconstrictory endothelin-1 gene expression (Park *et al.*, 2000b), upregulation of vascular adhesion molecules *in vitro* (Park *et al.*, 2000a). There is also evidence to suggest that the deleterious effects of oxLDL (Chapter 1.4.4.3) present in the plasma of hypercholesterolemic patients and the affected arteries of atherosclerosis patients on endothelial function may involve PKC (Deckert *et al.*, 2002).

In view of the important consequences of alterations to the activity of the endothelial L-Arg-NO pathway in CHF (Chapter 1.4), stimuli and mechanisms that affect either substrate provision or eNOS activity in this pathway are of major interest to our laboratory. Interestingly, findings of Chapter 5 suggest that the state of PKC activation may affect the provision of L-Arg in endothelial cells possibly by regulating the activity of the major L-Arg transporter, CAT-1. The current chapter examines potential mechanisms via which PKC may modulate L-Arg transport in endothelial cells

by i) influencing the CAT-1 (co-)localisation at the plasma membrane (Section 6.1), ii) direct phosphorylation of CAT-1 (Section 6.2) or, based on more recent evidence in the literature iii) modulating the activity of a cytoskeletal-associated protein, calpain (Section 6.3).

6.1 *Effect of PKC on CAT-1 (Co-)localisation Status in BAEC*

6.1.1 Introduction

Compartmentalisation of eNOS within the caveolae has a significant influence on NOS activity (Chapter 1.3.2.2). Within this context, a functional inhibitory association of caveolin with eNOS is now established (Chapter 1.3.2.2). Caveolin has also been shown to co-localise with CAT-1 in the caveolae of porcine pulmonary artery endothelial cells, although the precise function of the association is not yet known. Additionally, immunodepletion experiments in cultured endothelial cells have demonstrated that a more direct interaction may also exist between CAT-1 and eNOS (McDonald *et al.*, 1997). Localised expression in the caveolae is thought to be vital for targeting of the L-Arg transporter to the site of eNOS activity and may facilitate a functional eNOS complex that favours the delivery of extracellular L-Arg for conversion to NO (Chapter 1.5.4.3).

In endothelial cells, the caveolae is a major integration site for various receptors and signal transduction pathways including PKC pathways (Shaul *et al.*, 1998). Localisation of eNOS and CAT-1 in the immediate vicinity of these signal transduction pathways may contribute to their regulation. Although the mechanism of action and resulting effect is somewhat controversial (Li *et al.*, 1998), eNOS is regulated by PKC. Sustained PKC activation is known to increase NOS activity through a mechanism involving transcriptional activation of eNOS (Li et al., 1998). By contrast, targeted ablation of putative PKC sites on eNOS has clearly demonstrated a direct role for PKC in post-translational inhibition of the enzyme (Michell *et al.*, 2001). Thus, in the absence of more specific information about the specific PKC isotypes involved, current evidence suggests that PKC may have an inhibitory effect on eNOS post-translationally and an activational effect transcriptionally. Data obtained using primary endothelial cells (Chapter 5), and work of Graf *et al.* (Graf *et al.*, 2001) supports a role for PKC-mediated inhibition of L-Arg transport involving post-translational modifications. Taken together with the existing eNOS data, a coordinated form of regulation by PKC may exist at the post-translational level whereby L-arginine transporter and

NOS activity are regulated through a common signalling pathway. The major goal of the present study was to determine whether regulation of L-Arg transport activity in BAEC by PKC may involve changes in the plasma membrane localisation of CAT-1 or, altered expression of CAT-1 interacting proteins caveolin and eNOS.

6.1.2 Methods

6.1.2.1 Immunofluorescence

For the detection of CAT-1, BAEC were grown on poly-L-lysine coated glass coverslips in 12-well plates (Falcon) and maintained in DMEM + 10% FBS until confluency. Cells were treated in the absence (vehicle, 0.1% DMSO) or presence of 100 nM PMA (Sigma) for 0.5 hr or as indicated in Results. All cell treatments were terminated by aspiration and gentle rinsing of coverslips twice in D-PBS. A fixation step was performed by the addition of 3% paraformaldehyde and 3% sucrose in D-PBS for 10 min at RT. Cells were rinsed in D-PBS then incubated in D-PBS containing 2% BSA for 1 hr at RT in order to reduce any subsequent non-specific antibody binding effects. Coverslips were then rinsed three times over 15 min and incubated for 1 hr at RT with either CAT-1 antibody (1:200; Chapter 2.5.1) or non-immune rabbit serum (2.5 μg/mL) in D-PBS + 2% BSA. After incubation, coverslips were rinsed six times over 0.5 hr in D-PBS and then incubated for 0.5 hr at RT with secondary antibody coupled to a fluorescent marker, Alexa Fluor® 488 goat anti-rabbit (Molecular Probes) in D-PBS + 2% BSA. Excess antibody was then removed by six rinses in PBS over 0.5 hr. Coverslips were then mounted in Vectashield® medium (refractive index 1.45, Vector Laboratories Inc.). Images were captured with a BioRad MRC 1024 ES confocal microscope and analysed using acquisition software (LaserSharp 2000, BioRad).

6.1.2.2 Separation of membrane and cytosolic fractions from BAEC

Membrane and cytosolic fractions of BAEC were prepared in order to assess CAT-1 membrane association after PMA treatment. Briefly, at the appropriate time point, untreated (vehicle, 0.1% DMSO) and PMA-treated (100 nM for 0.5 hr) cells in 100 mm culture dishes were washed twice

with cold D-PBS, harvested using a rubber cell scraper in 1 mL cold D-PBS and transferred to eppendorf tubes. Cells were then pelleted in a centrifuge at maximum speed for 10 sec. The resulting D-PBS-containing supernatant was discarded and replaced with ice-cold detergent-free buffer (in mM: 20 Tris-HCL, pH 7.4, 10 EDTA, 5 EGTA, 5 2-mercaptoethanol, 5 μg/ml, leupeptin, 1 μg/mL pepstatin, 1mM PMSF, and 1 μg/ml aprotinin). Cells were sonicated and centrifuged at 100,000 x g for 0.5 hr at 4°C. The resulting supernatant was collected and defined as the cytosolic fraction. The pellet (membrane fraction) was resuspended in 200 μl of the solubilisation buffer (10 mM Tris-HCl, pH 7.4, 150 mM NaCl, 1% NP-40, 0.1% SDS, 0.5% sodium deoxycholate, 1 mM EDTA, 1 mM EGTA, 5 μg/ml, leupeptin, 1 μg/mL pepstatin, 1 mM PMSF, and 1 μg/ml aprotinin), incubated on ice for 0.5 hr, and sonicated (3 times for 10 sec bursts). The solubilised membrane fraction was then centrifuged at 100,000 x g for 0.5 hr at 4°C and, the resulting supernatant retained. Aliquots of both cytosolic and membrane fractions (100 μg) were treated with 20U N-glycosidase F and 0.1% SDS (v/v) for 3 hr at 37°C. Deglycosylated lysates were mixed with an equal volume of 2X Laemmli-Urea sample buffer (Laemmli sample buffer supplemented with 8M Urea (Laemmli, 1970), denatured at 65°C for 15 min and then used for further Western blot analysis

6.1.2.3 (Co)-Immunoprecipitation studies

Following PMA treatment, BAEC grown in 100 mm plates were lysed in 1 mL of RIPA buffer (50 mM Tris pH 7.4, 150 mM NaCl, 1% NP-40, 0.5% sodium deoxycholate, 5 μg/ml, leupeptin, 1 μg/mL pepstatin, 1 mM PMSF, and 1 μg/ml aprotinin). The lysate was passed through a 21-g syringe several times and clarified by brief centrifugation at 1000 x g for 5 min at 4°C. For immunoprecipitation, total lysates resulting from 100 mm plates were incubated with (where appropriate), 5 μg/ mL of either mouse anti-FLAG antibody (Sigma), mouse anti-caveolin (Transduction Laboratories), rabbit anti-FLAG (Sigma), rabbit anti-caveolin (Transduction Laboratories) or a polyclonal rabbit anti-CAT-1 ('home-made') at 4°C for 1 hr, followed by

overnight incubation at 4°C with 50 µL of pre-cleared protein A agarose. The immunoprecipitation step was followed by six sequential washes in high salt and low salt wash buffers recommended by the manufacturer of protein A agarose (Roche Diagnostics). The resulting bead pellet was resuspended in a total volume of 100 µL of modified RIPA buffer containing 0.1% w/v SDS and 5U of Glycosidase F. N-linked glycosidase digestion was performed by incubating this mixture for 1 hr at 37°C. Following digestion, beads were pelleted by centrifugation at 15 000 x g for 10 sec. The bead pellet was resuspended in 100 µL 2X Laemmli-Urea denaturing buffer (Section 6.1.2.2) and heated to 65°C for 15 min. Immunoprecipitates (30 µL per sample) were resolved alongside Benchmark pre-stained markers (Gibco) on either 12% (caveolin detection) or 10% (CAT-1 detection) SDS-PAGE and transferred to PVDF membranes according to standard methods (Chapter 2.5.2 and 2.5.3). Immunodetection was performed as described in 6.1.2.4.

6.1.2.4 Western blot analysis

For time-dependent analysis lysate containing either 40 µg of total protein for eNOS or 20 µg of total protein for caveolin expression was resolved by SDS-PAGE (7.5 or 12% acrylamide respectively) and transferred to PVDF for 1.5 hours at 100V according to standard methods (Chapter 2.5.2 and 2.5.3). All blots were pre-blocked in Tris-HCl, pH 7.5, buffered saline containing 0.1% Tween-20 (TBS-T) and 5% non-fat powdered milk. After 2 hr blocking at RT blots were then incubated with the appropriate primary antibody at 4°C overnight in fresh TBS-T + 5% milk solution. Primary antibodies used in this study were: purified polyclonal CAT-1 antibody (1:500 dilution, Chapter 2.5.1), monoclonal (1:1000 dilution) and polyclonal (1:2500 dilution) anti-FLAG anitbody (SIGMA), polyclonal anti-eNOS antibody (1:1000 dilution) and monoclonal anti-caveolin antibody (1:2500 dilution) (BD Transduction Laboratories). Blots were then incubated with the relevant secondary antibody coupled with horseradish peroxidase in TBS-T + 1% milk solution. Development of signal was achieved using Western blot enhanced chemiluminescence detection reagents (Amersham Biosciences, Inc.), X-OMAT film (Kodak) and a developer (Kodak).

6.1.2.5 NOS catalytic activity

Confluent BAEC monolayers in 6-well plates were exposed to vehicle (0.1% DMSO) or 100 nM PMA for either 0.5 and 24 hr. After treatment, NOS catalytic activity in BAEC cellular homogenates was quantitated as previously described by measuring the conversion of L-[^{3}H]Arg to L-[^{3}H]citrulline in 100 μg of cellular homogenates using additional eNOS co-factors (Chapter 2.4).

6.1.2.6 Statistical analysis

All data were analysed using SPSS for Windows (SPSS Inc. Chicago, Illinois, USA). Unless otherwise stated, results are presented as mean ± SEM and statistical significance was achieved when $P<0.05$.

6.1.3 Results

6.1.3.1 PKC does not affect plasma membrane localisation of CAT-1

Confocal imaging studies were performed in order to investigate whether inhibition of L-Arg transport activity in response to direct activation of PKC by PMA (100 nM for 0.5 hr; Chapter 5, Figure 5.4) occurs due to changes in the localisation of CAT-1 at the plasma membrane. Following treatment with PMA or vehicle (0.1% DMSO), CAT-1 antibody (Chapter 2.5.1) was used to detect the expression of endogenous CAT-1 protein in non-pemeabilised fixed cells. CAT-1 expression at the plasma membrane in both PMA-treated and untreated cells was measurable as the fluorescence intensity of AlexaFluor® 488 secondary antibody marker in planar XY confocal cell sections. As quantified, PKC activation in response to PMA exposure for 0.5 hr was not accompanied by significant alterations in the expression of CAT-1 at the cell surface (Figure 6.1). Similarly, subfractionation of BAEC after PMA exposure for 0.5 hr into cytosolic and membrane fractions did not reveal any alterations in the levels of expression or the membrane association of CAT-1 protein (Figure 6.2). Similar results were obtained using both confocal and subcellular fractionation

methodologies after longer-term PMA exposure (24 hr) to deplete PKC. Furthermore, no visible changes in BAEC morphology detected by transmitted light microscopy were evident after exposure to PMA for either 0.5 hr (Figure 6.1, compare panel A untreated with panel B treated) or 24 hr (results not shown).

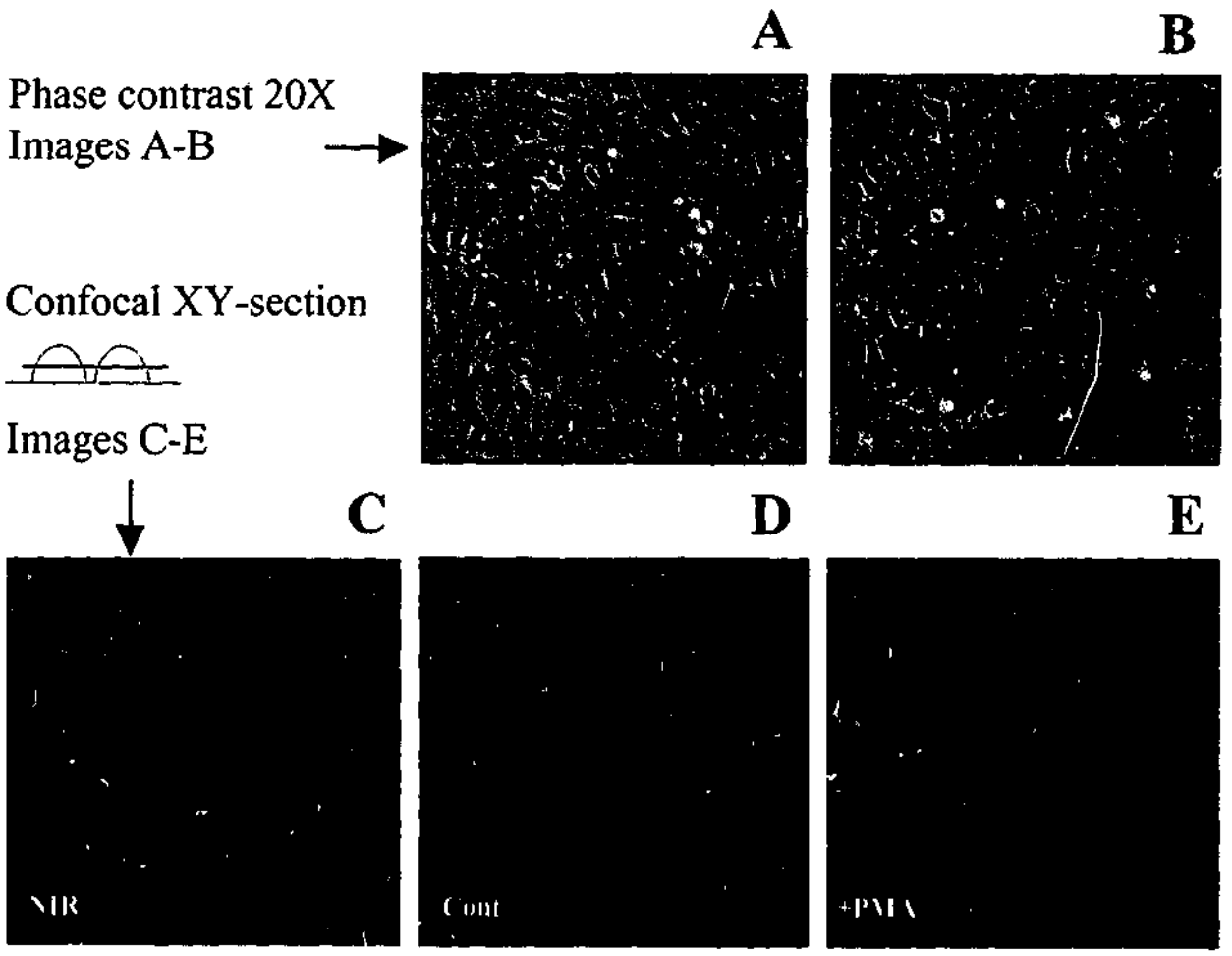

Figure 6.1 Activation of PKC does not affect CAT-1 plasma membrane localisation. Confocal images of BAEC stained with Alexa Flour 488 anti-CAT-1 (panels **D** and **E**) before (panel **D**) or after (panel **E**) treatment with 100 nM PMA for 0.5 hr. BAEC incubated with purified non-immune rabbit serum antibody (NIR) and detected with AlexaFlour 488 were used as a negative control (panel **C**). Images are XY planar sections through the approximated mid-point of cells. Panel **A** and **B** represent transmitted light images of untreated (0.1% DMSO vehicle, **A**) and treated (100nM PMA for 0.5 hr, **B**) BAEC. The scale bar length shown in the bottom right corner of panels D and E is 50 μM.

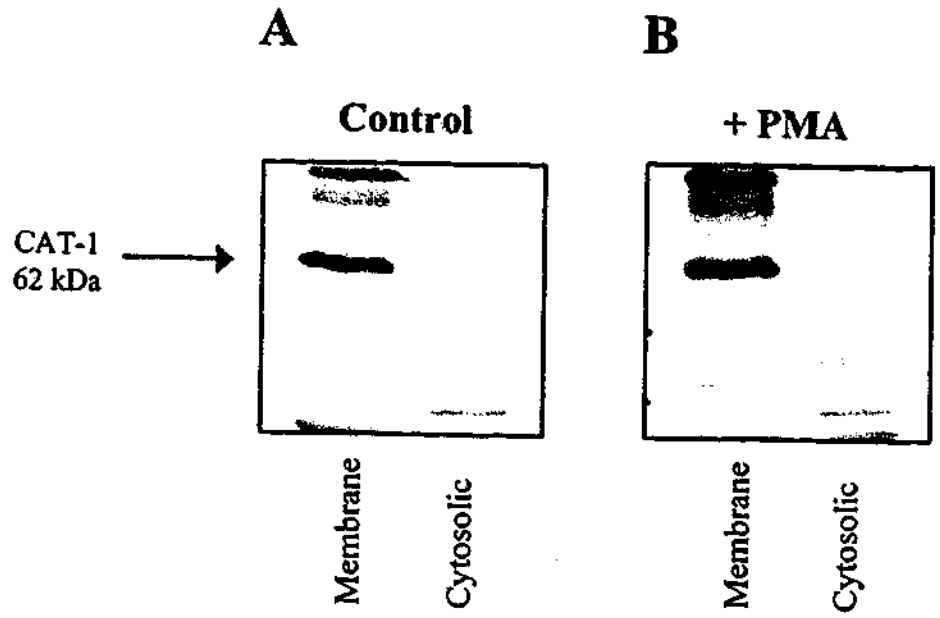

Figure 6.2 Subcellular fractionation of PMA-treated (B, 100 nM for 0.5 hr) and untreated (A) BAEC into membrane and cytosolic fractions. Deglycosylated membrane and cytosolic fractions were analysed on a 10 % SDS-PAGE and detected by Western blot using a specific CAT-1 antibody. Identical results were obtained after longer-term incubation with PMA for 24 hr. Results are representative of three separate experiments (n=3).

6.1.3.2 Effect of PKC on caveolin expression in BAEC.

The effects of PMA treatment (100 nM) time on the abundance of caveolin protein in the cell were measured in BAEC lysates by Western blot analysis (Figure 6.3, panel A) using a commercially available antibody. In confirmation with previous reports, basal expression of caveolin was detected in BAEC (Feron *et al.*, 1999). Expression of caveolin in this cell type was not found to vary significantly from baseline up to 12 hr after PMA treatment. However, a significant decrease in caveolin protein levels to 43±4.2% ($P<0.05$) of basal levels (Figure 6.3, panel B) was clearly evident after 24 hr of PMA exposure. In order to confirm equal loading, membranes used for the detection of caveolin were subsequently stripped and reprobed with an antibody directed against β–tubulin (Figure 6.3, top of panel A). A downregulation of total cellular caveolin protein expression has been previously demonstrated in proliferating cells (Galbiati *et al.*, 2001, Galbiati *et al.*, 1998). Since PMA is a known tumor promoting agent and can induce cellular proliferation

(Pintus *et al.*, 1998), a possible effect of this agent on endothelial growth was determined within a 24 hr time period of cell exposure by measuring total cellular protein content (Lowry assay). In the present study no significant increases in cell growth were detected up to 24 hr after PMA (100 nM) exposure.

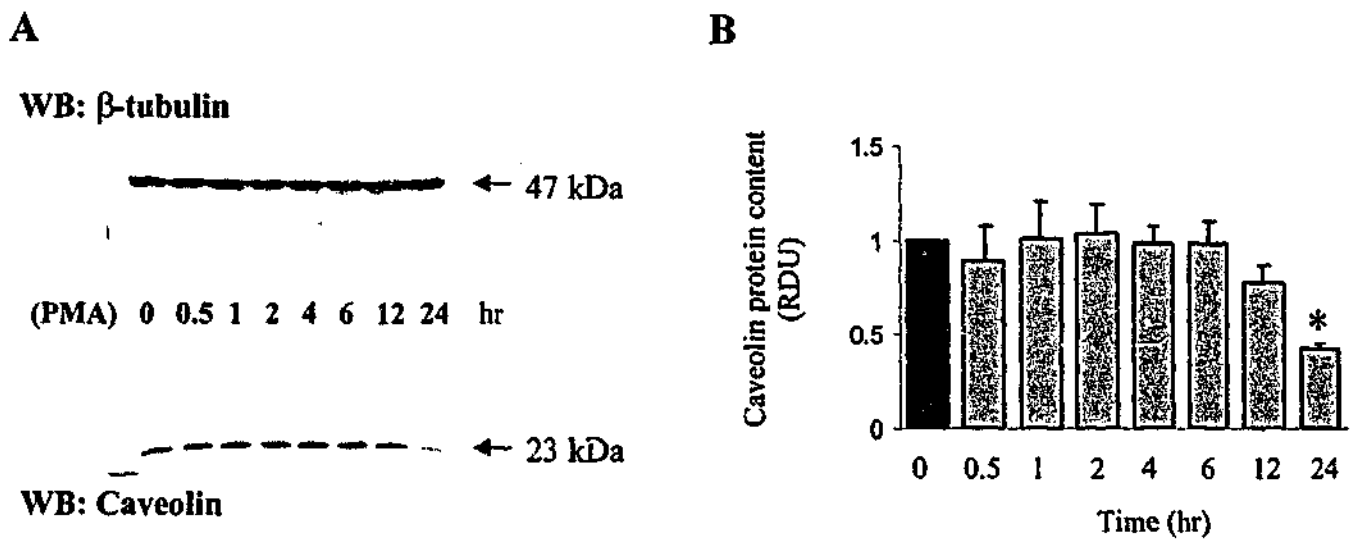

Figure 6.3 Effect of PMA treatment time on the expression of caveolin protein. BAEC were treated with 100 nM of PMA for various lengths of time indicated. Western blot analysis of BAEC lysates was performed using caveolin antibody (bottom, panel A). Signals were normalise by stripping the membrane and re-probing using β-tubulin antibody (top, panel A). A graphical depiction of caveolin protein abundance standardised according to β-tubulin levels and expressed as relative density units (RDU). Data represent the mean ± SEM of three independent experiments (n=3).

6.1.3.3 Effect of PKC on NOS expression in BAEC

Total NOS expression was also measured in BAEC by Western blotting over a 24 hr time course of 100 nM PMA exposure. Acute stimulation of PKC (PMA, 0.5 hr) with PMA did not alter the total expression of NOS (Figure 6.4). However, longer-term PMA treatment (24 hr) leading to PKC downregulation in this cell type led to a significantly increased NOS expression (Figure 6.4; 150% of basal expression, $P<0.05$). Induction of eNOS expression after PMA exposure relates temporally to the previously reported time course of PKC downregulation in BAEC in response to PMA (6-24

hr). The Ca^{2+}-independent NOS isoform, iNOS, was not detectable in BAEC by Western blot studies performed using an iNOS-specific antibody (BD Laboratories) over a 24 hr exposure period to PMA (results not shown).

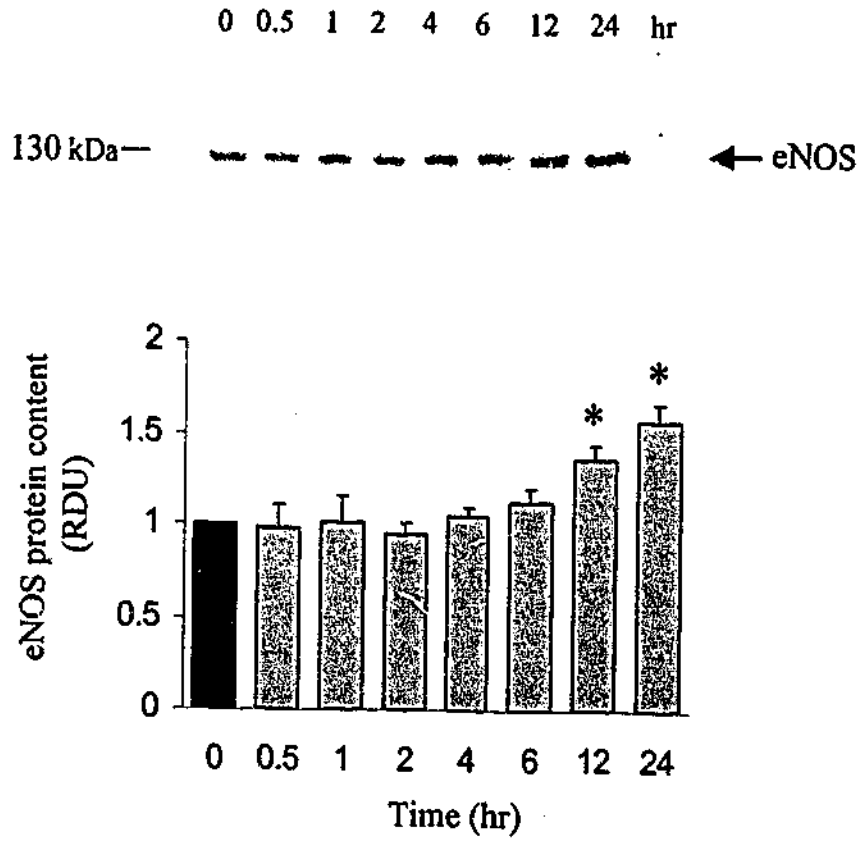

Figure 6.4 Effect of PMA treatment time on the expression of eNOS protein. BAEC were treated with 100 nM of PMA for various lengths of time indicated. Western blot analysis of BAEC lysates was performed using an anti-eNOS antibody (top panel). The bottom panel depicts the level of eNOS expression standardised according to β-tubulin levels and is expressed as relative density units (RDU). Data represent the mean ± SEM of three independent experiments (n=3).

6.1.3.4 Effects of PKC on NOS activity in BAEC

The effect of PMA exposure on the basal activity of eNOS was also determined in the present study. As shown in Figure 6.5, NOS activity from PKC-activated cells (PMA 0.5 hr) was not found to be significantly different from time-matched control (vehicle, 0.1%DMSO). By contrast, a significantly increased NOS activity (140 ± 9 %, $P<0.05$) was apparent in PKC-downregulated cells (PMA, 24 hr) compared with the time-matched control (Figure 6.5). More than 97% of NOS activity detected in the absence or presence of PMA (0.5 hr and 24 hr exposure) in BAEC was

found to be dependent on the presence of Ca^{2+} indicating a predominance of the eNOS isoform in BAEC (results not shown). These results demonstrate that activity of eNOS in BAEC is regulated by longer-term treatment with PMA.

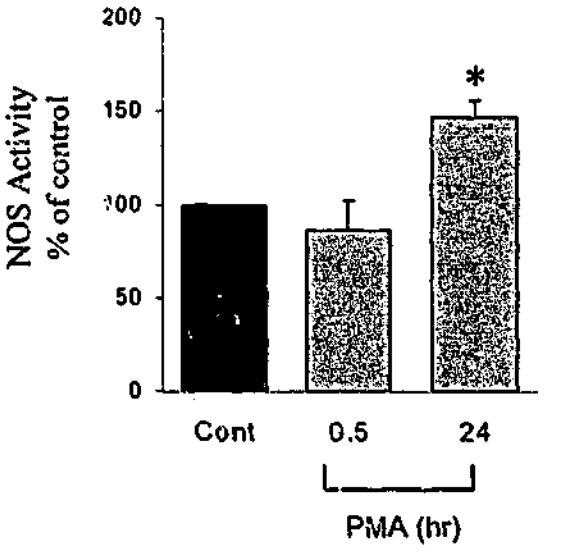

Figure 6.5 NOS activity in BAEC homogenates after PMA treatment. Cell monolayers were treated with either vehicle (0.1% DMSO, Cont) or 100 nM PMA for either 0.5 or 12 hr. After treatment, cells homogenates were prepared and basal NOS activity was measured as described in Methods. Data represent the mean ± SEM of three independent experiments (n=3).

6.1.3.5 Antioxidants do not affect PKC regulation of L-Arg transport.

PMA treatment of endothelial cells has previously been reported to cause an increased generation of reactive oxygen species (ROS), whose formation are linked to increased cell oxidative stress (Chapter 1.4.4.1). In order to investigate the potential effects of ROS on L-Arg transport in response to PMA exposure, cells were pre-treated with two known antioxidants, superoxide dismutase (SOD) and ascorbic acid (AA). At the concentrations previously reported to effectively reduce intracellular markers of oxidative stress, pre-treatment with either 200 U/mL SOD (Galle *et al.*, 1998) or 100 μM AA (May *et al.*, 2003) (Figure 6.8) was not able to prevent the effects of short-term (0.5 hr) or long-term (24 hr) exposure to PMA on L-Arg transport activity. Likewise, a wider dosage range of 0.1 – 5 mM (d'Uscio *et al.*, 2003) for AA and 1 – 200 U/mL for SOD

(Drummond *et al.*, 2000) did not alter PMA effects on L-Arg transport in the present study. NOS itself can generate ROS under conditions of low L-Arg substrate supply (Chapter 1, Section 4.4.1). Therefore, a possible role of PMA-induced NO or ROS production by eNOS in the modulation of L-Arg transport activity was investigated using the pharmacological NOS inhibitor, L-NAME. Cells were pre-treated in the presence and absence of 200 μM L-NAME at a dosage previously reported to block NOS activity in cultured endothelial cells (Huang *et al.*, 2000) and then exposed to 100 nM PMA. As shown (Figure 6.8), NOS inhibition with L-NAME did not prevent the effects of short-term or long-term PMA exposure on L-Arg transport.

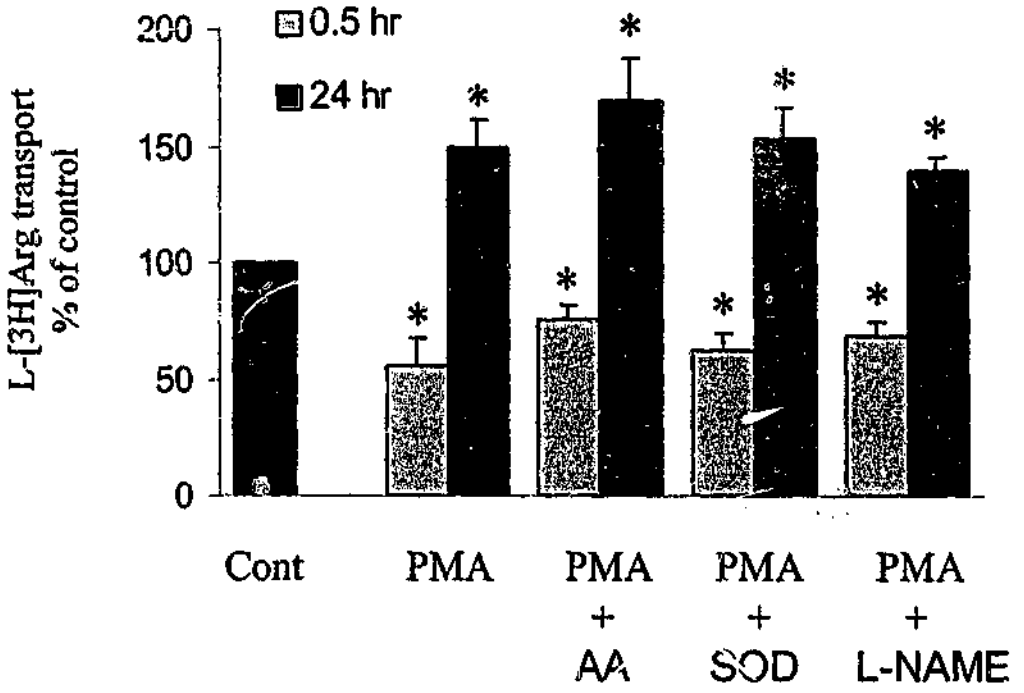

Figure 6.6 Effect of antioxidant treatment on PMA-modulated L-Arg transport. Confluent BAEC monolayers were pretreated with either ascorbic acid (AA), superoxide dismutase (SOD) or L-NAME for 30 min before the addition of 100 nM PMA. Incubation in the presence of antioxidants and/or PMA was continued for either 0.5 (open grey bars) or 24 hr (crossed grey bars). After this time L-Arg transport was measured. Data represent the mean ± SEM of four independent experiments (n=4).

6.1.3.6 Caveolin associates with CAT-1 under basal conditions in BAEC.

An interaction between caveolin and overexpressed CAT-1-gfp fusion protein has previously been demonstrated in hamster kidney cells (BHK) (Lu *et al.*, 2000). Further, eNOS and CAT-1 are also known to interact in pulmonary endothelial cells (McDonald et al., 1997). The aim of the present study was to initially establish whether CAT-1 associates with caveolin and/or eNOS in primary BAEC by performing co-immunoprecipitation analysis. An interaction between caveolin and endogenous CAT-1 was detected in BAEC since caveolin antibody co-immunoprecipitated CAT-1. This immunoprecipitated complex was detected using a home-made CAT-1 antibody (Figure 6.6, left panel). Vice versa, various strategies designed to co-immunoprecipitate caveolin or eNOS using the CAT-1 antibody were unsuccessful. Whilst CAT-1 antibodies have proven useful for Western blot studies in the literature they have generally showed poor performance in immunoprecipitation studies (Closs, 1996). In order to validate the current methodology used to show an association between caveolin and CAT-1 in BAEC, CAT-1 containing a single C-terminal FLAG epitope (Chapter 6.2.2.1) was expressed in BAEC. This allowed the use of an alternate commercially available FLAG antibody for immunoprecipitation of CAT-1. As shown, FLAG antibody immunoprecipitated FLAG-tagged CAT-1 and also co-immunoprecipitated caveolin (Figure 6.6, right panel). Expression of FLAG-tagged CAT-1 in this way provided further confirmation of a caveolin:CAT-1 association in BAEC. Evidence of an interaction between CAT-1 and eNOS was not detected using either the current methodology or that described by McDonald *et al.* (McDonald et al., 1997).

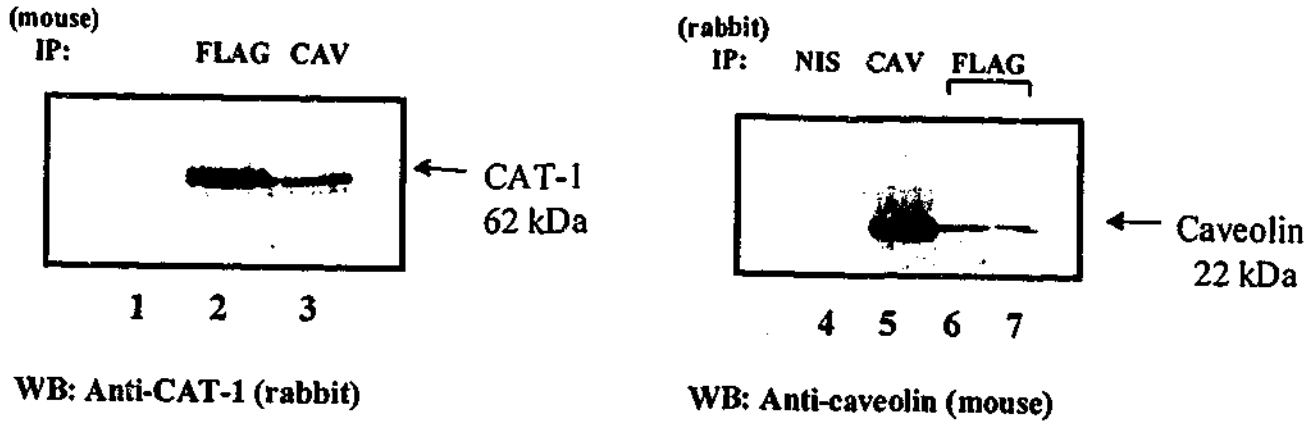

Figure 6.7 Interaction of caveolin with CAT-1 in BAEC under basal conditions. Untreated BAEC lysates were prepared in immunoprecipitation buffer as described in Methods. Lysates were immunoprecipitated (IP) with either anti-mouse (left panel) or anti-rabbit (right panel) non-immune serum (NIS), anti-FLAG, anti-caveolin (CAV) antibodies (Ab's) as indicated and then detected by Western blot (WB) with either anti-rabbit CAT-1 (left) or anti-mouse caveolin (right) Ab's. Please note that FLAG antibody was only used for IP in BAEC expressing the CAT1-FLAG fusion protein.

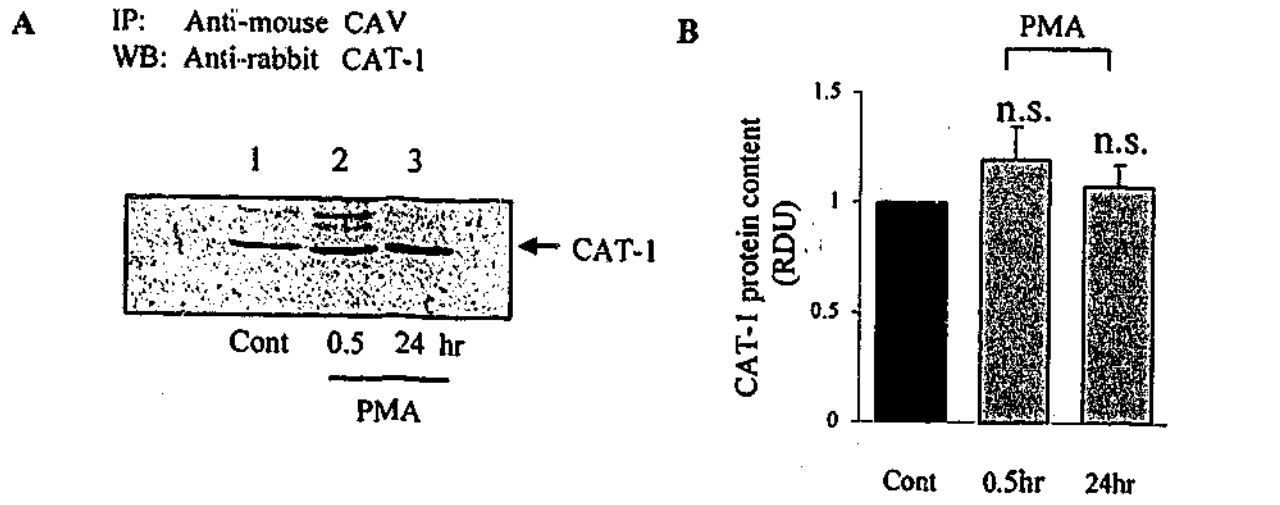

Figure 6.8 Association of CAT-1 with caveolin in response to PMA treatment in BAEC. A, PMA-treated (0.5 hr exposure lane 2 and 24 hr exposure lane 3) or –untreated (Lane 1) BAEC were prepared in immunoprecipitation buffer as described in Methods. All lysates were immunoprecipitated with anti-mouse caveolin (CAV) antibody and then detected with anti-rabbit CAT-1 antibody by Western blot. **B,** Amount of CAT-1 associated with caveolin after PMA exposure. Data from panel **A** expressed as relative density units (RDU), representing the total amount of CAT-1 protein co-immunoprecipitating with caveolin in BAEC. Three independent experiments were performed in order to verify the status of CAT-1 association with caveolin (n=3). n.s. means not significant.

6.1.3.7 PKC does not affect CAT-1 association with caveolin.

Having demonstrated an association between caveolin and CAT-1 in BAEC, the potential role of caveolin as a modulator of CAT-1 activity in response to PMA treatment was explored. The status of endogenous CAT-1 association with caveolin was assessed in BAEC after PMA treatment as outlined in the previous section (6.1.3.6). Briefly, cells were treated for either 0.5 hr with 100 nM PMA (100 nM) to assess either the effect of PKC activation or alternatively for 24 hr to examine the effect of PKC down-regulation. As shown in Figure 6.7 (panel A and B), association of CAT-1 with caveolin was not significantly altered in response to either PKC activation or downregulation.

6.1.4 Discussion

6.1.4.1 Membrane localisation of CAT-1 is not affected by PMA in BAEC

As a potential mechanism for the regulation of L-Arg transport by PKC in BAEC, localisation of CAT-1 at the plasma membrane was examined following PMA treatment. Using a specific CAT-1 antibody to detect cell surface expression of the transporter by confocal microscopy, no evidence of PMA-induced alterations in cell surface localisation of CAT-1 were detectable. Likewise separation of cellular proteins into membrane and cytosolic fractions following PMA treatment did not reveal any changes in the localisation of the CAT-1 at the membrane. Therefore, the present data indicates that PKC does not regulate CAT-1 activity via a membrane trafficking mechanism.

CAT-1 is distributed in distinct clusters on the plasma membrane of endothelial cells suggesting a more specialised plasma membrane localisation (Woodard *et al.*, 1994). Further imaging studies have suggested that CAT-1 is localised in Triton X-100 insoluble caveolar compartments since most of the CAT-1 detectable on the plasma membrane co-localises in clusters with caveolin (McDonald et al., 1997), possibly through direct association (Lu and Silver, 2000). Co-immunprecipitation data from the present study has confirmed the existence of a direct association of CAT-1 with caveolin in endothelial cells. The functional nature of a direct CAT-1:caveolin interaction is not yet known. In addition to the plasma membrane, CAT-1 and caveolin are both

known to localise within the Golgi-apparatus (Masuda *et al.*, 1999, Lu and Silver, 2000, Dupree *et al.*, 1993). This location is thought to be required for the post-translational glycosylation and processing of CAT1 before its insertion at the plasma membrane and also for the recycling of caveolin-enriched caveolar vesicles via the *trans*-Golgi network. Therefore it is possible that caveolin may assist in cell surface expression of the transporter within the caveolae and/or act as a docking protein for CAT-1, placing it in the vicinity of caveolar eNOS.

Caveolin is also known to play a more active role by inhibiting the activity of proteins through direct interaction such as that shown for PKC-α (Oka *et al.*, 1997), epidermal growth factor receptor (Wang *et al.*, 2002), G protein-coupled receptor kinases (Carman *et al.*, 1999) and eNOS (Chapter 1.3.2.2). Furthermore, PMA treatment is known to evoke changes in the association of caveolin with interacting proteins (Kim *et al.*, 1999). As a potential mechanism by which PKC may regulate L-Arg transport, the status of CAT1:caveolin association in BAEC was investigated following PMA treatment. Results of the present study (Figure 6.7) did not reveal changes in the association of caveolin with CAT-1 after PKC activation (PMA, 0.5 hr) or PKC downregulation (PMA, 24 hr). This clearly shows that caveolin does not mediate the effects of PMA on CAT-1 activity by either association or dissociation. Based on their recent work Kizhatil *et al.* (Kizhatil *et al.*, 2002) have suggested that plasma membrane localisation of CAT-1 in the caveolae may be inconsequential for its ability to transport L-Arg since human embryonic kidney cells were shown to exhibit a completely different cell surface distribution pattern of CAT-1 than endothelial cells.

Although immunofluorescence results from the present study show that there are no significant changes in the relative amount of CAT-1 at the plasma membrane after PKC activation these results do not exclude the possibility that PMA may cause the redistribution of CAT-1 away from the caveolae to another location at the plasma membrane. Redistribution of ion transporters at the plasma membrane such as Na+/K+-ATPase for example been reported in response to other stimuli such as ischemia by measuring changes in Triton X-100 solubility of the protein (Molitoris *et al.*,

1992). Since neither changes in caveolin localisation or CAT-1 Triton X-100 solubility were examined following PMA treatment no further conclusions can be made about the effects of PKC activation on CAT-1 caveolar localisation at this time. In addition, since a CAT1:caveolin association was measured in total cell lysates the present results may not exclude the possibility of PMA-induced changes CAT-1:caveolin association occurring exclusively within the caveolae. Investigation of this association using isolated caveolar fractions should help to clarify this further.

6.1.4.2 PMA modulation of caveolin and NOS expression in BAEC

PKC activation by PMA did not lead to changes in the expression or catalytic activity of NOS, or the expression of caveolin (Figure 6.3, 6.4 and 6.5). Taken together with major findings of Chapter 5, these results demonstrate that a decrease in L-Arg transport via PKC-induced inhibition of CAT-1 activity has no effect on the catalytic activity of NOS in endothelial cells. By contrast, downregulation of PKC activity by long-term PMA treatment resulted in a significantly elevated NOS expression and activity and, a significant decrease in caveolin expression. Increased L-Arg transport activity due to PKC downregulation might function to sustain the requirement for increased NO production in BAEC. These results may suggest a coordinated mechanism for removing the inhibitory effect of caveolin on NOS activity and increasing NOS substrate supply. Although measures of NOS catalytic activity are widely used as an indicator of NO production, a potential caveat in the interpretation of the present findings is that increased NOS activity can also be the source of increased superoxide production by alternate utilisation of molecular oxygen (Chapter 1). In this regard, production of ROS in response to PMA within the endothelium has previously been reported (Holland *et al.*, 2000). The effect of PMA-induced ROS on CAT-1 activity was explored in the present study by exposing cells to either antioxidants (ascorbic acid and superoxide dismutase) or the NOS inhibitor L-NAME in the presence of PMA (Figure 6.6). Since neither of these treatments prevented the effects of PMA on L-Arg transport activity I have concluded that ROS does not contribute to PKC-mediated inhibition of CAT-1 activity or longer-term effects of PMA treatment on CAT-1 activation.

6.2 *Effect of PKC on CAT-1 Phosphorylation Status in BAEC*

6.2.1 Introduction

Nitric oxide signalling, cellular proliferation and differentiation pathways are known to be regulated by PKC isotypes in various cell types (Siflinger-Birnboim and Johnson, 2003). Since L-Arg transport activity is also an essential component in these pathways (Chapter 1.5.1) it is conceivable that CAT-1 may also be subject to more direct regulation by PKC. In chapter 5, the phorbol ester phorbol 12-myristate 13-acetate (PMA), was shown to have a bi-phasic effect L-Arg transport activity by acutely (0.5- 4hr) decreasing and chronically (12-24hr) increasing transport. The acute effect of PMA has been attributed to an increase in direct phosphorylation and a corresponding decrease in the catalytic rate of transporter activity by activated protein kinase C (PKC) (Graf et al., 2001). However, there is no direct evidence that CAT-1 can be phosphorylated by PKC. Moreover, it is also not known whether the putative serine PKC phosphorylation sites can be modified by PKC. The major aim of the present study was to determine whether activated PKC could induce phosphorylation of CAT-1 as a mechanism for modulation of L-Arg transport activity. Subsequently, a major finding of this study has demonstrated the basal phosphorylation of CAT-1. As mentioned in the previous section, CAT-1 antibody raised for the purposes of this thesis work was not suitable in immunoprecipitation studies. To elucidate whether PKC can directly phosphorylate CAT-1 *in vivo*, FLAG-tagged CAT-1 (CAT1-FLAG) was expressed in BAEC and the PMA-induced incorporation of ^{32}P into immunoprecipitated CAT1-FLAG was examined.

Current CAT-1 modeling supports a 14 transmembrane topology that localises potential phosphophorlyation sites to five putative serine phosphorylation sites, two extracellularly (serine residues 4, 183) and three intracellularly (serine residues 469, 475 and 550). The three putative intracellular serine PKC phosphorylation sites are located in the fifth and sixth intracellular loops

according to the 14 transmembrane model by Albritton *et al.* (Albritton *et al.*, 1989). To identify what role putative PKC sites have in CAT-1 mediated L-Arg transport activity, the second part of this study reports on initial work performed with CAT mutants carrying alanine replacements at serine PKC sites intracellularly.

6.2.2 Methods

6.2.2.1 Plasmids

The mammalian expression vector pcDNA3 is from Invitrogen. A murine full length CAT-1 cDNA clone containing 3'untranslated regions (UTR) and 5'UTR sequence, inserted into pBluescriptII SK+/- at the *Eco*RI and *Bam*HI sites was generously provided by Dr. Daniel Markovich with permission of Dr. Donald Kakuda of the University of Queensland, Brisbane, Australia (Kakuda *et al.*, 1999). A C-terminally FLAG tagged full length CAT1 cDNA (62 kDa protein) was generated from this construct as follows. Full-length CAT1 cDNA was excised from pBluescript at the *Eco*RI and *Bam*HI sites and then subcloned into pcDNA3 (Invitrogen) at complementary restriction endonuclease sites. This plasmid is identified in the text as pcCAT-1. A single FLAG epitope sequence was incorporated upstream of the CAT-1 3' stop codon by polymerase chain reaction (PCR)-based mutagenesis methodology (Ausubel *et al.*, 1990) using the high-fidelity *pfu* polymerase (Promega Inc.) and, synthesised oligonucleotides (Genset Oligos) 5'-TCG TCC TTG TAG TCT TTG CAC TGG TCC AAG TTG-3' and 5' phosphate-CGA TGA CAA GTG ACT CGA GCA TGC ATC TAG AGG-3'. The resulting plasmid served as a template for amplifying the open reading frame including the newly incorporated FLAG epitope by PCR using synthesised oligonucleotides and *pfu* polymerase. The first oligonucleotide, 5'-GGT ACC GGA TCC ATG GGC TGC AAA AAC CTG CTC – 3' created unique *Kpn*I and *Bam*HI sites (underlined) upstream of the 5'ATG (underlined) start codon. The second nucleotide, 5'-TCT AGA CTC GAG TCA TTT GCA CTG GTC CAA GTT G-3' created unique *Xba*I and *Xho*I sites flanking the 3' FLAG stop codon. A *Bam*HI-*Xho*I fragment containing the CAT-1 protein coding region and a 3' terminus

FLAG epitope sequence was prepared from the 1.8 kb PCR product and then cloned in pcDNA3 using T4 DNA ligase according to standard methods (Ausubel et al., 1990). The resulting plasmid is identified in the text as CAT1-FLAG. All substitutions and additions were in-frame and confirmed by DNA sequencing.

6.2.2.2 Generation of CAT-1 mutants

The 3' terminus FLAG-tagged CAT-1 plasmid, CAT1-FLAG (see Section 6.2.2.1 for a description of this plasmid), was used as a template for replacement of the three putative PKC intracellular serine phosphorylation sites with alanine residues. Site-directed mutagenesis methodology (Appendix A) was used (Ausubel et al., 1990) to generate the following CAT-1 serine to alanine mutants:

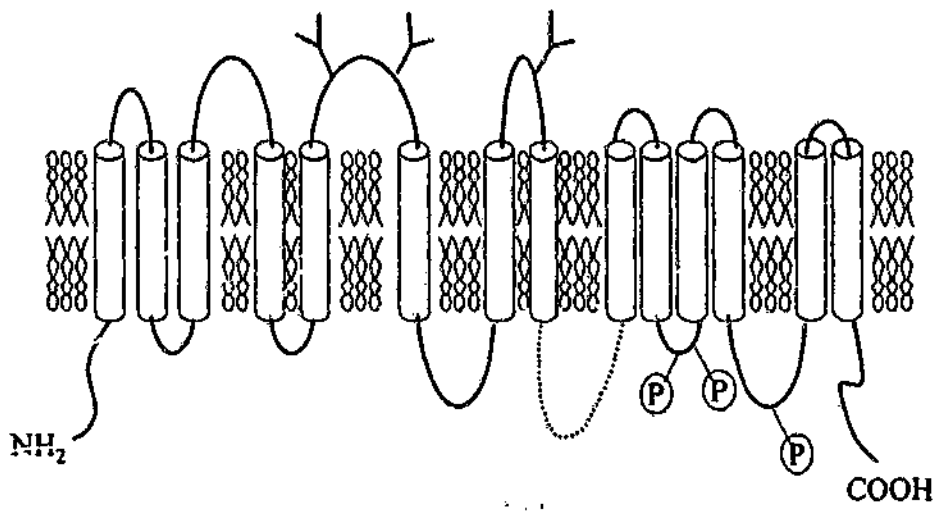

PKC Site #		Amino Acid Position (PubMed Accession # NP_031539)
Single mutant	1	469A
	2	475A
	3	550A
Double mutant	1,2	469A/475A
	2,3	475A/550A
	1,3	469A/550A
Triple mutant	123	469A/475A/550A

Figure 6. 9 Serine to alanine substitutions at intracellular PKC phosphorylation sites on CAT-1. Top panel depicts the proposed 14 transmembrane model for CAT-1 and its three putative intracellular PKC sites on the fifth and sixth loops. Bottom panel details the various CAT-1 PKC mutants produced.

6.2.2.3 Transfection of BAEC

Low passage primary BAEC, between split 1-6, were maintained in Dulbecco's modified Eagle's medium (DMEM) supplemented with 10% bovine calf serum and 100 U/mL penicillin/streptomycin at 37°C and 5% CO_2. Cells were transfected with LipofectAMINE 2000 (Invitrogen) using the manufacturers protocol. For metabolic labelling experiments, 1 x 10^6 cells plated the previous day in 100 mm Petri dishes, were incubated for 5 hours with a plasmid DNA (11.2 μg) –LipofectAMINE 2000 (56 μL) mixture in 14 mL of OptiMem (Gibco BRL) at 37°C in 5% CO_2. L-Arg transport studies were performed using 6 well plates (Falcon). Briefly, 4 x 10^5 cells per well that had been plated the previous day were incubated for 5 hr with the appropriate plasmid DNA (2 μg)-LipofectAMINE 2000 (10 μL) mixture in 2.5 mL of OptiMem. Where different sized tissue culture plates were used, transfection reagent volumes and DNA concentrations were scaled down accordingly with respect to surface area of the tissue culture well. Unless otherwise stated, the concentration of DNA and LipofectAMINE was adhered to for transfection and has been optimised for maximal transfection efficiency and minimum toxicity to cells. The plasmid pEGFP-N1 (CLONTECH) encoding the red-shifted variant of wild-type green fluorescent protein (GFP) was transfected alongside other plasmid DNA constructs in each independent experiment for evaluation of transfection efficiency. Expression of gfp was detected by inverted fluorescence microscopy with an excitation maximum of 488 nm and emission maximum at 507 nm. In comparison to cell lines, the transfection efficiency of primary endothelial cell types is known to be very low using standard lipid complex and electroporation methodologies. Of the cationic lipids tested, Lipofectamine 2000-based transfection was found to result in the highest efficiency and lowest cell toxicity to in BAEC. Between 10-30% of the total cell population were found to express proteins encoded by introduced plasmid DNA as detected visually by the expression of GFP in pEGFP-N1 transfected wells.

6.2.2.4 Metabolic labelling of BAEC

BAEC (S_1-S_6) were seeded in 6 well plates at a density of 4 x 10^5 cells/well or 100 mm plates (10^6 cells/plate) as indicated in Results. At ~95% confluency, cells were transfected with either pcDNA3 empty vector or FLAG-tagged wild type CAT1 cDNA using Lipofectamine 2000 according to the methods described (see Section 6.2.2.4). After transfection, the DNA mixture was replaced with DMEM + 10% FBS growth medium and cells were then left to recover for 48 hr. Prior to metabolic labelling, cell monolayers were washed twice using warm phosphate-free DMEM (P_i-free DMEM). Medium was replaced with P_i -free DMEM and incubated with either i) 200 μCi [^{32}P] orthophosphate (PerkinElmer Life Sciences) in a total volume of 1 mL per well for 6 well plates or ii) 1.0 mCi [^{32}P] orthophosphate in a total volume of 5 mL for 100 mm plates, for 4 hr at 37 °C to achieve steady-state labelling (Lawrence *et al.*, 1990). Metabolic labelling was performed in the presence and absence of either PMA, Bim I, okadaic acid or vehicle (0.1% DMSO) as indicated.

6.2.2.5 Immunoprecipitation of CAT-1 and Western blot analysis

Experimental conditions associated with metabolic labelling were stopped by transferring the plate to a pre-cooled ice pad and performing two washes using Hanks balanced salt solution (HBSS; SIGMA) in order to remove excess [^{32}P] orthophosphate and cell treatments. After the last traces of HBSS were removed cells were lysed with 750 μL of cold modified RIPA lysis buffer per well (50 mM Tris pH 7.4, 150 mM NaCl, 1% NP-40, 0.5% sodium deoxycholate, 5 μg/ml, leupeptin, 1 μg/mL pepstatin, 1 mM PMSF, and 1 μg/ml aprotinin). The cell plate was then transferred to a cold room (4°C) and incubated on a rocking platform for 1 hr. After this time, cell lysates were transferred to O-ring sealed tubes and centrifuged at 15000 x g for 15 min at 4°C to remove nuclear material and cellular debris. Clarified cell lysates were transferred to fresh O-ring tubes. An initial pre-clearing step was performed by adding 40 μL of protein A agarose (Roche Diagnostics) to these lysates and incubating on a rocking platform at 4°C overnight. The next day, protein A

agarose was removed by brief centrifugation at 15000 x g for 1 min at 4°C. Cell lysates were then transferred to fresh O-ring tubes containing a 35 µL bed volume of pre-washed (modified RIPA lysis buffer) M2 FLAG affinity beads (SIGMA) and then immunoprecipitated by incubating on a rocking platform for 2 hr at 4°C. The immunoprecipitation step was followed by six sequential washes: twice with modified RIPA lysis buffer, twice with high-salt buffer (50 mM Tris-HCl, pH 7.5, 500 mM NaCl, 0.1% NP-40 and 0.05% sodium deoxycholate) and twice with low salt buffer (50 mM Tris-HCl, pH 7.5, 0.1% NP-40 and 0.05% sodium deoxycholate) by centrifugation at 15 000 g for 30 sec at 4°C. FLAG immunoprecipitates (30 µL per sample) were resolved alongside Benchmark pre-stained markers by 10% SDS-PAGE and transferred onto PVDF membranes according to standard methods (Chapter 2.5.2 and 2.5.3). The membrane was air-dried then subjected to autoradiography using Kodak XAR film (PerkinElmer Life Sciences) and an intensifier screen at -80 °C in a cassette for at least 48 hr. Signals were detected using an X-Ray developer (Kodak). Band densities from scanned autoradiograph images were determined using Optimus software. Alternatively, the [^{32}P] signal was detected and quantified using a phosphoimager screen and a Fuji-Bas 100 Phosphoimager.

Following autoradiography, the membrane was re-used for CAT-1 immunodetection (Chapter 6.1.2.4). Either rabbit anti-FLAG primary antibody (1:5000 dilution; overnight at 4°C) or rabbit anti-CAT-1 primary antibody (1:500 dilution; overnight at 4°C), and a peroxidase-conjugated anti-rabbit (1:2500 dilution) secondary antibody were used for the detection of CAT1-FLAG fusion proteins. The density of the protein band from scanned X-Ray film images was determined using Optimus analysis software. The intensity of the ^{32}P signal resulting from the autoradiograph was normalised with the corresponding CAT-1 protein detected with either of the primary antibodies, rabbit anti-FLAG (SIGMA) or rabbit anti-CAT-1 antibody.

6.2.2.6 L-[^{3}H]Arg transport assay

L-[3H]Arg transport was assessed in BAEC in 6-well plates transiently expressing (Chapter 6, Section 2.2.3) either wildtype CAT-1, CAT-1 mutants or pcDNA3 as previously described in Chapter 5, Section 1.2.1.

6.2.3 Results

6.2.4.1 Activation of L-Arg transport due to overexpression of CAT-1

Prior to the investigation of CAT-1 phosphorylation, the properties of CAT1-FLAG in its uptake activity and sensitivity to PMA were examined and compared with native CAT-1. In CAT1-FLAG transfected BAEC, L-Arg transport activity was significantly increased to 153% of control cells transfected with pcDNA3 alone (Figure 6.10 B). CAT1-FLAG transport of L-[^{3}H]Arg did not significantly differ from that of transfected native CAT-1 (140% of control cells transfected with pcDNA3; Figure 6.10), suggesting that the addition of FLAG did not affect the transport properties of native CAT-1 protein. Of note, the magnitude of reported changes in transport activity after CAT-1 transfection in this cell type was found to relate to the different level of transfection efficiency achieved within each experiment as detected by the expression of GFP transfected cells in separate wells. An average transfection efficiency of 18 ±12 % was observed in BAEC using the protocol outlined in Methods (6.2.2.3). Expression of CAT1-FLAG protein was compared with endogenous CAT-1 protein by Western blot analysis using a commercially available FLAG antibody and a home-made CAT-1 antibody (Chapter 2.5.1). Consistent with CAT-1 properties, treatment with N-glycosidase reduced the size of both endogenous and FLAG tagged CAT-1 signals from a major 80 kDa form to the predicted 62 kDa size of CAT-1, revealing that CAT1-FLAG protein was also expressed in an N-glycosylated form (Figure 6.10 A). Overexpression of CAT-1 protein was also detected after transfection with either pcCAT1 or CAT1-FLAG using CAT-1 antibody (results not shown). Cell surface expression of CAT1-FLAG was confirmed by confocal imaging of fixed cells using an anti-rabbit FLAG antibody and a secondary antibody

coupled to the fluorescent marker, Alexa Fluor® 488 goat anti-rabbit (Section 6.1.2.1). In CAT1-FLAG transfected BAEC, treatment with PMA for 0.5 hr significantly inhibited L-[^{3}H]Arg transport activity from 183% to 98% of empty vector control (Figure 6. 11). PMA treatment is expected to affect both endogenous CAT-1 and CAT1-FLAG transport activity present in transfected BAEC. In accordance, a comparative level of inhibition for CAT-1 transfected cells was observed as in untransfected cells following PMA treatment.

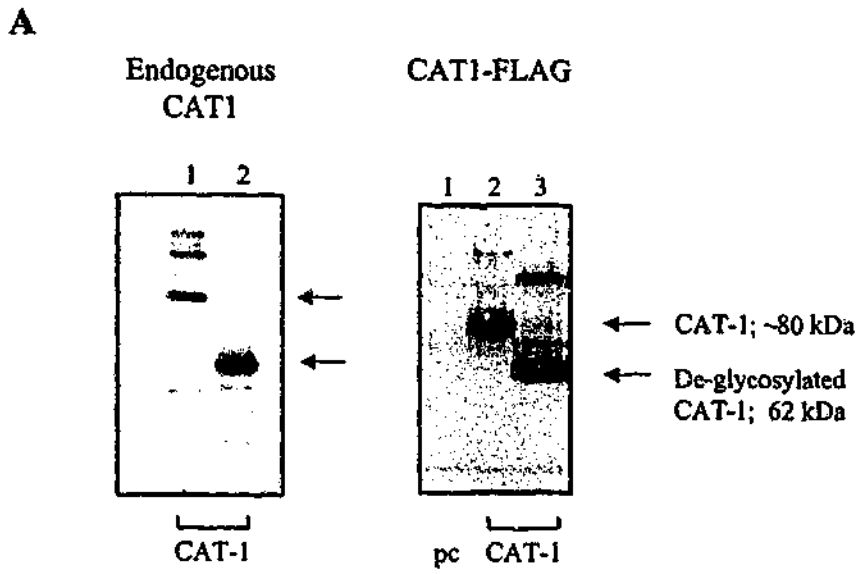

Figure 6.10 L-Arg transport activity and expression of CAT1-FLAG in BAEC. (A) Western blot analysis of transfected CAT1-FLAG cells (Lanes 2 and 3, right panel) and pcDNA3 (Lane 1, right panel) performed using a FLAG antibody that recognises the FLAG epitope at the C-terminus of CAT1-FLAG. This result was compared to the expression of endogenous CAT-1 protein in BAEC (Lane 1 and 2, left panel) using CAT-1 antibody. Both CAT1-FLAG lysates (Lane 3, right panel) and untransfected lysates (Lane 2, left panel) were subjected to N-Glycosidase treatment. **(B)** Untransfected (Un) BAEC or transfected BAEC with either empty vector (pcDNA3), pcCAT-1 or CAT1-FLAG were assessed for L-[^{3}H]Arg transport capacity 48 hr post-transfection. Data are expressed as dpm/ µg protein / min and represent the mean ± SEM of four independent experiments (n=4). * P<0.05 versus pcDNA3.

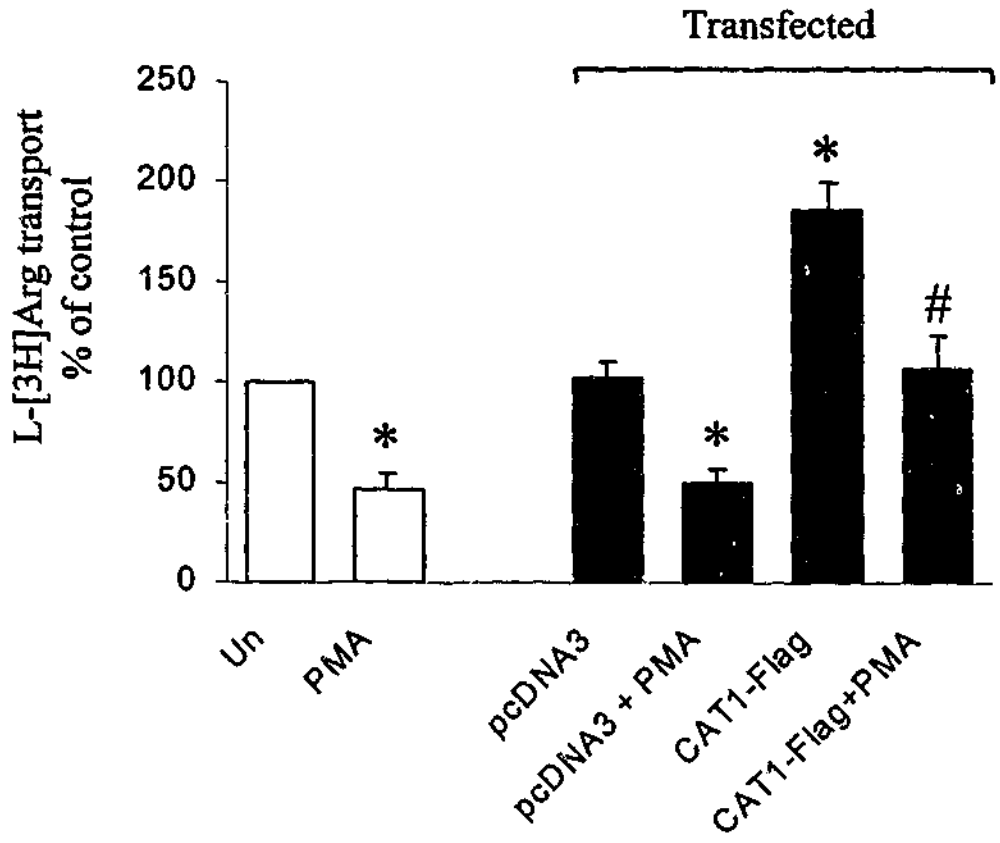

Figure 6.11 Effect of PKC activation on the activity of overexpressed CAT1-FLAG in BAEC. Untransfected BAEC are shown as open dotted bars in the absence (Un) or presence of PMA (PMA). Black bars show BAEC transfected with empty vector (pcDNA3) or CAT1-FLAG. L-[^{3}H]Arg transport was measured after incubation in the presence of absence of 100 nM PMA (0.5 hr) as indicated. Data are expressed % of control and represent the mean ± SEM of four independent experiments (n=4). Untransfected BAEC *P<0.05 versus untreated (Un) cells. Transfected BAEC *P<0.05 versus pcDNA3, # P<0.05 versus CAT1-FLAG.

6.2.4.2 CAT-1 is a phosphoprotein

To elucidate whether PKC can directly phosphorylate CAT-1 *in vivo*, FLAG-tagged CAT-1 was transiently expressed in BAEC. Cells were then metabolically labelled using ^{32}P-orthophosphate. Immunoprecipitated and de-glycosylated CAT1-FLAG was further subjected to SDS-PAGE in order to detect the efficacy of transfection and immunoprecipitation by Western blotting and, the phosphorylation level of CAT1-FLAG. As shown in Figure 6.12, a specific phosphorylation band was observed in immunoprecipitated CAT1-FLAG from untreated cells (left panel) that corresponded to the expected size of deglycosylated CAT-1 protein (62 kDa, right panel) detected using CAT-1 antibody. Phosphorylation of CAT1-FLAG could only be detected after de-glycosylation of immunoprecipitates since FLAG- antibody also precipitated other phosphorylated species in both empty vector and FLAG transfected lysates that interfered with the detection of

higher molecular weight glycosylated forms of CAT-1 (see Figure 6.12 and 6.13, panel A). These results suggest that CAT-1 is basally phosphorylated and is a substrate of kinase activity in CAT-1 transfected BAEC.

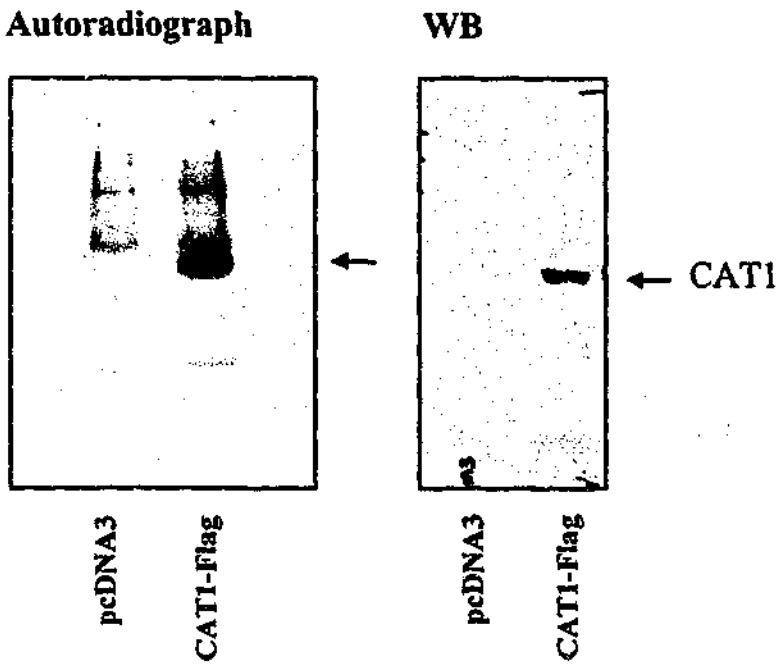

Figure 6.12 Basal phosphorylation of CAT-1. BAEC were transfected with either empty vector (pcDNA3) or CAT1-FLAG. BAEC immunoprecipitates were prepared using FLAG antibody and resolved by 10% SDS-PAGE and transferred to PVDF membranes. Air-dried membranes were exposed to film for 2 weeks in order to detect ^{32}P signal. A representative autoradiograph is shown on the left panel. After exposure to film, the membrane was used for Western blot analysis using CAT-1 antibody (WB, right panel).

6.2.4.3 Effect of PKC activation on CAT-1 phosphorylation status

Activation of PKC with 100 nM PMA for 0.5 hr did not lead to any significant alterations in the basal phosphorylation of CAT-1 (Figure 6.13). Under the same treatment conditions, PMA caused a significant decrease in L-[^{3}H]Arg transport activity in CAT-1 transfected cells (Figure 6.11). Likewise, the PKC inhibitor Bim I, which reversed the inhibitory effects of PMA on L-Arg transport (Chapter 5, Figure 5. 5) did not influence the phosphorylation status of CAT-1 in BAEC either alone or in the presence of PMA (results not shown). These results suggest that CAT-1 is not a direct target of PKC in CAT1-FLAG transfected BAEC.

Phosphorylation-dependent regulation of target proteins is a balance between the actions and of kinases and phosphatases. Okadaic acid, a broad-spectrum protein phosphatase inhibitor (PP1 and PP2A) has previously been reported to prevent protein dephosphorylation (Fleming *et al.*, 2001). Since CAT-1 was found to be basally phosphorylated, the potential role of phosphatases in regulation of L-Arg transport was explored in BAEC. Purified preparations of PP1 and PP2A show half-maximal inhibition by okadaic acid *in vitro* at 10–15 and 0.1 nM, respectively (Cohen, 1989). Treatment with phosphatase inhibitor okadaic acid within a dosage range (0.1 nM – 1000 nM) reported to prevent dephosphorylation of proteins in cultured cells did not affect either basal L-Arg transport or PKC-inhibited L-Arg transport (100 nM PMA, 0.5 hr) in BAEC (results not shown). Similarly, okadaic acid did not affect CAT-1 phosphorylation either basally or following PMA treatment (results not shown).

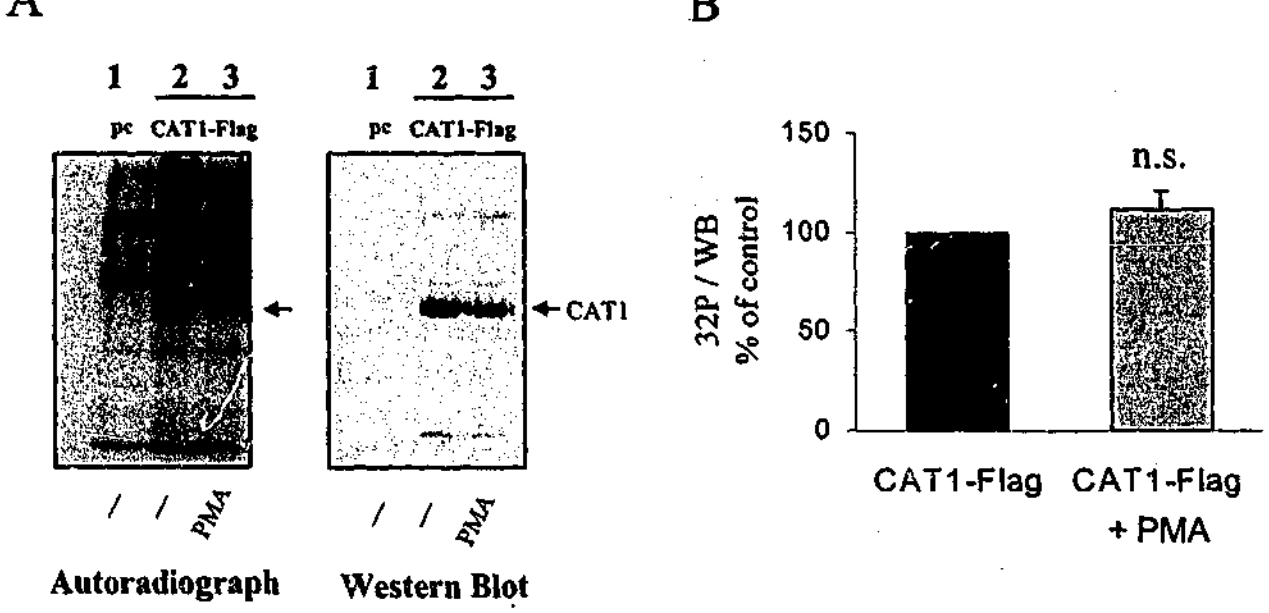

Figure 6.13 Phosphorylation status of CAT-1 after PKC activation. BAEC were transfected with either empty vector (pc) or CAT1-FLAG. Metabolic labelling of cells using ^{32}P orthophosphate was performed as described in Methods. During the last 0.5 hr of labelling 100 nM PMA was added as indicated. FLAG antibody immunoprecipitates bound to PVDF membranes were exposed to film (left image, panel **A**) and then used for immunodetection with CAT-1 antibody (right image, panel **A**). Phosphorylation levels were calculated as a ratio of ^{32}P to Western blot signal (relative density units). Data are expressed as a percentage of CAT1-FLAG without PMA treatment (Panel **B**), mean ± SEM of four independent experiments (n=4).

6.2.4.4 *A role for putative PKC sites in basal expression of CAT-1*

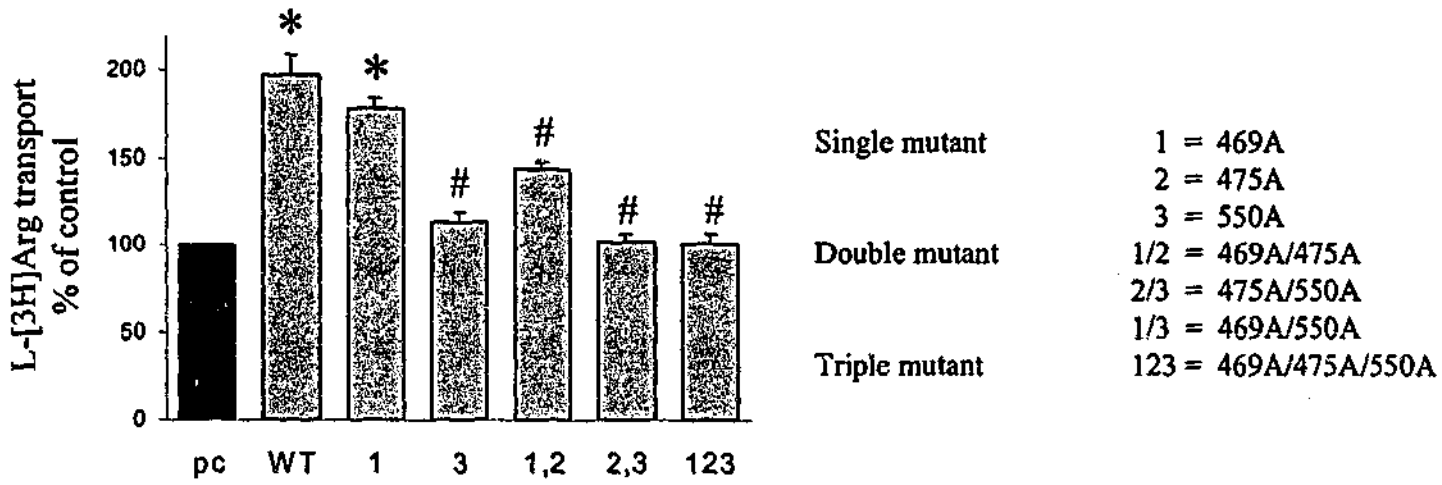

Figure 6.14 Ablation of putative PKC sites on CAT-1 reduces basal L-Arg transport. BAEC were transfected with either pcDNA3 empty vector (pc), wild-type CAT-1 (WT) or various site-directed PKC mutants as indicated on the left and right panels. L-[^{3}H]Arg transport was measured 48 hr post-transfection. Data are expressed as a percentage of empty vector (pc) transport values and are expressed as mean±SEM (n=3).*P<0.05 versus empty vector control. #P<0.05 versus wild-type CAT-1.

To further assess the role of phosphorylation of CAT-1 for its L-Arg transport activity, putative PKC phosphorylation sites within the fifth and sixth intracellular loops were ablated by mutational analysis (Figure 6.9). Different combinations of single, double and triple mutations were constructed using CAT1-FLAG as a template, in which serine positions 469, 475 and 550 (PubMedAccession #NP_031539, mouse CAT-1) were replaced by nonphosphorylatable alanine residues. DNA sequence analysis of each individual mutant was carried out in order to verify that the correct substitutions had successfully occurred. Immunoblot analysis of CAT-1 showed that equivalent amounts of transporter proteins were expressed in BAEC transfected with wild-type and mutated CAT-1 cDNA (results not shown). After 48 hr post-transfection with wildtype CAT1-FLAG and PKC phosphorylation defective mutants (469A, 550A, 469/475A, 475/550A,

469/475/550A) transport of L-[^{3}H]Arg was determined. Results were expressed as the percentage change in L-Arg transport measured in cells transfected with the appropriate empty vector (pcDNA3). Ablation of all three putative PKC phosphorylation sites (469/475/550A) prevented the upregulation of L-Arg transport activity observed in wild type CAT1-FLAG transfected cells (Figure 6.14). Transfection with the single mutant 469A resulted in an upregulation of L-Arg transport activity that was comparable to wild type CAT1-FLAG transport activity. By contrast, transfection with either 550A, 469/475A or 475/550A mutants significantly prevented upregulation of CAT1-FLAG transport activity. This initial data suggests that the putative PKC phosphorylation site serine residues 475 and 550 are important determinants of basal L-Arg transport activity.

6.2.4 Discussion

L-Arg transport is regulated in endothelial cells by the activity of kinases such as PKC and p42/44 MAPK (Flores *et al.*, 2003, Pan *et al.*, 1995, Pan *et al.*, 2002). Conserved putative PKC phosphorylation sites in the consensus sequence for CAT-1 suggests that this regulation may occur by a mechanism involving direct phosphorylation of the transporter by PKC. The present study outlines a method that has been developed for the determination of CAT-1 phosphorylation status using a commercially available antibody to selectively immunoprecipitate CAT-1 after initial metabolic labelling with ^{32}P-orthophosphate. Use of this metholodogy has led to the identification of CAT-1 as a phosphoprotein in endothelial cells. Furthermore, the existence of phosphorylated CAT-1 in untreated cells suggests that kinase activity may play an important role in the maintenance of basal transporter activity. Activation of PKC by PMA resulted in no further change to CAT-1 basal phosphorylation status. Treatment of BAEC (30 min) with either the PKC inhibitor Bim I, or the PP1/PP2A phosphatase inhibitor okadaic acid also had no effect on the level of CAT-1 phosphorylation or activity either in the presence or absence of PMA. Taken together, these results demonstrate that activated PKC inhibits CAT-1 activity by an indirect mechanism that does not involve direct phosphorylation by PKC.

A site-directed mutagenesis approach was also utilised in order to further explore the role of putative PKC phosphorylation sites in the regulation and maintenance of L-Arg transport by CAT-1. Replacement of all three intracellular serine PKC phosphorylation sites with alanine substitutions led to the complete abolition of L-Arg transport activity. Initial data from this study indicates that both Ser-475 and 550 play major roles in the maintenance of L-Arg transport activity. Further expression studies are required to investigate whether PKC site-defective CAT-1 mutants are correctly processed and trafficked through the Golgi network and, expressed at the plasma membrane. Certainly, PKC is known to regulate the cell surface expression of other membrane transporters (van Balkom *et al.*, 2002, Lin *et al.*, 2002). Such additional data would certainly reveal functionally important putative PKC phosphorylation sites in CAT-1 and their relationship to transport regulation by PKC.

In conclusion, acute activation of PKC leads to an inhibition of CAT-1 activity that occurs independently of CAT-1 phosphorylation status. Initial work from site-directed mutagenesis studies suggests that CAT-1 is a substrate of PKC. Furthermore, PKC may play an essential role in the processing and trafficking of newly expressed CAT-1 protein.

6.3 PKC –Modulated L-Arg Transport is Mediated by a Cytoskeletal-Associated Protease

6.3.1 Introduction

The fodrin-actin based cytoskeleton acts as a support underneath the endothelial plasma membrane. In addition, fodrin is known to be involved in the regulation of membrane transporters and various other integral membrane proteins. A previous report by Zharikov *et al.*(Zharikov *et al.*, 2000) has presented evidence to suggest that actin-binding cytoskeletal fodrin has a major regulatory influence on CAT-1 activity in endothelial cells. The authors have proposed that proteolysis of fodrin by a cytoskeletal-associated cysteine protease, calpain, during hypoxia is one of the mechanisms responsible for inhibition of CAT-1 activity under these conditions (Zharikov and Block, 2000). In this section, I have tested the hypothesis that PKC activation by PMA also leads to activation of calpain causing an inhibition of CAT-1 mediated L-Arg transport. The involvement of a similar CAT-1 regulatory mechanism occurring after PKC activation in BAEC was investigated in preliminary studies through pharmacologic inhibition of calpain.

6.3.2 Methods

6.3.2.1 L-[^{3}H]Arg transport assay

Transport assays were performed as previously described (Chapter 5.1.2.1). Briefly, confluent cell monolayers in 24-well plates were serum deprived overnight. The next day, cells were pretreated for 30 min with 20 μM calpain inhibitor I (N-Acetyl-Leu-Leu-NorLeu-al; Sigma) where indicated. PMA was then added to the culture medium and incubated for a further 0.5 hr. Following exposure to drugs, monolayers were incubated in Transport buffer containing a 100 μM L-[^{3}H]Arg mixture for 60 sec at 37°C in order to determine transport activity. Additional parallel transport assays were performed in the presence of a system y+ competitor, 10 mM L-lysine. Specific L-Arg transport was calculated as the difference between transport in the absence and presence of 10 mM lysine in

the transport buffer. All transport values were normalised to total cellular protein content and the rate expressed as pmol L-Arg/ μg protein / min.

6.3.2.2 Western blot analysis of isolated membrane fractions

Serum-deprived cell monolayers grown in 100 mm plates were exposed to the relevant drug treatments. Following treatment, cytosolic and membrane fractions were prepared as previously described (Chapter 6.1.2.2). Deglycosylated membrane fractions (20 μg) were subjected to Western blot analysis as previously described (Chapter 6.1.2.4) using a 7.5% polyacrylamide gel, 1:500 dilution of CAT-1 antibody (overnight incubation) and a 1:5000 dilution of goat anti-rabbit HRP secondary antibody.

6.3.3 Results

In order to explore the possible role of calpain in the inhibition of L-Arg transport by activated PKC, cells were treated with PMA for 0.5 hr in the presence of absence of calpain inhibitor I, at a concentration of 20 μM previously used in the study by Zharikov *et al.* (Zharikov and Block, 2000). The efficacy of calpain inhibitor I to block calpain activity (IC50) is reported to be 0.09 μM (Perrin *et al.*, 2002). As shown in Figure 6.15A, exposure of cells to PMA in the presence of calpain inhibitor significantly blocked the inhibition of L-Arg transport by PMA. Interestingly, exposure of cells in the presence of calpain inhibitor I alone (0.5 hr) resulted in a significantly increased L-Arg transport activity. Both effects did not correspond with changes in the membrane association of CAT-1 protein (Figure 6.15 B).

6.3.3.1 Calpain inhibition prevents effects of activated PKC on L-Arg transport

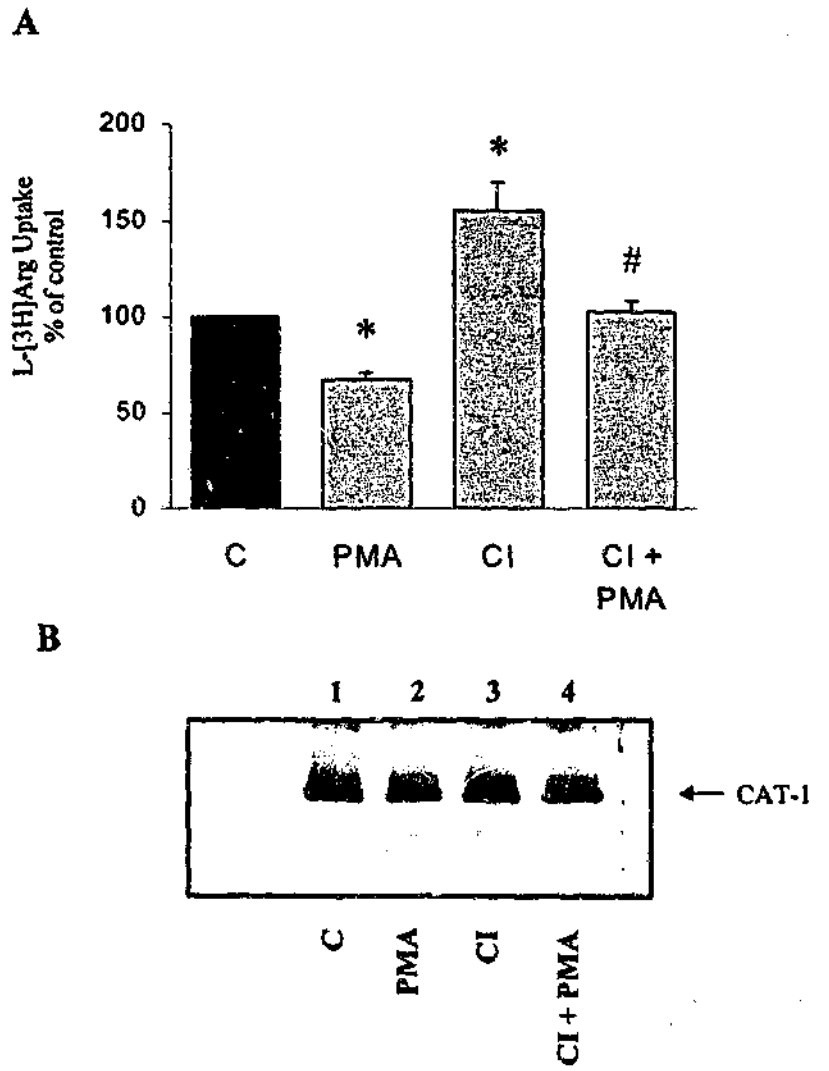

Figure 6.15 Effect of calpain inhibition on PKC mediated inhibition of L-Arg transport. BAEC were pre-treated with calpain inhibitor (CI) where indicated for 30 min. 100 nM PMA was added to culture media for 0.5 hr. After this time, (**A**) L-[^{3}H]Arg transport was determined as well as (**B**) the expression of CAT-1 protein in isolated membrane fractions. Data are expressed as a percentage of control untreated cells and are mean ±SEM (n=4). *P<0.05 versus untreated cells.

6.3.3.2 Calpain inhibition prevents the long-term effects of PMA

The effect of calpain inhibition on the activation of L-Arg transport after long-term treatment with PMA was also determined (Figure 6.16). As shown, activation of L-Arg transport associated with long-term PMA treatment was completely blocked in the presence of calpain inhibitor 1. Effects of calpain inhibitor 1 alone on increased L-Arg transport at 0.5 hr were not observed after longer incubation times. Results of a previous section demonstrated that long-term treatment of BAEC

with PMA was also associated with alterations in the expression of eNOS and caveolin (Chapter 6.1.3.2 and 6.1.3.3). These PMA-mediated effects were further examined in the presence of calpain inhibitor 1. Upregulation of eNOS associated with long-term PMA treatment (12-24 hr) was completely blocked in the presence of calpain inhibitor 1 (Figure 6.17A top and bottom panel). Likewise, downregulation of caveolin associated with long-term PMA treatment (12-24 hr) was prevented in the presence of calpain inhibitor 1 (Figure 6.17B top and bottom panel).

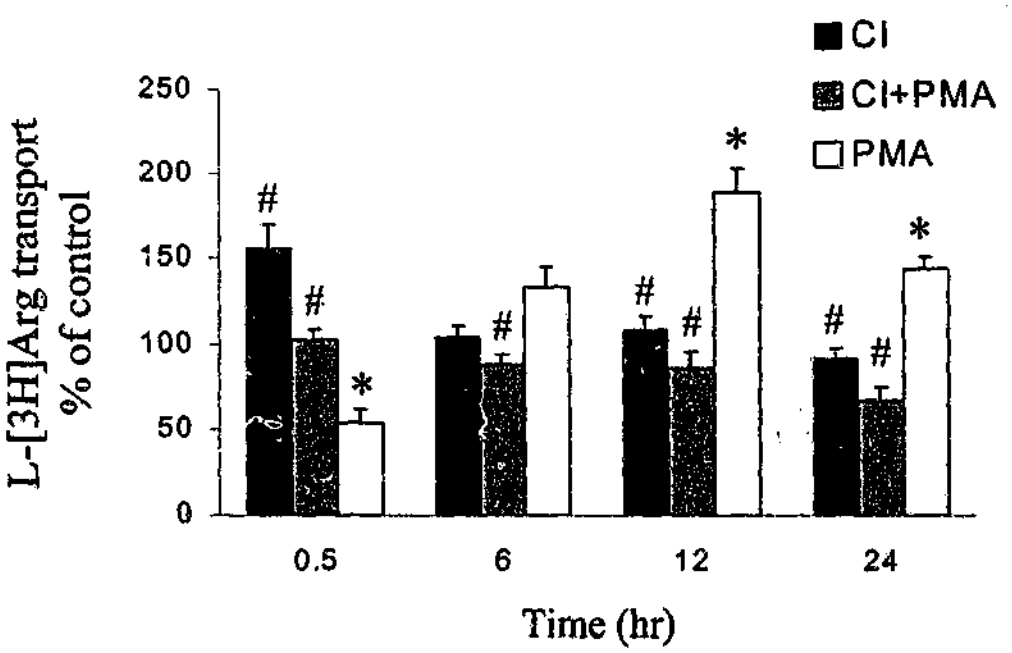

Figure 6.16 Calpain inhibition prevents the induction of L-Arg transport caused by long-term PMA treatment. BAEC were pre-treated with calpain inhibitor (CI) where indicated for 30 min. 100 nM PMA was added to culture media for various lengths of time indicated. After the appropriate incubation time point L-[^{3}H]Arg transport was determined. Data are expressed as % of control untreated cells and are mean ±SEM (n=3). *P<0.05 PMA treated versus untreated cells.#P<0.05 versus time-matched PMA treated cells.

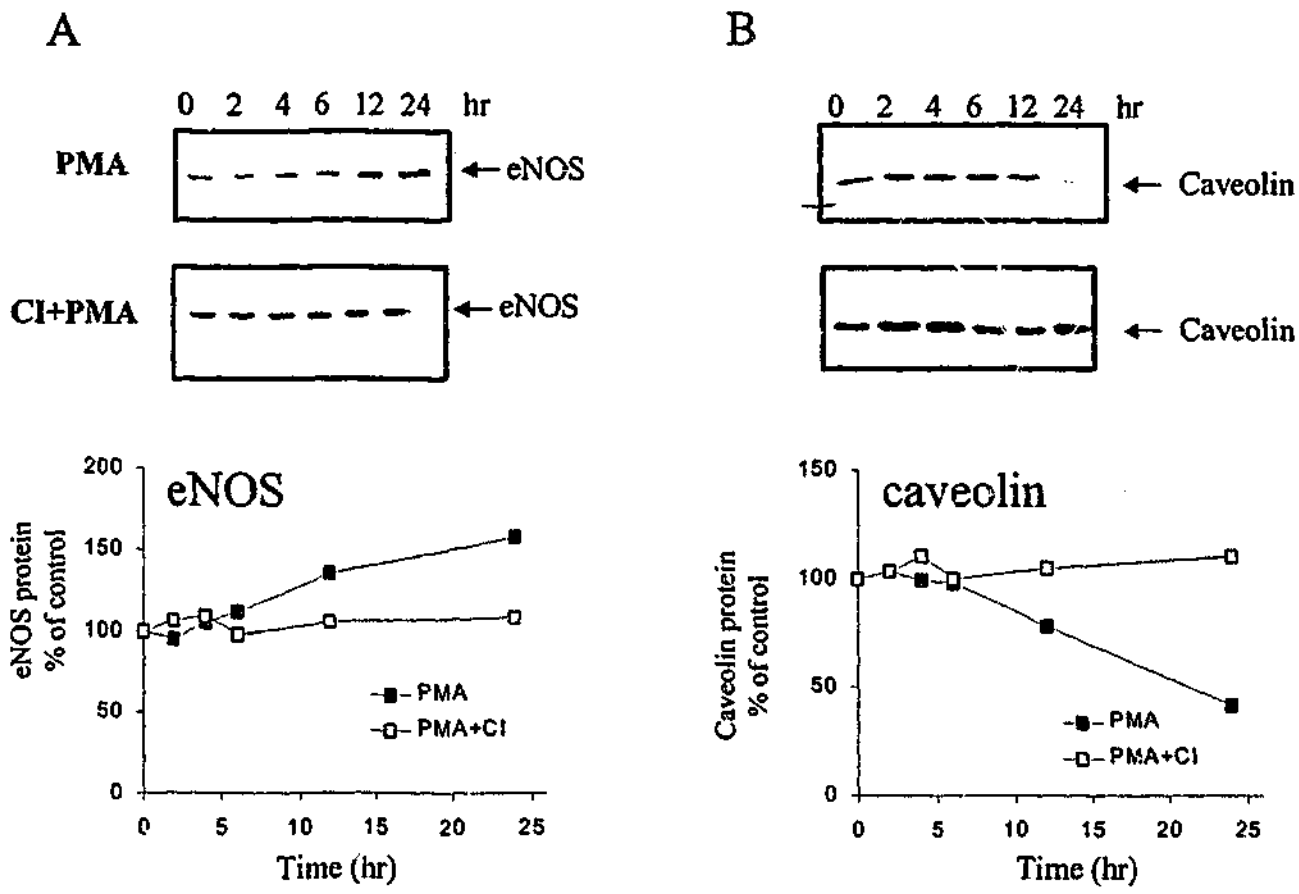

Figure 6.17 Calpain inhibition prevents the effects of long-term PMA treatment on caveolin and NOS expression. BAEC were pre-treated with calpain inhibitor (CI) where indicated for 30 min. 100 nM PMA was added to culture media for various lengths of time indicated. Protein expression levels of (**A**) eNOS and (**B**) caveolin were then determined. Data are expressed as a percentage of control untreated cells and are mean ±SEM (n=2).

6.3.4 Discussion

PKC isotypes regulate endothelial cell cytoskeleton and shape by regulating cell to cell adherence proteins (catenin-cadherin complex), cell-matrix linking proteins (vinculin, paxillin, and focal adhesion kinase) and also proteins that control actin polymerisation and microtubule assembly. Treatment of endothelial cells with phorbol esters such as PMA can evoke changes in cytoskeletal reorganisation by stimulating the formation of actin stress fibers and the re-organisation of fodrin and actin filaments. High-resolution microscopy studies have indicated that PKC activation by PMA causes fodrin to closely associate at focal adhesion points forming ring-like structures around actin filaments that are organised in dot structures (Sobue *et al.*, 1988). Under the same conditions there is also a decrease of peripheral actin microfilaments and an increase in central microfilaments (Gotlieb, 1990). Long-term cell exposure to PMA that promotes PKC downregulation has been

shown to destabilise the fodrin cytoskeleton, releasing fodrin from the lateral walls of cells and leading to a diffuse cytoplasmic distribution (Huotari *et al.*, 1992).

Calpains have a prominent role in severing cytoskeletal/membrane attachments. Cytoskeletal fodrin is a major substrate of calpain proteolytic activity (Goll *et al.*, 2003). Both association of fodrin with CAT-1 and also the state of actin microfilament assembly are known to influence CAT-1 activity (Zharikov *et al.*, 2000, Zharikov *et al.*, 2001). Results of the present study show that inhibition of L-Arg transport due to PKC activation (PMA treatment) can be prevented by the presence of a calpain inhibitor (Figure 6.15). The effects of calpain inhibitor I on L-Arg transport in PMA-treated BAEC could be explained by calpain-mediated proteolysis of CAT-1. However, calpain inhibitor I did not affect the levels of membrane-associated CAT-1 (Figure 6.15). Surprisingly, calpain inhibitor I was found to cause an activation of CAT-1 activity in the absence of PMA suggesting that calpain might regulate basal CAT-1 mediated L-Arg transport. This effect was not however observed after longer-term treatment (>1 hr) with calpain inhibitor (Figure 6.16).

Without further supporting evidence, the current data can be interpreted in different ways (see Chapter 7, Figure 7.1). Firstly, PKC isotypes can also serve as major substrates of cytoskeletal-associated proteins. Although this has not yet been clearly established a relationship between PKC and calpain is known to exist (Goll *et al.*, 2003). For instance PKC-α, β and γ isotypes can all be rapidly cleaved by calpain to smaller sized fragments that become constitutively active being no longer subject to regulation by calcium and phospholipids. Once activated, calpain is known to form a tight complex with PKC-α and has been linked to the formation of the constitutively active PKC proteolytic fragment PKM (Aragon *et al.*, 2002). Upregulation of both PKC and m-calpain by phorbol esters has been demonstrated and is thought to be related to a role of m-calpain in regulation of PKC activity (Goll *et al.*, 2003). One theory might be that activated calpain forms a complex with PKC-α after acute PMA exposure leading to downregulation of CAT-1 activity

through a direct association of PKC-α/PKM with CAT-1. Or alternatively, through a PKC-α/PKM evoked association/dissociation of CAT-1 with an unknown regulatory protein.

Secondly, fodrin dissociation from CAT-1 may help to explain the inhibition of CAT-1 activity in response to PMA treatment similar to that shown during hypoxia (Zharikov *et al.*, 2000). Co-immunoprecipitation studies of Zharikov *et al.* have demonstrated that proteolysis of fodrin due to hypoxia-induced calpain activation inhibits CAT-1 activity through the dissociation of a complex between fodrin and CAT-1. While their data does exclude a role for actin-binding ankyrin, there is an additional possibility that other fodrin-binding proteins may be involved in a CAT-1 regulatory process. For example, cytoskeletal associated adducin forms a ternary complex with actin and fodrin and is also known to be a major substrate for PKC phosphorylation (Matsuoka *et al.*, 2000).

Thirdly, commonly employed synthetic inhibitors of calpain including calpain inhibitor I are known to have effects in addition to the inhibition of calpain and may confound interpretation of the current data. At effective inhibitory doses for calpain, calpain inhibitor I is also a good inhibitor of cathepsins B and L and the proteasome (Goll *et al.*, 2003). For example, proteasomal inhibition might explain why caveolin is not degraded in response to long-term PMA treatment (Figure 6.17). Further work using highly selective biological inhibitors of calpain such as calpastatin or calpastatin inhibitory domain peptide fragments are required in order to more clearly dissect the role of calpain in L-Arg transport regulation.

In conclusion, the present data suggests that calpain may be a major mediator of PKC-regulated L-Arg transport in the endothelium. Furthermore calpain seems to play a role in the preventing long-term effects of PMA treatment such as increased CAT-1 and NOS activity, and decreased caveolin expression (Figure 6.17). The functional significance of these observations is not yet known. This current data provides further supporting evidence (Zharikov *et al.*, 2000, Zharikov *et al.*, 2001) for a role of the endothelial cytoskeleton in regulation of L-Arg transport.

Chapter Seven

Conclusions

7.1 L-Arg transport abnormalities in human congestive heart failure

The major finding of this thesis demonstrates a significant depression of L-Arg transport activity in CHF. In concurrence with the findings of Dr.Kaye, a decrease in L-Arg transport rate both in the peripheral and coronary vasculature demonstrates a generalised abnormality in CHF (Chapter 3). Although we were unable to provide more direct evidence at this time, we believe that this generalised abnormality also extends to the endothelium in human CHF. Additionally, no evidence was found to suggest that this abnormality is related to gender or aging (Chapter 3). Extensive clinical and experimental studies documenting endothelial dysfunction in CHF have consistently provided evidence of diminished endothelium-dependent vasodilation attributable to reduced NO availability both in the peripheral and coronary circulation (Chapter 1, Section 4.3). A reduction of L-Arg transport detected in CHF provides a plausible explanation for the beneficial actions of supplemental L-Arg in clinical studies (Chapter 1, Section 4.5.7). Findings of the present study support a proposal that reduced L-Arg transport may contribute to a deficiency of intracellular L-Arg available for eNOS catalysed conversion to NO, ultimately leading to reduced NO synthesis. The functional nature of this dysregulation *in vivo* has not yet been formally proven.

More recent studies performed by others within this laboratory have provided evidence of reduced L-Arg transport in the forearm vasculature and the peripheral circulation of patients with hypertension and normotensive individuals with a positive hypertensive family history (Schlaich *et al.*, 2002). Hypertensive individuals also exhibit endothelial dysfunction. Additionally, increased L-Arg transport is evident in the peripheral vasculature of individuals with advanced liver cirrhosis, a pathophysiological condition associated with excessive splanchnic and systemic vasodilation (Rasaratnum *et al.*, 1999). Such studies also allude to an important role for L-Arg transport in the maintenance of NO production and vascular function.

Depressed L-Arg transport in CHF was attributed to a decrease of the system y+/CAT-1 transport capacity (V_{max}) without affecting transporter affinity for L-Arg (K_m) (Chapter 3, Section 2). A

decrease in maximal transporter capacity in the absence of a change in transport affinity is indicative of a decrease in functional CAT-1 transporter expression. In accordance, a downregulation of CAT-1 expression was observed both in the peripheral circulation and coronary vasculature (Chapter 3, Section 2). These results suggest that the primary cause of reduced L-Arg transport is due to a decrease in CAT-1 expression in CHF. Underlying mechanisms responsible for a reduction in CAT-1 mRNA expression and L-Arg transport rate and both in circulating mononuclear cells and the failing heart in CHF remains unknown. Clearly, an investigation of the factors that regulate L-Arg transport in CHF are warranted.

7.2 Regulation of L-Arg transport in the endothelium

Feasibility of CAT-1 as a therapeutic target

In addition to the supply of L-Arg for the NO pathway, CAT-1 activity is also vital for other processes such as cell proliferation and differentiation (Nicholson *et al.*, 1993). Therefore, an investigation of the mechanisms underlying depressed L-Arg transport in CHF must first be undertaken in order to devise a rational basis for effective treatment regimens in the restoration of endothelial dysfunction. Little evidence exists about factors which affect CAT-1 mediated L-Arg transport in the myocardium or endothelium *in vivo*. Hormones such as insulin, dexamethasone, bradykinin and histamine have been shown to selectively increase L-Arg transport and/or CAT-1 mRNA *in vitro*. Increases in eNOS activity induced by vasodilators such as histamine and bradykinin are closely correlated with increased L-Arg transport into cells (Hardy *et al.*, 2002). Cytokine treatment with either IL-1β, IFN-γ or TNF-α has been reported to increase L-Arg transport due to upregulation of CAT isoforms -1, -2A and –2B expression. However, cytokine treatment is also associated with pathological levels of NO production attributed to inducible expression of iNOS (Chapter 1, Section 7.2.1).

The major finding of this thesis (Chapter 7, Section 1) may be explained by elevated levels of circulating neurohormones and cytokines that are known to be present in CHF. However, adoption

of a screening approach to examine the effects of some pathophysiologically relevant CHF factors (Ang II, ANP, NA, ET-1 and TNF-α) on L-Arg transport *in vitro* did not reveal any candidates that would help explain reduced L-Arg transport in CHF (Chapter 4). In the present study, conventional CHF medications were continued because of concerns about the severity of left ventricular dysfunction in these patients. Therefore, there is the possibility that our observations were influenced by the presence of antifailure medications. A novel finding of the screening approach was the ability of Ang II to upregulate CAT-1 expression and activity in the human endothelium (Chapter 4, Section 2). Subsequent investigation of this observation using pharmacological inhibitors suggests that Ang II mediated L-Arg transport requires prior conversion of Ang II to a metabolically active fragment, Ang IV, and subsequent AT_4 receptor binding (Chapter 4, Section 2). Treatment of human endothelial cells with Ang II was also accompanied by an increase in intracellular eNOS activity (142 ± 11% of control; Ang II cells vs untreated cells). If proven physiologically relevant *in vivo*, the mechanism by which Ang IV may stimulate the L-Arg-NO pathway could potentially be exploited therapeutically in CHF.

Regulation of L-Arg transport by PKC

An investigation of the mechanism leading to Ang II induction of CAT-1 activity in endothelial cells revealed that PKC was significantly involved in mediating this response (Chapter 4, Section 2). For this reason, further studies were undertaken to determine the mechanism via which PKC may modulate CAT-1 activity using the synthetic PKC activator, PMA (Chapter 5 and 6). PKC activation by PMA caused a significant downregulation of CAT-1 mediated L-Arg transport. This response was not due to changes in the level of CAT-1 at the plasma membrane (Chapter 6, Section 1), association status of CAT-1 with caveolin (Chapter 6, Section 1) or the phosphorylation status of CAT-1 (Chapter 6, Section 2). Instead, inhibition of a cytoskeletal-associated protease, calpain, was found to completely block the effects of PKC on L-Arg transport (Chapter 6, Section 3). A summary of these results is presented in Figure 7.1 below.

Figure 7.1 Proposed model for PKC regulation of L-Arg transport in the endothelium.

A. Acute treatment of cells with PMA leads cytoskeletal reorganisation by stimulating the formation of actin stress fibers and the reorganisation of fodrin and actin filaments. Activation of PKC by PMA causes translocation of PKC-α from the cytosol to the plasma membrane. Activated PKC may result in L-Arg transport inhibition by i) calpain-mediated hydrolysis of fodrin due to PKC activation leading to an inhibition of CAT-1 activity through the dissociation of a complex between fodrin and CAT-1, ii) the direct association of PKC-α with CAT-1, iii) proteolysis of translocated PKC-α by PMA-activated calpain resulting in the production of a smaller constitutively active PKC fragment, PKM. Subsequent inhibition of CAT-1 activity may occur through a direct association of PKM with CAT-1 or possibly iv) via PKC-α/PKM evoked association/dissociation of CAT-1 with an unknown regulatory protein.

B. Long-term cell exposure to PMA depletes PKC isotypes and has been shown to destabilise the fodrin cytoskeleton, releasing fodrin from the lateral walls of cells and leading to a diffuse cytoplasmic distribution. Long-term treatment with PMA does not cause changes in CAT-1 protein expression. In the absence of any supporting evidence, no further explanations can be given. Calpain inhibition blocks the effect of long-term PMA treatment on CAT-1 activation suggestive of a mechanism that may involve the proteolytic actions of calpain, such as hydrolysis of fodrin. However, synthetic inhibitors of calpain including calpain inhibitor I (used in this thesis) are known to have effects in addition to the inhibition of calpain and confounds the interpretation of data resulting from their usage. At effective inhibitory doses for calpain, calpain inhibitor I is also a good inhibitor of cathepsins B and L and the proteasome. Therefore treatment with calpain inhibitor I may lead to proteasomal inhibition, preventing the depletion of PKC isotypes associated with long-term PMA treatment, fodrin or other unknown CAT-1 regulatory proteins.

(See Chapter 6 for further detail and references relating to this proposed model)

A

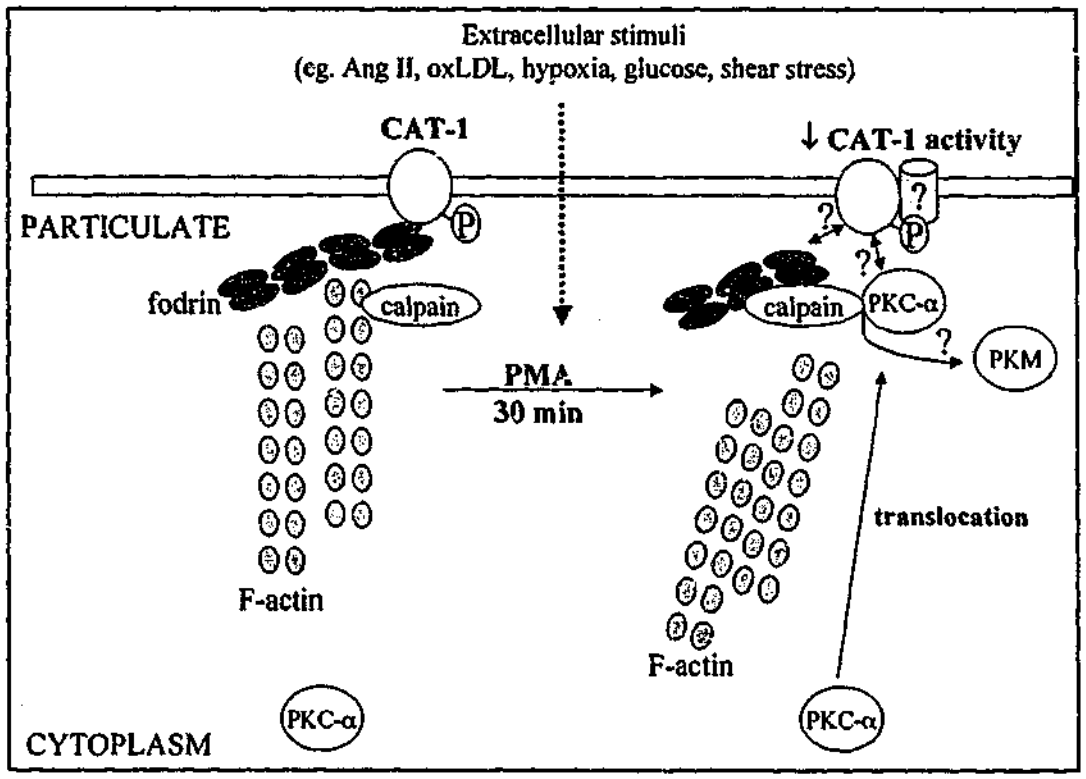
Extracellular stimuli
(eg. Ang II, oxLDL, hypoxia, glucose, shear stress)
CAT-1
↓ CAT-1 activity
PARTICULATE
P
fodrin
calpain
F-actin
PMA
30 min
calpain
PKC-α
PKM
translocation
F-actin
PKC-α
CYTOPLASM
PKC-α

B

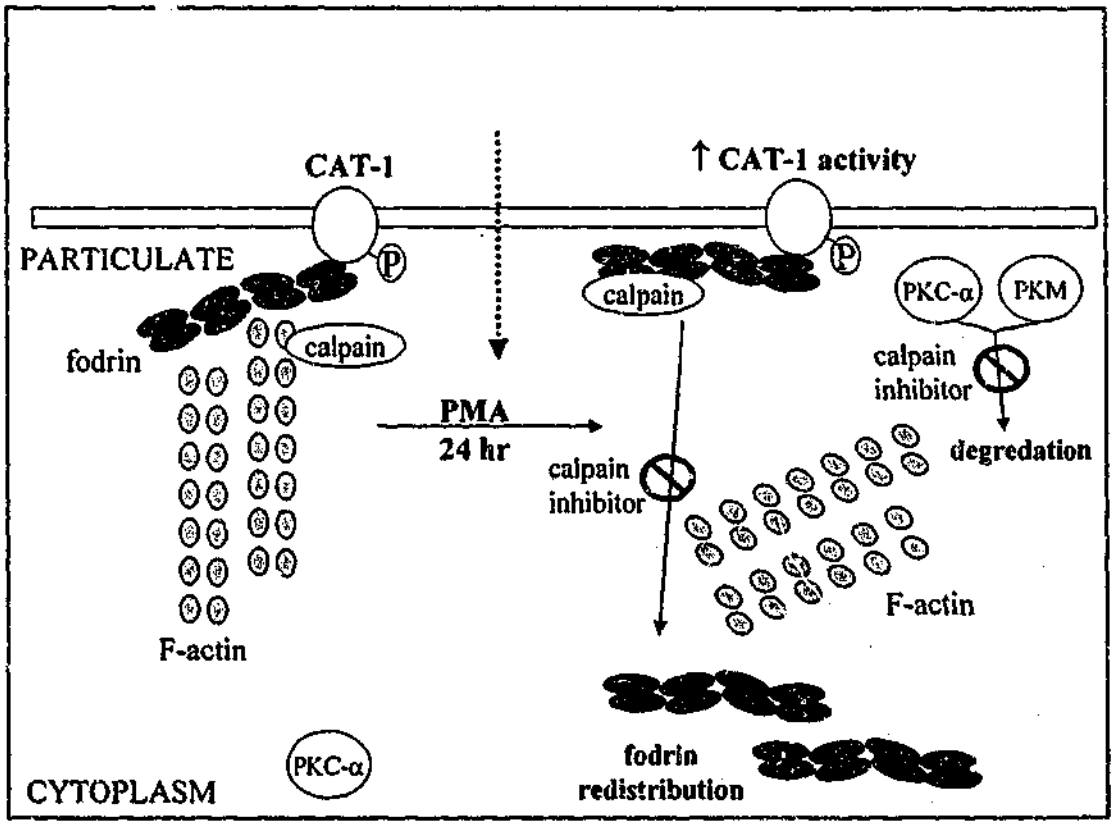
CAT-1
↑ CAT-1 activity
PARTICULATE
P
fodrin
calpain
F-actin
PMA
24 hr
calpain
calpain
inhibitor
PKC-α
PKM
calpain
inhibitor
degredation
F-actin
fodrin
redistribution
PKC-α
CYTOPLASM

The state of cytoskeletal organisation within the endothelium is known to have a significant influence on CAT-1 mediated L-Arg transport (Zharikov *et al.*, 2001, Zharikov *et al.*, 2000). In addition, activation of PKC by PMA is known to cause rearrangement of the actin-fodrin based cytoskeleton in endothelial cells (Smirnov *et al.*, 1989). Therefore, it is plausible that the effect of PKC on CAT-1 mediated L-Arg transport may be due to an effect on cytoskeletal processes. Interestingly, there is various accumulating evidence to suggest that cytoskeletal abnormalities may participate in many forms of heart failure (Towbin *et al.*, 2002).

Since PMA is a broad activator of novel and classical isotypes (-δ, -ε, -θ, -η, -α, -β1, -β2,and -γ) it is not possible to draw direct conclusions about the specific PKC isotype(s) involved in modulating L-Arg transport. Thus, PMA gives only an indication of the class of PKC involved in this response. Since α- and ε- are the only classical and novel isotypes present in BAEC this allowed the discrimination of two likely candidates for the regulation of L-Arg transport activity by PMA. During the writing of this thesis, new published evidence by Krotova *et al.* (Krotova *et al.*, 2003) has indicated that the effects of PMA on L-Arg transport in endothelial cells are attributed specifically to the actions of the PKC-α isotype. The authors demonstrate that an inhibitory effect of PMA on L-Arg transport is accompanied by a translocation of PKC-α from the cytosol to the membrane fraction, whereas activation of L-Arg transport by PMA is temporally related to a total depletion of PKC-α expression in porcine aortic endothelial cells.

This thesis contains one of the first reports to demonstrate the involvement of endothelial signalling pathways in the post-translational regulation of CAT-1 activity. The functional significance of endothelial L-Arg transport regulation by PKC is not yet known. Likewise, factors that may lead regulation of endothelial L-Arg transport by PKC *in vivo* are not known. Physiologically, PKC activators are known to include fluid/shear stress and the binding of various endotoxins, growth factors, and cytokines to membrane receptors. Those factors potentially relevant in the setting of heart failure for example include Ang II, endothelin-1, phenylephrine, norepinephrine, oxLDL and

hypoxia. Newly proposed therapies for CHF now include the inhibition of specific PKC isotypes due to their involvement in some potentially detrimental effects like myocardial hypertrophy, apoptosis, impaired calcium handling and cytoskeletal arrangement (Vlahos *et al.*, 2003). PKC-α, -β and –δ have been reported to be elevated in CHF (Koide *et al.*, 2003, Vlahos *et al.*, 2003). Since PKC isotypes are also known to have opposing roles within the same cell type, which may be either detrimental or beneficial to the cell, further progress in this area will ultimately rely on a more complete understanding of individual PKC isotype functions (Rosales *et al.*, 1998, Vlahos *et al.*, 2003).

7.3 Major Limitations

CAT-1 expression

Many previous investigations of CAT-1 protein expression have been hindered by the difficulty in producing reliable antibodies for use in Western blot and immunoprecipitation studies. To overcome this, a polyclonal CAT-1 antibody was successfully generated during this PhD according to a previously described method by Woodard *et al.* (Woodard *et al.*, 1994). Whereas Woodard *et al.* (Woodard et al., 1994) had reported using the same type of antibody for detection in human cell types (human embryonic kidney cell line) CAT-1 was only detectable in cells and tissues of mouse and bovine origin in the authors hands. This meant that no conclusions could made about expression of CAT-1 protein in peripheral blood mononuclear cells or myocardial tissue isolated from CHF patients (Chapter 3). Likewise, the induction of CAT-1 mRNA and L-Arg transport activity by Ang II in the human endothelial cell line, EA.hy926 could not be related temporally to CAT-1 protein expression levels (Chapter 4).

With these limitations in mind, BAEC was chosen as a model for investigating the regulation of CAT-1 by PKC because it allowed measurement of CAT-1 protein expression and an investigation of post-translational regulation using CAT-1 antibody. For this purpose, CAT-1 antibody proved extremely useful for Western blotting and confocal imaging studies in BAEC (Chapter 5 and 6). Previous studies have demonstrated that the L-Arg transport properties of mouse and human CAT-

1 are almost identical (Kim *et al.*, 1991, Wang *et al.*, 1991, Closs *et al.*, 1997). Based on this evidence, it is believed that the results derived from BAEC may reflect the same type of regulation of endothelial CAT-1 by PKC in humans. However, through the course of these PhD studies major differences became apparent in the way in which CAT-1 can be regulated in different species. For example, activation of PKC by PMA treatment of EA.hy926 and BAEC resulted in a significant inhibition of L-Arg transport activity. However, depletion of PKC through long-term PMA treatment causes activation of L-Arg transport in BAEC whilst an inhibition of L-Arg transport activity is evident in EA.hy926. In further paradox, Ang II treatment caused an increase in L-Arg transport in EA.hy926 cells, an effect that was mediated by PKC. Further identification of the specific PKC isotypes involved in regulation of CAT-1 activity by Ang II and PMA may help to explain this paradox.

Nitric oxide measurements

Changes in NO production were detected on the basis of a currently established and accepted method of determining the catalytic activity of NOS. However, these measurements are not able to reveal changes in NO bioavailability due inactivation by reactive oxygen species. Under conditions of limited L-Arg availability, both iNOS and eNOS are capable of generating superoxide radicals by utlising molecular oxygen with no apparent changes in NOS catalytic activity. Generation of ROS either by NOS or through other cellular sources in CHF is thought to play a significant role in the development of endothelial dysfunction (Chapter 1, Section 4.4.1). Reliable measures of NO bioavailability are of ultimate significance to the validation of studies presented within this PhD thesis. Further efforts to detect real-time NO production are currently underway in this laboratory.

7.4 Concluding Remark

It is hoped that studies contained within this thesis will serve to open up new avenues for exploring some of the potential mechanisms that may lead to the development and/or contribute to the progression of endothelial dysfunction in heart failure.

References

Aberle, S., *et al.* (1997) Quantitative measurement for endothelial constitutive nitric oxide synthase in cultured human endothelial cells. *Nitric Oxide,* **1,** 226-33.

Abrams, J. (1991) The mystery of nitrate resistance. *Am J Cardiol,* **68,** 1393-6.

Abrams, J. (1996) Beneficial actions of nitrates in cardiovascular disease. *Am J Cardiol,* **77,** 31C-7C.

Agnoletti, L., *et al.* (1999) Serum from patients with severe heart failure downregulates eNOS and is proapoptotic: role of tumor necrosis factor-alpha. *Circulation,* **100,** 1983-91.

Aisaka, K., *et al.* (1989) L-arginine availability determines the duration of acetylcholine-induced systemic vasodilation in vivo. *Biochem Biophys Res Commun,* **163,** 710-7.

Albiston, A. L., *et al.* (2001) Evidence that the angiotensin IV (AT(4)) receptor is the enzyme insulin-regulated aminopeptidase. *J Biol Chem,* **276,** 48623-6.

Albritton, L. M., *et al.* (1993) Envelope-binding domain in the cationic amino acid transporter determines the host range of ecotropic murine retroviruses. *J Virol,* **67,** 2091-6.

Albritton, L. M., *et al.* (1989) A putative murine ecotropic retrovirus receptor gene encodes a multiple membrane-spanning protein and confers susceptibility to virus infection. *Cell,* **57,** 659-66.

Amin, A. R., *et al.* (1995) Expression of nitric oxide synthase in human peripheral blood mononuclear cells and neutrophils. *J Inflamm,* **47,** 190-205.

Andrawis, N., *et al.* (2000) Aging is associated with endothelial dysfunction in the human forearm vasculature. *J Am Geriatr Soc,* **48,** 193-8.

Andrews, R. K., *et al.* (1998) Binding of purified 14-3-3 zeta signaling protein to discrete amino acid sequences within the cytoplasmic domain of the platelet membrane glycoprotein Ib-IX-V complex. *Biochemistry,* **37,** 638-47.

Anker, S. D., *et al.* (1998) Tumour necrosis factor alpha as a predictor of impaired peak leg blood flow in patients with chronic heart failure. *Qjm,* **91,** 199-203.

Arnal, J. F., *et al.* (1999) Endothelium-derived nitric oxide and vascular physiology and pathology. *Cell Mol Life Sci,* **55,** 1078-87.

Arnal, J. F., *et al.* (1995) Interactions between L-arginine and L-glutamine change endothelial NO production. An effect independent of NO synthase substrate availability. *J Clin Invest,* **95,** 2565-72.

Arnold, J. M., *et al.* (1991) Large artery function in patients with chronic heart failure. Studies of brachial artery diameter and hemodynamics. *Circulation,* **84,** 2418-25.

Aulak, K. S., *et al.* (1996a) Molecular sites of regulation of expression of the rat cationic amino acid transporter gene. *J Biol Chem,* **271,** 29799-806.

Aulak, K. S., *et al.* (1996b) Molecular sites of regulation of expression of the rat cationic amino acid transporter gene. *J Biol Chem,* **271,** 29799-806.

Aulak, K. S., *et al.* (1999) Post-transcriptional regulation of the arginine transporter Cat-1 by amino acid availability. *J Biol Chem,* **274,** 30424-32.

Ausubel, F. M., *et al.* (Eds.) (1990) *Current Protocols in Molecular Biology,* Greene Publishing Associates and John Wiley & Sons, New York.

Autelitano, D. J. (1998) Cardiac expression of genes encoding putative adrenomedullin/calcitonin gene-related peptide receptors. *Biochem Biophys Res Commun,* **250,** 689-93.

Bank, A. J., *et al.* (2000) Endothelial dysfunction in patients with heart failure: relationship to disease severity. *J Card Fail,* **6,** 29-36.

Bank, A. J., *et al.* (1994) Endothelium-dependent vasodilation of peripheral conduit arteries in patients with heart failure. *J Card Fail,* **1,** 35-43.

Barbul, A. (1995) In *Amino acid metabolism and therapy in health and nutritional disease.*(Ed, Cynober, L. A.) CRC Press; 1995., New York, pp. 361-372.

Barbul, A., *et al.* (1990) Arginine enhances wound healing and lymphocyte immune responses in humans. *Surgery,* **108,** 331-6; discussion 336-7.

Barbul, A., *et al.* (1984) High arginine levels in intravenous hyperalimentation abrogate post-traumatic immune suppression. *J Surg Res,* **36,** 620-4.

Bauersachs, J., *et al.* (1999) Endothelial dysfunction in chronic myocardial infarction despite increased vascular endothelial nitric oxide synthase and soluble guanylate cyclase expression: role of enhanced vascular superoxide production. *Circulation,* **100,** 292-8.

Bauersachs, J., *et al.* (2001) Improvement of left ventricular remodeling and function by hydroxymethylglutaryl coenzyme a reductase inhibition with cerivastatin in rats with heart failure after myocardial infarction. *Circulation,* **104,** 982-5.

Baydoun, A. R., *et al.* (1990) Substrate-dependent regulation of intracellular amino acid concentrations in cultured bovine aortic endothelial cells. *Biochem Biophys Res Commun,* **173,** 940-8.

Baydoun, A. R., *et al.* (1999) Transmembrane signalling mechanisms regulating expression of cationic amino acid transporters and inducible nitric oxide synthase in rat vascular smooth muscle cells. *Biochem J,* **344 Pt 1,** 265-72.

Beckman, J. A., *et al.* (2002) Inhibition of protein kinase Cbeta prevents impaired endothelium-dependent vasodilation caused by hyperglycemia in humans. *Circ Res,* **90,** 107-11.

Bertran, J., *et al.* (1992) Expression of Na(+)-independent amino acid transport in Xenopus laevis oocytes by injection of rabbit kidney cortex mRNA. *Biochem J,* **281 (Pt 3),** 717-23.

Birks, E. J., *et al.* (1997) The role of nitric oxide and cytokines in heart failure. *Coron Artery Dis,* **8,** 389-402.

Block, E. R., *et al.* (1995) Hypoxia inhibits L-arginine uptake by pulmonary artery endothelial cells. *Am J Physiol,* **269,** L574-80.

Bode, B. P., *et al.* (1998) Protein kinase C regulates nutrient uptake and growth in hepatoma cells. *Surgery,* **124,** 260-7; discussion 267-8.

Boger, R. H. (1999) Nitric oxide and the mediation of the hemodynamic effects of growth hormone in humans. *J Endocrinol Invest,* **22(5,** 75-81.

Boger, R. H., *et al.* (1998) Asymmetric dimethylarginine (ADMA): a novel risk factor for endothelial dysfunction: its role in hypercholesterolemia. *Circulation,* **98,** 1842-7.

Bogle, R. G., *et al.* (1996) Regulation of L-arginine transport and nitric oxide release in superfused porcine aortic endothelial cells. *J Physiol,* **490,** 229-41.

Bonapace, S., *et al.* (2003) Aortic distensibility independently affects exercise tolerance in patients with dilated cardiomyopathy. *Circulation,* **107,** 1603-8.

Boo, Y. C., *et al.* (2002) Shear stress stimulates phosphorylation of eNOS at Ser(635) by a protein kinase A-dependent mechanism. *Am J Physiol Heart Circ Physiol,* **283,** H1819-28.

Booyse, F. M., *et al.* (1975) Culture of arterial endothelial cells: characterization and growth of bovine aortic cells. *Thromb Diath Haemorrh,* **34,** 825-39.

Boucher, J. L., *et al.* (1994) N omega-hydroxyl-L-arginine, an intermediate in the L-arginine to nitric oxide pathway, is a strong inhibitor of liver and macrophage arginase. *Biochem Biophys Res Commun,* **203,** 1614-21.

Boucher, J. L., *et al.* (1999a) Nitric oxide biosynthesis, nitric oxide synthase inhibitors and arginase competition for L-arginine utilization. *Cell Mol Life Sci,* **55,** 1015-28.

Boucher, J. L., *et al.* (1999b) Nitric oxide biosynthesis, nitric oxide synthase inhibitors and arginase competition for L-arginine utilization. *Cell Mol Life Sci,* **55,** 1015-28.

Boulanger, C. M., *et al.* (1995) Endothelial AT1-mediated release of nitric oxide decreases angiotensin II contractions in rat carotid artery. *Hypertension,* **26,** 752-7.

Boyd, C. A., *et al.* (1992) Activation of cationic amino acid transport through system y+ correlates with expression of the T-cell early antigen gene in human lymphocytes. *Pflugers Arch,* **422,** 87-9.

Braga, M., *et al.* (1999) Perioperative immunonutrition in patients undergoing cancer surgery: results of a randomized double-blind phase 3 trial. *Arch Surg,* **134,** 428-33.

Brandes, R. P., *et al.* (2000) L-arginine supplementation in hypercholesterolemic rabbits normalizes leukocyte adhesion to non-endothelial matrix. *Life Sci,* **66,** 1519-24.

Braunwald, E., *et al.* (2000) Congestive heart failure: fifty years of progress. *Circulation,* **102,** IV14-23.

Bredt, D. S., *et al.* (1990) Isolation of nitric oxide synthetase, a calmodulin-requiring enzyme. *Proc Natl Acad Sci U S A,* **87,** 682-5.

Broer, A., *et al.* (2000) The heterodimeric amino acid transporter 4F2hc/y+LAT2 mediates arginine efflux in exchange with glutamine. *Biochem J,* **349 Pt 3,** 787-95.

Brosnihan, K. B., *et al.* (1996) Angiotensin-(1-7) dilates canine coronary arteries through kinins and nitric oxide. *Hypertension,* **27,** 523-8.

Brunner, F., *et al.* (2001a) Myocardial contractile function and heart rate in mice with myocyte-specific overexpression of endothelial nitric oxide synthase. *Circulation,* **104,** 3097-102.

Brunner, F., *et al.* (2001b) Endothelial NO/cGMP system contributes to natriuretic peptide-mediated coronary and peripheral vasodilation. *Microvasc Res,* **61,** 102-10.

Budworth, J., *et al.* (1995) Differential inhibition of cytosolic and membrane-derived protein kinase C activity by staurosporine and other kinase inhibitors. *FEBS Lett,* **362,** 139-42.

Buga, G. M., *et al.* (1996) Arginase activity in endothelial cells: inhibition by NG-hydroxy-L-arginine during high-output NO production. *Am J Physiol,* **271,** H1988-98.

Burton, G. W., *et al.* (1983) Is vitamin E the only lipid-soluble, chain-breaking antioxidant in human blood plasma and erythrocyte membranes? *Arch Biochem Biophys,* **221,** 281-90.

Busconi, L., *et al.* (1993) Endothelial nitric oxide synthase. N-terminal myristoylation determines subcellular localization. *J Biol Chem,* **268,** 8410-3.

Busse, R., *et al.* (1998) Pulsatile stretch and shear stress: physical stimuli determining the production of endothelium-derived relaxing factors. *J Vasc Res,* **35,** 73-84.

Butt, E., *et al.* (1993) The cGMP-dependent protein kinase--gene, protein, and function. *Neurochem Res,* **18,** 27-42.

Capponi, A. M. (1996) Distribution and signal transduction of angiotensin II AT1 and AT2 receptors. *Blood Press Suppl,* **2,** 41-6.

Cardillo, C., *et al.* (1999) Insulin stimulates both endothelin and nitric oxide activity in the human forearm. *Circulation,* **100,** 820-5.

Carey, R. M., *et al.* (2000) Update: role of the angiotensin type-2 (AT(2)) receptor in blood pressure regulation. *Curr Hypertens Rep,* **2,** 198-201.

Carr, A., *et al.* (2000) The role of natural antioxidants in preserving the biological activity of endothelium-derived nitric oxide. *Free Radic Biol Med,* **28,** 1806-14.

Carr, A. C., *et al.* (1999) Toward a new recommended dietary allowance for vitamin C based on antioxidant and health effects in humans. *Am J Clin Nutr,* **69,** 1086-107.

Carville, C., *et al.* (1998) Relation between impairment in nitric oxide pathway and clinical status in patients with congestive heart failure. *J Cardiovasc Pharmacol,* **32,** 562-70.

Castillo, L., *et al.* (1994) Plasma arginine kinetics in adult man: response to an arginine-free diet. *Metabolism,* **43,** 114-22.

Castillo, L., *et al.* (1993) Plasma arginine and citrulline kinetics in adults given adequate and arginine-free diets. *Proc Natl Acad Sci U S A,* **90,** 7749-53.

Chauhan, A., *et al.* (1996) Aging-associated endothelial dysfunction in humans is reversed by L-arginine. *J Am Coll Cardiol,* **28,** 1796-804.

Chavakis, E., *et al.* (2001) Oxidized LDL inhibits vascular endothelial growth factor-induced endothelial cell migration by an inhibitory effect on the Akt/endothelial nitric oxide synthase pathway. *Circulation,* **103,** 2102-7.

Chen, J. X., *et al.* (2001) Nitric oxide donors regulate nitric oxide synthase in bovine pulmonary artery endothelium. *J Cell Physiol,* **186,** 116-23.

Chen, L. Y., *et al.* (1996a) Variable effects of L-arginine analogs on L-arginine-nitric oxide pathway in human neutrophils and platelets may relate to different nitric oxide synthase isoforms. *J Pharmacol Exp Ther,* **276,** 253-7.

Chen, L. Y., *et al.* (1998) Evidence for the presence of L-arginine-nitric oxide pathway in human red blood cells: relevance in the effects of red blood cells on platelet function. *J Cardiovasc Pharmacol,* **32,** 57-61.

Chen, L. Y., *et al.* (1996b) Oxidized LDL decreases L-arginine uptake and nitric oxide synthase protein expression in human platelets: relevance of the effect of oxidized LDL on platelet function. *Circulation,* **93,** 1740-6.

Chen, S., *et al.* (2000) Angiotensin IV-mediated pulmonary artery vasorelaxation is due to endothelial intracellular calcium release. *Am J Physiol Lung Cell Mol Physiol,* **279,** L849-56.

Chiariello, M., *et al.* (1999) Pathophysiology of heart failure. *Miner Electrolyte Metab,* **25,** 6-10.

Chomczynski, P., *et al.* (1987) Single-step method of RNA isolation by acid guanidinium thiocyanate-phenol-chloroform extraction. *Anal Biochem,* **162,** 156-9.

Chou, T. C., *et al.* (1998) Alterations of nitric oxide synthase expression with aging and hypertension in rats. *Hypertension,* **31,** 643-8.

Christensen, H. N. (1990) Role of amino acid transport and countertransport in nutrition and metabolism. *Physiol Rev,* **70,** 43-77.

Christensen, H. N., *et al.* (1965) An amino acid transport system of unassigned function in the Ehrlich ascites tumor cell. *J Biol Chem,* **240,** 3601-8.

Closs, E. I. (1996) CATs, a family of three distinct mammalian cationic amino acid transporters. *Amino Acids,* **11,** 193-208.

Closs, E. I. (2002) Expression, regulation and function of carrier proteins for cationic amino acids. *Curr Opin Nephrol Hypertens,* **11,** 99-107.

Closs, E. I., *et al.* (1999) Cationic amino acid transporters (CATs). Targets for the manipulation of NO-synthase activity? *Pharm Biotechnol,* **12,** 229-49.

Closs, E. I., *et al.* (2000) Substrate supply for nitric-oxide synthase in macrophages and endothelial cells: role of cationic amino acid transporters. *Mol Pharmacol,* **57,** 68-74.

Cocks, T. M., *et al.* (1985a) In *Vascular Neuroeffector Mechanisms*(Eds, Bevan, J. A., Godfraind, T., Maxwell, R. A., Stoclet, J. S. and Worcel, M.) Elsevier, Amsterdam, pp. 131-6.

Cocks, T. M., *et al.* (1985b) Release and properties of endothelium-derived relaxing factor (EDRF) from endothelial cells in culture. *J Cell Physiol,* **123,** 310-20.

Coleman, J. K., *et al.* (1998) Autoradiographic identification of kidney angiotensin IV binding sites and angiotensin IV-induced renal cortical blood flow changes in rats. *Peptides,* **19,** 269-77.

Colton, C. A., *et al.* (2001) Apolipoprotein E acts to increase nitric oxide production in macrophages by stimulating arginine transport. *Biochim Biophys Acta,* **1535,** 134-44.

Comini, L., *et al.* (1996) Aorta and skeletal muscle NO synthase expression in experimental heart failure. *J Mol Cell Cardiol,* **28,** 2241-8.

Cooke, J. P. (2000) Does ADMA cause endothelial dysfunction? *Arterioscler Thromb Vasc Biol,* **20,** 2032-7.

Cosentino, F., *et al.* (2001) Reactive oxygen species mediate endothelium-dependent relaxations in tetrahydrobiopterin-deficient mice. *Arterioscler Thromb Vasc Biol,* **21,** 496-502.

Creager, M. A., *et al.* (1992) L-arginine improves endothelium-dependent vasodilation in hypercholesterolemic humans. *J Clin Invest,* **90,** 1248-53.

Csiszar, A., *et al.* (2002) Aging-induced phenotypic changes and oxidative stress impair coronary arteriolar function. *Circ Res,* **90,** 1159-66.

Cynober, L. A. (2002) Plasma amino acid levels with a note on membrane transport: characteristics, regulation, and metabolic significance. *Nutrition,* **18,** 761-6.

Dachman, W. D., *et al.* (1992) Bradykinin-induced venodilation is not impaired with aging in humans. *J Gerontol,* **47,** M166-70.

Daniels, G. M., *et al.* (1999) Regulated trafficking of the human dopamine transporter. Clathrin-mediated internalization and lysosomal degradation in response to phorbol esters. *J Biol Chem,* **274,** 35794-801.

Dargie, H. (1999) Diagnosis and assessment in heart failure. *Congest Heart Fail,* **5,** 275-282.

Davis, M. E., *et al.* (2003) Role of c-Src in regulation of endothelial nitric oxide synthase expression during exercise training. *Am J Physiol Heart Circ Physiol,* **284,** H1449-53.

de Belder, A. J., *et al.* (1993) Nitric oxide synthase activities in human myocardium. *Lancet,* **341,** 84-5.

De Jonge, W. J., *et al.* (2002) Arginine deficiency affects early B cell maturation and lymphoid organ development in transgenic mice. *J Clin Invest,* **110,** 1539-1548.

Deves, R., *et al.* (1993) N-ethylmaleimide discriminates between two lysine transport systems in human erythrocytes. *J Physiol (Lond),* **468,** 753-66.

Deves, R., *et al.* (1998) Transporters for cationic amino acids in animal cells: discovery, structure, and function. *Physiol Rev,* **78,** 487-545.

Deves, R., *et al.* (1992) Identification of a new transport system (y+L) in human erythrocytes that recognizes lysine and leucine with high affinity. *J Physiol (Lond),* **454,** 491-501.

Dibbs, Z., *et al.* (1999) Natural variability of circulating levels of cytokines and cytokine receptors in patients with heart failure: implications for clinical trials. *J Am Coll Cardiol,* **33,** 1935-42.

Dieber-Rotheneder, M., *et al.* (1991) Effect of oral supplementation with D-alpha-tocopherol on the vitamin E content of human low density lipoproteins and resistance to oxidation. *J Lipid Res,* **32,** 1325-32.

Dillon, P. F., *et al.* (2000) Natural electrophoresis of norepinephrine and ascorbic acid. *Biophys J,* **79,** 370-6.

Dohi, Y., *et al.* (1990) Activation of endothelial L-arginine pathway in resistance arteries. Effect of age and hypertension. *Hypertension,* **16,** 170-9.

Drab, M., *et al.* (2001) Loss of caveolae, vascular dysfunction, and pulmonary defects in caveolin-1 gene-disrupted mice. *Science,* **293,** 2449-52.

Drew, B., *et al.* (2002) Aging and the role of reactive nitrogen species. *Ann N Y Acad Sci,* **959,** 66-81.

Drexler, H. (1999a) Nitric oxide and coronary endothelial dysfunction in humans. *Cardiovasc Res,* **43,** 572-9.

Drexler, H. (1999b) Nitric oxide synthases in the failing human heart: a doubled-edged sword? [editorial; comment]. *Circulation,* **99,** 2972-5.

Drexler, H., *et al.* (1999) Endothelial dysfunction in human disease. *J Mol Cell Cardiol,* **31,** 51-60.

Drummond, G. R., *et al.* (2000) Transcriptional and posttranscriptional regulation of endothelial nitric oxide synthase expression by hydrogen peroxide. *Circ Res,* **86,** 347-54.

Durante, W. (2001) Regulation of L-arginine transport and metabolism in vascular smooth muscle cells. *Cell Biochem Biophys,* **35,** 19-34.

Durante, W., *et al.* (1996a) Selective induction of a cationic amino acid transporter by tumor necrosis factor-alpha in vascular endothelium. *Proc Assoc Am Physicians,* **108,** 356-61.

Durante, W., *et al.* (1996b) Platelet-derived growth factor regulates vascular smooth muscle cell proliferation by inducing cationic amino acid transporter gene expression. *J Biol Chem,* **271,** 11838-43.

Durante, W., *et al.* (1997) Lysophosphatidylcholine regulates cationic amino acid transport and metabolism in vascular smooth muscle cells. Role in polyamine biosynthesis. *J Biol Chem,* **272,** 30154-9.

Durante, W., *et al.* (2001) Transforming growth factor-beta(1) stimulates L-arginine transport and metabolism in vascular smooth muscle cells: role in polyamine and collagen synthesis. *Circulation,* **103,** 1121-7.

Egashira, K., *et al.* (1993) Effects of age on endothelium-dependent vasodilation of resistance coronary artery by acetylcholine in humans. *Circulation,* **88,** 77-81.

Elkayam, U., *et al.* (1999) Double-blind, placebo-controlled study to evaluate the effect of organic nitrates in patients with chronic heart failure treated with angiotensin-converting enzyme inhibition. *Circulation,* **99,** 2652-7.

Elkayam, U., *et al.* (2002) Impaired endothelium-mediated vasodilation in heart failure: clinical evidence and the potential for therapy. *J Card Fail,* **8,** 15-20.

Elsner, D., *et al.* (1995) Efficacy of prolonged infusion of urodilatin [ANP-(95-126)] in patients with congestive heart failure. *Am Heart J,* **129,** 766-73.

Ennezat, P. V., *et al.* (2001) Physical training in patients with chronic heart failure enhances the expression of genes encoding antioxidative enzymes. *J Am Coll Cardiol,* **38,** 194-8.

Escobales, N., *et al.* (2000) Relationship between NO synthesis, arginine transport, and intracellular arginine levels in vascular smooth muscle cells. *Amino Acids,* **19,** 451-68.

Esterbauer, H., *et al.* (1992) The role of lipid peroxidation and antioxidants in oxidative modification of LDL. *Free Radic Biol Med,* **13,** 341-90.

Everson, W. V., *et al.* (2001) Influence of caveolin, cholesterol, and lipoproteins on nitric oxide synthase: implications for vascular disease. *Trends Cardiovasc Med,* **11,** 246-50.

Fang, Z. Y., *et al.* (2002) Vascular dysfunction and heart failure: epiphenomenon or etiologic agent? *Am Heart J,* **143,** 383-90.

Farquharson, C. A., *et al.* (2002) Aldosterone induces acute endothelial dysfunction in vivo in humans: evidence for an aldosterone-induced vasculopathy. *Clin Sci (Lond),* **103,** 425-31.

Fernandez, J., *et al.* (2002a) Translation mediated by the internal ribosome entry site of the cat-1 mRNA is regulated by glucose availability in a PERK kinase-dependent manner. *J Biol Chem,* **277,** 11780-7.

Fernandez, J., *et al.* (2001) Internal ribosome entry site-mediated translation of a mammalian mRNA is regulated by amino acid availability. *J Biol Chem,* **276,** 12285-91.

Fernandez, J., *et al.* (2002b) Regulation of internal ribosomal entry site-mediated translation by phosphorylation of the translation initiation factor eIF2alpha. *J Biol Chem,* **277,** 19198-205.

Feron, O., *et al.* (1999) Hypercholesterolemia decreases nitric oxide production by promoting the interaction of caveolin and endothelial nitric oxide synthase. *J Clin Invest,* **103,** 897-905.

Feron, O., *et al.* (1998) The endothelial nitric-oxide synthase-caveolin regulatory cycle. *J Biol Chem,* **273,** 3125-8.

Ferrari, R., *et al.* (1998) Endothelial function and dysfunction in heart failure. *Eur Heart J,* **19 Suppl G,** G41-7.

Fichtlscherer, S., *et al.* (2001) Tumor necrosis factor antagonism with etanercept improves systemic endothelial vasoreactivity in patients with advanced heart failure. *Circulation,* **104,** 3023-5.

Finley, K. D., *et al.* (1995) A mammalian arginine/lysine transporter uses multiple promoters. *Proc Natl Acad Sci U S A,* **92,** 9378-82.

Flam, B. R., *et al.* (2001) Caveolar localization of arginine regeneration enzymes, argininosuccinate synthase, and lyase, with endothelial nitric oxide synthase. *Nitric Oxide,* **5,** 187-97.

Fleming, I., *et al.* (2003) Molecular mechanisms involved in the regulation of the endothelial nitric oxide synthase. *Am J Physiol Regul Integr Comp Physiol,* **284,** R1-R12.

Flores, C., *et al.* (2003) Rapid stimulation of L-arginine transport by D-glucose involves p42/44(mapk) and nitric oxide in human umbilical vein endothelium. *Circ Res,* **92,** 64-72.

Forstermann, U., *et al.* (1994) Nitric oxide synthase isozymes. Characterization, purification, molecular cloning, and functions. *Hypertension,* **23,** 1121-31.

Forstermann, U., *et al.* (1990) Regional distribution of EDRF/NO-synthesizing enzyme(s) in rat brain. *Biochem Biophys Res Commun,* **168,** 727-32.

Forstermann, U., *et al.* (1991) Calmodulin-dependent endothelium-derived relaxing factor/nitric oxide synthase activity is present in the particulate and cytosolic fractions of bovine aortic endothelial cells. *Proc Natl Acad Sci U S A,* **88,** 1788-92.

Fulton, D., *et al.* (2001) Post-translational control of endothelial nitric oxide synthase: why isn't calcium/calmodulin enough? *J Pharmacol Exp Ther,* **299,** 818-24.

Furchgott, R. F., *et al.* (1980) The obligatory role of endothelial cells in the relaxation of arterial smooth muscle by acetylcholine. *Nature,* **288,** 373-6.

Gambaryan, S., *et al.* (1996) Expression of type II cGMP-dependent protein kinase in rat kidney is regulated by dehydration and correlated with renin gene expression. *J Clin Invest,* **98,** 662-70.

Garcia-Cardena, G., *et al.* (1998) Dynamic activation of endothelial nitric oxide synthase by Hsp90. *Nature,* **392,** 821-4.

Garcia-Cardena, G., *et al.* (1996a) Endothelial nitric oxide synthase is regulated by tyrosine phosphorylation and interacts with caveolin-1. *J Biol Chem,* **271,** 27237-40.

Garcia-Cardena, G., *et al.* (1997) Dissecting the interaction between nitric oxide synthase (NOS) and caveolin. Functional significance of the nos caveolin binding domain in vivo. *J Biol Chem,* **272,** 25437-40.

Garcia-Cardena, G., *et al.* (1996b) Targeting of nitric oxide synthase to endothelial cell caveolae via palmitoylation: implications for nitric oxide signaling. *Proc Natl Acad Sci U S A,* **93,** 6448-53.

Garlichs, C. D., *et al.* (2000) Decreased plasma concentrations of L-hydroxy-arginine as a marker of reduced NO formation in patients with combined cardiovascular risk factors. *J Lab Clin Med,* **135,** 419-25.

Gazzola, G. C., *et al.* (1981) The cluster-tray method for rapid measurement of solute fluxes in adherent cultured cells. *Anal Biochem,* **115,** 368-74.

Gewaltig, M. T., *et al.* (2002) Vasoprotection by nitric oxide: mechanisms and therapeutic potential. *Cardiovasc Res,* **55,** 250-60.

Gielen, S., *et al.* (2002) Exercise training and endothelial dysfunction in coronary artery disease and chronic heart failure. From molecular biology to clinical benefits. *Minerva Cardioangiol,* **50,** 95-106.

Gill, D. J., *et al.* (1996) Interleukin-1 beta and tumor necrosis factor-alpha stimulate the cat-2 gene of the L-arginine transporter in cultured vascular smooth muscle cells. *J Biol Chem,* **271,** 11280-3.

Giugliano, D., *et al.* (1997a) Vascular effects of acute hyperglycemia in humans are reversed by L-arginine. Evidence for reduced availability of nitric oxide during hyperglycemia. *Circulation,* **95,** 1783-90.

Giugliano, D., *et al.* (1997b) The vascular effects of L-Arginine in humans. The role of endogenous insulin. *J Clin Invest,* **99,** 433-8.

Godecke, A., *et al.* (2001) Inotropic response to beta-adrenergic receptor stimulation and anti-adrenergic effect of ACh in endothelial NO synthase-deficient mouse hearts. *J Physiol,* **532,** 195-204.

Goineau, S., *et al.* (2002) Systemic and regional hemodynamic and cardiac remodeling effects of candesartan in dilated cardiomyopathic hamsters with advanced congestive heart failure. *J Cardiovasc Pharmacol,* **40,** 189-200.

Goligorsky, M. S., *et al.* (2002) Relationships between caveolae and eNOS: everything in proximity and the proximity of everything. *Am J Physiol Renal Physiol,* **283,** F1-F10.

Goll, D. E., *et al.* (2003) The calpain system. *Physiol Rev,* **83,** 731-801.

Gonzalez-Fernandez, F., *et al.* (2001) Cerivastatin prevents tumor necrosis factor-alpha-induced downregulation of endothelial nitric oxide synthase: role of endothelial cytosolic proteins. *Atherosclerosis,* **155,** 61-70.

Gorelik, G., *et al.* (1998) Angiotensin 1-7 induces bradykinin-mediated relaxation in porcine coronary artery. *J Pharmacol Exp Ther,* **286,** 403-10.

Gorlach, A., *et al.* (2000) A gp91phox containing NADPH oxidase selectively expressed in endothelial cells is a major source of oxygen radical generation in the arterial wall. *Circ Res,* **87,** 26-32.

Gotlieb, A. I. (1990) The endothelial cytoskeleton: organization in normal and regenerating endothelium. *Toxicol Pathol,* **18,** 603-17.

Graf, P., *et al.* (2001) The transport activity of the human cationic amino acid transporter hCAT-1 is downregulated by activation of protein kinase C. *Br J Pharmacol,* **132,** 1193-200.

Gragasin, F. S., *et al.* (2003) Estrogen reduces angiotensin II-induced nitric oxide synthase and NAD(P)H oxidase expression in endothelial cells. *Arterioscler Thromb Vasc Biol,* **23,** 38-44.

Gratton, J. P., *et al.* (2000) Reconstitution of an endothelial nitric-oxide synthase (eNOS), hsp90, and caveolin-1 complex in vitro. Evidence that hsp90 facilitates calmodulin stimulated displacement of eNOS from caveolin-1. *J Biol Chem,* **275,** 22268-72.

Greene, B., *et al.* (1993) Characterization of L-arginine transport by pulmonary artery endothelial cells. *Am J Physiol,* **264,** L351-6.

Gregg, A. R., *et al.* (1998) Limb reduction defects in endothelial nitric oxide synthase-deficient mice. *Am J Physiol,* **275,** H2319-24.

Griendling, K. K., *et al.* (1994) Angiotensin II stimulates NADH and NADPH oxidase activity in cultured vascular smooth muscle cells. *Circ Res,* **74,** 1141-8.

Gryglewski, R. J., *et al.* (1996) Treatment with L-arginine is likely to stimulate generation of nitric oxide in patients with peripheral arterial obstructive disease. *Wien Klin Wochenschr,* **108,** 111-6.

Hall, K. L., *et al.* (1993) Identification and characterization of a novel angiotensin binding site in cultured vascular smooth muscle cells that is specific for the hexapeptide (3-8) fragment of angiotensin II, angiotensin IV. *Regul Pept,* **44,** 225-32.

Hall, K. L., *et al.* (1995) Characterization of a functional angiotensin IV receptor on coronary microvascular endothelial cells. *Regul Pept,* **58,** 107-15.

Hambrecht, R., *et al.* (2000) Effect of exercise on coronary endothelial function in patients with coronary artery disease. *N Engl J Med,* **342,** 454-60.

Hamilton, C. A., *et al.* (2002) NAD(P)H oxidase inhibition improves endothelial function in rat and human blood vessels. *Hypertension,* **40,** 755-62.

Hammermann, R., *et al.* (2000) Nuclear factor-kappaB mediates simultaneous induction of inducible nitric-oxide synthase and Up-regulation of the cationic amino acid transporter CAT-2B in rat alveolar macrophages. *Mol Pharmacol,* **58,** 1294-302.

Hanssen, H., *et al.* (1998) Increased L-arginine transport in human erythrocytes in chronic heart failure [published erratum appears in Clin Sci (Colch) 1998 Mar;94(3):333]. *Clin Sci (Colch),* **94,** 43-8.

Harding, J. W., *et al.* (1992) Identification of an AII(3-8) [AIV] binding site in guinea pig hippocampus. *Brain Res,* **583,** 340-3.

Harding, J. W., *et al.* (1994) AT4 receptors: specificity and distribution. *Kidney Int,* **46,** 1510-2.

Hardy, T. A., *et al.* (2002) Coordinate regulation of L-arginine uptake and nitric oxide synthase activity in cultured endothelial cells. *Free Radic Biol Med,* **32,** 122-31.

Harrison, J. R., *et al.* (1990) Interleukin-1 alpha and phorbol ester inhibit collagen synthesis in osteoblastic MC3T3-E1 cells by a transcriptional mechanism. *Mol Endocrinol,* **4,** 184-90.

Hayakawa, H., *et al.* (1997) The link among nitric oxide synthase activity, endothelial function, and aortic and ventricular hypertrophy in hypertension. *Hypertension,* **29,** 235-41.

Hayashi, T., *et al.* (1999) Endothelium-dependent relaxation of rabbit atherosclerotic aorta was not restored by control of hyperlipidemia: the possible role of peroxynitrite (ONOO(-)). *Atherosclerosis,* **147,** 349-63.

Haywood, G. A., *et al.* (1996) Expression of inducible nitric oxide synthase in human heart failure. *Circulation,* **93,** 1087-94.

Hecker, M., *et al.* (1990) The metabolism of L-arginine and its significance for the biosynthesis of endothelium-derived relaxing factor: cultured endothelial cells recycle L-citrulline to L-arginine. *Proc Natl Acad Sci U S A,* **87,** 8612-6.

Helenius, A., *et al.* (2001) Intracellular functions of N-linked glycans. *Science,* **291,** 2364-9.

Hemmens, B., *et al.* (1998) Enzymology of nitric oxide synthases. *Methods Mol Biol,* **100,** 1-32.

Herbst, J. J., *et al.* (1997) Insulin stimulates cell surface aminopeptidase activity toward vasopressin in adipocytes. *Am J Physiol,* **272,** E600-6.

Hernandez-Perera, O., *et al.* (1998) Effects of the 3-hydroxy-3-methylglutaryl-CoA reductase inhibitors, atorvastatin and simvastatin, on the expression of endothelin-1 and endothelial nitric oxide synthase in vascular endothelial cells. *J Clin Invest,* **101,** 2711-9.

Herrera, E., *et al.* (2001) Vitamin E: action, metabolism and perspectives. *J Physiol Biochem,* **57,** 43-56.

Herrmann, J., *et al.* (2001) The endothelium: dysfunction and beyond. *J Nucl Cardiol,* **8,** 197-206.

Heymes, C., *et al.* (2000) Cyclo-oxygenase-1 and -2 contribution to endothelial dysfunction in ageing. *Br J Pharmacol,* **131,** 804-10.

Higashi, Y., *et al.* (1995) Intravenous administration of L-arginine inhibits angiotensin-converting enzyme in humans. *J Clin Endocrinol Metab,* **80,** 2198-202.

Higashi, Y., *et al.* (1997) Aging and severity of hypertension attenuate endothelium-dependent renal vascular relaxation in humans. *Hypertension,* **30,** 252-8.

Hinschen, A. K., *et al.* (2001) Age-related changes in adenosine-mediated relaxation of coronary and aortic smooth muscle. *Am J Physiol Heart Circ Physiol,* **280,** H2380-9.

Hirono, A., *et al.* (1996) [Human red cell metabolism and its pathophysiology]. *Nippon Rinsho,* **54,** 2326-30.

Hogg, N., *et al.* (1993) Peroxynitrite and atherosclerosis. *Biochem Soc Trans,* **21,** 358-62.

Hortelano, S., *et al.* (1993) Phorbol esters induce nitric oxide synthase and increase arginine influx in cultured peritoneal macrophages. *FEBS Lett,* **320,** 135-9.

Hosokawa, H., *et al.* (1999) Neuron-specific expression of cationic amino acid transporter 3 in the adult rat brain. *Brain Res,* **838,** 158-65.

Hosokawa, H., *et al.* (1997) Cloning and characterization of a brain-specific cationic amino acid transporter. *J Biol Chem,* **272,** 8717-22.

Howes, L. G., *et al.* (1997) Lipoproteins and cardiovascular reactivity. *Br J Clin Pharmacol,* **44,** 319-24.

Huang, P. L., *et al.* (1995) Hypertension in mice lacking the gene for endothelial nitric oxide synthase. *Nature,* **377,** 239-42.

Hughes, A. D. (1998) Molecular and cellular mechanisms of action of angiotensin II (AT1) receptors in vascular smooth muscle. *J Hum Hypertens,* **12,** 275-81.

Huotari, V., *et al.* (1992) Different organizational states of fodrin in cultured MDCK cells are induced by treatment with low pH, calmodulin antagonist TFP, and tumor promoter PMA. *J Cell Physiol,* **153,** 340-52.

Hyatt, S. L., *et al.* (1997) Adaptive regulation of the cationic amino acid transporter-1 (Cat-1) in Fao cells. *J Biol Chem,* **272,** 19951-7.

Ignarro, L., *et al.* (1995) *Nitric Oxide: Biochemistry, Molecular Biology, and Therapeutic Implications,* Academic Press, San Diego.

Ignarro, L. J., *et al.* (1987) Endothelium-derived relaxing factor from pulmonary artery and vein possesses pharmacologic and chemical properties identical to those of nitric oxide radical. *Circ Res,* **61,** 866-79.

Ikeda, U., *et al.* (1995) Angiotensin II augments cytokine-stimulated nitric oxide synthesis in rat cardiac myocytes. *Circulation,* **92,** 2683-9.

Ikeda, U., *et al.* (1997) Nitric oxide and cardiac failure. *Clin Cardiol,* **20,** 837-41.

Imaizumi, T., *et al.* (1992) Effects of L-arginine on forearm vessels and responses to acetylcholine. *Hypertension,* **20,** 511-7.

Irie, K., *et al.* (1997) Cationic amino acid transporter-2 mRNA induction by tumor necrosis factor-alpha in vascular endothelial cells. *Eur J Pharmacol,* **339,** 289-93.

Ischiropoulos, H., *et al.* (1992) Peroxynitrite-mediated tyrosine nitration catalyzed by superoxide dismutase. *Arch Biochem Biophys,* **298,** 431-7.

Ishibashi, Y., *et al.* (2001) An inhibitor of inducible nitric oxide synthase decreases forearm blood flow in patients with congestive heart failure. *J Am Coll Cardiol,* **38,** 1470-6.

Ito, K., *et al.* (1997) A new member of the cationic amino acid transporter family is preferentially expressed in adult mouse brain. *J Biol Chem,* **272,** 26780-6.

Jakob, G., *et al.* (1995) Ergometric exercise testing and sensitivity of cyclic guanosine 3',5'-monophosphate (cGMP) in diagnosing asymptomatic left ventricular dysfunction. *Br Heart J,* **73,** 145-50.

Jay, M. T., *et al.* (1997) Modulation of vascular tone by low density lipoproteins: effects on L-arginine transport and nitric oxide synthesis. *Exp Physiol,* **82,** 349-60.

Jess, U., *et al.* (2002) Interaction of the C-terminal region of the rat serotonin transporter with MacMARCKS modulates 5-HT uptake regulation by protein kinase C. *Biochem Biophys Res Commun,* **294,** 272-9.

Jimenez, A., *et al.* (2001) Regulation of endothelial nitric oxide synthase expression in the vascular wall and in mononuclear cells from hypercholesterolemic rabbits. *Circulation,* **104,** 1822-30.

Jin, L., *et al.* (2001) Endothelial cell dysfunction in a model of oxidative stress. *Med Sci Monit,* **7,** 585-91.

Johnson, A. R., *et al.* (1977) Metabolism of vasoactive peptides by human endothelial cells in culture. Angiotensin I converting enzyme (kininase II) and angiotensinase. *J Clin Invest,* **59,** 684-95.

Ju, H., *et al.* (1997) Direct interaction of endothelial nitric-oxide synthase and caveolin-1 inhibits synthase activity. *J Biol Chem,* **272,** 18522-5.

Kakuda, D. K., *et al.* (1999) CAT2-mediated L-arginine transport and nitric oxide production in activated macrophages. *Biochem J,* **340,** 549-53.

Kalandadze, A., *et al.* (2002) Protein kinase C activation decreases cell surface expression of the GLT-1 subtype of glutamate transporter. Requirement of a carboxyl-terminal domain and partial dependence on serine 486. *J Biol Chem,* **277,** 45741-50.

Kamada, Y., *et al.* (2001) Vascular endothelial dysfunction resulting from L-arginine deficiency in a patient with lysinuric protein intolerance. *J Clin Invest,* **108,** 717-24.

Kanai, Y., *et al.* (2001) Heterodimeric amino acid transporters: molecular biology and pathological and pharmacological relevance. *Curr Drug Metab,* **2,** 339-54.

Kang, E. S., *et al.* (2000) Normal circulating adult human red blood cells contain inactive NOS proteins. *J Lab Clin Med,* **135,** 444-51.

Katusic, Z. S. (2001) Vascular endothelial dysfunction: does tetrahydrobiopterin play a role? *Am J Physiol Heart Circ Physiol,* **281,** H981-6.

Katz, S. D. (1995) The role of endothelium-derived vasoactive substances in the pathophysiology of exercise intolerance in patients with congestive heart failure. *Prog Cardiovasc Dis,* **38,** 23-50.

Katz, S. D. (1997) Mechanisms and implications of endothelial dysfunction in congestive heart failure. *Curr Opin Cardiol,* **12,** 259-64.

Katz, S. D., *et al.* (1999) Decreased activity of the L-arginine-nitric oxide metabolic pathway in patients with congestive heart failure. *Circulation,* **99,** 2113-7.

Katz, S. D., *et al.* (1994) Pathophysiological correlates of increased serum tumor necrosis factor in patients with congestive heart failure. Relation to nitric oxide-dependent vasodilation in the forearm circulation. *Circulation,* **90,** 12-6.

Kayanoki, Y., *et al.* (1999) Reduced nitric oxide production by L-arginine deficiency in lysinuric protein intolerance exacerbates intravascular coagulation. *Metabolism,* **48,** 1136-40.

Kaye, D. M., *et al.* (2000) In vivo and in vitro evidence for impaired arginine transport in human heart failure. *Circulation,* **102,** 2707-12.

Kaye, D. M., *et al.* (1998) The failing human heart does not release nitrogen oxides. *Life Sci,* **62,** 883-7.

Kaye, D. M., *et al.* (2002) Reduced myocardial and systemic L-arginine uptake in heart failure. *Circ Res,* **91,** 1198-203.

Kaye, D. M., *et al.* (1997) S-nitrosothiols inhibit neuronal norepinephrine transport. *Am J Physiol,* **272,** H875-83.

Khan, A. S., *et al.* (2002) Growth hormone, insulin-like growth factor-1 and the aging cardiovascular system. *Cardiovasc Res,* **54,** 25-35.

Kiemer, A. K., *et al.* (2001) Induction of L-arginine transport is inhibited by atrial natriuretic peptide: a peptide hormone as a novel regulator of inducible nitric-oxide synthase substrate availability. *Mol Pharmacol,* **60,** 421-6.

Kikuta, K., *et al.* (1998) High-affinity arginine transport of bovine aortic endothelial cells is impaired by lysophosphatidylcholine. *Circ Res,* **83,** 1088-96.

Kilberg, M. S., *et al.* (1993) Recent advances in mammalian amino acid transport. *Annu Rev Nutr,* **13,** 137-65.

Kim, J. W., *et al.* (1991) Transport of cationic amino acids by the mouse ecotropic retrovirus receptor [see comments]. *Nature,* **352,** 725-8.

Koide, M., *et al.* (1994) Expression of nitric oxide synthase by cytokines in vascular smooth muscle cells. *Hypertension,* **23,** I45-8.

Koide, Y., *et al.* (2003) Differential induction of protein kinase C isoforms at the cardiac hypertrophy stage and congestive heart failure stage in Dahl salt-sensitive rats. *Hypertens Res,* **26,** 421-6.

Komers, R., *et al.* (2000) Effect of ACE inhibition and angiotensin AT1 receptor blockade on renal and blood pressure response to L-arginine in humans. *J Hypertens,* **18,** 51-9.

Kramar, E. A., *et al.* (1998) Role of nitric oxide in angiotensin IV-induced increases in cerebral blood flow. *Regul Pept,* **74,** 185-92.

Krantz, D. E., *et al.* (1997) Phosphorylation of a vesicular monoamine transporter by casein kinase II. *J Biol Chem,* **272,** 6752-9.

Krizbai, I., *et al.* (1995) Expression of protein kinase C family members in the cerebral endothelial cells. *J Neurochem,* **65,** 459-62.

Krotova, K. Y., *et al.* (2003) Classical isoforms of PKC as regulators of CAT-1 transporter activity in pulmonary artery endothelial cells. *Am J Physiol Lung Cell Mol Physiol,* **284,** L1037-44.

Kugiyama, K., *et al.* (1992) Lysophosphatidylcholine inhibits surface receptor-mediated intracellular signals in endothelial cells by a pathway involving protein kinase C activation. *Circ Res,* **71,** 1422-8.

Lancaster, J. R., Jr. (1994) Simulation of the diffusion and reaction of endogenously produced nitric oxide. *Proc Natl Acad Sci U S A,* **91,** 8137-41.

Landmesser, U., *et al.* (2002) Vascular oxidative stress and endothelial dysfunction in patients with chronic heart failure: role of xanthine-oxidase and extracellular superoxide dismutase. *Circulation,* **106,** 3073-8.

Lang, D., *et al.* (2000) Coronary microvascular endothelial cell redox state in left ventricular hypertrophy : the role of angiotensin II. *Circ Res,* **86,** 463-9.

Lantin-Hermoso, R. L., *et al.* (1997) Estrogen acutely stimulates nitric oxide synthase activity in fetal pulmonary artery endothelium. *Am J Physiol,* **273,** L119-26.

Latchman, D. S. (2001) Heat shock proteins and cardiac protection. *Cardiovasc Res,* **51,** 637-46.

Laughlin, M. H., *et al.* (2001) Training induces nonuniform increases in eNOS content along the coronary arterial tree. *J Appl Physiol,* **90,** 501-10.

Laurent, S., *et al.* (1996) The arterial wall: a new pharmacological and therapeutic target. *Fundam Clin Pharmacol,* **10,** 243-57.

Lerman, A., *et al.* (1992) Plasma endothelin concentrations in humans with end-stage heart failure and after heart transplantation. *J Am Coll Cardiol,* **20,** 849-53.

Lerner, R. A., *et al.* (1981) Chemically synthesized peptides predicted from the nucleotide sequence of the hepatitis B virus genome elicit antibodies reactive with the native envelope protein of Dane particles. *Proc Natl Acad Sci U S A,* **78,** 3403-7.

Levine, B., *et al.* (1990) Elevated circulating levels of tumor necrosis factor in severe chronic heart failure. *N Engl J Med,* **323,** 236-41.

Li, H., *et al.* (1998) Activation of protein kinase C alpha and/or epsilon enhances transcription of the human endothelial nitric oxide synthase gene. *Mol Pharmacol,* **53,** 630-7.

Li, H., *et al.* (2002) Physiological mechanisms regulating the expression of endothelial-type NO synthase. *Nitric Oxide,* **7,** 132-47.

Liao, J. K., *et al.* (1995a) Regulation of G-protein alpha i2 subunit expression by oxidized low-density lipoprotein. *J Clin Invest,* **95,** 1457-63.

Liao, J. K., *et al.* (1995b) Oxidized low-density lipoprotein decreases the expression of endothelial nitric oxide synthase. *J Biol Chem,* **270,** 319-24.

Liu, S. F., *et al.* (1996) Differential regulation of the constitutive and inducible nitric oxide synthase mRNA by lipopolysaccharide treatment in vivo in the rat. *Crit Care Med,* **24,** 1219-25.

Liu, W. S., *et al.* (1998) The sevenfold way of PKC regulation. *Cell Signal,* **10,** 529-42.

Loscalzo, J. (2000) What we know and don't know about L-arginine and NO. *Circulation,* **101,** 2126-9.

Low, B. C., *et al.* (1995) Angiotensin II stimulates system y+ and cationic amino acid transporter gene expression in cultured vascular smooth muscle cells. *J Biol Chem,* **270,** 27577-83.

Lowry, O. H., *et al.* (1951) Protein measurement with the Folin Phenol reagent. *J Biol Chem,* **193,** 265-75.

Lu, J. L., *et al.* (1996) Downregulation of endothelial constitutive nitric oxide synthase expression by lipopolysaccharide. *Biochem Biophys Res Commun,* **225,** 1-5.

Lu, X., *et al.* (2000) Ecotropic murine leukemia virus receptor is physically associated with caveolin and membrane rafts. *Virology,* **276,** 251-8.

Luo, Z., *et al.* (2000) Acute modulation of endothelial Akt/PKB activity alters nitric oxide-dependent vasomotor activity in vivo. *J Clin Invest,* **106,** 493-9.

Luscher, T. F., *et al.* (1996) Endothelial function as an end-point in interventional trials: concepts, methods and current data. *J Hypertens Suppl,* **14,** S111-9; discussion S119-21.

Ma, R., *et al.* (2001) Protein kinase C activates store-operated Ca(2+) channels in human glomerular mesangial cells. *J Biol Chem,* **276,** 25759-65.

MacAllister, R. J., *et al.* (1995) Vascular and hormonal responses to arginine: provision of substrate for nitric oxide or non-specific effect? *Clin Sci (Lond),* **89,** 183-90.

MacLeod, C. L., *et al.* (1990) Activated T cells express a novel gene on chromosome 8 that is closely related to the murine ecotropic retroviral receptor. *Mol Cell Biol,* **10,** 3663-74.

MacLeod, C. L., *et al.* (1994) y(+)-type cationic amino acid transport: expression and regulation of the mCAT genes. *J Exp Biol,* **196,** 109-21.

Macleod, C. L., *et al.* (1996) Regulation of CAT: Cationic amino acid transporter gene expression. *Amino Acids,* **11,** 171-191.

Mak, S., *et al.* (2001) The oxidative stress hypothesis of congestive heart failure: radical thoughts. *Chest,* **120,** 2035-46.

Mann, G. E., *et al.* (2003) Regulation of Amino Acid and Glucose Transporters in Endothelial and Smooth Muscle Cells. *Physiol Rev,* **83,** 183-252.

Massberg, S., *et al.* (1999) Increased adhesion and aggregation of platelets lacking cyclic guanosine 3',5'-monophosphate kinase I. *J Exp Med,* **189,** 1255-64.

Masuda, M., *et al.* (1999) Analysis of receptor usage by ecotropic murine retroviruses, using green fluorescent protein-tagged cationic amino acid transporters. *J Virol,* **73,** 8623-9.

Matsuoka, H. (2001) Endothelial dysfunction associated with oxidative stress in human. *Diabetes Res Clin Pract,* **54 Suppl 2,** S65-72.

Matsuoka, Y., *et al.* (2000) Adducin: structure, function and regulation. *Cell Mol Life Sci,* **57,** 884-95.

Matthews, J. C., *et al.* (1999) Placental anionic and cationic amino acid transporter expression in growth hormone overexpressing and null IGF-II or null IGF-I receptor mice. *Placenta,* **20,** 639-50.

Matz, R. L., *et al.* (2000) Age-related endothelial dysfunction with respect to nitric oxide, endothelium-derived hyperpolarizing factor and cyclooxygenase products. *Physiol Res,* **49,** 11-8.

Mayhan, W. G., *et al.* (1990) Effects of aging on responses of cerebral arterioles. *Am J Physiol,* **258,** H1138-43.

McAllister, R. M., *et al.* (1995) Contribution of endothelium-derived nitric oxide (EDNO) to the skeletal muscle blood flow response to exercise. *Med Sci Sports Exerc,* **27,** 1145-51.

McCabe, T. J., *et al.* (2000) Enhanced electron flux and reduced calmodulin dissociation may explain "calcium-independent" eNOS activation by phosphorylation. *J Biol Chem,* **275,** 6123-8.

McDonald, K. K., *et al.* (1997) A caveolar complex between the cationic amino acid transporter 1 and endothelial nitric-oxide synthase may explain the "arginine paradox". *J Biol Chem,* **272,** 31213-6.

McQuillan, L. P., *et al.* (1994) Hypoxia inhibits expression of eNOS via transcriptional and posttranscriptional mechanisms. *Am J Physiol,* **267,** H1921-7.

McVeigh, G. E., *et al.* (2003) Endothelial dysfunction and the metabolic syndrome. *Curr Diab Rep,* **3,** 87-92.

Mehta, J. L., *et al.* (1995) Identification of constitutive and inducible forms of nitric oxide synthase in human platelets. *J Lab Clin Med,* **125,** 370-7.

Melikian, H. E., *et al.* (1999) Membrane trafficking regulates the activity of the human dopamine transporter. *J Neurosci,* **19,** 7699-710.

Mellor, H., *et al.* (1998) The extended protein kinase C superfamily. *Biochem J,* **332 (Pt 2),** 281-92.

Mendes Ribeiro, A. C., *et al.* (2001) Abnormalities in L-arginine transport and nitric oxide biosynthesis in chronic renal and heart failure. *Cardiovasc Res,* **49,** 697-712.

Mendes Ribeiro, A. C., *et al.* (1999) Identification of system y+L as the high-affinity transporter for L-arginine in human platelets: up-regulation of L-arginine influx in uraemia. *Pflugers Arch,* **438,** 573-5.

Meneilly, G. S., *et al.* (2001) Contrasting effects of L-arginine on insulin-mediated blood flow and glucose disposal in the elderly. *Metabolism,* **50,** 194-9.

Michell, B. J., *et al.* (2001) Coordinated control of endothelial nitric-oxide synthase phosphorylation by protein kinase C and the cAMP-dependent protein kinase. *J Biol Chem,* **276,** 17625-8.

Mitchell, J. A., *et al.* (1990) Cultured endothelial cells maintain their L-arginine level despite the continuous release of EDRF. *Eur J Pharmacol,* **182,** 573-6.

Moeller, I., *et al.* (1999) Up regulation of AT4 receptor levels in carotid arteries following balloon injury. *Regul Pept,* **83,** 25-30.

Mollnau, H., *et al.* (2002a) Effects of angiotensin II infusion on the expression and function of NAD(P)H oxidase and components of nitric oxide/cGMP signaling. *Circ Res,* **90,** E58-65.

Mollnau, H., *et al.* (2002b) Effects of angiotensin II infusion on the expression and function of NAD(P)H oxidase and components of nitric oxide/cGMP signaling. *Circ Res,* **90,** E58-65.

Mombouli, J. V. (1997) ACE inhibition, endothelial function and coronary artery lesions. Role of kinins and nitric oxide. *Drugs,* **54,** 12-22.

Mombouli, J. V., *et al.* (1999) Endothelial dysfunction: from physiology to therapy. *J Mol Cell Cardiol,* **31,** 61-74.

Moncada, S., *et al.* (1993) The L-arginine-nitric oxide pathway. *N Engl J Med,* **329,** 2002-12.

Mori, M., *et al.* (2000) Regulation of nitric oxide production by arginine metabolic enzymes. *Biochem Biophys Res Commun,* **275,** 715-9.

Mukherjee, S., *et al.* (2001) Effects of oxidized low density lipoprotein on nitric oxide synthetase and protein kinase C activities in bovine endothelial cells. *Cell Mol Biol (Noisy-le-grand),* **47,** 1051-8.

Mungrue, I. N., *et al.* (2002) The role of NOS in heart failure: lessons from murine genetic models. *Heart Fail Rev,* **7,** 407-22.

Murata, T., *et al.* (2001) Hypoxia impairs endothelium-dependent relaxation in organ cultured pulmonary artery. *Eur J Pharmacol,* **421,** 45-53.

Murohara, T., *et al.* (1999) Effects of atrial and brain natriuretic peptides on lysophosphatidylcholine-mediated endothelial dysfunction. *J Cardiovasc Pharmacol,* **34,** 870-8.

Muzykantov, V. R., *et al.* (1996) Immunotargeting of antioxidant enzyme to the pulmonary endothelium. *Proc Natl Acad Sci U S A,* **93,** 5213-8.

Nadaud, S., *et al.* (1996) Sustained increase in aortic endothelial nitric oxide synthase expression in vivo in a model of chronic high blood flow. *Circ Res,* **79,** 857-63.

Napoli, C., *et al.* (2001) Nitric oxide and atherosclerosis. *Nitric Oxide,* **5,** 88-97.

Napoli, R., *et al.* (2002) Growth hormone corrects vascular dysfunction in patients with chronic heart failure. *J Am Coll Cardiol,* **39,** 90-5.

Nelin, L. D., *et al.* (2001) Cytokine treatment increases arginine metabolism and uptake in bovine pulmonary arterial endothelial cells. *Am J Physiol Lung Cell Mol Physiol,* **281,** L1232-9.

Nguyen, T. T., *et al.* (1996) N-linked oligosaccharides are required for cell surface expression of the norepinephrine transporter but do not influence substrate or inhibitor recognition. *J Neurochem,* **67,** 645-55.

Nichols, W. W., *et al.* (2001) Arterial elastance and wave reflection augmentation of systolic blood pressure: deleterious effects and implications for therapy. *J Cardiovasc Pharmacol Ther,* **6,** 5-21.

Nicholson, B., *et al.* (2001) Sustained nitric oxide production in macrophages requires the arginine transporter CAT2. *J Biol Chem,* **276,** 15881-5.

Nicholson, B., *et al.* (1998) Increased Cat3-mediated cationic amino acid transport functionally compensates in Cat1 knockout cell lines. *J Biol Chem,* **273,** 14663-6.

Nilius, B., *et al.* (2001) Ion channels and their functional role in vascular endothelium. *Physiol Rev,* **81,** 1415-59.

Nishida, K., *et al.* (1992) Molecular cloning and characterization of the constitutive bovine aortic endothelial cell nitric oxide synthase. *J Clin Invest,* **90,** 2092-6.

Noris, M., *et al.* (1995) Nitric oxide synthesis by cultured endothelial cells is modulated by flow conditions. *Circ Res,* **76,** 536-43.

Nussler, A. K., *et al.* (1994) Coinduction of nitric oxide synthase and argininosuccinate synthetase in a murine macrophage cell line. Implications for regulation of nitric oxide production. *J Biol Chem,* **269,** 1257-61.

Ogonowski, A. A., *et al.* (2000a) Effects of NO donors and synthase agonists on endothelial cell uptake of L-Arg and superoxide production. *Am J Physiol Cell Physiol,* **278,** C136-43.

Ogonowski, A. A., *et al.* (2000b) Effects of NO donors and synthase agonists on endothelial cell uptake of L-Arg and superoxide production. *Am J Physiol Cell Physiol,* **278,** C136-43.

Olson, S. C., *et al.* (1997) ANG II stimulates endothelial nitric oxide synthase expression in bovine pulmonary artery endothelium. *Am J Physiol,* **273,** L315-21.

Opie, L. H. (2002) The neuroendocrinology of congestive heart failure. *Cardiovasc J S Afr,* **13,** 171-8.

Ozaki, M., *et al.* (2002) Overexpression of endothelial nitric oxide synthase accelerates atherosclerotic lesion formation in apoE-deficient mice. *J Clin Invest,* **110,** 331-40.

Packer, M. (1995) Is tumor necrosis factor an important neurohormonal mechanism in chronic heart failure? *Circulation,* **92,** 1379-82.

Palacin, M., *et al.* (1998) Molecular biology of mammalian plasma membrane amino acid transporters. *Physiol Rev,* **78,** 969-1054.

Palacin, M., *et al.* (2001) The amino acid transport system b(o,+) and cystinuria. *Mol Membr Biol,* **18,** 21-6.

Palmer, R. M., *et al.* (1988) Vascular endothelial cells synthesize nitric oxide from L-arginine. *Nature,* **333,** 664-6.

Palmer, R. M., *et al.* (1987) Nitric oxide release accounts for the biological activity of endothelium-derived relaxing factor. *Nature,* **327,** 524-6.

Pan, M., *et al.* (1995a) Protein kinase C-dependent regulation of L-arginine transport activity in Caco-2 intestinal cells. *Biochim Biophys Acta,* **1239,** 27-32.

Pan, M., *et al.* (1995b) TNF-stimulated arginine transport by human vascular endothelium requires activation of protein kinase C. *Ann Surg,* **221,** 590-600; discussion 600-1.

Panza, J. A., *et al.* (1993) Effect of increased availability of endothelium-derived nitric oxide precursor on endothelium-dependent vascular relaxation in normal subjects and in patients with essential hypertension. *Circulation,* **87,** 1475-81.

Papapetropoulos, A., *et al.* (1999) Molecular control of nitric oxide synthases in the cardiovascular system. *Cardiovasc Res,* **43,** 509-20.

Patel, J. M., *et al.* (1999) Increased expression of calreticulin is linked to ANG IV-mediated activation of lung endothelial NOS. *Am J Physiol,* **277,** L794-801.

Patel, J. M., *et al.* (1998) Angiotensin IV receptor-mediated activation of lung endothelial NOS is associated with vasorelaxation. *Am J Physiol,* **275,** L1061-8.

Patel, V., *et al.* (1996) Protein kinase C isoforms in bovine aortic endothelial cells: role in regulation of P2Y- and P2U-purinoceptor-stimulated prostacyclin release. *Br J Pharmacol,* **118,** 123-30.

Pedersen, E. B., *et al.* (1986) Angiotensin II, aldosterone and arginine vasopressin in plasma in congestive heart failure. *Eur J Clin Invest,* **16,** 56-60.

Pfeiffer, R., *et al.* (1999) Amino acid transport of y+L-type by heterodimers of 4F2hc/CD98 and members of the glycoprotein-associated amino acid transporter family. *Embo J,* **18,** 49-57.

Phelps, D. T., *et al.* (1995) TNF-alpha induces peroxynitrite-mediated depletion of lung endothelial glutathione via protein kinase C. *Am J Physiol,* **269,** L551-9.

Pollock, J. S., *et al.* (1991) Purification and characterization of particulate endothelium-derived relaxing factor synthase from cultured and native bovine aortic endothelial cells. *Proc Natl Acad Sci U S A,* **88,** 10480-4.

Pollock, J. S., *et al.* (1992) Endothelial nitric oxide synthase is myristylated. *FEBS Lett,* **309,** 402-4.

Posch, K., *et al.* (1999) Selective stimulation of L-arginine uptake contributes to shear stress-induced formation of nitric oxide. *Life Sci,* **64,** 663-70.

Prabhakar, P., *et al.* (1998) Receptor-regulated translocation of endothelial nitric-oxide synthase. *J Biol Chem,* **273,** 27383-8.

Preik-Steinhoff, H., *et al.* (1995) Transport of L-arginine in arginine-deprived endothelial cells. *Biochem Biophys Res Commun,* **213,** 447-53.

Preli, R. B., *et al.* (2002) Vascular effects of dietary L-arginine supplementation. *Atherosclerosis,* **162,** 1-15.

Pueyo, M. E., *et al.* (1998) Angiotensin II stimulates the production of NO and peroxynitrite in endothelial cells. *Am J Physiol,* **274,** C214-20.

Quyyumi, A. A. (1998) Endothelial function in health and disease: new insights into the genesis of cardiovascular disease. *Am J Med,* **105,** 32S-39S.

Quyyumi, A. A., *et al.* (1995) Nitric oxide activity in the human coronary circulation. Impact of risk factors for coronary atherosclerosis. *J Clin Invest,* **95,** 1747-55.

Quyyumi, A. A., *et al.* (1997) Effect of L-arginine on human coronary endothelium-dependent and physiologic vasodilation. *J Am Coll Cardiol,* **30,** 1220-7.

Racke, K., *et al.* (1998) Activation of L-arginine transport by protein kinase C in rabbit, rat and mouse alveolar macrophages. *J Physiol,* **511 (Pt 3),** 813-25.

Ramesh, G., *et al.* (1999) Increased plasma nitrite level in cardiac failure. *J Mol Cell Cardiol,* **31,** 1495-500.

Razani, B., *et al.* (2001) Caveolin-1 null mice are viable but show evidence of hyperproliferative and vascular abnormalities. *J Biol Chem,* **276,** 38121-38.

Recchia, F. A., *et al.* (1998) Reduced nitric oxide production and altered myocardial metabolism during the decompensation of pacing-induced heart failure in the conscious dog. *Circ Res,* **83,** 969-79.

Rector, T. S., *et al.* (1996) Abnormal desmopressin-induced forearm vasodilatation in patients with heart failure: dependence on nitric oxide synthase activity. *Clin Pharmacol Ther,* **60,** 667-74.

Reiling, N., *et al.* (1996) Nitric oxide synthase: expression of the endothelial, Ca2+/calmodulin-dependent isoform in human B and T lymphocytes. *Eur J Immunol,* **26,** 511-6.

Reizer, J., *et al.* (1993) Mammalian integral membrane receptors are homologous to facilitators and antiporters of yeast, fungi, and eubacteria. *Protein Sci,* **2,** 20-30.

Reynolds, J. V., *et al.* (1990) Immunologic effects of arginine supplementation in tumor-bearing and non-tumor-bearing hosts. *Ann Surg,* **211,** 202-10.

Reynolds, J. V., *et al.* (1988) Arginine, protein malnutrition, and cancer. *J Surg Res,* **45,** 513-22.

Robinson, L. J., *et al.* (1995) Agonist-modulated palmitoylation of endothelial nitric oxide synthase. *J Biol Chem,* **270,** 995-8.

Rodeheffer, R. J., *et al.* (1992) Increased plasma concentrations of endothelin in congestive heart failure in humans. *Mayo Clin Proc,* **67,** 719-24.

Rosales, O. R., *et al.* (1998) Overexpression of protein kinase C alpha and beta1 has distinct effects on bovine aortic endothelial cell growth. *Cell Signal,* **10,** 589-97.

Ross, J. (1996) Control of messenger RNA stability in higher eukaryotes. *Trends Genet,* **12,** 171-5.

Saito, S., *et al.* (1996) Angiotensin II activates endothelial constitutive nitric oxide synthase via AT1 receptors. *Hypertens Res,* **19,** 201-6.

Sala, R., *et al.* (2002) Two-way arginine transport in human endothelial cells: TNF-alpha stimulation is restricted to system y(+). *Am J Physiol Cell Physiol,* **282,** C134-43.

Sambrook, J., *et al.* (1989) *Molecular Cloning: A laboratory manual.,* Cold Spring Harbour Laboratory Press, Cold Spring Harbour, New York.

Samih, N., *et al.* (2003) The impact of N- and O-glycosylation on the functions of Glut-1 transporter in human thyroid anaplastic cells. *Biochim Biophys Acta,* **1621,** 92-101.

Sanchez de Miguel, L., *et al.* (1999) Evidence that an endothelial cytosolic protein binds to the 3'-untranslated region of endothelial nitric oxide synthase mRNA. *J Vasc Res,* **36,** 201-8.

Sarkar, D., *et al.* (2001) Nitric oxide: not just a negative inotrope. *Eur J Heart Fail,* **3,** 527-34.

Sase, K., *et al.* (1995) Expression of constitutive endothelial nitric oxide synthase in human blood platelets. *Life Sci,* **57,** 2049-55.

Sato, I., *et al.* (1993) Reduction of nitric oxide producing activity associated with in vitro aging in cultured human umbilical vein endothelial cell. *Biochem Biophys Res Commun,* **195,** 1070-6.

Schapira, R. M., *et al.* (1998) L-arginine uptake and metabolism by lung macrophages and neutrophils following intratracheal instillation of silica in vivo. *Am J Respir Cell Mol Biol,* **19,** 308-15.

Schiffrin, E. L. (2002) Vascular and cardiac benefits of angiotensin receptor blockers. *Am J Med,* **113,** 409-18.

Schlaich, M. P., *et al.* (2000) Is l-arginine infusion an adequate tool to assess endothelium-dependent vasodilation of the human renal vasculature? *Clin Sci (Lond),* **99,** 293-302.

Schmidt, H. H., *et al.* (1991) Purification and characterization of a human NO synthase. *Biochem Biophys Res Commun,* **181,** 1372-7.

Schulz, E., *et al.* (2002) Functional and biochemical analysis of endothelial (dys)function and NO/cGMP signaling in human blood vessels with and without nitroglycerin pretreatment. *Circulation,* **105,** 1170-5.

Schulz, R., *et al.* (1994) Role of NO in vascular smooth muscle and cardiac muscle function. *Trends Pharmacol Sci,* **15,** 255-9.

Schwartz, I. F., *et al.* (2001) Tetrahydrobiopterin augments arginine transport in rat cardiac myocytes through modulation of CAT-2 mRNA. *J Lab Clin Med,* **137,** 356-62.

Sessa, W. C. (1994) The nitric oxide synthase family of proteins. *J Vasc Res,* **31,** 131-43.

Sessa, W. C., *et al.* (1992) Molecular cloning and expression of a cDNA encoding endothelial cell nitric oxide synthase. *J Biol Chem,* **267,** 15274-6.

Sessa, W. C., *et al.* (1994) Chronic exercise in dogs increases coronary vascular nitric oxide production and endothelial cell nitric oxide synthase gene expression. *Circ Res,* **74,** 349-53.

Seyedi, N., *et al.* (1995) Coronary kinin generation mediates nitric oxide release after angiotensin receptor stimulation. *Hypertension,* **26,** 164-70.

Shah, A. M., *et al.* (2000) Paracrine and autocrine effects of nitric oxide on myocardial function. *Pharmacol Ther,* **86,** 49-86.

Shaul, P. W. (2002) Regulation of endothelial nitric oxide synthase: location, location, location. *Annu Rev Physiol,* **64,** 749-74.

Shaul, P. W., *et al.* (1998) Role of plasmalemmal caveolae in signal transduction. *Am J Physiol,* **275,** L843-51.

Shi, X., *et al.* (2001) A novel casein kinase 2 alpha-subunit regulates membrane protein traffic in the human hepatoma cell line HuH-7. *J Biol Chem,* **276,** 2075-82.

Shuttleworth, C. W., *et al.* (1995) Recycling of L-citrulline to sustain nitric oxide-dependent enteric neurotransmission. *Neuroscience,* **68,** 1295-304.

Siflinger-Birnboim, A., *et al.* (2003) Protein kinase C modulates pulmonary endothelial permeability: a paradigm for acute lung injury. *Am J Physiol Lung Cell Mol Physiol,* **284,** L435-51.

Sigal, R. K., *et al.* (1992) Parenteral arginine infusion in humans: nutrient substrate or pharmacologic agent? *JPEN J Parenter Enteral Nutr,* **16,** 423-8.

Silacci, P., *et al.* (2000) Unidirectional and oscillatory shear stress differentially modulate NOS III gene expression. *Nitric Oxide,* **4,** 47-56.

Simmons, W. W., *et al.* (1996) Cytokines and insulin induce cationic amino acid transporter (CAT) expression in cardiac myocytes. Regulation of L-arginine transport and no production by CAT-1, CAT-2A, and CAT-2B. *J Biol Chem,* **271,** 11694-702.

Singh, N., *et al.* (2002) Ageing is associated with impairment of nitric oxide and prostanoid dilator pathways in the human forearm. *Clin Sci (Lond),* **102,** 595-600.

Sloan, J. L., *et al.* (1999) Cloning and functional expression of a human Na(+) and Cl(-)-dependent neutral and cationic amino acid transporter B(0+). *J Biol Chem,* **274,** 23740-5.

Smirnov, V. N., *et al.* (1989) Effects of forskolin and phorbol-myristate-acetate on cytoskeleton, extracellular matrix and protein phosphorylation in human endothelial cells. *J Mol Cell Cardiol,* **21 Suppl 1,** 3-11.

Smith, C. J., *et al.* (1996) Reduced gene expression of vascular endothelial NO synthase and cyclooxygenase-1 in heart failure. *Circ Res,* **78,** 58-64.

Smith, P. A., *et al.* (1997) Electrogenic arginine transport mediates stimulus-secretion coupling in mouse pancreatic beta-cells. *J Physiol,* **499 (Pt 3),** 625-35.

Smits, P., *et al.* (1993) Possibility of downregulation of atrial natriuretic peptide receptor coupled to guanylate cyclase in peripheral vascular beds of patients with chronic severe heart failure. *Circulation,* **88,** 811-3.

Sobue, K., *et al.* (1988) Tumor promoter induces reorganization of actin filaments and calspectin (fodrin or nonerythroid spectrin) in 3T3 cells. *Proc Natl Acad Sci U S A,* **85,** 482-6.

Sperandeo, M. P., *et al.* (1998) The gene encoding a cationic amino acid transporter (SLC7A4) maps to the region deleted in the velocardiofacial syndrome. *Genomics,* **49,** 230-6.

Srivastava, J., *et al.* (2002) Phosphorylation is required for PMA- and cell-cycle-induced degradation of protein kinase Cdelta. *Biochem J,* **368,** 349-55.

Stanek, B., *et al.* (2001) Prognostic evaluation of neurohumoral plasma levels before and during beta-blocker therapy in advanced left ventricular dysfunction. *J Am Coll Cardiol,* **38,** 436-42.

Stathopulos, P. B., *et al.* (2001) Increased L-arginine uptake and inducible nitric oxide synthase activity in aortas of rats with heart failure. *Am J Physiol Heart Circ Physiol,* **280,** H859-67.

Stein, B., *et al.* (1998) Increased expression of constitutive nitric oxide synthase III, but not inducible nitric oxide synthase II, in human heart failure. *J Am Coll Cardiol,* **32,** 1179-86.

Stein, W. (1990) *Channels, Carriers, and Pumps: An Introduction to Membrane Transport.,* Academic Press, San Diego.

Steinberg, H. O., *et al.* (1994) Insulin-mediated skeletal muscle vasodilation is nitric oxide dependent. A novel action of insulin to increase nitric oxide release. *J Clin Invest,* **94,** 1172-9.

Stepp, D. W., *et al.* (2002) Native LDL and minimally oxidized LDL differentially regulate superoxide anion in vascular endothelium in situ. *Am J Physiol Heart Circ Physiol,* **283,** H750-9.

Struthers, A. D. (2002) Impact of aldosterone on vascular pathophysiology. *Congest Heart Fail,* **8,** 18-22.

Stuehr, D. J. (1999) Mammalian nitric oxide synthases. *Biochim Biophys Acta,* **1411,** 217-30.

Stuehr, D. J., *et al.* (1991) Purification and characterization of the cytokine-induced macrophage nitric oxide synthase: an FAD- and FMN-containing flavoprotein. *Proc Natl Acad Sci U S A,* **88,** 7773-7.

Su, Y., *et al.* (2002) Microtubule-active agents modify nitric oxide production in pulmonary artery endothelial cells. *Am J Physiol Lung Cell Mol Physiol,* **282,** L1183-9.

Sukumaran, S. K., *et al.* (2002) Escherichia coli K1 internalization via caveolae requires caveolin-1 and protein kinase Calpha interaction in human brain microvascular endothelial cells. *J Biol Chem,* **277,** 50716-24.

Sullivan, M. J., *et al.* (1995) Exercise intolerance in patients with chronic heart failure. *Prog Cardiovasc Dis,* **38,** 1-22.

Sumi, D., *et al.* (2001) Estrogen prevents destabilization of endothelial nitric oxide synthase mRNA induced by tumor necrosis factor alpha through estrogen receptor mediated system. *Life Sci,* **69,** 1651-60.

Sutsch, G., *et al.* (1999) Endothelin in heart failure. *Curr Hypertens Rep,* **1,** 62-8.

Szabo, C., *et al.* (1996) DNA strand breakage, activation of poly (ADP-ribose) synthetase, and cellular energy depletion are involved in the cytotoxicity of macrophages and smooth muscle cells exposed to peroxynitrite. *Proc Natl Acad Sci U S A,* **93,** 1753-8.

Taddei, S., *et al.* (2000) Physical activity prevents age-related impairment in nitric oxide availability in elderly athletes. *Circulation,* **101,** 2896-901.

Taddei, S., *et al.* (1995) Aging and endothelial function in normotensive subjects and patients with essential hypertension. *Circulation,* **91,** 1981-7.

Takemoto, M., *et al.* (2001) Pleiotropic effects of 3-hydroxy-3-methylglutaryl coenzyme a reductase inhibitors. *Arterioscler Thromb Vasc Biol,* **21,** 1712-9.

Taubman, M. B., *et al.* (1989) Angiotensin II induces c-fos mRNA in aortic smooth muscle. Role of Ca2+ mobilization and protein kinase C activation. *J Biol Chem,* **264,** 526-30.

Thorup, C., *et al.* (1999) AT1 receptor inhibition blunts angiotensin II-stimulated nitric oxide release in renal arteries. *J Am Soc Nephrol,* **10 Suppl 11,** S220-4.

Toomtong, P., *et al.* (2001) Nitric oxide production by human peripheral blood mononuclear cells. *Ann Acad Med Singapore,* **30,** 270-3.

Toullec, D., *et al.* (1991) The bisindolylmaleimide GF 109203X is a potent and selective inhibitor of protein kinase C. *J Biol Chem,* **266,** 15771-81.

Tsutsui, T., *et al.* (2002) Plasma oxidized low-density lipoprotein as a prognostic predictor in patients with chronic congestive heart failure. *J Am Coll Cardiol,* **39,** 957-62.

Udvardy, M., *et al.* (1997) Effect of L-arginine on in vitro plasmin-generation and fibrinogenolysis. *Thromb Res,* **87,** 75-82.

Uemura, S., *et al.* (2000) Rapid and efficient vascular transport of arginine polymers inhibits myointimal hyperplasia. *Circulation,* **102,** 2629-35.

Uemura, S., *et al.* (2002) Short polymers of arginine rapidly translocate into vascular cells. *Circ J,* **66,** 1155-60.

Urakami-Harasawa, L., *et al.* (1997) Importance of endothelium-derived hyperpolarizing factor in human arteries. *J Clin Invest,* **100,** 2793-9.

Usui, M., *et al.* (1998) Increased endogenous nitric oxide synthase inhibitor in patients with congestive heart failure. *Life Sci,* **62,** 2425-30.

Vallance, P., *et al.* (1989) Effects of endothelium-derived nitric oxide on peripheral arteriolar tone in man. *Lancet,* **2,** 997-1000.

van der Zypp, A., *et al.* (2000) Age-related involvement of the endothelium in beta-adrenoceptor-mediated relaxation of rat aorta. *Eur J Pharmacol,* **397,** 129-38.

van Iwaarden, P. R., *et al.* (1992) What we can learn from the effects of thiol reagents on transport proteins. *Biochim Biophys Acta,* **1113,** 161-70.

Van Winkle, L. J., *et al.* (1988) Na+-independent transport of basic and zwitterionic amino acids in mouse blastocysts by a shared system and by processes which distinguish between these substrates. *J Biol Chem,* **263,** 3150-63.

Vanhoutte, P. M. (1996) Endothelium-dependent responses in congestive heart failure. *J Mol Cell Cardiol,* **28,** 2233-40.

Vapaatalo, H., *et al.* (2001) Clinically important factors influencing endothelial function. *Med Sci Monit,* **7,** 1075-85.

Vasquez-Vivar, J., *et al.* (1998) Superoxide generation by endothelial nitric oxide synthase: the influence of cofactors. *Proc Natl Acad Sci U S A,* **95,** 9220-5.

Vaziri, N. D., *et al.* (1999) cGMP-mediated negative-feedback regulation of endothelial nitric oxide synthase expression by nitric oxide. *Hypertension,* **34,** 1237-41.

Vejlstrup, N. G., *et al.* (1998) Inducible nitric oxide synthase (iNOS) in the human heart: expression and localization in congestive heart failure. *J Mol Cell Cardiol,* **30,** 1215-23.

Vekony, N., *et al.* (2001) Human cationic amino acid transporter hCAT-3 is preferentially expressed in peripheral tissues. *Biochemistry,* **40,** 12387-94.

Viner, R. I., *et al.* (1996) The oxidative inactivation of sarcoplasmic reticulum Ca(2+)-ATPase by peroxynitrite. *Free Radic Res,* **24,** 243-59.

Violi, F., *et al.* (1999) Nitric oxide and its role in lipid peroxidation. *Diabetes Metab Res Rev,* **15,** 283-8.

Visek, W. J. (1986) Arginine needs, physiological state and usual diets. A reevaluation. *J Nutr,* **116,** 36-46.

Vlahos, C. J., *et al.* (2003) Kinases as therapeutic targets for heart failure. *Nat Rev Drug Discov,* **2,** 99-113.

Wagner, A. H., *et al.* (2000) Improvement of nitric oxide-dependent vasodilatation by HMG-CoA reductase inhibitors through attenuation of endothelial superoxide anion formation. *Arterioscler Thromb Vasc Biol,* **20,** 61-9.

Wagner, C. A., *et al.* (2001) Function and structure of heterodimeric amino acid transporters. *Am J Physiol Cell Physiol,* **281,** C1077-93.

Walter, R., *et al.* (2000) Pharmacological concentrations of arginine influence human whole blood viscosity independent of nitric oxide synthase activity in vitro. *Biochem Biophys Res Commun,* **269,** 687-91.

Wang, H., *et al.* (1991) Cell-surface receptor for ecotropic murine retroviruses is a basic amino-acid transporter [see comments]. *Nature,* **352,** 729-31.

Wascher, T. C., *et al.* (1997) Vascular effects of L-arginine: anything beyond a substrate for the NO-synthase? *Biochem Biophys Res Commun,* **234,** 35-8.

Wassmann, S., *et al.* (2001) HMG-CoA reductase inhibitors improve endothelial dysfunction in normocholesterolemic hypertension via reduced production of reactive oxygen species. *Hypertension,* **37,** 1450-7.

Wassmann, S., *et al.* (2002) Cellular antioxidant effects of atorvastatin in vitro and in vivo. *Arterioscler Thromb Vasc Biol,* **22,** 300-5.

White, M., *et al.* (1997) Age- and gender-related changes in endothelin and catecholamine release, and in autonomic balance in response to head-up tilt. *Clin Sci (Lond),* **93,** 309-16.

Wideman, L., *et al.* (2000) Synergy of L-arginine and GHRP-2 stimulation of growth hormone in men and women: modulation by exercise. *Am J Physiol Regul Integr Comp Physiol,* **279,** R1467-77.

Wolf, S., *et al.* (2002) Expression of solute carrier 7A4 (SLC7A4) in the plasma membrane is not sufficient to mediate amino acid transport activity. *Biochem J,* **364,** 767-75.

Woodman, O. L. (1999) Approaches to the prevention of coronary vascular dysfunction caused by myocardial ischaemia and reperfusion. *Curr Pharm Des,* **5,** 1077-87.

Wright, J. W., *et al.* (1995a) Brain angiotensin receptor subtypes AT1, AT2, and AT4 and their functions. *Regul Pept,* **59,** 269-95.

Wright, J. W., *et al.* (1995b) The angiotensin IV system: functional implications. *Front Neuroendocrinol,* **16,** 23-52.

Wu, G., *et al.* (1999) Dietary protein or arginine deficiency impairs constitutive and inducible nitric oxide synthesis by young rats. *J Nutr,* **129,** 1347-54.

Wu, G., *et al.* (2000) Arginine nutrition and cardiovascular function. *J Nutr,* **130,** 2626-9.

Wu, G., *et al.* (1998) Arginine metabolism: nitric oxide and beyond. *Biochem J,* **336,** 1-17.

Wu, J. Y., *et al.* (1994) Hormonal regulation of the gene for the type C ecotropic retrovirus receptor in rat liver cells. *J Virol,* **68,** 1615-23.

Xie, L., *et al.* (1997) Argininosuccinate synthetase overexpression in vascular smooth muscle cells potentiates immunostimulant-induced NO production. *J Biol Chem,* **272,** 16624-30.

Xiong, Y., *et al.* (2001) Elevated serum endogenous inhibitor of nitric oxide synthase and endothelial dysfunction in aged rats. *Clin Exp Pharmacol Physiol,* **28,** 842-7.

Yamashita, T., *et al.* (2000) Mechanisms of reduced nitric oxide/cGMP-mediated vasorelaxation in transgenic mice overexpressing endothelial nitric oxide synthase. *Hypertension,* **36,** 97-102.

Yang, J., *et al.* (2000) Decreased SLIM1 expression and increased gelsolin expression in failing human hearts measured by high-density oligonucleotide arrays. *Circulation,* **102,** 3046-52.

Yasue, H., *et al.* (1990) Responses of angiographically normal human coronary arteries to intracoronary injection of acetylcholine by age and segment. Possible role of early coronary atherosclerosis. *Circulation,* **81,** 482-90.

Yokoyama, K., *et al.* (2002) HMG-CoA reductase inhibitors suppress intracellular calcium mobilization and membrane current induced by lysophosphatidylcholine in endothelial cells. *Circulation,* **105,** 962-7.

Yoshimoto, T., *et al.* (1992) Enhanced gene expression of the murine ecotropic retroviral receptor and its human homolog in proliferating cells. *J Virol,* **66,** 4377-81.

Yoshizumi, M., *et al.* (1993) Tumor necrosis factor downregulates an endothelial nitric oxide synthase mRNA by shortening its half-life. *Circ Res,* **73,** 205-9.

Yu, B. P., *et al.* (2001) Oxidative stress and vascular aging. *Diabetes Res Clin Pract,* **54 Suppl 2,** S73-80.

Zhang, C., *et al.* (2001) Constitutive expression of arginase in microvascular endothelial cells counteracts nitric oxide-mediated vasodilatory function. *Faseb J,* **15,** 1264-6.

Zhang, H., *et al.* (1999) Angiotensin II-induced superoxide anion generation in human vascular endothelial cells: role of membrane-bound NADH-/NADPH-oxidases. *Cardiovasc Res,* **44,** 215-22.

Zhao, G., *et al.* (1996) Loss of nitric oxide production in the coronary circulation after the development of dilated cardiomyopathy: a specific defect in the neural regulation of coronary blood flow. *Clin Exp Pharmacol Physiol,* **23,** 715-21.

Zharikov, S. I., *et al.* (1998) Characterization of L-arginine uptake by plasma membrane vesicles isolated from cultured pulmonary artery endothelial cells. *Biochim Biophys Acta,* **1369,** 173-83.

Zharikov, S. I., *et al.* (2000) Association of L-arginine transporters with fodrin: implications for hypoxic inhibition of arginine uptake. *Am J Physiol Lung Cell Mol Physiol,* **278,** L111-7.

Zharikov, S. I., *et al.* (1997) Role of membrane potential in hypoxic inhibition of L-arginine uptake by lung endothelial cells. *Am J Physiol,* **272,** L78-84.

Zharikov, S. I., *et al.* (2001) Cytoskeletal regulation of the L-arginine/NO pathway in pulmonary artery endothelial cells. *Am J Physiol Lung Cell Mol Physiol,* **280,** L465-73.

ADDENDUM

8.1 Statistical tests applied to the data presented in this thesis

Significance of the difference among two or more groups of experimental data as in Chapter 3 (Figures 3.1, 3.2, 3.6, 3.12), Chapter 4 (Figure 4.2, 4.3, 4.5, 4.9), Chapter 5 (Figure 5.1, 5.3) and Chapter 6 (Figures 6.6, 6.11, 6.16) have been analysed by either one-way or two-way ANOVA where appropriate with subsequent post-hoc testing eg. Tukey test. Taking one group of data and repeatedly comparing it against different groups, was not applied in these instances and is inappropriate for two reasons: 1) non-independence of hypothesis tests and 2) the problem of multiple hypothesis tests. However, in experiments which the means of two groups of independent samples were compared the two-tailed unpaired Student's t-test was applied. This includes experimental data presented in Chapter 3 (Figures 3.2, 3.7, 3.9, 3.10, 3.11), Chapter 4 (Figure 4.2, 4.6, 4.7, 4.8), Chapter 5 (Figure 5.2, 5.4, 5.5, 5.6) and Chapter 6 (Figures 6.2, 6.3, 6.4, 6.5, 6.8, 6.10, 6.12, 6.13, 6.14, 6.15, 6.17). Results were all expressed as mean ± SEM. SigmaStat 2.0 software (Jandel Scientific, San Rafael, CA, USA) was utilised for all statistical analyses. Values were considered to be statistically different at a value of $P<0.05$.

8.2 Further discussion of experimental data

Additional information provided for Chapter 3.1.2

There was no description provided in the methods section of Chapter 3.1.2 (page 103) concerning subject characteristics from which peripheral blood mononuclear cells (PBM) were collected. Male and female staff from the Alfred and Baker Medical Unit, within an age range of 19-69 years, were recruited in order to develop an *ex vivo* assay for assessing L-Arginine transport in humans. Healthy subjects had blood pressure, glucose, cholesterol and triglycerides within the normal range. All subjects were non-smokers with no history of cardiovascular disease and were not taking medication. All staff participated after giving informed consent, and the study was conducted with the approval of the Alfred Hospital Ethics Review Committee. Data obtained from these healthy subjects using the concentration-dependent L-[^{3}H]Arg transport protocol described in Chapter 3.1.2.3 (page 104) was also used for healthy age-matched controls in the analysis of L-Arg transport in CHF (Chapter 3.2) and aging (Chapter 3.3).

Chapter 3.2.2

Experiments carried out on PBM no longer in the circulation are classified as *ex-vivo* rather then *in-vivo* experiments.

Statistical analysis of data presented in figure 3.6

The description of statistical analysis methods applied to the data in Chapter 3.2.2.5 (page 123) is incomplete. The description provided in the text only applies to ribonuclease protection assay data (Figure 3.7, 3.9 and 3.10), RT-PCR data (Figure 3.8) and Western blot data (Figure 3.11) that were all subject to statistical analysis using the two-tailed unpaired Student's t-test. However, it is important to note that two-way ANOVA was used to analyse L-Arg transport rate as a function of group [control versus heart failure] and [L-Arg] concentration for the data presented in Figure 3.6. A significant group effect difference was detectable $p<0.001$.

Modification to concluding remark in Chapter 4.1.4

In the concluding paragraph of the discussion (Chapter 4.1.4, page 161) I stated that since major neurohormones relevant in the setting of heart failure do not account for depressed L-Arg transport observed in CHF, it is likely that reduced shear stress has a major causal role in this effect. Since this has not yet been tested experimentally, a modification of this paragraph now reads: "Potential effects of structural and mechanical alterations to the vasculature of CHF patients may be a determinant of L-Arg transport activity (Posch et al., 1999). Data presented within this chapter does not exclude this possibility. For example, changes in endothelial L-Arg transport (Posch et al., 1999), NOS activity and expression, and antioxidant enzyme activity have previously been detected in humans, and in animal and culture models of shear stress (Gielen et al., 2002). Further investigation of this topic is warranted."

Modification of concluding remark in Chapter 6.1.4.2

Data presented in Figure 6.6 shows that treatment with either superoxide dismutase, ascorbic acid or L-NAME was unable to prevent the acute and chronic effects of PMA on L-Arg transport in bovine endothelial cells. In the concluding paragraph of Chapter 6.1.4.2 (page 223, lines 21-26) I have stated that on the basis of these results, ROS does not contribute to PKC-mediated inhibition of CAT-1 activity or longer-term effects of PMA treatment on CAT-1 activation. This is conclusion is inaccurate since the experiments performed only assessed the role of superoxide in PMA-related effects on L-Arg transport and not that of other free radical species such as ROS produced from various sources including NADH/NADPH oxidase (Gorlach et al., 2000), xanthine oxidase (Landmesser et al., 2002), cyclooxygenases and, side products resulting from the mitochondrial respiratory chain (Mak and Newton, 2001).

The concluding remark now reads: "Potential effects of PMA-induced superoxide on CAT-1 activity were explored in the present study by exposing cells to either antioxidants (ascorbic acid and superoxide dismutase) or the NOS inhibitor L-NAME in the presence of PMA (Figure 6.6). Since neither of these treatments prevented the effects of PMA on L-Arg transport activity I conclude that superoxide does not contribute to PKC-mediated inhibition of CAT-1 activity or longer-term effects of PMA treatment on CAT-1 activation. The present data does not exclude the potential effects of PMA-generated free radical species by other sources such as NADH/NADPH oxidase, xanthine oxidase and cyclooxygenases, and should be further investigated."

Chapter 6.2.2.2

A reference in the text to Appendix A (page 225, line 9), which should have been omitted because Appendix A is not included the final thesis format. The original Appendix A contained a detailed description about site-directed mutagenesis methodology in addition to the exact primer sequences used to convert serine residues to alanine residues at putative PKC phosphorylation sites within the CAT-1 open reading frame. As an suitable alternative to Appendix A inclusion I have referred the reader to Ausubel et al., 1990 (Page 225, line 9) which is a standard molecular biology methodology text book.

Chapter 6.2 Methods

The statistical methods used for the analysis of data presented in Chapter 6.2 are outlined above in Amendments, Chapter 8.1.

Data for single Ala mutation substitution at Ser-475; Chapter 6.2, Figure 6.14.

Data presented in Figure 6.14 (Chapter 6.2, page 236) using putative PKC site double mutants PKC 1,2 (Ser-469 to Ala, Ser-475 to Ala) and PKC 2,3 (Ser-475 to Ala, Ser-550 to Ala) suggest a potentially important role for Ser-475 in basal CAT-1 mediated L-Arg transport. However, no L-Arg transport data has been obtained for the single Ser-475 to Ala PKC site mutation (PKC 2). The presence of this specific mutation introduced using PCR-based mutagenesis methodology had not been positively confirmed by sequence analysis at the time of investigation. Selection for this mutation delayed since the Baker Institute was experiencing technical difficulties with the core facility ABI Prism DNA sequencer. This problem was encountered towards the end of my PhD studies and I was unable to determine the importance of Ser-475 for basal CAT-1 mediated L-Arg transport. I have since constructed and sequence verified a plasmid containing this mutation.

Dr.Kaye's laboratory is currently in the process of completing the experiments described in Chapter 6.2 using the PKC 2 single mutant.

Asymmetric-dimethyl arginine (ADMA), a NOS inhibitor, and its effects on L-Arg transport
The role of ADMA in hypercholesterolemia and CHF is an area of increasing interest in NOS pharmacology and biology. With respect to CHF, elevated plasma levels of ADMA have been detected both experimentally (Feng et al., 1998) and clinically (Saitoh et al., 2003, Usui et al., 1998). Furthermore, levels of ADMA have been shown to negatively correlate with the level of NOx in moderate to severe CHF (Saitoh et al., 2003, Usui et al., 1998). It has not yet been definitively proven whether ADMA serves as a surrogate marker of endothelial dysfunction or whether it is causally involved in endothelial dysfunction associated with CHF. Clearly this topic needs further investigation.

I did not test the acute effects of ADMA on L-Arg transport in cultured endothelial cells since it is already a known competitor of L-Arg uptake *in vitro* (Closs et al., 1997, Xiao et al., 2001). Although, much higher concentrations of ADMA (~100μM) are required to inhibit transport of plasma L-Arg concentrations. L-Arg is preferentially taken up by cells under normal conditions since the level of circulating L-Arg in humans is reported to be 80-120 μM whereas the level of normal circulating ADMA is reported to be much lower ~1 μM. In vascular disorders such as hypercholesterolemia plasma ADMA levels are increased by up to 2 fold whereas in HF levels are increased by severity regardless of aetiology but by smaller margins (Feng et al., 1998, Usui et al., 1998). Plasma L-Arg levels in CHF are controversial since some groups have not detected alterations while others have reported a decreased level of L-Arg from 125 μM in healthy subjects compared with 59 μM in CHF (Hanssen et al., 1998). Since plasma levels of ADMA are well below the K_M for CAT-1 mediated transport, regardless of the pathology, it seems unlikely that ADMA affects endothelial function by acute competitive inhibition of L-Arg transport. In accordance, L-Arg transport was depressed in mononuclear cells removed from the plasma of CHF patients (versus normal, Chapter 3), to a similar magnitude as reduced L-Arg clearance measured in CHF forearm studies (Kaye et al., 2000).

Increases in the intracellular level of ADMA however may lead to a longer-term inhibition of L-Arg transport activity via effects of ADMA within the cell, for example, by causing an uncoupling of the functional association of CAT-1 with NOS. I did not explore this possibility during my PhD. The ratio of L-Arg to ADMA concentration in the cell is known to be a determinant of the level of NO production. Endothelial cells cultured at hypercholesterolemic L-Arg/ADMA ratios (25:1) exhibit increased monocyte adhesiveness (a feature of endothelial dysfunction), similar to that exhibited in patients with this disorder (Chan et al., 2000). Normalisation of L-Arg/ADMA ratios (normocholesterolemic 50:1) through a 2-12 week oral administration of L-Arg (14-21 g/d L-Arginine hydrochloride 3 times daily) can reverse this effect *in vivo* (Chan et al., 2000). One way in which higher levels of ADMA can result intracellularly is through a decreased metabolism within the cell. In this respect, the activity of dimethylarginine dimethylaminohydrolase (DDAH), the major enzyme for ADMA conversion to L-citrulline is known to be depressed in certain disorders associated with endothelial dysfunction (Cooke, 2000). Various other detrimental effects of increased ADMA have also been proposed within the endothelium (Boger et al., 2003).

It would be interesting to determine the long-term effects of ADMA (24-72 hr; added to culture medium at normal and CHF L-Arg/ADMA ratios) on L-Arg transport and NO synthesis in cultured endothelial cells to explore the possibility of changes in the CAT-1/NOS interaction. Determination of expression and enzymatic activity of the ADMA metabolising enzyme DDAH from experimental/clinical CHF tissue samples in combination with the measurement of the stable intermediate in the biosynthesis of NO, N^G-hydroxy-L-Arginine (NOHA; Chapter 1.5.2) by HPLC analysis would help contribute towards a better understanding of alterations in the metabolic utilisation of L-Arg by NOS which may exist in CHF.

8.3 Editing corrections

Chapter 5, page 191, text line 9 (Figure 6.3A). The correction is (Figure 5.3A).
Chapter 5, page 191, text line 13 (Figure 6.3B). The correction is (Figure 5.3B).
Chapter 5, page 194, text line 9, (Figures 6.5 A/B). The correction is (Figure 5.5A and B).
Chapter 5, page 195, text line 11, (Figure 6.6A and B). The correction is (Figure 5.6A and B).
Chapter 5, page 195, text line 18, Figure 6.6A. The correction is Figure 5.6A.
Chapter 5, page 195, text line 20, Figure 6.6A. The correction is Figure 5.6A.
Chapter 5, page 195, text line 22, Figure 6.6A. The correction is Figure 5.6A.
Chapter 6, page 217, text line 11, (Figure 6.8). The correction is Figure 6.6.
Chapter 6, page 218, text line 7, (Figure 6.8). The correction is Figure 6.6.
Chapter 6, page 219, text line 8, (Figure 6.6, left panel). The correction is (Figure 6.7, left panel).
Chapter 6, page 219, text line 17, (Figure 6.6, right panel). The correction is (Figure 6.7, right panel).
Chapter 6, page 221, text line 7, Figure 6.7 (panel A and B). The correction is Figure 6.8 (panel A and B).
Chapter 6, page 222, text line 13, Figure 6.7. The correction is Figure 6.8.

8.4 Additional references

Boger, R. H., Zoccali, C., Mallamaci, F., Tripepi, G., Annuk, M., Zilmer, M., Fellstrom, B., Fliser, D., Kielstein, J. T., Haller, H., Bode-Boger, S. M., Maas, R., Schwedhelm, E., Albsmeier, J., Chan, N. N., Chan, J. C., Kurowska, E. M., Cooke, J. P., Tsao, P. S., Hedner, T. and Sun, X. (2003) Association of asymmetric dimethylarginine and endothelial dysfunction *Clin Chem Lab Med,* **41,** 1467-72.

Chan, J. R., Boger, R. H., Bode-Boger, S. M., Tangphao, O., Tsao, P. S., Blaschke, T. F. and Cooke, J. P. (2000) Asymmetric dimethylarginine increases mononuclear cell adhesiveness in hypercholesterolemic humans. *Arterioscler Thromb Vasc Biol,* **20,** 1040-6.

Cooke, J. P. (2000) Does ADMA cause endothelial dysfunction? *Arterioscler Thromb Vasc Biol,* **20,** 2032-7.

Feng, Q., Lu, X., Fortin, A. J., Pettersson, A., Hedner, T., Kline, R. L. and Arnold, J. M. (1998) Elevation of an endogenous inhibitor of nitric oxide synthesis in experimental congestive heart failure. *Cardiovasc Res,* **37,** 667-75.

Gielen, S., Erbs, S., Schuler, G. and Hambrecht, R. (2002) Exercise training and endothelial dysfunction in coronary artery disease and chronic heart failure. From molecular biology to clinical benefits. *Minerva Cardioangiol,* **50,** 95-106.

Saitoh, M., Osanai, T., Kamada, T., Matsunaga, T., Ishizaka, H., Hanada, H. and Okumura, K. (2003) High plasma level of asymmetric dimethylarginine in patients with acutely exacerbated congestive heart failure: role in reduction of plasma nitric oxide level. *Heart Vessels,* **18,** 177-82.

Xiao, S., Wagner, L., Mahaney, J. and Baylis, C. (2001) Uremic levels of urea inhibit L-Arginine transport in cultured endothelial cells. *Am J Physiol Renal Physiol,* **280,** F989-95.